THE UNIVERSITY
of EDINBURGH

UNIVERSITY OF EDINBURGH

Computational and neuroimaging approaches to major depressive disorder

Author:
Samuel RUPPRECHTER

Supervisors:
Dr. Peggy SERIÈS
Prof. J. Douglas STEELE

Doctor of Philosophy
Institute for Adaptive and Neural Computation
School of Informatics
University of Edinburgh
2020

Abstract

Major depression is a severely debilitating psychiatric condition with high prevalence and substantial economic impact. However, its aetiology is largely unknown, mechanistic understanding remains limited, and treatment outcomes are hard to predict. Recently, a "computational psychiatry" approach has emerged which embraces the idea of using computational models to link brain function, behaviour and psychiatric illness. This thesis describes the use of computational psychiatry tools and techniques to advance understanding of abnormalities in decision-making and neuronal activity associated with depressive illness.

Behaviour during novel reward learning tasks was analysed from patients diagnosed with major depressive disorder and healthy controls. Formal computational modelling was used to show behavioural impairments associated with depression during both learning and decision-making phases. Depressed participants displayed lower memory of rewards and decreased ability to use internal value estimations during decision-making. Functional MRI results showed decreased reward signals in areas including the striatum were associated with depression symptoms. Computational models were used to generate latent variable time-series of internal value estimations which were used for model-based fMRI analyses. Reward value encoding in hippocampus and rostral anterior cingulate was abnormal in depression and anterior mid-cingulate (aMCC) activity was altered during decision-making. A signal encoding the difference between the values of the two options was also found in the aMCC, linking the behavioural model to localised brain function. Depressed patients showed decreased event-related connectivity between aMCC and rostral cingulate regions, implying impaired communication between value estimation and decision-making regions. A large community-based sample of participants reporting a range of depressive symptoms performed a different probabilistic reward learning task. Mood symptoms were associated with blunted striatal reward signals. Event-related directed medial prefrontal cortex to ventral striatum effective connectivity was abnormally decreased related to the severity of depression symptoms. A generative-embedding machine learning approach was used to classify never-depressed healthy controls from participants with current or past major depression. A support vector machine classifier achieved 72% diagnostic accuracy using estimated connectivity parameters as features.

The thesis replicates previous reports of abnormal depression-related neural activity in areas including the striatum, hippocampus and prefrontal cortex using novel reward learning tasks. Findings support the theory about abnormal neural reward valuation in major depression being a core pathophysiological process which could be a target for treatment. The thesis also provides important novel evidence for decreased connectivity between prefrontal and limbic brain regions, and within

different prefrontal areas in depression. It shows how abnormalities in reward value based decision-making may be related to abnormal reward activation and connectivity in the brain, supporting glutamatergic and cortical-limbic related theories of depression.

Lay Summary

Clinical depression has an enormous impact, not only affecting the afflicted but also their loved ones, employers and the wider society. It is not yet known how exactly processes in the brain are related to depression and how to objectively identify who is ill, and it is hard to predict which therapy (if any) would work for a specific patient.

Various groups of participants, including depressed patients, healthy controls, and participants reporting various depression symptoms, performed decision-making tasks while in a functional magnetic resonance imaging (fMRI) scanner. Computational models were used to succinctly describe and compare behaviour of participants, which revealed decision-making abnormalities in depression. Patients showed lower memory of previously observed rewards and difficulties using estimated reward values to guide their decisions. This behaviour was related to alterations in brain activity of several regions, including areas in the prefrontal cortex and the basal ganglia, which are known to be involved in value estimation and decision-making. Connectivity between implicated brain regions, that is the information flow between them, was estimated. Results indicated impaired communication between value estimation and decision-making regions in depression. Based on the strengths of connectivity between brain regions, machine learning was used to classify participants into never-depressed healthy versus current or past depression groups with 72% accuracy.

The thesis replicates and significantly extends previous reports of abnormal behaviour, brain activity and brain connectivity related to major depression. It provides important evidence for an association between mood symptoms and decreased connectivity between brain regions which are implicated in reward value based decision-making, supporting prominent theories about depression.

Declaration of Authorship

I declare that this thesis was composed by myself and the work contained is my own, except where explicitly stated otherwise. This work has not been submitted for any other degree or professional qualification except as specified. Where necessary, my contributions are clearly stated at the beginning of each chapter.

Samuel Rupprechter

Contents

For Sarah

Chapter 1

Introduction

Depression is immensely devastating and the common conception of it being mere "low mood" does not begin to capture the severity of this disease. Those who have suffered from it tell tales of absolute blackness and hopelessness beyond measure. "It is like living in a body that fights to survive with a mind that tried to die." (Anonymous, 2016). In his memoir, William Styron described his suffering in a brutally honest way:

> *"Depression is a disorder of mood, so mysteriously painful and elusive in the way it becomes known to the self — to the mediating intellect — as to verge close to being beyond description. It thus remains nearly incomprehensible to those who have not experienced it in its extreme mode."*
>
> — William Styron, Darkness Visible: A Memoir of Madness

Indeed, due to its debilitating impact and high prevalence, depression ranks as one of the greatest burdens on societies around the world (Üstün, Ayuso-Mateos, Chatterji, et al., 2004). It is extremely costly and responsible for one of the highest rates of "years lived with disability" (YLDs), only rivalled by other extremely common diseases such as low back pain and migraine (Vos, Flaxman, Naghavi, et al., 2012; Vos, Abajobir, Abate, et al., 2017). The World Health Organisation projects that depression will become the leading cause of disease burden by 2030 (WHO report 2007[1]).

Unfortunately, too little is known about this crushing disease and the general consensus is that clinical practice in psychiatry has not advanced significantly in over 50 years (Stephan, Bach, Fletcher, et al., 2016; Stephan, Binder, Breakspear, et al., 2016). Treatment outcomes are hard to predict and many patients never fully recover (Steele and Paulus, 2019).

Nevertheless, there is hope. Technology and neuroimaging techniques are advancing rapidly and are leading to exciting new discoveries about the brain, and finally allow some long standing theories to be tested. The use of computational models

[1] https://www.who.int/healthinfo/global_burden_disease/GBD_report_2004update_full.pdf

and machine learning techniques is especially promising which has given rise to the field of "computational psychiatry" (Montague, Dolan, Friston, and Dayan, 2012), which is promising to lead psychiatry into a new "golden age" (Vinogradov, 2017).

There is substantial evidence for behavioural and neuronal abnormalities during the performance of reward learning and decision-making tasks in depression (see Chapter 2). This thesis uses computational models to succinctly capture participants' behaviour during such tasks and then combines this modelling with observed brain activity during the task to test novel hypotheses about depressive illness.

1.1 Computational Models

Computational or mathematical models have been used prominently in many areas of science and engineering for a long time. Nowadays they are also used in neuroscience, such as in computational neuroscience. Models can be used to capture and describe the essence of a concept or system by abstracting and simplifying it and eliminating unnecessary complexities.

Marr (1982) famously proposed three levels at which an information-processing device such as the brain should be understood and models can span one or more of these levels: (a) the computational level, specifying the goal of the computation, (b) the algorithmic level, explaining how the goal can be achieved, and (c) the implementation level, specifying how the algorithm can be physically realised. It should be noted that although the levels are often practically useful, they are not necessarily complete nor does every published work fit neatly into one of these three levels.

In this thesis, I model the behaviour and decision making of participants by trying to find a model which best captures the choices they make during a controlled experiment. This is then followed by comparing the models (or parameters of these models) of participants suffering from depression with healthy control participants, allowing the analysis of how groups differ.

Computational modelling of behavioural data commonly involves a sequence of steps and I briefly highlight some here. For more detailed descriptions, explanations and discussion the reader may want to consult one of the many previous introductions (e.g. see Wilson and Collins, 2019). Here I focus on conceptual understanding. More mathematical details about the methods used in this thesis are provided in the appendices and the cited literature.

The first step is usually to design a model (or a model space consisting of multiple models), ideally in combination with the design of the experiment, to address a scientific question. It is important not to forget that all models are an approximation, so in a sense "wrong", and the more appropriate question is if they can be useful (see also Box and Draper, 1987).

Once the models are defined and data from the experiment is collected, models are then "fitted" to the data. This means searching for parameters which result in a model performance most similar to the observed choice behaviour. There are different approaches one could take but in this thesis I generally use a maximum likelihood or maximum a posteriori approach which means I let models assign a probability to each possible action and then try to maximise the probability of producing the whole sequence of observed actions. Gradient descent is commonly used to find these maxima.

While this can be done on a per-participant basis, in this thesis the prior assumption is sometimes made that in general, participants will behave similarly to one another. Formally this means that first parameter estimation is performed for each participant and then all these estimates are combined into a single empirical group level prior, which is used to constrain subsequent parameter estimations of individuals.

Model comparison is a crucial next step and is used to choose the most parsimonious model, meaning a model which is as simple as possible but no simpler. There are again different approaches but importantly one should always remember that model comparison is conditional on the defined model space and so a chosen "best" model should always be viewed relative to the other "worse" models.

Once a model is selected it can then be used to test the original scientific question. For example, in this thesis I look at potential differences in estimated parameters between groups of healthy and depressed participants. These parameters might correspond to underlying constructs of interest not easily detectable from the raw behavioural data, such as a "learning rate parameter" intended to capture how fast participants update their previously held beliefs with new information.

So far, a profoundly important property of the discussed models has been neglected: they can be simulated to generate artificial data. This can and should be done throughout the process of computational modelling. Ideally models are simulated before any real data is collected so that, for example, the researcher can identify how much data will be needed for reliable parameter estimation and model selection. The method of "parameter recovery" involves simulating data with known parameters and then recovering the parameters by fitting the model to the generated data. If the original and recovered parameters are very different it might be an indication of an underpowered experiment or the use of inappropriate methods. Similarly, "model recovery" can be used to check if the model comparison procedures works as intended given a set of data and models. Data is simulated from one of the models (in turn) and then each model is fitted to the artificial data, and model comparison is used to identify the best fitting model. If the chosen model is different from the model which actually generated the data this again might be an indication of a lack of data, or the choice of an inappropriate model comparison method.

1.1.1 Computational psychiatry

In recent years computational psychiatry has emerged as a subfield of computational neuroscience (Huys, Moutoussis, and Williams, 2011; Montague, Dolan, Friston, and Dayan, 2012; Friston, Stephan, Montague, and Dolan, 2014; Wang and Krystal, 2014; Maia, 2015; Adams, Huys, and Roiser, 2016; Huys, Maia, and Frank, 2016; Stephan, Bach, Fletcher, et al., 2016; Vinogradov, 2017). It embraces the idea of using computational models to advance understanding of mental illness with the goal of improving their prediction and treatment.

Both data-driven (applying machine learning) and theory-driven approaches are used (Huys, Maia, and Frank, 2016). In these thesis I primarily focus on the latter approach and use prior knowledge or hypotheses about possible mechanisms to inform our work although I also explore machine learning (classification) techniques. Computational psychiatry is not restricted to a single level of description and, for example, in this thesis I aim to link (depression-related) behaviour with (abnormal) neuronal function.

Despite the many promises, computational psychiatry has yet to prove itself by changing real clinical practice (Stephan and Mathys, 2014). It has been argued that it is already possible for computational research to have an impact in clinical settings as for example machine learning techniques make it possible to predict diagnosis or treatment outcomes (Steele and Paulus, 2019). However, practical implementation is currently hindered by a lack of routine collection of quantitative data and will require a collective effort from researchers, policy and funding agencies, and practitioners, and a general cultural change (Steele and Paulus, 2019; McGuire, Sato, Mechelli, et al., 2015).

1.2 Functional magnetic resonance imaging

In this thesis I analyse functional magnetic resonance imaging (fMRI) data. The use of fMRI has skyrocketed since its development in the early 1990s because it allows researchers to non-invasively investigate brain activity (Poldrack, Mumford, and Nichols, 2011; see Figure 1.1). More specifically, it measures changes in the blood oxygenation level dependent (BOLD) signal. When neurons become active they need more energy including oxygen which is provided to them through a local increase in blood flow (haemodynamic response). MRI technology depends on the observation that haemoglobin has different magnetic properties depending on how much oxygen it is carrying. An MRI scanner can be used to detect these small changes in the magnetic signal. For more details about the history and physics of (functional) MRI please refer to previous literature such as Poldrack, Mumford, and Nichols (2011) who provide a more detailed overview of the history of fMRI and its relationship to PET imaging and Buxton (2009) who discusses related physical

concepts in details. In this thesis I am primarily concerned with making inferences from fMRI data collected while participants performed a (cognitive) task.

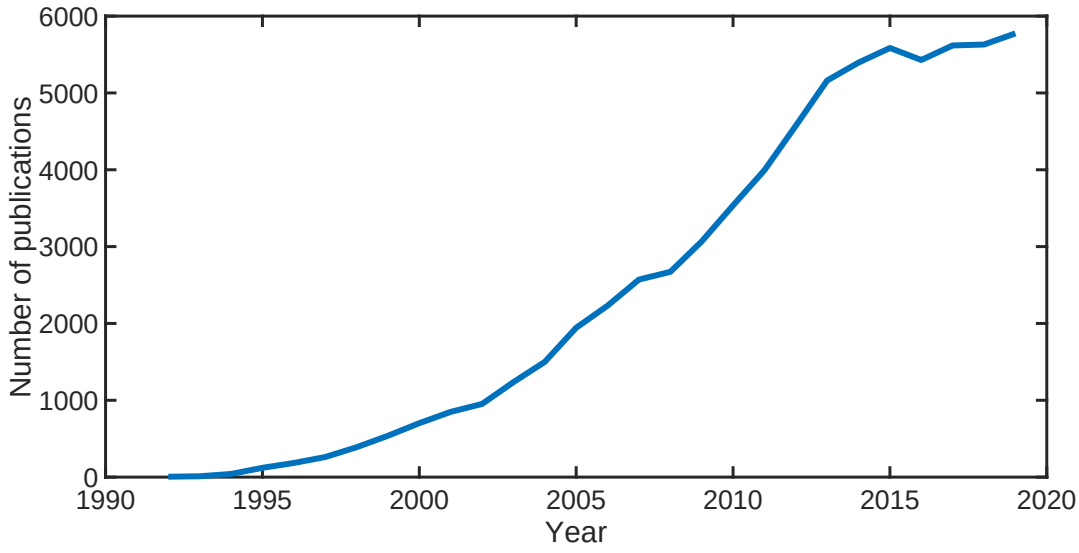

FIGURE 1.1: The number of matches to a PubMed query of `"fMRI"[All Fields] OR "functional MRI"[All Fields] OR "functional magnetic resonance imaging"[All Fields] AND ("YEAR/01/01"[PDAT] : "YEAR/12/31"[PDAT])` for YEAR between 1992 and 2019. This was inspired by Poldrack, Mumford, and Nichols (2011) who showed a similiar plot up to 2010.

While the analysis of fMRI data is complex there are dedicated toolboxes and software packages such as SPM (Friston, Ashburner, Kiebel, et al., 2007; Ashburner, 2012), FSL (Jenkinson, Beckmann, Behrens, et al., 2012) and AFNI (Cox, 1996) available which simplify this task. Analysis usually proceeds in two parts, namely pre-processing and statistical inference, both of which involve a series of steps. For example, pre-processing commonly includes a step in which the individual scans (i.e. the time-series of scans which usually means a whole-brain scan roughly every two seconds) are realigned to account for head movements. The scans of all individuals also need to be anatomically normalised to a standard template brain space so they can be compared and used for group analysis. Spatial smoothing and temporal filtering are used to reduce noise. Visual quality control is routinely used to spot possible artefacts although this becomes impractical with very large sets of data which can, for example, affect machine learning performance (Johnston, Mwangi, Matthews, et al., 2013).

For the statistical modelling a general linear model (GLM) is commonly used. The BOLD signal acts as the dependent variable and a design matrix defines the experimental design with a row for each scan and a column for each explanatory variable such as stimulus timings. The parameters are estimated and used to produce contrast images for each individual; for example to find areas which are more active (compared to an implicit baseline) when a stimulus is shown. These “first level”

images of individuals are then taken to the "second level" to look at overall group activation or to compare different groups. The "significance" of these activations or activation differences can be assessed using t-tests, but given the mass-univariate approach (i.e. one test is run for every single voxel), voxel significance needs to be corrected for multiple comparisons (Nichols, 2012).

In addition to this "model-free" approach I also use a "model-based" approach in this thesis (e.g. see Gläscher and O'Doherty, 2010). Importantly, "model-free" here does not mean the absence of any model (it clearly relies on multiple models, including the GLM), but rather that it is not incorporating a computational model of a cognitive process. In the model-based approach such a model is defined and some aspect of it is incorporated into the GLM. For example, a model about how participants learn about the values of certain stimuli and how they then use these values to make decisions is fitted to their behavioural data. A latent (hidden) variable such as the value of a certain stimulus at each timepoint throughout the experiment is then extracted and included as regressor in the GLM (after convolution with a haemodynamic response function). This allows the researcher to find areas of the brain which are "encoding" this value (i.e. areas with activity which are correlated with the predicted signal).

Lastly, it is worth mentioning "connectivity" in the brain which is increasingly becoming a focus in the field (Kahan and Foltynie, 2013). There are at least three types to distinguish. Structural connectivity refers to the anatomical connections between regions. This type of connectivity is not directly accessible using fMRI, but can be studied using diffusion tensor imaging and it can be used as prior to constrain other types of connectivity (Friston, 2011). Functional connectivity refers to undirected statistical dependencies (correlations) between regions (Kahan and Foltynie, 2013). A high functional connectivity between two regions would mean their BOLD signals show similar fluctuations over the course of an experiment (Kahan and Foltynie, 2013). Effective connectivity goes a step further and its aim is to infer directed influence from one region to another. In this thesis I use the dynamic causal modelling (DCM) framework (Friston, Harrison, and Penny, 2003) to estimate this directed connectivity. Models are built to describe how activity in a region (and external stimuli) might change activity in other regions, then model comparison is used to select the most parsimonious explanation.

1.3 Organisation of this thesis

The aim of this thesis is to use computational modelling and fMRI to investigate the relationship between depression symptoms, (abnormal) behaviour and brain activity and connectivity. This work was done in the context of "reward learning" as there is a large body of evidence suggesting abnormalities are associated with depression. More specifically, I asked whether mood symptoms are associated with

(a) anomalous behaviour, (b) blunted striatal response to reward, (c) value encoding and the use of values during decision making, and (d) a change in the connectivity related to prefrontal cortex regions.

Chapter 2 reviews the literature on depression from a computational perspective. It starts by describing symptoms, diagnosis and statistics of the disorder. Existing theories are introduced, including possible biological underpinnings which also forms the basis of the work in the following chapters. A number of studies using computational approaches are reviewed and a 'case study' is used to give an example of the usefulness of computational models.

Chapters 3 and 4 present the results of an fMRI study involving a group of unmedicated patients suffering from depression and a group of healthy controls. The participants had to estimate the probability that a certain fractal would lead to a rewarding outcome based on a small number of passive fractal-reward association trials. Intermittently, participants had to make an active choice between (the reward probability of) one of the observed fractals and an explicit probability displayed as a (percentage) number.

Chapter 3 describes the behavioural and computational modelling analyses. Patients performed worse than controls and the modelling revealed that this was based on impairments during both the passive observation and the active decision making phases. Specifically, depressed participants displayed lower memory or increased discounting of observed rewards and a decreased ability to use the internal estimations of the reward probabilities to make decisions.

Chapter 4 builds on these results and examines the neuronal basis for the group behavioural differences. Specifically, I used model-based fMRI to look at value encoding and brain activity during decision making and their relationship with depression. Replicating previous studies, we found blunted striatal reward activation in the depressed group. Value encoding was decreased in depression within brain regions including hippocampus and rostral anterior cingulate, regions which have been reported to show reward value encoding in healthy subjects. An anterior mid-cingulate region showed increased activity and decreased (functional) connectivity to rostral cingulate regions in depression. Linking the behavioural model to brain function, this suggests a possible impairment in the communication of value estimates from rostral to dorsal prefrontal regions.

Chapter 5 expands on this hypothesis of abnormal connectivity but uses Dynamic Causal Modelling to also infer the directed effect of one brain region on another. A large community-based sample of participants took part in a reward learning study and computational modelling of behaviour, model-free and model-based fMRI, and DCM were used for analyses. Increased depression symptom severity was associated with decreased medial prefrontal cortex to ventral striatum top-down

effective connectivity. This is consistent with a number of theories (see Chapter 2) positing a role of abnormal cortico-limbic connectivity in depression.

Chapter 6 explores how a combination of data-driven and theory-driven ("generative embedding") approaches might help with the detection of past or present depressive episodes. A machine learning classifier was built to differentiate between never-depressed healthy participants and lifetime depression patients using estimated DCM effective connectivity parameters as input features. A cross-validated balanced accuracy of 72% was achieved.

Chapter 7 discusses and brings together the different strands of research and shows how they integrate into previous research and advance the current understanding of depression. It addresses a number of common limitations within the wider area of computational research on depression. Finally, it discusses unexplored avenues and open questions which will need to be addressed to move research forward in this field.

Chapter 2

Background

This chapter reviews the literature about depressive illness and previous computational approaches towards this devastating disease which inspired the work described in the following chapters. The contents of this chapter will appear in a shorter form as chapter in a textbook: S. Rupprechter, V. Valton, and P. Seriès (2020). "Depressive Disorders from a Computational Perspective". In: *Computational Psychiatry: A Primer*. Ed. by P. Seriès. Cambridge, MA, USA: MIT Press. Chap. 7.

My contributions
A selection of papers to review and the general outline of the textbook chapter were discussed with my coauthors in the beginning. I drafted the first version of the chapter which then went through multiple rounds of editing from all authors. I created Figures 2.1–2.3 and assembled and adapted Figures 2.4 and 2.5 from (Huys, Pizzagalli, Bogdan, and Dayan, 2013). I also wrote the extended version of the chapter for this thesis.

2.1 Depressive disorders

Depression and anxiety disorders are the two most common psychiatric disorders world-wide (Alonso, Angermeyer, Bernert, et al., 2004; Ayuso-Mateos, Vázquez-Barquero, Dowrick, et al., 2001; Üstün, Ayuso-Mateos, Chatterji, et al., 2004; Vos, Flaxman, Naghavi, et al., 2012) and display a high level of co morbidity: patients suffering from one of these illnesses are often affected by the other one as well (Kessler, Berglund, Demler, et al., 2003). In the United States, Kessler, Berglund, Demler, et al. (2003) estimated the lifetime prevalence of major depressive disorder (MDD) at over 16%. Similar figures have been reported for Europe at 13% (Alonso, Angermeyer, Bernert, et al., 2004).

Diagnosis for MDD is commonly based on the Diagnostics and Statistical Manual of mental disorders (DSM-V; American Psychiatric Association, 2013). The manual lists two core symptoms of MDD: depressed mood and loss of interest or pleasure (anhedonia), of which at least one has to be present for diagnosis. Other symptoms

include a significant change in weight, insomnia, hypersomnia, psychomotor agitation or retardation, fatigue or loss of energy, feelings of worthlessness or guilt, a diminished ability to think or concentrate, and recurrent thoughts of death or suicide. Overall, five or more symptoms have to be present for at least two weeks, cause significant impairments in important areas of daily life, and should not be better explained by other psychiatric disorders. The International Classification of Diseases (ICD-10; World Health Organization, 1992) has similar criteria for diagnosis of (single) depressive episodes and recurrent depressive disorder. For research studies, DSM and ICD diagnoses are frequently established using diagnostic systems such as the Structured Clinical Interview for DSM disorders (SCID, First, Spitzer, Gibbon, Williams, et al., 2002 or the Mini International Neuropsychiatric Interview (MINI, Sheehan, Lecrubier, Sheehan, et al., 1998).

Patients often show cognitive deficits on a broad range of tasks probing executive function and memory (Snyder, 2013; Rock, Roiser, Riedel, and Blackwell, 2014), and impairments often remain (to some degree) after remission (Rock, Roiser, Riedel, and Blackwell, 2014). Rock and colleagues argue that cognitive impairments should be viewed as core features of depression rather than secondary symptoms.

Strikingly, according to the DSM definition, it is possible (in theory; although unlikely in clinical practice) for two people to receive the same diagnosis of MDD without sharing a single symptom. One MDD patient may experience depressed mood, weight gain, constant tiredness and fatigue, and regularly think about ending their life. Another MDD patient may experience anhedonia, lose a lot of weight, and go through psychomotor and concentration difficulties while being unable to sleep properly. The existence of these non-overlapping profiles partly stems from the fact that categories and symptoms of depression originated from clinical consensus and do not necessarily have a basis in biology (Insel, Cuthbert, Garvey, et al., 2010; Fried, Nesse, Zivin, et al., 2014).

As a consequence, some research has started to focus on individual symptoms—for example anhedonia (Pizzagalli, 2014; see also the case study in Section 2.3)—in addition to categorical group differences. In the clinical and drug trial literature, Hamilton Depression Rating (HRSD-17) and Montgomery-Åsberg Depression Rating Scale (MADRS) are two of the most popular rating scales. In research environments, the Beck depression inventory (BDI; Beck, Ward, Mendelson, et al., 1961) is also a popular choice to measure overall depressive severity and a sub-score can be extracted from items of the questionnaire to quantify anhedonic symptom severity. These questionnaires also allow a dimensional (as opposed to categorical) approach, which is emphasised in current research (see below). Compared to SCID or MINI these dimensional ratings are not diagnostic and, for example, a high anhedonia score does not necessarily indicate depression and could be related to substance use or withdrawal (Destoop, Morrens, Coppens, and Dom, 2019).

Recently, much cognitive research has focused on decreased sensitivity to reward in depression. There are at least two important reasons for this focus: First, reward processing appears to align with a lack of interest or pleasure (anhedonia), a core symptom of depression and one to which we will come back again in the case study section of this chapter. Second, reward processes are arguably better understood than mood processes, both at the neurobiological and at the behavioural level. Indeed, cognitive neuroscience has started to dissociate and delineate different sub-domains of reward processing, which can be studied independently in relation to anhedonia (Treadway and Zald, 2013). For example, "incentive salience" ("desire" or "want") can be distinguished from "motivation" and "hedonic response" (enjoyment) and we may want to independently study the association of each of these sub-domains with depression. For instance, your attention and focus on a piece of chocolate (a potentially rewarding stimulus) is different from how much you enjoy the chocolate while you are eating it. These two subdomains may also be independent from your willingness to expend effort to obtain that piece of chocolate.

Cléry-Melin, Schmidt, Lafargue, et al. (2011) tested depressed patients and healthy controls on a task in which they could exert physical effort (through grip force on a handle) to attain monetary rewards of varying magnitudes. They found that depressed participants did not exert more physical effort to obtain higher rewards (as opposed to lower rewards). However, they believed they had exerted more effort for higher rewards, as evidenced by their higher effort ratings. Controls, on the other hand, objectively exerted more effort for greater rewards, but reported subjectively reduced effort ratings for higher rewards compared to lower rewards. In another study (Treadway, Bossaller, Shelton, and Zald, 2012), participants were able to obtain varying amounts of money if they managed to make a large number of button presses within a short time window. Depressed patients exerted less effort (made less button presses) than controls in order to obtain reward. Together these studies suggest that depression, and anhedonia in particular, may be related to impairments in the motivation and willingness to exert effort for rewards. This may also explain why behavioural activation therapies have been reported to work well for depressed patients: these practices specifically target decreased motivation (Treadway, Bossaller, Shelton, and Zald, 2012). However, how such psychological therapies can be applied successfully in real clinical environments and how effective they are for severe depression is still debated (DeRubeis, Hollon, Amsterdam, et al., 2005; Cuijpers, Straten, Bohlmeijer, et al., 2010; Driessen, Cuijpers, Hollon, and Dekker, 2010).

Some researchers have advocated for a network analysis approach to psychopathology, in which major depression and other psychological disorders are conceptualised as clusters of causally connected symptoms (Borsboom and Cramer, 2013). This drops the assumption that symptoms stem from a single latent cause, but acknowledges that current psychiatric classifications are not arbitrary as they label

groups of symptoms which create "reliable patterns of covariance" (Borsboom and Cramer, 2013).

It is difficult to set a boundary between healthy and pathological mood and indeed it is unclear whether such a boundary exists at all (Ruscio, 2019). There does not appear to be a discontinuity at the MDD diagnostic threshold (i.e. five symptoms) and sub-threshold levels of symptoms can come with noticeable impairment and may predict escalation and relapse (Ruscio, 2019). Currently, however, there is no consensus about how to reconcile this apparent continuum of pathological mood with clinical diagnoses and treatment (Ruscio, 2019).

Recently, the National Institute of Mental Health (NIMH) in the US launched the Research Domain Criteria (RDoC) project to create a framework for research in psychiatry (Insel, Cuthbert, Garvey, et al., 2010). Rather than defining categories of disorders, RDoC uses a dimensional system which recognises the full range of observable behaviour and neurobiological function. It groups research into different domains including positive valence systems, negative valence systems and cognitive systems. Each of these can then be studied using different "units" of analysis, including genes, neural circuits and behaviours. In the future, a practitioner could then supplement a diagnosis of "major depressive episode" with behavioural and neuroimaging data from a reward-based learning task to determine the best treatment (Insel, Cuthbert, Garvey, et al., 2010). However, at least in the near future, RDoC is not expected to replace DSM or ICD, but rather co-exist beside them to guide research while being continually updated and improved (Insel, Cuthbert, Garvey, et al., 2010; Lilienfeld and Treadway, 2016).

2.1.1 Cognitive theories of depression

An early influential theory, inspired by a wealth of animal studies, is that of learned helplessness (Seligman, 1972; Maier and Seligman, 1976; Abramson, Seligman, and Teasdale, 1978). The theory suggests that continued exposure to aversive (stressful) environments over which animals do not have any control lead to behavioural deficits similar to those observed in depression. In such a framework, the patients' distress is believed to stem from their perception of a lack of control over the environment and ensuing rewards or penalties. This, in turn, could explain patients' distress and lack of motivation to initiate actions. Stress has been proposed as a mechanism for memory impairments in depression (Dillon and Pizzagalli, 2018) and Pizzagalli (2014) hypothesised that dysfunctional interactions between stress and the brain reward system can lead to anhedonia.

A complementary and not necessarily alternative influential theory about depression concentrated on "negative biases" involved in the development and maintenance of depression (Beck, 2008), and which led to the emergence of cognitive behavioural therapies (CBT). This line of research hypothesised that negative schemas

about the self, the world, and the future form due to adverse early-life experiences. According to this framework, negative schemas could lead patients to downplay the magnitude of positive events, or attribute negative valence to objectively neutral events. Patients would effectively perceive the world through "dark tainted" glasses.

A recent extension of this cognitive theory suggested that negative biases play a causal role in the development and maintenance of depression (Roiser, Elliott, and Sahakian, 2012): both low-level perceptual and reinforcement biases and high-level cognitive control biases could influence negative schemas. It has also been suggested that common antidepressant medications target the negative, presumably bottom-up perceptual biases rather than targeting mood directly (Harmer, Goodwin, and Cowen, 2009). This would be consistent with observations that while medications typically have an effect at the synapse level within hours, recovery from depression is often more gradual and can take several weeks (Roiser, Elliott, and Sahakian, 2012). In contrast, CBT is proposed to work in a top-down manner, helping to improve and re-learn affective cognitive control, negative schemas and expectations (Roiser, Elliott, and Sahakian, 2012).

An alternative extension of Beck's cognitive theory by Joormann and colleagues emphasised the role of deficits in emotion regulation in depression (Joormann and Vanderlind, 2014; Joormann and Stanton, 2016). Most (first) major depressive episodes follow a significant negative life event, but only few people who live through such events develop the disorder (Joormann and Stanton, 2016). These observations, they argue, point towards the importance of emotional self-regulation in MDD (Joormann and Stanton, 2016) and they refer to a substantial amount of literature showing a distortion of emotion regulation strategies in depression (increased rumination and suppression, decreased distraction and reappraisal). Underlying these emotion regulation difficulties may be biases in attention, interpretation and memory which can all be linked to the emotional response, and deficits in cognitive control, which may hinder an improvement of these strategies (Joormann and Stanton, 2016).

Overall, there is large overlap between the different theories of depression. Most cognitive theories place a large emphasis on biases influencing emotional processing (Gotlib and Joormann, 2010), but some differ in their explanation of the development of these biases; for example whether they develop in response to early stressful life experiences (Beck, 2008; Pizzagalli, 2014) or stem from biased perceptual and reinforcement processes (Roiser, Elliott, and Sahakian, 2012). A lack of control (real or imagined) could contribute to the emergence and maintenance of such biases.

2.1.2 Biological basis for depression

Helen Mayberg was one of the earliest to point out that rather than depression being related to the failure of a single brain region, it is likely to be a system wide disorder affecting multiple regions and the pathways between them (Mayberg, 1997; Mayberg, Lozano, Voon, et al., 2005; Mayberg, 2009). Mayberg and colleagues proposed a circuit model of depression in which regions are grouped into four clusters reflecting impaired dimensions in depression (Mayberg, 2009): Medial prefrontal cortical regions ("mood regulation", active cognitive control, reinforcement, contingencies), dorsal and parietal cortical regions ("exteroception", attention, appraisal, action), ventral limbic regions including subgenual cingulate, anterior insula, hippocampus, and brainstem ("interoception", drive states, autonomic function, circadian rhythms), and other subcortical regions including amygdala, ventral striatum, caudate, thalamus and midbrain / ventral tegmental area ("mood monitoring", novelty, salience, learning, habit).

These regions have been highlighted in a large number of functional imaging studies, and Mayberg focused on the subgenual section of the anterior cingulate, Brodmann area 25, which is interconnected with many of them and had been found to be hyperactive in (treatment resistant) major depression (Mayberg, 2009). This region was the target of a deep brain stimulation trial involving six treatment resistant MDD patients of which four were deemed to show sustained remission (Mayberg, Lozano, Voon, et al., 2005) which led to the initiation of additional stimulation studies (Mayberg, 2009). The trial ultimately did not work as it did not result in statistically significant differences between stimulation and control groups and was halted early (Holtzheimer, Husain, Lisanby, et al., 2017).

Disner, Beevers, Haigh, and Beck (2011) reviewed Beck's cognitive model and proposed an underlying neurobiological system largely consistent with Mayberg's limbic-cortical dysregulation model. Two key processes were identified which initiate and sustain cognitive biases. An impaired bottom-up pathway, involving a hyperactive amygdala, the subgenual cingulate, ACC, striatum (blunted NAc response and abnormal caudate and putamen functioning), and hippocampus ending in the frontal lobe, leads to abnormal responses to emotional stimuli. An impaired top-down pathway, from the PFC through anterior cingulate and thalamus and ending in subcortical regions, is related to diminished cognitive control which allows biases to persist.

Several neurotransmitters, most commonly serotonin and dopamine, are implicated in reward and punishment processing in depression (Eshel and Roiser, 2010). Dopamine is implicated in reinforcement learning processes (Schultz, 2002) and has consistently been associated with depression in humans and animals (Pizzagalli, 2014). Serotonin has long been implicated in the processing of aversive stimuli, response inhibition and learned helplessness and depression may be related to a

failure of stopping such aversive processes (Deakin, 2013). Antidepressant medications have their most obvious effect altering brain serotonin levels (Eshel and Roiser, 2010).

Deakin and Graeff (Deakin and Graeff, 1991; Deakin, 2013) made a number of predictions regarding the involvement of the serotonin system in depressed mood and anxiety. Instead of conceptualizing depression as a serotonin deficit disorder, they proposed an overactive dorsal raphe nucleus (DRN) which would affect amygdala and striatum with overactive projections and an underactive median raphe nucleus with underactive projections to the hippocampus (Johnston, Tolomeo, Gradin, et al., 2015).

Notably, Johnston, Tolomeo, Gradin, et al. (2015) used a combined loss-avoidance and win-gain paradigm and found neuroimaging results consistent with Deakin and Graeff's predictions in treatment resistant depression. DRN and amygdala activity was significantly increased and nucleus accumbens decreased in patients. During loss events, depressed individuals failed to regulate the hippocampus resulting in overactivity and this was also correlated with BDI (depression severity) and HADS-A (anxiety severity) scores.

Dopamine is heavily linked to reward processing and the role of blunted dopamine transmission in depression has received much attention (Pizzagalli, 2014). This could potentially help explain behavioural and neuroimaging reports of abnormal prediction-error based reinforcement learning (Kumar, Waiter, Ahearn, et al., 2008), but direct human evidence of reduced dopamine transmission during reward learning tasks is missing (Pizzagalli, 2014; Dunlop and Nemeroff, 2007). Pizzagalli (2014) hypothesised that stress affects dopamine (reward) pathways which could induce anhedonia leading to depression.

A large number of neuroimaging studies have repeatedly revealed associations between depressive mood and changes in activation of various brain regions (Bartra, McGuire, and Kable, 2013; Zhang, Chang, Guo, et al., 2013; Chase, Kumar, Eickhoff, and Dombrovski, 2015; Keren, O'Callaghan, Vidal-Ribas, et al., 2018). Hyperactivity of the amygdala in response to or anticipation of sad or negative stimuli in MDD has consistently been found, consistent with the conception that the amygdala is part of the emotion generation and regulation system (Joormann and Stanton, 2016). Another part of the emotion generation system is the ventral striatum (Joormann and Stanton, 2016) and multiple studies have shown blunted reward responses in this area (Bartra, McGuire, and Kable, 2013; Keren, O'Callaghan, Vidal-Ribas, et al., 2018; Pizzagalli, 2014).

Reduced activation of other subcortical regions, including caudate, putamen, and thalamus during reward processing in MDD has been reported (Zhang, Chang, Guo, et al., 2013; Bartra, McGuire, and Kable, 2013; Keren, O'Callaghan, Vidal-Ribas,

et al., 2018). Gradin, Kumar, Waiter, et al. (2011) described decreased reward value encoding in the hippocampus in treatment resistant depression.

Prefrontal areas are frequently conceptualised as higher level processing parts, exerting cognitive control and regulating emotions (Joormann and Stanton, 2016). The orbitofrontal cortex (OFC) and ventromedial prefrontal cortex (vmPFC) are implicated in the representation of internal values (Chase, Kumar, Eickhoff, and Dombrovski, 2015). Depression is associated with abnormal activation in these regions (Pizzagalli, 2014; Cléry-Melin, Jollant, and Gorwood, 2018), possibly related to abnormal use of reward values during decision-making (see Chapters 3 and 4).

As described previously, abnormal connectivity between prefrontal cortical and limbic/subcortical areas is assumed to play a major role in the onset and continuation of depression (Mayberg (2009), Joormann and Stanton (2016), Pizzagalli (2014), and Roiser, Elliott, and Sahakian (2012) and see also Chapter 5).

There is some evidence for volume changes in depression in various areas including amygdala, hippocampus, and prefrontal areas (Mayberg, 2009). Particularly noteworthy are large meta-analyses which have concluded that MDD is associated with reduced hippocampal volume (Schmaal, Veltman, Erp, et al., 2016) and alterations in cortical thickness, especially in OFC (Schmaal, Hibar, Sämann, et al., 2017). However, there is considerable variability in findings of changes in volume (Mayberg, 2009), and it is important to note that acute lesions in these areas do not seem to initiate depressive symptoms (Mayberg, 2009).

Genetics and environmental influences likely play important roles in the aetiology of depression (Sullivan, Neale, and Kendler, 2000). A genome-wide association study identified 44 significantly associated genomic regions with depressive symptoms (Wray, Ripke, Mattheisen, et al., 2018) which was increased to approximately 100 loci in a recent follow-up meta-analysis (Howard, Adams, Clarke, et al., 2019). However, effect sizes are small and the explained variance is typically less than 2% (Wray, Ripke, Mattheisen, et al., 2018) which means these effects will likely not be useful for individual patient predictions in the near future (Steele and Paulus, 2019).

2.1.3 Treatment

One of the reasons why advances in this field are desperately needed is because existing treatment options are inadequate for many patients (Taghva, Malone, and Rezai, 2013; Culpepper, 2010).

It has been reported that treatment of depression is ineffective in about half to two thirds of patients (Culpepper, 2013; Cohen and DeRubeis, 2018). Recently, a large study in the United States concluded that only about a third of adults who had been positively screened for depression actually received treatment and only roughly a

third of adults who did receive treatment for depression had screened positive for the disorder (Olfson, Blanco, and Marcus, 2016), revealing the inappropriateness and mismatch between diagnosis and treatment of depression.

The most common treatments are antidepressant medication and psychotherapy (Olfson, Blanco, and Marcus, 2016) and the combination of the two may further enhance recovery (Khan, Faucett, Lichtenberg, et al., 2012). Typical antidepressant classes include selective serotonin reuptake inhibitors (SSRI), selective serotonin-norepinephrine reuptake inhibitors (SNRI), tricyclic antidepressants (TCA), and monoamine oxidase (MAO) inhibitors (Shultz and Malone Jr, 2013). Behavioural therapies typically focus on targeting negative cognitive biases, thoughts and beliefs, to improve emotion regulation (Beck, 2008; Joormann and Stanton, 2016).

Some studies indicate that deep brain stimulation for treatment resistant depression might become a viable therapeutic option, but results are still inconsistent and further work is needed to improve target selection (Taghva, Malone, and Rezai, 2013). Subgenual cingulate (Mayberg, 2009) and ventral striatum are two promising targets, but small changes of the exact location might lead to substantially different outcomes (Taghva, Malone, and Rezai, 2013). Other possible therapies for treatment resistant depression include transcranial magnetic stimulation (TMS) and electroconvulsive therapy (ECT). Advantages of such stimulation techniques in comparison to lesioning procedures (for example, anterior cingulotomy; Steele, Christmas, Eljamel, and Matthews, 2008) include reversibility and the possibility of adjusting features such as the stimulation frequency (Taghva, Malone, and Rezai, 2013), but rely on permanently implanted hardware.

Treatment selection is a difficult problem and there currently is no obvious way to choose a treatment for a particular patient and it can take many months to Find a treatment which works (Steele and Paulus, 2019). It has been suggested that neuroscience techniques could be used to make clinically useful predictions about treatment outcomes without necessarily understanding the underlying nosology or mechanisms (Steele and Paulus, 2019). Recently, the availability of larger and larger amounts of data has enabled machine learning approaches to be used for treatment outcome predictions with some initial success (Chekroud, Zotti, Shehzad, et al., 2016).

2.2 Past and current computational approaches

A variety of different computational approaches, ranging from connectionist and neural networks, to drift diffusion models, reinforcement learning and Bayesian decision theory, have been used to study the behaviour of MDD patients. I will briefly describe some of the findings from each of these approaches as well as more recent models of mood.

2.2.1 Connectionist models

One early approach that has been used to model depression is a connectionist approach, which is inspired by the idea that complex functions can naturally arise from the interaction of simple units ("neurons") in a network.

Siegle, Steinhauer, and Thase (2004) asked groups of depressed and healthy individuals to perform a Stroop colours naming task. In this task, colour words are presented on each trial with different ink colours matching or not matching the word (e.g. the word "red" written in blue ink), and participants have to name the ink colour while refraining from reading the word itself (Figure 2.1). The task is typically used to probe attentional control. Pupil dilation measurements were used as an indicator for cognitive load, because pupils reliably dilate under cognitively demanding conditions (Siegle, Steinhauer, and Thase, 2004). Previous studies had shown impairments within groups of depressed subjects, but the nature of these impairments varied, with patients sometimes showing slower responses and other times increased error rates. Siegle, Steinhauer, and Thase (2004) found similar performance patterns for the two groups, but differences in pupil dilation. Depressed individuals showed decreased pupil dilation, consistent with decreased cognitive control. A neural network was used to identify possible mechanisms that could have resulted in these group differences. The modelling suggested that decreased prefrontal cortex activity could lead to the observed cognitive control differences in this experiment. Such a disruption might also explain attentional deficits commonly observed in depression (Siegle, Steinhauer, and Thase, 2004).

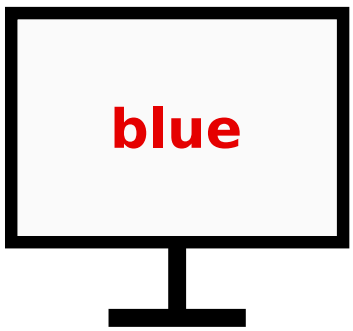

FIGURE 2.1: A sketch of the Stroop colour-naming task, as used by Siegle, Steinhauer, and Thase (2004). Participants had to respond by indicating the colour of the ink of the word (here *red*), while ignoring the written word (here *blue*).

Siegle and Hasselmo (2002) provided another example of how neural network models can be used to better understand deficits in depression during (negatively biased) emotional information processing. The task considered was one where emotional word stimuli were observed, which participants had to label as positive, negative, or neutral. Patients typically show biases in emotional information processing, for example quicker responses to negative information (Siegle and Hasselmo, 2002).

A neural network model was used to simulate classification of emotional stimuli. It could reproduce the typically observed behaviour of depressed patients: it was quicker to identify negative information than positive information and showed larger sustained activity when confronted with negative words. Different mechanisms could lead to these observed abnormalities in the network, including over-learning of negative information, which can be related to rumination, i.e. the tendency to repetitively think about the causes, situational factors, and consequences of one's negative emotional experience. A network that had over-learned on negative information could be retrained using positive information (akin to a cognitive behavioural therapy), which resulted in the normalisation of network activity in response to negative information. The longer the network had "ruminated", the longer it took for the "therapy" (i.e. retraining) to work, providing insights into the recovery from depression using CBT and its interactions with rumination. Siegle and Hasselmo (2002) therefore suggested that rumination can be predictive of treatment response and should be routinely assessed in depressed individuals. Based on Siegle's work, a simulation study looked at the impact of hippocampal atrophy in depression (Gradin and Pomi, 2008). They reported evidence for links between atrophy and both cognitive impairments and the maintenance of depression, consistent with a large meta-analysis which reported reduced hippocampal volume in MDD (Schmaal, Veltman, Erp, et al., 2016).

2.2.2 Drift diffusion models

Drift diffusion models (DDMs) have also been used to better understand the mechanisms underlying depressive illness. These models are especially useful when the modelling of reaction time and accuracy in combination is of primary interest.

For example, Pe, Vandekerckhove, and Kuppens (2013) modelled behaviour on the emotional flanker task to analyse negative biases in depression. In this task, participants are shown a positively or negatively valenced word that they are asked to classify according to valence. The central stimulus is flanked by two additional words with positive, negative or neutral valence (Figure 2.2). The authors hypothesised that higher depressive symptomatology and rumination (as measured by self report questionnaires) are related to negative attentional biases (i.e. a bias towards negative target words). Classical analyses showed that the higher the rumination score, the stronger the facilitation effect (computed from accuracy scores) of negative distracters on negative targets and the weaker the facilitation effect of positive distracters on positive targets. After controlling for depression, only the former effect remained. A DDM analysis on the other hand revealed more effects involving the drift rate, which corresponds to the rate at which information is being processed. The drift rate was negatively correlated with rumination scores on trials where a negative target word was flanked by positive words and was positively correlated with rumination scores on trials where negative words flanked a negative or positive

word. After controlling for depression scores, rumination still predicted attentional bias for negative information, but depression scores were no longer predictive after controlling for rumination. The computational modelling therefore revealed that rumination was associated with an enhanced processing of words flanked by negative words and decreased processing in the presence of positive flankers.

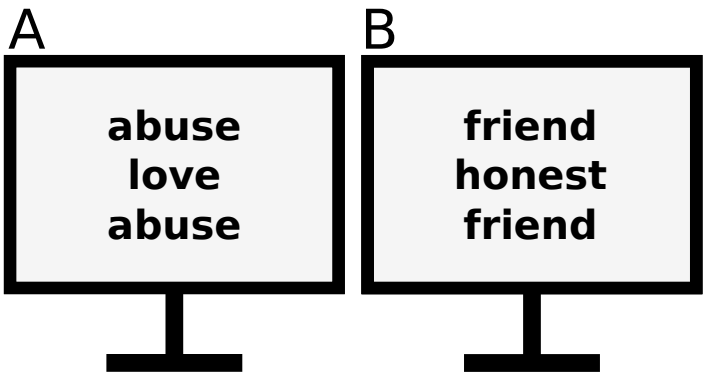

FIGURE 2.2: A sketch of two types of trials of the emotional flanker task, as used by (Pe, Vandekerckhove, and Kuppens, 2013). Participants had to classify the word in the centre according to its valence. (A) An incongruent trial, in which the target word love and the flanking word abuse have differing valence. (B) A congruent trial, in which the valence of the flanking word is the same as the valence of the target. (Note that Dutch, four letters long, monosyllabic words were used by Pe, Vandekerckhove, and Kuppens (2013)).

In addition to negative biases, depression is also associated with impairments in executive function (Snyder, 2013). Dillon, Wiecki, Pechtel, et al. (2015) used a combination of three drift diffusion processes to account for behaviour on a different (non-emotional) version of the flanker task. In this version, stimuli and distracters were three arrows pointing left or right. The central and flanking arrows could either be congruent (pointing in the same direction) or incongruent. Depressed and healthy participants had to indicate the direction of the arrow in the middle. The authors' goal was again to address inconsistent findings of previous studies, which had sometimes found enhanced executive functioning in depression during tasks that demand careful thought. Depression can lead to increased analytical information processing (c.f. rumination), which results in worse performance during tasks requiring fast decisions, but can also lead to increased accuracy when careful approach is necessitated and reflexive responses need to be inhibited. Dillon, Wiecki, Pechtel, et al. (2015) found that depressed participants were more accurate but slower than controls on incongruent trials. They decomposed behaviour on the flanker task into three different mechanisms that might be affected by depression, and which were modelled by separate drift diffusion processes: (1) a reflexive mechanism biased to respond according to the flankers, (2) a response inhibition mechanism able to suppress the reflexive response, and (3) executive control responsible for correct responses in the presence of incongruent flankers.

The analysis of model parameters showed that the drift rate for the executive control mechanism was lower in depression, which on its own would lead to slower, but also less accurate responses. However, this executive control deficit was offset by an additional decreased drift rate in the reflexive mechanism. This could explain impaired executive function but highly accurate responses in MDD (Dillon, Wiecki, Pechtel, et al., 2015).

One more example comes from Vallesi, Canalaz, Balestrieri, and Brambilla (2015), who used DDMs to better understand deficits in the regulation of speed-accuracy trade-offs in depression. At the beginning of each trial, a cue signalled whether participants should focus on speed or accuracy. It was found that MDD patients, unlike controls, adjusted their decision threshold based on the instructions for the previous trial, with speed instructions decreasing the decision boundary (independently of the cue for the current trial). That is, patients had difficulties overcoming instructions from the previous trial and flexibly switching between fast and accurate decision-making. In addition, drift rates within the patient group were generally lower than in the control group, indicating a slowing down of cognitive processing, which is commonly found in MDD patients.

2.2.3 Reinforcement learning models

In reinforcement learning models, behaviour is captured on a trial-by-trial basis. An agent makes a decision based on some internal valuation of the objects in the environment, observes an outcome, and then uses this outcome to update the internal values. There exists substantial behavioural and neural evidence, often supported by computational modelling, for impaired reinforcement learning during depression (see Chen, Takahashi, Nakagawa, et al., 2015 for a review).

Chase, Frank, Michael, et al. (2010) fitted a Q-learning model to the behaviour of MDD patients and healthy controls on a probabilistic selection task. On each trial, one of three possible stimulus pairs was displayed and participants had to choose one of the stimuli, which were followed by positive or negative feedback according to different probabilities. They did not find evidence for their initial hypothesis that patients would preferentially learn from negative outcomes due to a tendency in depression to focus on negative events. Participants' anhedonia scores, however, negatively correlated with positive and negative learning rate as well as the exploration-exploitation (softmax) parameter. The study therefore provided evidence that depression, and specifically anhedonia, is related to altered reinforcement learning. Huys, Pizzagalli, Bogdan, and Dayan (2013) performed a meta-analysis on the Signal Detection Task (Pizzagalli, Jahn, and O'Shea, 2005). In contrast to the previous study, they concluded that anhedonia is principally associated with blunted sensitivity to reward as opposed to an impaired ability to learn from experienced rewards. The task and their approach is covered in more detail in the case study section below.

Temporal difference (TD) prediction-error learning signals have been linked to the firing of dopamine neurons in the brain (Montague, Dayan, and Sejnowski, 1996; Schultz, 1998; Schultz, 2002; O'Doherty, Dayan, Schultz, et al., 2004) and there exists substantial evidence that these neurons play an important part in the experience of pleasure and reward (Dunlop and Nemeroff, 2007). Using fMRI and a Pavlovian reward-learning task, Kumar, Waiter, Ahearn, et al. (2008) investigated whether TD learning signals would be reduced in MDD patients. The authors indeed found blunted reward prediction error signals in the patient group and additionally a correlation between such blunting and illness severity ratings. This provides a link between an impaired physiological TD learning mechanism and reduced reward learning behaviour as observed in anhedonia.

The previous study by Kumar, Waiter, Ahearn, et al. (2008) investigated Pavlovian learning during which participants passively observed stimulus-outcome associations. An early study to look at instrumental learning through active decision-making in depression was performed by Gradin, Kumar, Waiter, et al. (2011). Stimuli were associated with different reward probabilities, which slowly changed. Prediction errors and expected values of a Q-learning model were regressed against fMRI brain activity. Compared to healthy controls, depressed patients did not display behavioural differences. However, physiologically they showed reduced expected reward signals as well as blunted prediction error encoding in dopamine-rich areas of the brain. This blunting correlated with anhedonia scores. This shows that model-based fMRI can reveal differences in reward learning; even in the absence of behavioural effects.

2.2.4 Bayesian decision theory

At a more abstract level, Bayesian decision theory (BDT) has been used to explain common symptoms of depression such as anhedonia, helplessness and pessimism (Huys, Vogelstein, Dayan, and Bottou, 2008; Trimmer, Higginson, Fawcett, et al., 2015; Huys, Daw, and Dayan, 2015). Bayesian decision theory allows formulation of optimal behaviour during a task and then analysis of how sub-optimal behaviour can arise.

Huys, Vogelstein, Dayan, and Bottou (2008) fitted a Bayesian reinforcement learning model to the behaviour of depressed and healthy participants in two reward learning tasks. Importantly, their formulation of the model included two parameters, describing sensitivity to reward and a prior belief about control (cf. helplessness). Higher values of the control parameter corresponded to stronger beliefs about the predictability of outcomes following an action. Individuals who believe they have a lot of control over their environment would predict that previously rewarded actions will likely be rewarded again, while someone with a low control prior would expect weaker associations between action and reward. Huys, Vogelstein, Dayan, and Bottou (2008) then showed how a linear classifier could be used to distinguish

between healthy and depressed participants after they had played a slot machine game, based purely on the two values of individuals' parameters. This suggests that model parameters obtained by fitting a behavioural task, such as a probabilistic learning task, could be used to classify MDD to a high accuracy. The objective classification of illness is an important goal of computational psychiatry (Stephan and Mathys, 2014).

A comprehensive evaluation framework formulated through BDT was introduced by Huys, Daw, and Dayan (2015), in which they discuss how depressive symptoms can arise from impairments in utility evaluation and prior beliefs about (the control over) outcomes. They theorised that it is primarily model-based reinforcement learning, rather than model-free learning, which is abnormal in depression.

A theoretical description of how optimal decision-making can lead to (seemingly) depressed behaviour and inaction similar to learned-helplessness in a probabilistic environment can also be found in (Trimmer, Higginson, Fawcett, et al., 2015). They concluded that to understand a patient's current depressed behaviour, the history of the individual should be considered by describing it much further back in the past than what is the current norm. Imagine, for example, that Bob gets fired from his job due to "corporate restructuring" due to an economic crisis. Further, no other company seems interested in hiring while the economy is in this downswing, which is unlikely to change for the foreseeable future. Best efforts and repeated attempts to get a new job fail and adverse events in the environment increase (e.g. he loses friends or family or becomes homeless). Bob starts to learn that his actions do not seem to influence his environment. Negative outcomes appear unavoidable and over time his willingness to try to escape his situation decreases. Distressed and desperate, Bob starts to show symptoms reminiscent of depression. He has "learned to be helpless".

2.2.5 A model of momentary happiness

Rutledge, Skandali, Dayan, and Dolan (2014) developed a computational model to describe healthy participants' "momentary happiness" during a decision-making task including gain and loss components. Subjects repeatedly chose between a fixed option which would always result in the indicated outcome and a risky option which would yield one of two possible indicated outcomes with equal probabilities. After every two to three trials, participants were asked to rate their current happiness on a sliding scale. Overall earnings increased over the course of the experiment but overall happiness did not change although trial-by-trial variance was observed. The computational model which best described the variation in happiness over time indicated that momentary happiness was best described as a function of recent reward expectations and prediction errors, rather than simply as a function of recent rewards.

The model has been applied multiple times and it has been shown that activity in the ventral striatum is correlated with future happiness ratings and that fluctuations in momentary happiness can reliably be related to expectations, rewards and RPEs in a quantitative fashion (Rutledge, Skandali, Dayan, and Dolan, 2014; Rutledge, Skandali, Dayan, and Dolan, 2015; Rutledge, De Berker, Espenhahn, et al., 2016; Eldar, Rutledge, Dolan, and Niv, 2016).

Based on previous studies (c.f. Sections 2.1.2-2.2.3) linking depression to altered reward prediction errors and dopamine function, the same computational happiness model was used in an fMRI study as well as a large smartphone-based study both including MDD subjects and healthy controls (Rutledge, Moutoussis, Smittenaar, et al., 2017). Depression did not reduce the emotional impact of RPEs on happiness, but the estimated base happiness was significantly negatively associated with severity of depression symptoms. In contrast to earlier studies (Kumar, Waiter, Ahearn, et al., 2008; Gradin, Kumar, Waiter, et al., 2011), RPE signals in the ventral striatum were not significantly different between groups. Rutledge, Moutoussis, Smittenaar, et al. (2017) concluded that the underlying dopaminergic system responsible for producing RPEs (Rutledge, Skandali, Dayan, and Dolan, 2015) is likely intact in depression and previous results (Pizzagalli, Holmes, Dillon, et al., 2009; Kumar, Waiter, Ahearn, et al., 2008; Gradin, Kumar, Waiter, et al., 2011; Robinson, Cools, Carlisi, et al., 2012) may reflect other downstream changes in the brain's reward learning system (e.g. see Kumar, Goer, Murray, et al., 2018). This also supports the previously mentioned idea that depression is primarily characterised by altered goal-directed decision-making and model-based reasoning (Huys, Daw, and Dayan, 2015). Importantly, there was no learning and no ambiguity involved in the task used by Rutledge, Skandali, Dayan, and Dolan (2014) and Rutledge, Moutoussis, Smittenaar, et al. (2017), and altered ventral striatal signals from previous studies may be related to an impairment in the model-based system active during reinforcement learning. While the computation of the (dopaminergic) prediction error may not fundamentally be affected in depression, the inputs to the computation might be different in depression (see also the concept of *reward sensitivity* in the case study described in Section 2.3), especially when task and environment are complex. Depression is associated with learning abnormalities, especially in rewarding contexts, and the disorder might be related to difficulties in estimating or keeping track of uncertainty (Pulcu and Browning, 2019).

The precise mathematical description of the generative process which results in (a change in) happiness ratings has the advantage of showing exactly what is formally described in the model. For example, as pointed out by Pulcu and Browning (2017), a possible influence of (negative) self-appraisal is not considered. It also becomes clear from the model that it can only describe momentary changes in emotional state, but not long-term changes in mood which will be important to consider when studying depression. Repeatedly asking participants how they feel during a task

may also result in "demand effects" as they might believe they should report higher happiness after a win (Pulcu and Browning, 2017). It is perhaps a bit surprising that small unexpected rewards or losses could repeatedly change subjects' emotional state from "very unhappy" to "very happy" and back within minutes. These considerations might also help explain the fact that although participants reported variations in momentary happiness, their overall mood did not change between start and end of the experiment. The monetary compensation earned throughout the task did not appear to change overall happiness at all. It is worth noting that in a study involving successful mood induction (Vinckier, Rigoux, Oudiette, and Pessiglione, 2018) the model best describing mood variation did not include expected value or RPEs but only the effect of (positive and negative) feedback. Nevertheless, the computational approach of describing momentary changes in happiness is promising and has been shown to work well within both healthy and ill participants (Rutledge, Skandali, Dayan, and Dolan, 2014; Rutledge, Moutoussis, Smittenaar, et al., 2017). It is now necessary to look at longer time-scales (i.e. long-term mood rather than momentary happiness) and study how variations in mood can be related to major depression (see Eldar, Roth, Dayan, and Dolan, 2018 for initial work looking at mood variation within healthy participants during a period of seven days).

In this thesis I assume that the mood of participants remains essentially stable over the course of the experiments. More specifically, I assume that any small variation in the mood of a participant would not change their depression severity rating. In the study described in Chapters 3 and 4 participants were not shown the potentially rewarding outcomes after their choices so (the lack of) feedback should not have influenced their momentary mood. More interestingly, in Chapter 5 I describe a study in which participants did receive rewards (in the form of points) depending on their choices and the study also included an element of (lack of) control. Although it is possible that their momentary happiness changed following the outcomes and their corresponding prediction errors, we assumed that any such variation would not (systematically) change their self-reported depression severity ratings.

2.3 A case study: How does reward learning relate to anhedonia?

This section will provide a "case study" of the use of computational modelling in depression: a meta-analysis published by Huys, Pizzagalli, Bogdan, and Dayan (2013) of a behavioural task that has consistently revealed reward-learning impairments in depressed and anhedonic individuals and other closely related groups.

Anhedonia is a core symptom of depression. Different behavioural tasks have been used to show that reward feedback objectively has less impact on participants who subjectively report anhedonia (Huys, Pizzagalli, Bogdan, and Dayan, 2013). However, there are different ways through which such a relationship could be realised.

The goal of the meta-analysis was to find out whether anhedonia was principally associated with the initial rewarding experience of stimuli, or the subsequent learning from these rewards. The two mechanisms are important to disentangle, as they would likely correspond to distinct aetiologies and different strategies for therapies (Huys, Pizzagalli, Bogdan, and Dayan, 2013).

2.3.1 Signal detection task

The Signal Detection Task (see Figure 2.3) consists of many (often 300) trials. In each trial one of two possible stimulus pictures (cartoon faces) is shown and the participant is prompted to indicate which picture was observed. This can be quite difficult, because the stimuli look very similar—they only differ slightly in the length of their mouth—and are only displayed for a fraction of a second. If participants correctly identify a stimulus, they sometimes receive a reward (e.g. in the form of points) and sometimes receive no feedback. Participants are told to maximize their reward.

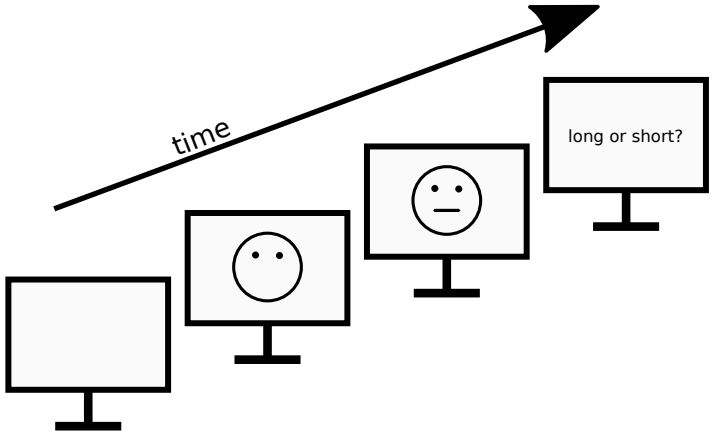

FIGURE 2.3: A sketch of the signal detection task (Huys, Pizzagalli, Bogdan, and Dayan, 2013). On each trial participants observe one of two possible cartoon faces which only differ slightly in the lengths of their mouths. They have to indicate which face they observed. The reward structure is asymmetrical with one of the stimuli being rewarded more frequently than the alternative.

The most important aspect of the task is the asymmetrical reward structure. Unbeknownst to participants, one of the stimuli (called the “rich” stimulus) is followed by reward approximately three times as often as the alternative “lean” stimulus. If participants are not certain about the stimulus, they can incorporate knowledge about their reward history into their decision and choose the rich stimulus so as to maximize their chances to accumulate rewards. Healthy individuals have consistently shown to develop a response bias towards the rich option (Huys, Pizzagalli, Bogdan, and Dayan, 2013).

Using the Signal Detection Task, Pizzagalli, Jahn, and O'Shea (2005) found a reduced ability in (healthy) participants with high depression (BDI) scores to adjust their behaviour based on their reward history, while low BDI participants developed a stronger response bias towards the rich stimulus. Similarly, worse performance has been observed in MDD patients (Pizzagalli, Iosifescu, Hallett, et al., 2008), stressed individuals (Bogdan and Pizzagalli, 2006), euthymic (i.e. neutral mood) bipolar outpatients (Pizzagalli, Goetz, Ostacher, et al., 2008), as well as volunteers receiving medication (Pizzagalli, Evins, Schetter, et al., 2008), and even healthy participants with a history of MDD (Dutra, Brooks, Lempert, et al., 2009; Pechtel, Dutra, Goetz, and Pizzagalli, 2013).

These studies used signal detection theory and summary statistics from raw behaviour to analyse the data. Huys, Pizzagalli, Bogdan, and Dayan (2013) extended this by using trial-by-trial reinforcement learning (RL) modelling to better understand the evolution of the behaviour through time, and get to a finer granularity in the analysis of the behaviour.

While anhedonia has been associated with a diminished ability to use rewards to guide decision-making (such as in studies listed above), there exist varied possibilities for this impairment. Of primary interest in this case study was the distinction between the primary reward sensitivity, the immediately experienced consummatory pleasure following reward, and the learning from reward. Huys, Pizzagalli, Bogdan, and Dayan (2013) included these two factors as parameters into a reinforcement learning model. Figure 2.4 shows how changes in either reward sensitivity (ρ) or learning rate (ε) could lead to the empirically observed changes in response bias.

2.3.2 A basic RL model

A standard Q-learning update rule incorporates learning rate in the following way:

$$Q_{t+1}(a_t, s_t) = Q_t(a_t, s_t) + \varepsilon \times \delta_t \tag{2.1}$$

where s_t is the displayed stimulus on trial t, a_t is the action on trial t (i.e. which button was pressed), $Q_t(a_t, s_t)$ denotes the internal value assigned to the stimulus action pair (a_t, s_t) at trial t, $r \in 0, 1$ is the observed outcome, and $\delta_t = \rho r - Q_t(a_t, s_t)$ is the prediction error. Note that Huys, Pizzagalli, Bogdan, and Dayan (2013) included a reward sensitivity parameter ρ that scales the true value of the reward. A lowering of the learning rate ε increases the time needed to learn about the stimulus-action pairs, while a lowering of the reward sensitivity ρ alters the asymptotic (average) values of Q that are associated with each pair.

In addition, Huys, Pizzagalli, Bogdan, and Dayan (2013) included a term, $\gamma I(a_t, s_t)$, encoding participants' ability to follow the task instructions (i.e. press one key for the short mouth stimulus, and the other key for the long mouth stimulus), where:

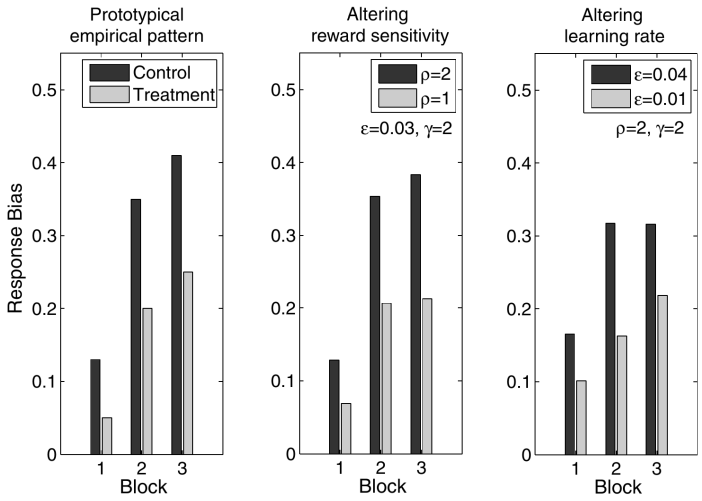

FIGURE 2.4: Modeling the signal detection task. Response bias on simulated data (adapted from Huys, Pizzagalli, Bogdan, and Dayan (2013)). Three blocks of 100 trials were simulated and the development of the response bias is shown across these blocks in each bar chart. On the left, a typical pattern of group differences is shown, with controls developing a strong response bias over the three blocks, and patients showing a reduced bias. The middle chart shows how a reduced reward sensitivity (ρ) could lead to these observed differences. The right chart shows how a reduced learning rate (ε) could also lead to similar differences.

$I(a_t, s_t) = 1$ if stimulus s_t required action a_t, and

$I(a_t, s_t) = 0$ if action a_t is the wrong response to stimulus s_t.

Higher values for the parameter γ indicate a better ability to follow instructions and will result in generally higher accuracy. The two terms for I and Q were added together to form a "weight" for a particular stimulus-action pair (on trial t):

$$W_t(a_t, s_t) = \gamma I(a_t, s_t) + Q_t(a_t, s_t) \tag{2.2}$$

These weights are related to the probability of choosing action a when stimulus s was presented. From the above equation we can see that the probability of choosing an action does not only depend on following the task instructions (I), but also on the internal value based on previous experience (Q). Huys, Pizzagalli, Bogdan, and Dayan (2013) used the popular softmax decision function to map these weights to action probabilities:

$$p(a|s_t) = \frac{1}{1 + \exp(-(W_t(a_t, s_t) - W_t(\bar{a}_t, s_t)))} \tag{2.3}$$

$W_t(\bar{a}_t, s_t)$ is the weight associated with choosing the wrong action for stimulus s at trial t. The softmax gives the probability that individuals choose the correct action

given a certain stimulus. While individuals' parameters are not directly accessible, it is possible to infer them by fitting the model to their sequence of actions, i.e. by finding parameters that maximize the probability that the model would produce a similar sequence of actions when presented with the same sequence of stimuli.

2.3.3 Including uncertainty in the model

The above model ignores one central aspect of the Signal Detection Task: stimuli are only displayed very briefly and so participants can never be certain about which of the two stimuli they actually observed. To account for perceptual uncertainty about the stimulus, Huys, Pizzagalli, Bogdan, and Dayan (2013) expanded the model to assume that when participants compute their internal weights that guide their decision, they incorporate the possibility for both stimuli to have been presented. This leads to an updated equation for the weights, which now includes a term for stimulus s as well as a term for the alternative stimulus s:

$$W_t(a_t, s_t) = \gamma I(a_t, s_t) + \zeta Q_t(a_t, s_t) + (1 - \zeta) Q_t(a_t, \bar{s}_t) \tag{2.4}$$

Huys, Pizzagalli, Bogdan, and Dayan (2013) used the parameter ζ to capture the average certainty (i.e. their belief) about which stimulus they actually observed, and called this model "Belief".

2.3.4 Testing more hypotheses

Reinforcement learning models can be used to describe specific hypotheses about the behaviour of participants while performing the task. Model comparison then allows one to find the model that "best fits" the data, by which is generally meant that the model is neither too simplistic nor too complex and can explain how the data was generated. Usually, model comparison is used to test different hypotheses, heuristics, or strategies that participants may employ to solve the task. One other such hypothesis about performance in the Signal Detection Task is that participants could feel as if they are being punished when they do not receive a reward on a given trial. In the models described above, the reward r was coded as 1 or 0 (presence or absence of reward). Huys, Pizzagalli, Bogdan, and Dayan (2013) changed the model to test the possibility that participants would perceive a lack of reward as punishment by including a punishment sensitivity parameter ρ^-. The prediction error term therefore becomes

$$\delta_t = \rho r_t + \rho^-(1 - r_t) - Q_t(a_t, s_t) \tag{2.5}$$

A final possibility is that participants might completely ignore the stimuli and only focus on the values of actions. Huys, Pizzagalli, Bogdan, and Dayan (2013)

formalised an "Action" model by setting the ζ parameter of the model "Belief" (in Eq. 2.4) to 0.5, which results in the weights equation randomly. Huys, Pizzagalli, Bogdan, and Dayan (2013) then attempted to relate the estimated model parameters to measures of depressive symptoms severity, and in particular to anhedonia. The authors used the anhedonic depression (AD) questionnaire and an anhedonia sub-score from the BDI. They performed a correlation analysis to investigate whether primary reward sensitivity (ρ) or learning (ε) was most associated with anhedonia (Figure 2.5B). They found a negative correlation between ρ and AD, but no significant correlation between ε and AD. This suggested that reward sensitivity rather than learning rate is primarily impaired in anhedonic depression.

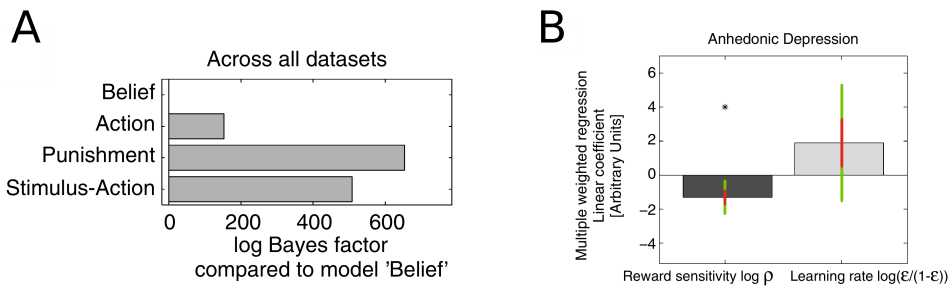

FIGURE 2.5: Results of the signal detection task (adapted from Huys, Pizzagalli, Bogdan, and Dayan (2013)). (A) Results of the model comparison. Compared to the three alternative models, the model "Belief" was shown to be the most parsimonious explanation for the data. (B) Linear correlation coefficients between anhedonic depression and reward sensitivity (left; significant at $p < .05$) and learning rate (right; not significant) parameters. (See Huys, Pizzagalli, Bogdan, and Dayan (2013) for details on this hierarchical regression analysis.)

2.3.5 Limitations

There are limitations to these results. For example, Huys, Pizzagalli, Bogdan, and Dayan (2013) found that reward sensitivity and learning rate were strongly negatively correlated, meaning changes in one of the parameters could be compensated by changes in the other parameter. The authors addressed this by showing that the relationship between AD and reward sensitivity (but not learning rate) remained significant in the majority of simulated data-sets (i.e. choices simulated using the estimated parameters). In addition, they reported that the significant correlation remained after orthogonalising reward sensitivity parameter with respect to the learning rate parameter. Nevertheless, the two parameter can, at least to some extent, explain similar features of the data, and future work will need to address this using a different tasks. Huys, Pizzagalli, Bogdan, and Dayan, 2013 did not provide exact details of some of the estimated statistics such as the estimated linear coefficients and their scales of the hierarchical regression model. It is possible that a slight increase in power would have led to an additional positive association of AD with learning rate (c.f. Figure 2.5).

Additionally, the reward sensitivity parameter could not be distinguished from a temperature parameter typically included in the softmax decision rule. Indeed, in the formulation of the model these two parameters could be substituted for each other exactly. This means that differences in the reward sensitivity parameter might have masked differences in the exploration-exploitation behaviour of participants.

Huys, Pizzagalli, Bogdan, and Dayan, 2013 found a negative correlation between ρ and anhedonic depression but no significant correlations between ρ and BDI anhedonia subscore. This is surprising given the strong correlation between the two questionnaires and further increases the difficulty of interpreting the presence or absence of associations between (correlated) questionnaire scores and (correlated) model parameters. More work is required to pinpoint which depression and anhedonia symptoms are related to a difference in reward sensitivity and in which contexts this association is important. Notably, when individual data-sets of this meta-analysis were analysed separately it was shown that neither model parameter categorically separated any of the groups (such as MDD patients from healthy controls; Huys, Pizzagalli, Bogdan, and Dayan, 2013).

One aspect of reward processing that the study did not explore is effort, which is a large part of everyday decision making. Because in the signal detection task participants always have to exert the same amount of effort (a button press) independent of the stimulus they chose, it was not possible to address this here.

2.4 Discussion

Depression is a devastating disease with a major societal impact and rising prevalence (Vos, Flaxman, Naghavi, et al., 2012), which make it an important area of study. Due to unclear boundaries between categorical definitions of psychiatric disorders, current research often focuses on dimensional measures such as neuroticism or depression symptoms such as anhedonia, both of which have been identified as promising endophenotypes of depression (Pizzagalli, 2014). However, it has been noted that anhedonia itself encompasses various subdomains (e.g. hedonic response to pleasurable stimuli, but also motivation to pursue such stimuli) and these also need to be teased apart (Treadway and Zald, 2013).

Patients suffering from depression routinely display impairments in a range of different experimental paradigms (Snyder (2013), Rock, Roiser, Riedel, and Blackwell (2014), and Chen, Takahashi, Nakagawa, et al. (2015) and see also Chapter 3). Different computational tools and techniques (connectionist models, diffusion models, reinforcement learning techniques, Bayesian decision theory) have been used to describe this (abnormal) behaviour and brain activity in depression, to gain insight into cognitive and neural processes, and to make predictions.

An important aim for computational psychiatry is the development of computational assays that can be used to separate patients into subgroups, generate treatment recommendations, and make predictions for the outcome of those treatments (Stephan, Bach, Fletcher, et al., 2016; Stephan and Mathys, 2014; Chekroud, Zotti, Shehzad, et al., 2016). As Huys, Maia, and Frank (2016) put it, "Aspects of decision-making that have predictive value may become useful for the guidance of treatment or for alternative (and complementary) classifications of psychiatric disorders and individual patients." Reinforcement learning has been described as especially promising in this regard (Hitchcock, Radulescu, Niv, and Sims, 2017) and has indeed shown potential for classification of depression from purely behavioural data without the need for (subjective) questionnaires (Huys, Vogelstein, Dayan, and Bottou, 2008).

Commonly observed pessimistic cognitive biases and thoughts in depression have been explained using prior beliefs within the framework of Bayesian decision theory (Huys, Daw, and Dayan, 2015; Stankevicius, Huys, Kalra, and Seriès, 2014). Simulations of neural network models have shown that biases could arise from a combination of different mechanisms including over-learning of negative information and rumination (Siegle and Hasselmo, 2002). Drift diffusion models have been used to explain how aberrant behaviour relates to executive control deficits (Dillon, Wiecki, Pechtel, et al., 2015; Vallesi, Canalaz, Balestrieri, and Brambilla, 2015) and rumination (Pe, Vandekerckhove, and Kuppens, 2013).

RL models in which behaviour is fitted on a trial-by-trial basis make it possible to measure group differences in behaviour that are not obvious from raw data. The described case study (Huys, Pizzagalli, Bogdan, and Dayan, 2013) pooled data from various studies using the same experimental paradigm and fitted different reinforcement learning models according to hypotheses of the behaviour of participants. The goal was to better understand anhedonia and how it is related to aberrant reward processing. Results indicated that the symptom is primarily associated with the initial experience of reward, rather than the reward learning mechanism.

At a neuronal level, there is substantial evidence that dopamine neuron activity encodes reward prediction errors (among other things; Schultz, 1998; Iglesias, Tomiello, Schneebeli, and Stephan, 2017). Work by Kumar, Waiter, Ahearn, et al. (2008) and Gradin, Kumar, Waiter, et al. (2011) revealed that in depression prediction error signals appear reduced in the striatum and other dopamine rich regions of the brain, suggesting that symptoms of depression are associated with an abnormal encoding of reward learning signals.

It is worth noting that in the meta-analysis of Huys, Pizzagalli, Bogdan, and Dayan (2013), the authors found the two parameters of interest (reward sensitivity and learning rate) to be highly negatively correlated. Small changes in one of the parameters could therefore be compensated by changes in the other parameter, and

Huys, Pizzagalli, Bogdan, and Dayan (2013) had to perform additional analyses in order to increase their confidence in the fitted parameter values. The authors used the popular softmax function to model decision probabilities, but decided against adding a temperature (or exploration-exploitation) parameter, because it would have traded off against the important reward sensitivity parameter. Changes in one of these parameters could have been compensated by changes in the other parameter. The larger question here is how to reliably distinguish between parameters. At least some computational variables are thought to be encoded in the brain (Iglesias, Tomiello, Schneebeli, and Stephan, 2017), for example dopamine neurons' activity is believed to encode prediction errors. However, to discover these biological correlates we need reliable estimates that are not confounded by other parameters. The signal detection task was not initially designed with RL modelling in mind for example, and one could think about running a subtask to isolate exploration-exploitation behaviour and estimate the temperature parameter independently. Replication of results, especially involving a larger number of participants, will also be important before useful computational assays can be developed. Paulus, Huys, and Maia (2016) proposed a pipeline, consisting of phases analogous to generic drug development stages, which will allow computational psychiatry to translate findings from neuroscience into clinical practice.

Current research has often focused on reward. While the omission of a reward might be felt as punishment by participants (as was assumed by Huys, Pizzagalli, Bogdan, and Dayan, 2013), Chen, Takahashi, Nakagawa, et al. (2015) point out that reward and punishment processing involve different neural bases. They hypothesise that depression might be characterised by a gain-loss asymmetry, so that patients experience decreased reward sensitivity but increased punishment sensitivity (see also Johnston, Tolomeo, Gradin, et al., 2015). As mentioned above, reward processing can also further be sub-divided into different domains. The association between anhedonia and the motivation to exert effort could not be addressed in our case study. In natural settings, patients weigh the pros (reward outcome) against the cons (effort required) to make a decision (cost-benefit analysis). Therefore, when an individual displays an abnormally large effort sensitivity, perceiving efforts as more effortful than they objectively are, they may decide against engaging in a potentially rewarding activity. The effort cost might be perceived as outweighing the potential reward outcome. This is also related to what is observed in Parkinsons' patients who display high levels of apathy (a symptom akin to anhedonia; Husain and Roiser, 2018). In the future, scientists may want to design tasks that enable them to test hypotheses about different reward learning domains such as effort sensitivity and reward sensitivity.

While much research points towards behavioural deficits of patients suffering from MDD, there is also evidence for improved performance in depression (Beevers, Worthy, Gorlick, et al., 2013). Replications and robust (computational) techniques will

be needed to pinpoint exactly when impairments occur and how they relate to aberrant brain activity. Memory impairments are common in depression (Rock, Roiser, Riedel, and Blackwell, 2014; Snyder, 2013), but computationally they seem as of yet still largely unexplored. Notably, Dombrovski, Clark, Siegle, et al. (2010) included a memory parameter in their reinforcement-learning model and found that depressed suicide attempters discounted previously observed rewards more than healthy controls. It has been proposed that many observed impairments in schizophrenia could potentially be explained by deficits in the memory of patients (Strauss, Robinson, Waltz, et al., 2010; Collins, Brown, Gold, et al., 2014). Future research might want to consider whether memory (encoding and/or retrieval) impairments could also be a (partial) explanation for many of the observed abnormalities in depression.

2.5 Summary

Behavioural impairments are prevalent in depression and computational methods provide a useful tool to tease apart different (neural) mechanisms that might influence learning and decision-making. Computational modelling of behaviour in participants with depression has provided refinement and additional evidence for theories of MDD, which suggest that negative (perceptual) biases, deficient cognitive control, impaired reward learning, and beliefs about the controllability of the environment are all important aspects of the disease. Clever task design and replication involving larger samples, combined with robust computational techniques, are now needed to advance the field. It is important as well not to neglect the study of patients with moderate-severe mood disorder (rather than participants with low mood or mild forms of depression, who are often easier to study) and particularly treatment resistant patients who are common in secondary care psychiatric services. We need to move from methods which are able to distinguish between groups of patients and healthy control participants, to methods which show convincing individual patient differences along symptom dimensions. This will ultimately be necessary to allow objective treatment recommendations and predictions of outcomes for individuals.

The work described in this thesis uses tools and techniques from computational psychiatry to test for behavioural and brain imaging differences between patients suffering from depression, participants showing various depressive symptoms, and healthy controls. Behaviour during reward learning tasks was analysed and modelled in a similar way as described in the case study report of this chapter. It was found that patients were impaired in their use of internal value estimations (Chapter 3; Rupprechter, Stankevicius, Huys, Steele, et al., 2018). These results were used to describe hypotheses about differences in the underlying neuronal function of value encoding and decision making (Chapter 4; Rupprechter, Stankevicius, Huys,

Series, et al., 2020). Consistent with studies reviewed in this chapter, we reported abnormal activity in striatum, hipppocampus and anterior cingulate (Chapter 4).

Given these results and the evidence for abnormal activity (and functional connectivity) of cortical and limbic regions in depression, I set out to directly test the hypothesis of abnormal cortico-limbic reward-related effective connectivity being associated with depressive symptoms. Corroborating a number of theories reviewed in this chapter, I found that increased severity of depressive symptoms was associated with decreased connectivity from the medial prefrontal cortex to the ventral striatum (Chapter 5). In a last "proof of concept" study I then tested whether estimated effective connectivity parameters could be used as features for a data-driven (machine learning) computational psychiatry approach: differentiating never-depressed healthy controls from participants with past or present major depression (Chapter 6). Results were promising and yielded good classification performance.

Chapter 3

Major Depression Impairs the Use of Reward Values for Decision-Making

This chapter consists of a slightly modified version of a published journal article: S. Rupprechter, A. Stankevicius, Q. J. M. Huys, J. D. Steele, et al. (2018). "Major Depression Impairs the Use of Reward Values for Decision-Making". In: *Scientific Reports* 8.13798. *Supplementary Materials for this chapter are included in Appendix A.*

The study was designed as a follow up to the work of Stankevicius, Huys, Kalra, and Seriès (2014) in which the authors used computational modelling to show a relationship between optimism and prior belief about reward in a healthy sample. The experiment consisted of about 240 observation trials intermitted by exactly 60 decision trials. Participants observed brief displays of various fractal stimuli which were followed by a binary reward outcome signal in the form of a full (reward) or empty (no reward) treasure chest. Sixty different fractals were shown (each followed by a treasure chest) and on average each type of fractal was observed 4 times. The exact number of how often a particular fractal stimulus was displayed was drawn from a Poisson distribution with mean 4. After a fractal had been shown its allotted number of times it was then included in a single decision trial at a later time point. A choice had to be made between an explicit reward probability (the proportion of filled circles out of 10 total circles) and a previously observed fractal for which subjects had to estimate the reward probability. For example, a simple model might assume participants keep track of the total number of times a fractal was observed and the number of times it was followed by reward. They could use this to calculate the proportion of rewarded events and compare it to the explicit proportion to choose the more rewarding option. Stankevicius, Huys, Kalra, and Seriès (2014) expanded on this idea and assumed participants behaved as Bayesian observers who also integrated their prior belief about the probability of reward into their decision making. This prior belief (or more precisely the mean of the assumed

prior distribution) significantly correlated with participants' self-reported optimism scores. More optimistic subjects had a higher prior belief that fractal stimuli would lead to a reward.

Cognitive biases in depression are closely related to the absence of an optimism bias (Sharot, 2011) and increased pessimistic biases (see Chapter 2) and therefore future research about the effects of depressive symptoms on the performance in this task was indicated (Stankevicius, Huys, Kalra, and Seriès, 2014). It was decided that in addition to potential behavioural differences between a group of depressed patients and healthy controls, the neural basis of the value estimation and decision making was of interest and so an fMRI study was designed. Because two separate groups were recruited, analysis focused on group comparisons, but correlation analyses are also provided in the Supplement (Appendix A). To capture the BOLD signal, a few important changes to the timings of the task had to be made which are also discussed in the Supplement (Appendix A). Overall, these changes probably contributed to the fact that we did not replicate the relationship between optimism scores and a prior belief about reward. Nevertheless, other behavioural group differences are described in this paper. Computational modelling was used to analyse smaller components of the behaviour and results indicated lower memory of observed rewards and an impaired ability to use internal value estimations when making a choice in the depressed group.

My contributions

I specified and implemented the models and analysis. I also created the figures, wrote the first version of the manuscript, and drafted the first response to the peer reviewers. All this was only made possible through invaluable contributions by my coauthors with whom I discussed the analysis strategy and the results and who edited multiple versions of the manuscript. They had also already optimised the experiment for fMRI and collected the data at the start of my Ph.D. program.

Major Depression Impairs the Use of Reward Values for Decision-Making

Samuel Rupprechter[1], *Aistis Stankevicius*[1], *Quentin J. M. Huys*[2,3], *J. Douglas Steele*[4], *Peggy Seriès*[1]

[1]Institute for Adaptive and Neural Computation, University of Edinburgh, United Kingdom. [2]Centre for Addictive Disorders, Hospital of Psychiatry, University of Zurich, Switzerland. [3]Translational Neuromodeling Unit, Institute of Biomedical Engineering, University of Zurich and ETH Zurich, Switzerland. [4]Division of Imaging Science and Technology, Medical School, University of Dundee, United Kingdom.

Abstract

Depression is a debilitating condition with a high prevalence. Depressed patients have been shown to be diminished in their ability to integrate their reinforcement history to adjust future behaviour during instrumental reward learning tasks. Here, we tested whether such impairments could also be observed in a Pavlovian conditioning task. We recruited and analysed 32 subjects, 15 with depression and 17 healthy controls, to study behavioural group differences in learning and decision-making. Participants had to estimate the probability of some fractal stimuli to be associated with a binary reward, based on a few passive observations. They then had to make a choice between one of the observed fractals and another target for which the reward probability was explicitly given. Computational modelling was used to succinctly describe participants' behaviour. Patients performed worse than controls at the task. Computational modelling revealed that this was caused by behavioural impairments during both learning and decision phases. Depressed subjects showed lower memory of observed rewards and had an impaired ability to use internal value estimations to guide decision-making in our task.

3.1 Introduction

Although major depressive disorder (MDD) is a debilitating condition with a high prevalence and substantial economic impact (Pizzagalli, 2014). A core symptom of clinical depression is anhedonia (World Health Organization, 1992) and patients often display impairments in executive function, working memory and attention (McIntyre, Cha, Soczynska, et al., 2013; Rock, Roiser, Riedel, and Blackwell, 2014).

Another common symptom during depressive episodes is "bleak and pessimistic views of the future" (World Health Organization, 1992). The theory of learned helplessness posits that people with a pessimistic explanatory style (attributing

their helplessness to a stable, global, internal cause) are at greater risk of developing depression (Abramson, Seligman, and Teasdale, 1978). There exists extensive evidence that patients diagnosed with MDD exhibit features of Beck's Negative Cognitive Triad, which is characterized by negative and pessimistic views about oneself, the world and the future (Beck, Rush, Shaw, and Emery, 1979), consistent with a pervasive pessimistic cognitive bias. The Beck Depression Inventory (BDI, Beck, Ward, Mendelson, et al., 1961) and the Beck Hopelessness Scale (BHS, Beck and Steer, 1988) both measure aspects of this triad and Cognitive Behavioural Therapy (CBT), which targets these negative biases can be an effective treatment for depression (Beck, 2005; Butler, Chapman, Forman, and Beck, 2006). Here we used a novel experimental paradigm and computational models of decision-making in order to supplement these subjective clinical interviews and rating scales with objective behavioural evidence.

Behavioural impairment in MDD has consistently been found with at least two tasks (see Chen, Takahashi, Nakagawa, et al. (2015) for a review): the Iowa Gambling Task (see Must, Horvath, Nemeth, and Janka (2013) for a mini review) and the Signal Detection Task (see Huys, Pizzagalli, Bogdan, and Dayan (2013) for a meta-analysis). In both paradigms, participants repeatedly choose between options and observe probabilistic reward outcomes based on their choices. Depressed patients are impaired in their ability to properly integrate their reinforcement history to adjust future behaviour.

We used a probabilistic reward-learning task, which has previously been reported to demonstrate individual behavioural differences that were associated with Life Orientation Test - Revised (LOT-R; which measures optimism) scores (Stankevicius, Huys, Kalra, and Seriès, 2014), as well as neuroticism scores (see Supplement) in healthy subjects. In the task, participants were asked to maximize their rewards by choosing between fractal stimuli, for which they could estimate the probability of reward from previous passive observations, and another target associated with an explicit reward probability value. Here we tested patients with depression as well as healthy controls and used a computational modelling approach to describe their behaviour. This allowed us to formulate specific hypotheses, corresponding to distinct computational models, about both the learning and the decision process during the task. While focusing on group differences, we also explored how participants' ratings of depression severity, optimism and neuroticism affected their performance across groups.

Specifically, we tested whether there was objective evidence for: (a) a behavioural difference in learning and decision-making between MDD subjects and healthy controls, and (b) a pessimistic bias about the likelihood of reward in MDD, and then performed exploratory analyses, probing for (c) a correlation between computational model parameters and ratings of depression severity or neuroticism.

3.2 Methods and Materials

3.2.1 Participants

The main dataset analysed here consists of thirty-nine subjects (Tables 3.1 and S1) including 19 patients meeting DSM-IV criteria for a diagnosis of MDD and 20 control participants without a history of depression or other psychiatric disorder. The task was performed during fMRI scanning and in the following this will be referred to as "fMRI dataset". Importantly, patients were unmedicated. Diagnosis was made according to the MINI PLUS (v5.0) structured diagnostic interview (Sheehan, Lecrubier, Sheehan, et al., 1998). The mean BDI score of the patient group (24.7) can be regarded as "moderate severity" depression (see Supplement for additional information on questionnaire scores). Data collection took place at the Clinical Research Imaging Centre, Ninewells Hospital and Medical School, Dundee. The study was approved by the East of Scotland Research Ethics Service (UK Research Ethics Committee, study reference 13/ES/0043) and all experiments were performed in accordance with relevant guidelines and regulations. Written informed consent was obtained from all subjects.

MDD and control groups of the fMRI dataset were matched for age, sex and National Adult Reading Test (NART) scores, which were used to estimate premorbid IQ (Bright, Jaldow, and Kopelman, 2002). Exclusion criteria included claustrophobia, serious physical illness, pre-existing cerebrovascular, neurological disease, previous history of significant head injury, and receipt of any medication likely to affect brain function. All subjects were recruited using the University of Dundee advertisement system HERMES and were paid £20 plus up to £10 dependent on task performance. Four patients and three controls were excluded from further analysis from the fMRI dataset, after performance results showed that they did not choose the higher reward (in the 48 trials in which the reward probability was not the same) in at least 50% of cases. Two additional participants were excluded from all analysis, because they did not complete the study. Model comparison and primary data analysis, which used the fMRI dataset, therefore included 15 participants with MDD and 17 controls.

To further validate our results, we also analysed a second dataset we had previously collected to validate the experiment outside the scanner. In the following, this will be referred to as "Pilot dataset". It included 3 MDD and 21 control participants (Tables 3.1 and S1). Recruitment and assessment was performed in the same way as above and the same ethics statement applies. Model comparison was performed on the fMRI dataset and the best performing model was then separately fitted to the Pilot dataset.

Group	N	Age	Sex (F/M)	BDI	Neuroticism	LOT-R	NART
fMRI Patients	15	17 – 41	12 / 3	24.7 ± 13.1	46.3 ± 7.1	9.1 ± 5.5	46.8 ± 4.2
fMRI Controls	17	18 – 33	13 / 4	4.2 ± 5.6	29.8 ± 8.0	18.4 ± 3.1	46.6 ± 3.2
Pilot Patients	3	N/A	N/A	27.7	50.7	9.3	45.3
Pilot Controls	21	N/A	N/A	10.1 ± 12.2	34.4 ± 11.5	14.5 ± 5.5	44.0 ± 11.3

TABLE 3.1: Demographics of participants from both dataset versions (see Table S1 for more details). BDI, Beck Depression Inventory; LOTR, Life Orientation Test - Revised; NART, National Adult Reading Test; Data given as n or mean ± std. Due to the small number of Pilot patients, standard deviations are not shown for this group.

3.2.2 Experiment

The paradigm (Figure 3.1) was adapted from Stankevicius and colleagues (Stankevicius, Huys, Kalra, and Seriès, 2014). The experiment was implemented in MATLAB R2007b (The MathWorks, Inc., Natick, MA) using the Psychophysics Toolbox (Brainard, 1997; Pelli, 1997; Kleiner, Brainard, Pelli, et al., 2007). Additional details about the experiment are provided in the Supplement and the fMRI analysis will be reported elsewhere. Here we focus on behavioural differences, model fitting and best model identification.

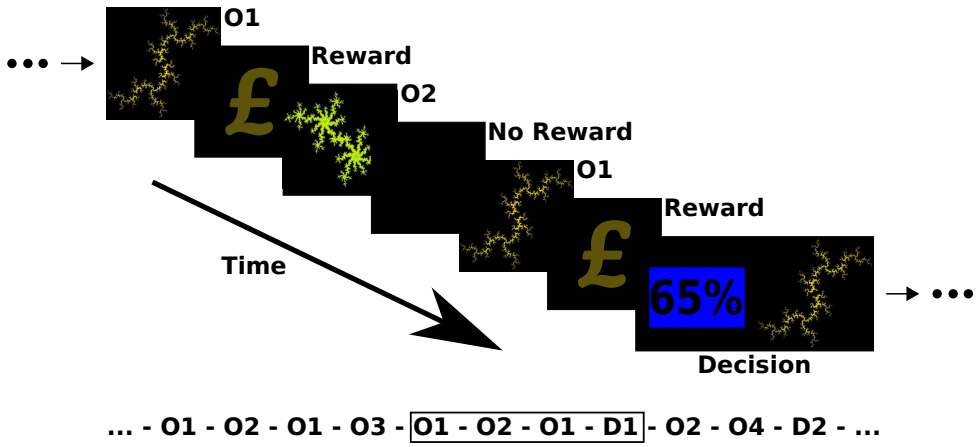

FIGURE 3.1: Experimental paradigm. Subject passively observed different fractal stimuli which were followed by reward (a pound symbol) or no reward (blank screen). Interleaved with these observations were decision prompts in which they had to make a choice between one of the observed fractals (for which they could estimate reward probability) and an explicit numeric probability value in order to maximize their reward. An example of a longer sequence is shown at the bottom with the encased subsequence depicted above.

Participants passively observed fractal stimuli, which were followed by either a reward (depicted by a pound symbol) or no reward (no symbol). Interleaved with these observations were decision screens, during which they were asked to make a choice between one of the fractal stimuli they had observed, and an explicit

numeric probability value. Participants were asked to choose the higher probability (or reward) value option, which required them to estimate the value of the fractal stimuli they had observed. There were seven possible differences in the numeric value probability. Either option could have a higher probability value of 10%, 20% or 30% (each of which was the case for 8 decision trials) or they could have the same probability of reward (in 12 trials). Our Pilot dataset used a slightly different task, in which possible differences ranged from -90% to +90% instead (in 10% intervals, each displayed in 4 decision trials).

Participants observed a variable number of fractals between decision screens, but each fractal was observed exactly four times before it was used within a decision. Each fractal was used in a single decision and in total participants made 60 decisions (and therefore observed fractals 240 times). The sequence of observations and decisions was pseudo-random, and identical for all subjects. Performance feedback was only given at the end of the experiment. Data collection for each subject lasted approximately 2 hours, which included collection of rating scale data (see Table S1).

3.2.3 Behavioural Performance Data Analysis

We tested for differences in average reaction time, IQ (NART) and other questionnaire scores between the groups using Welch's t-tests. We measured participants' performance in terms of how often the fractal was chosen as a function of the difference between the probabilities of the two options (assuming exact estimations for the fractal probabilities; i.e. if a fractal was followed by reward three times, and followed by non-reward once, the fractal probability would be 75%). We fitted a sigmoid function with two parameters (intercept α, slope β) to the psychometric curves of individuals:

$$\varsigma(x) = \alpha + \frac{1}{1 + \exp(-\beta \times x)}. \tag{3.1}$$

3.2.4 Computational Modelling

Three different families of models were fitted to the data (see Table 3.2 for a summary), representing distinct hypotheses about how participants make decisions during the task. All models assume that participants estimate an internal "value" for each fractal they observe and compare this value to the displayed probability when asked to make a choice.

First, we fitted variations of a family of reinforcement learning (RL) models that incorporate trial-by-trial prediction errors and a learning rate parameter. During each trial, the fractal is associated with an expectation about reward based on the internal value and this expectation is updated after observing the reward or lack thereof. Such RL models have been used extensively to describe reward-based learning and much research has gone into understanding the connection between

Name	V update	p(choose fractal i)	Parameters
RL-basic	$V_i^{t+1} = V_i^t + \varepsilon(r_i^t - V_i^t)$	$\sigma(\beta(V_i^t - \phi_i))$	v_0, ε, β
RL-learning	$V_i^{t+1} = V_i^t + \varepsilon^+(1 - V_i^t)r_i^t + \varepsilon^- V_i^t(1 - r_i^t)$	$\sigma(\beta(V_i^t - \phi_i))$	$v_0, \varepsilon^+, \varepsilon^-, \beta$
RL-unbiased	$V_i^{t+1} = V_i^t + \varepsilon(r_i^t - V_i^t)$	$\sigma(\beta(V_i^t - \phi_i))$	ε, β
RL-learning-unbiased	$V_i^{t+1} = V_i^t + \varepsilon^+(1 - V_i^t)r_i^t + \varepsilon^- V_i^t(1 - r_i^t)$	$\sigma(\beta(V_i^t - \phi_i))$	$\varepsilon^+, \varepsilon^-, \beta$
Leaky	$V_i^{t+1} = AV_i^t + r_i^t$	$\sigma(\beta(V_i^t/4 - \phi_i))$	A, β
Leaky-ρ	$V_i^{t+1} = AV_i^t + \rho r_i^t$	$\sigma(\beta(V_i^t/4 - \phi_i))$	A, ρ, β
Bayesian	$V_i = \frac{n_i+\alpha}{N_i+\alpha+\gamma}$	$\sigma(\beta(V_i - \phi_i))$	α, β, γ

TABLE 3.2: Model specification. The second column shows how internal values for a fractal i are updated after observing an outcome r in trial t. The *Bayesian* model does not model learning on a trial-by-trial basis. The third column depicts the choice rule that is used to calculate the probability of choosing the fractal over the alternative option (Equation 3.3). The initial value is set to zero or modelled by v_0. ϕ_i is the displayed probability when asked to make a choice for fractal i. ε is the learning rate; β is the inverse temperature parameter; A is the memory parameter; ρ is the reward sensitivity parameter; α and γ are the parameters of the Beta prior. N_i and n_i are the number of times a fractal i was observed and followed by reward respectively. See main text and Supplement for additional details.

prediction errors and the dopamine system (Schultz, 2002). In two of the models ("RL-basic" and "RL-learning"), the initial value parameter was allowed to vary between 0 and 1, and could therefore act in a similar way as the mean of the prior belief in the Bayesian model (see below). The other two RL models ("RL-unbiased" and "RL-learning-unbiased") kept the bias parameter fixed at 0.5, which corresponded to a prior belief that reward was equally likely from the fractal or the explicit option. Two of these models ("RL-learning" and "RL-learning-unbiased") aimed at testing whether learning was different following rewards versus no-rewards ("punishment") by including separate learning parameters for each outcome. It has been proposed that there may be heightened asymmetry between learning from positive and negative outcomes in depression and separate learning rate parameters can be used to account for this (see Chen, Takahashi, Nakagawa, et al. (2015) for a review). They were also used in the previous version of this task (Stankevicius, Huys, Kalra, and Seriès, 2014).

Next, we fitted the winning model of Stankevicius, Huys, Kalra, and Seriès (2014) (see Table 3.2 and Supplement), which tests the hypothesis that subjects behave as Bayesian observers during the task. This model assumed that at the decision time for a given fractal, participants estimate the number of times the fractal was followed by a reward (the likelihood) and combine this evidence with a prior belief about the probability of rewards associated with the fractals. Although the observations are not modelled on a trial-by-trial basis, this model assumes that the likelihood is computed by (implicitly) counting, and perfectly remembering, the number of times each fractal is associated with reward. In the original experiment, Stankevicius,

Huys, Kalra, and Seriès (2014) found that the mean of the participants' prior belief distribution correlated positively with their optimism scores (LOT-R). A more recent analysis of the same data also revealed a negative correlation of the prior mean with neuroticism scores (see Supplement). This means optimists and people scoring low on neuroticism overestimated the reward associated with fractal stimuli and that in this task, optimism and neuroticism acted as a prior belief, biasing performance in situations of uncertainty.

This Bayesian model comes with some limitations. First of all, it does not allow us to distinguish between observation and decision phases, because it ignores individual observation trials. More importantly, the model assumes perfect memory of observations, which is an unrealistic assumption, especially since memory impairments in MDD are exceedingly common (McIntyre, Cha, Soczynska, et al., 2013; Rock, Roiser, Riedel, and Blackwell, 2014; Ebmeier, Donaghey, and Steele, 2006; McDermott and Ebmeier, 2009; Gotlib and Joormann, 2010).

To overcome these limitations, we therefore also fitted two additional trial-by-trial models ("Leaky" and "Leaky-ρ"), which include neither a learning rate nor a prediction error, but which include a discounting factor (also termed a "memory" parameter). Note that the Leaky model is equivalent to the Bayesian model assuming a flat prior and non-optimal ("leaky") memory. Internal value estimates are updated after observing fractal i and associated reward r at observation t as

$$V_i^{t+1} = A \times V_i^t + r_i^t, \tag{3.2}$$

where A ($0 < A < 1$) is the memory parameter (the closer it is to 0, the more a subject "forgets" about their observations and the less they take into account previously observed rewards) and $r_i^t = +1$ if observation t of fractal i was rewarded and 0 otherwise. Initial internal values were set to zero. A second model in this family (Leaky-ρ) includes a scaling ("reward sensitivity") parameter on observed rewards, to capture participants' subjective valuations of observed rewards. Notably, reward processing (dysfunction) has been identified as a promising phenotype of depression (Pizzagalli, 2014).

The probability of choosing an action was calculated by passing estimated and explicitly displayed reward probability values through a softmax function. For the Leaky model, fractal i was chosen (as opposed to the displayed reward probability ϕ_i) with probability

$$p(\text{choose fractal i}) = \sigma(\beta \times (f(V_i) - \phi_i)) = \frac{1}{1 + \exp(-\beta \times (f(V_i) - \phi_i))}, \tag{3.3}$$

where $f(x) = x/4$ is a deterministic function which transforms the internal value estimates to a probability comparable to ϕ. The shape of the sigmoid function was determined by the β parameter. The higher this inverse temperature parameter, the more deterministic decisions become, while lower values lead to "noisier" decision-making. When the values of actions are unknown, this parameter governs the balancing of exploration and exploitation in reinforcement learning (Sutton and Barto, 1998). Higher values mean actions are chosen more greedily, lower values lead to suboptimal actions being chosen more often to explore the environment. Here participants were asked to maximize their reward, which means they were asked to always choose the option with the higher probability of reward and there was no advantage of "exploring" the other option. Each fractal was only associated with a single decision and feedback was only given at the end of the experiment and not after each decision. This makes it unlikely that individuals consciously decided to choose the option they thought had a lower probability just to explore the alternative. More plausibly, participants made wrong choices when they either were not certain about what they had observed or had incorrectly estimated the probability of a certain fractal leading to reward. Note that variations in the two parameters (A and β) produce separable behavioural effects. Beta affects the probability of choosing the option estimated to have higher probability of reward on all decision-trials. Memory primarily affects the trials in which the fractal should have a higher chance of reward (if perfectly estimated) than the displayed numeric probability (see Supplement).

3.2.5 Model Fitting and Model Comparison

We used model fitting and comparison procedures previously described by Huys and colleagues (Dombrovski, Clark, Siegle, et al., 2010). Parameters were maximum a posteriori (MAP) estimates incorporating an empirical prior, estimated from the data. Parameters were initialized with maximum likelihood values; then an expectation-maximization procedure was used to iteratively update the estimates (see Supplement). We calculated the integrated Bayesian Information Criterion (iBIC; Huys, Cools, Gölzer, et al., 2011) for all fitted models to find the model that best fitted the data, taking into account complexity. Simulations were run to verify that both the fitting and comparison procedure recovered reasonable parameters and chose the correct type of model when generating and re-fitting data using known parameters and models (see Supplement).

3.3 Results

3.3.1 Model-free Analysis

A summary of all questionnaire scores of the two groups is displayed in Table S1. National Adult Reading Test (NART) scores indicated no difference in IQ between

the groups ($t(26.3) = 0.158$, $p = 0.876$). Overall, participants did not respond in 17 of 1920 trials (0.89%). Mean response times were not significantly different between groups (RT patients $\mu \pm \sigma = 2286 \pm 455$ms; RT controls $\mu \pm \sigma = 2185 \pm 360$ms; $t(26.6) = 0.692$, $p = 0.495$).

Figure 3.2 shows the fitted sigmoid curves using the average of the fitted parameters for each group. The fitted offset parameter (α) was not significantly different between groups ($t(28.1) = 0.023$, $p = 0.982$), but the slope parameter (β) was significantly different ($t(26.3) = -2.383$, $p = 0.025$), with controls having steeper curves (β controls $\mu \pm \sigma = 0.566 \pm 0.316$), indicating they were significantly better at learning (β patients $\mu \pm \sigma = 0.350 \pm 0.185$). Stankevicius, Huys, Kalra, and Seriès (2014) recorded a systematic bias in optimistic people towards choosing fractals. We did not find such a systematic bias in healthy participants (as compared to MDD patients) towards choosing fractals, but the difference in the slope parameters indicated performance differences between the groups that we further examined using computational modelling. We were particularly interested in understanding whether those differences stemmed from observation phase or decision phase abnormalities.

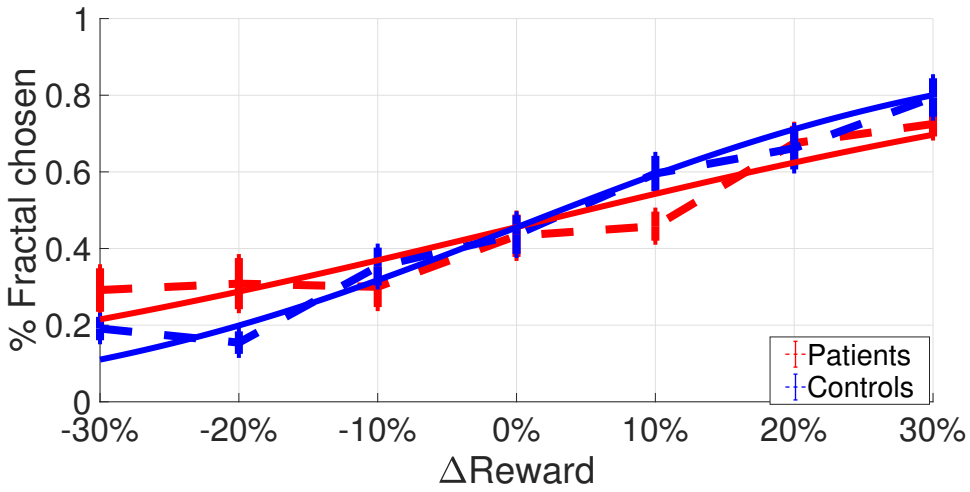

FIGURE 3.2: Average sigmoid functions (solid lines) fitted to psychometric curves (dashed lines) of the two groups of the fMRI dataset. Dashed lines depict the average proportion of responses in which the fractal was chosen as a function of the difference between estimated and explicit reward probabilities. Solid lines show the average of simple sigmoid functions fitted to the psychometric curves of individuals. A perfect observer would never choose the fractal when the explicit probability is higher (-30%, -20%, -10%) and always choose the fractal when the estimated probability is higher (10%, 20%, 30%). An unbiased observer would be expected to choose the fractal in half of the trials when reward probability is the same for both options. Error bars represent between subjects standard errors.

3.3.2 Model-based Analysis

Model selection using iBIC showed that the Leaky model best described participants' performance in our data (Figure 3.3), indicating that in our dataset participants did not seem to rely on their prior beliefs, but were limited by their episodic memory.

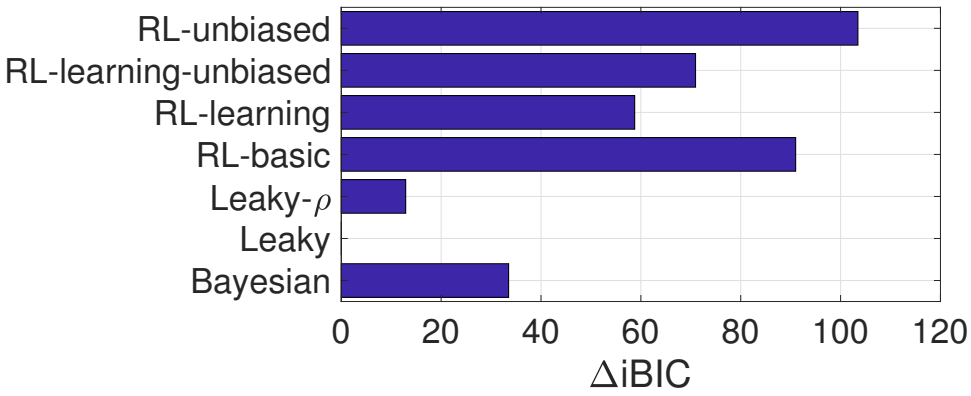

FIGURE 3.3: Results of the model comparison. iBIC values of different models relative to the best fitting model Leaky. A difference of 10 or higher is considered strong evidence for the model with the lower value (Huys, Pizzagalli, Bogdan, and Dayan, 2013).

The memory parameter differed significantly between groups ($z = -2.153$, $p = 0.031$; A patients $\mu \pm \sigma = 0.90 \pm 0.04$, median $= 0.91$; A controls $\mu \pm \sigma = 0.92 \pm 0.09$, median $= 0.96$). This indicates that patients discounted their estimated values more than controls on each trial, possibly indicating impairments in episodic memory. The choice sensitivity parameter (β) was also significantly different between groups ($z = -2.341$, $p = 0.019$; β patients $\mu \pm \sigma = 4.67 \pm 1.45$, β controls $\mu \pm \sigma = 5.89 \pm 1.33$), meaning that controls found it easier to follow their internal estimations, while patients chose more randomly. There was a trend suggesting a correlation between parameter estimates ($r = 0.349$, $p = 0.051$). We performed additional simulations by systematically varying the parameters to see if parameter recovery of one parameter was systematically influenced by the other parameter and convinced ourselves that parameter correlation did not cause problems during inference (see Supplement).

We were also interested in understanding whether there existed interesting relationships between model parameters and questionnaire scores. This exploratory analysis revealed a negative relationship between beta and neuroticism across the two groups (see Supplement). As this was indistinguishable from a group level effect, we then combined our fMRI dataset with our Pilot dataset and focused on healthy participants only. Within the pooled control groups, there was also a significant negative relationship between beta and neuroticism ($t(35) = -2.679$, $p = 0.011$) after controlling for dataset version (Figure S6). This means high neuroticism was related to more variable decision-making in controls.

Further analyses details are reported in the Supplement.

3.4 Discussion

Here we used a probabilistic reward-learning task associated with computational modelling to capture behavioural differences between groups of depressed and healthy participants. We found evidence for impairments in MDD subjects during both learning and decision-making. Our results demonstrate a strong association between depression and participants' inability to make decisions based on their internal value estimations. MDD patients also showed decreased memory of observed rewards throughout the task. We did not find evidence for a systematic pessimistic bias about the likelihood of reward in depressed participants (see Supplement for a discussion).

Depression is characterized by behavioural, emotional and cognitive symptoms (Gotlib and Joormann, 2010). It is well established that MDD patients display cognitive impairments including deficits in executive function, working memory, attention and psychomotor processing speed (McIntyre, Cha, Soczynska, et al., 2013; Rock, Roiser, Riedel, and Blackwell, 2014). Behavioural differences in reinforcement learning performance between groups of depressed and healthy participants have been reported previously (see Chen, Takahashi, Nakagawa, et al. (2015) for a review). In the Iowa Gambling Task subjects repeatedly choose from one of four different decks of cards with different reward and punishment contingencies (unknown to the player). High immediate rewards (or losses in an adapted version) are followed by even higher losses (or rewards) at unpredictable points for some decks. Other decks are associated with lower immediate rewards but even lower unpredictable losses. MDD patients typically choose more often from disadvantageous decks, displaying a worsened sensitivity to discriminating reward and punishment (see Must, Horvath, Nemeth, and Janka (2013) for a mini review). In the Signal Detection Task participants observe in each trial one of two hard to distinguish stimuli for a very short time and are asked to indicate which stimulus they observed. Correct answers are sometimes rewarded, but unbeknownst to subjects, one of the stimuli is rewarded three times as often as the alternative. Whilst healthy people show a bias towards choosing the more frequently rewarded option, MDD patients do not develop this bias (see Huys, Pizzagalli, Bogdan, and Dayan (2013) for a meta-analysis), an effect thought to be related to anhedonia.

In both the Iowa Gambling Task and the Signal Detection Task participants undergo instrumental conditioning, in which chosen actions are reinforced or punished. Subjects learn from their individual choices and the rewards that follow, and will not experience the same reinforcement history, because their rewards depend on their choices. Findings of differences in behaviour or neural activity between groups therefore have to deal with potentially confounding effects of unequal reinforcement histories. Our experiment contains a Pavlovian conditioning phase, during which conditioned stimuli (fractals) are paired with reward and no choices are

made. All participants passively observed the exact same sequence of stimuli and these rewards. Participants could not learn from their instrumental choices in our task, because each fractal stimulus was only associated with a single decision and feedback was only displayed at the end of the experiment.

Computational modelling was used to capture the behaviour of participants during the task and formal model comparison to choose the best fitting model, from which we identified the best fitting parameters for each participant. MDD patients performed worse on our task and the model-based analysis showed that this was due to differences in two model parameters. First, patients discounted (or forgot) previous reward history more than comparison subjects, consistent with reported impairments in memory and attentional deficits (McIntyre, Cha, Soczynska, et al., 2013; Rock, Roiser, Riedel, and Blackwell, 2014). Dombrovski and colleagues found suicide attempters (but intriguingly not non-suicidal depressed elderly people) had lower memory parameter values than control participants in a probabilistic reversal learning task (Dombrovski, Clark, Siegle, et al., 2010). Our finding is also consistent with another recent study by Pulcu and colleagues which reported increased discounting of rewards in MDD (Pulcu, Trotter, Thomas, et al., 2014), although discounting in our task was related to past rewards, while Pulcu and colleagues' task involved future rewards. Notably, a link between memory and delay discounting has previously been reported (Bickel, Yi, Landes, et al., 2011; Wesley and Bickel, 2014). Second, we found MDD patients had more difficulty following their internal value estimations of different stimuli, making decisions more randomly. It is possible that patients had a lower confidence in their ability to perform the task, similar to how learned helplessness theories view depression as a consequence of an organism's diminished belief about its ability to influence outcomes (Abramson, Seligman, and Teasdale, 1978). Taken together, our results therefore suggest that MDD is associated with dysfunctions in both learning and decision-making.

Neuroticism is associated with a vulnerability to many common psychiatric disorders including depression (Widiger and Oltmanns, 2017; Ormel, Bastiaansen, Riese, et al., 2013). Stress reactivity is thought to be a core aspect of neuroticism, with individuals scoring highly on neuroticism showing greater sensitivity to aversive (stressful) events (Ormel, Bastiaansen, Riese, et al., 2013). A large population based study concluded that neuroticism increases vulnerability to depression because of increased sensitivity to stressful life events (Kendler, Kuhn, and Prescott, 2004). In addition to group differences discussed above, we were interested in exploring possible relationships between participants' fitted model parameter values and questionnaire scores. Within control participants, across two different versions of the task, we recorded a negative relationship between self-reported neuroticism and a model parameter capturing a subject's ability to use internal value estimates, meaning higher neuroticism scores were associated with a more variable decision process. Taking this exploratory analysis further, we found that this association also

existed across healthy and MDD groups. However, we could not reliably distinguish this from a group-level effect, and future work is needed to address this.

In conclusion, our results demonstrate impairments in MDD in a probabilistic reward-learning task during both learning and decision-making phases of the experiment. Patients, naturally scoring higher on neuroticism than controls, had a decreased memory of previous rewards and were less able use internally estimated values to guide decision-making in our task.

Future work

As mentioned in the preamble of this chapter, I was not involved in the design of this study. This section briefly explores a few things that could have been done differently and/or might be fruitful avenues for future work with regard to study design.

Ideally study design goes hand in hand with model and parameter recovery simulations as, for example, this makes it possible to estimate the minimum number of trials and participants which should be included. For example, I ran additional parameter recovery simulations which showed considerably better parameter estimates for the Leaky model when the number of trials was doubled (i.e. number of fractals doubled, but each fractal still only observed four times). Thirty-two sets of parameters were drawn randomly from the estimated group prior distribution (from the real data) and then used to generate artificial data. This was repeated ten times, including five times for which double the amount of data (120 fractals) was generated. Unsurprisingly, the mean of the root mean square errors for the inverse temperature parameter was lower by 0.38 (which is approximately $1/6$ of the variance of beta values fitted to the real data) when the recovery simulations included more data. The estimation of the memory parameter showed almost no change (< 0.003 difference).

Under idealised assumptions, one could therefore estimate how many trials are needed for some maximum desired error. Similarly, one could use simulations to estimate how many participants would be needed per group to be able to reliably distinguish between models or find a difference in parameters. That is, similar to classical power analysis, for some assumed effect size one could estimate the number of required participants. Importantly however, experimental design (which as mentioned above should happen hand in hand with model design and simulations) is always critical to be able to achieve the desired effect and answer the experimenters' question and can greatly affect how well models can be fit.

It is important to note that fMRI stipulates additional constraints, such as a maximum time an experiment may run, which need to be considered. The scanner is a loud and uncomfortable environment and participants will lose concentration and motivation. While short scanning sessions might therefore be preferable, the BOLD response is sluggish and usually requires trials to be at least a few seconds long. In addition, while events were jittered to optimise disambiguation of the haemodynamic response, power estimation in fMRI is generally difficult and in our case impossible as no similar data previously existed. Experimental designs therefore always involve a trade-off between optimal computational requirements and practical feasibility, and the current study relied on expert knowledge of one of the authors (J.D. Steele) to achieve this.

In the original experiment (Stankevicius, Huys, Kalra, and Seriès, 2014) the authors reported a relationship between self-reported optimism scores and participants' prior belief about reward associated with fractal stimuli which we did not replicate in this study. Notably, Stankevicius, Huys, Kalra, and Seriès (2014) also performed control experiments and found that reducing the uncertainty by showing each fractal much more often would eliminate the difference between optimistic and pessimistic participants.

For the current study the paradigm was changed in various ways to optimise it for fMRI. Trials lasted longer and fractals were observed for several seconds rather than only a fraction of a second. Participants also had to undergo a lengthy training session and each fractal was observed exactly 4 times rather than a random number of times between 2 and 10. These adjustments likely decreased participant's uncertainty about the reward probabilities and might have been part of the reason for the non-replication (see also Appendix A).

It might have been worth to adjust the paradigm a bit more to increase the chance of replication. I might have suggested that each fractal should be involved in multiple decisions, after they have been observed a various number of times. Outcomes would still not be shown after decisions and so participants would still only learn from passive observations and not their own choices. For example, each fractal could be involved in three decisions; after it had been observed three, four and five times. Not only would this likely have kept some of the uncertainty of the original experiment about the number of times a certain fractal had been observed, but might also have allowed us to study the effects of a change in this uncertainty and might have improved the ability to estimate and interpret memory parameters. Simulations could show if parameter or model recovery could be improved by having different fractals be observed different number of times which would further increase uncertainty.

While our models differed in how they assumed people observed and updated their internal value estimations, they all used the same softmax decision model. (The Leaky models can be rewritten to move the division by four to the value update equations.) The softmax function first calculates the difference between estimated and explicit probabilities and uses this to calculate a "probability" between zero and one. It is worth noting that for most models of all three families of models, the estimated value is sometimes underestimated. For example, in the Leaky model if A is 0.9 the value of a fractal would be around $3.44/4 = 0.86$ rather than 1 after four reward observations. Similarly, for a learning rate of 0.25 in the RL-unbiased model, the estimated value would be around 0.75 after four reward observations[1], and because α and γ in the Bayesian model are constrained to be positive the model can also underestimate the internal value. The reward sensitivity parameter of the

[1]The RL model would eventually converge to the correct value, but that requires many more observations.

Leaky-ρ model could compensate for such possible underestimation, but model comparison showed that even though the model in a sense is "more correct", the data did not support the added complexity and the simpler Leaky model was the "better" model.

Note that if the proposed changes to the study paradigm above were implemented the Leaky model might need to be reworked or extended because it would be less likely that participants would assume a fixed number of four observations. Simulations could be used to check if a scaling parameter within the decision model could reliably be estimated.

It would have been possible to adjust the explicit probability, ϕ, in the decision model to account for the potential underestimation bias. As the underestimation depends on A, the most obvious way to adjust exactly would be to just get rid of the memory parameter as otherwise it might not be estimable. This means A could simply be set to 1, which would result in a model equivalent to the Bayesian model assuming no (or a flat) prior. I implemented this model, but model comparison showed that it was "worse" than the Leaky model ($\Delta iBIC = 15.5$, which is very similar to the Leaky-ρ model).

Another possibility would have been to allow A to be greater than 1, which might be interpreted as participants overvaluing rewards received farther in the past. I again implemented this model and model comparison slightly favoured this new model compared to the Leaky model ($\Delta iBIC = 6.4$). Parameter estimates of both A and β were highly correlated between the two models ($r = 0.91$ and $r = 0.97$ respectively). While the group difference in the inverse temperature parameter remained significantly different, the difference in the A parameter was not significant using this model ($z = -1.511$, $p = 0.131$; A patients $\mu \pm \sigma = 0.94 \pm 0.05$, median $= 0.93$; A controls $\mu \pm \sigma = 0.96 \pm 0.08$, median $= 0.99$).

Due to the strong correlations between parameter estimates of our Leaky model and the new potentially better model it is unlikely that results of Chapter 4, for which we did not directly rely on a significant group difference, would have been very different had the new model be used instead. To be completely certain, a re-analysis of the model-based results would be necessary. Note however that before drawing strong conclusions from the model comparison results above, it will be necessary to perform simulations using these models to make sure they can adequately explain the data, and parameter and model recovery show acceptable performance. Future work might consider the exact implications of possible overvaluation of rewards and whether such a model should be included. As always with computational modelling work, there might be models which explain the data "even better", and any inference we drew in Chapters 3–4 should be seen as implicitly conditioned on the model space we considered.

Chapter 4

Abnormal Reward Valuation and Event-Related Connectivity in Unmedicated Major Depressive Disorder

This chapter consists of a slightly modified version of a published journal article: S. Rupprechter, A. Stankevicius, Q. J. M. Huys, P. Series, et al. (2020). "Abnormal reward valuation and event-related connectivity in unmedicated major depressive disorder". In: *Psychological Medicine*, pp. 1–9. *Supplementary Materials for this chapter are included in Appendix B.*

The work described in this chapter directly follows our behavioural analysis in the previous chapter in which we had identified behavioural abnormalities in depression. We reported a lower memory or higher discounting factor in the MDD group, possibly signalling impairments in working memory. In addition, the depressed group had a significantly lower choice sensitivity parameter, indicating that they found it more difficult to base their decisions on their internal value estimations.

Here, we aimed to identify the neural substrates of these abnormalities. More specifically, we wanted to look at possible group differences in the strength of the value encoding signal. Our "best" behavioural model was used to simulate the evolution of their internally estimated values for each participant and these estimated values were then used as model-based parametric modulators. During fractal trials the value of the displayed fractal was of interest. During decision trials we used the difference between the two displayed values (i.e. the difference between estimated and explicit probability value). This difference of the values corresponded exactly to the input the decision model received.

Altered value encoding signals were found in areas including hippocampus and rostral anterior cingulate regions, while differences during decision making were

especially pronounced in an anterior mid cingulate area. Due to the hypothesis that MDD is associated with abnormalities in a distributed network rather than changes in isolated areas of the brain, we then turned to connectivity analysis. We wanted to identify if areas exhibiting abnormal encoding or use of reward values would also show a change in connectivity. We indeed found weaker connectivity between mid cingulate ("decision making") and rostral anterior cingulate ("value encoding") areas in MDD patients.

My contributions

I preprocessed the fMRI data and performed the model-free and model-based analysis. I considered and proposed specific testable hypotheses relevant to this work and discussed them with my coauthors. I interpreted the results in the context of the translational neuroscience background literature after discussing it with my coauthors. I created the figures, wrote the first version of the manuscript, and drafted the first response to the peer reviewers. All this was only made possible through invaluable contributions by my coauthors with whom I discussed the analysis strategy and the results, and who edited multiple versions of the manuscript.

Abnormal reward valuation and event-related connectivity in unmedicated major depressive disorder

Samuel Rupprechter[1], *Aistis Stankevicius*[1], *Quentin J. M. Huys*[2,3], *Peggy Seriès*[1], *J. Douglas Steele*[4,5]

[1]Institute for Adaptive and Neural Computation, University of Edinburgh, Edinburgh, UK; [2]Max Planck Centre for Computational Psychiatry and Ageing Research, UCL, London, UK; [3]Camden and Islington NHS Foundation Trust, London, UK; [4]Division of Imaging Science and Technology, Medical School, University of Dundee, Dundee, UK and [5]Department of Neurology, Ninewells Hospital, NHS Tayside, Dundee, UK

Abstract

Background. Experience of emotion is closely linked to valuation. Mood can be viewed as a bias to experience positive or negative emotions and abnormally biased subjective reward valuation and cognitions are core characteristics of major depression.

Methods. Thirty-four unmedicated subjects with major depressive disorder and controls estimated the probability that fractal stimuli were associated with reward, based on passive observations, so they could subsequently choose the higher of either their estimated fractal value or an explicitly presented reward probability. Using model-based functional magnetic resonance imaging, we estimated each subject's internal value estimation, with psychophysiological interaction analysis used to examine event-related connectivity, testing hypotheses of abnormal reward valuation and cingulate connectivity in depression.

Results. Reward value encoding in the hippocampus and rostral anterior cingulate was abnormal in depression. In addition, abnormal decision-making in depression was associated with increased anterior mid-cingulate activity and a signal in this region encoded the difference between the values of the two options. This localised decision-making and its impairment to the anterior mid-cingulate cortex (aMCC) consistent with theories of cognitive control. Notably, subjects with depression had significantly decreased event-related connectivity between the aMCC and rostral cingulate regions during decision-making, implying impaired communication between the neural substrates of expected value estimation and decision-making in depression.

Conclusions. Our findings support the theory that abnormal neural reward valuation plays a central role in major depressive disorder (MDD). To the extent that

emotion reflects valuation, abnormal valuation could explain abnormal emotional experience in MDD, reflect a core pathophysiological process and be a target of treatment.

4.1 Introduction

Psychiatric disorders are the leading cause of disability world-wide with major depressive disorder (MDD) the commonest cause (Whiteford, Degenhardt, Rehm, et al., 2013). Severe and enduring mental illness is associated with a reduction in lifespan of 5–15 years (Chang, Hayes, Perera, et al., 2011) and suicide is a leading cause of death in young adults (WHO, 2018). However, understanding of illness mechanisms remains rudimentary, there are no biomarkers in clinical use, clinical outcomes are difficult to predict for individual patients and it is widely recognised clinical practice in psychiatry has not progressed significantly in the past 50 years (Stephan, Bach, Fletcher, et al., 2016; Stephan, Binder, Breakspear, et al., 2016). Better understanding of illness mechanisms is crucial for progress.

Dolan has argued that emotional experience is closely linked to valuation (Dolan, 2002). Normal mood can be viewed as a bias to experience positive or negative emotions and abnormally biased subjective reward valuation (anhedonia) and cognitions are core characteristics of MDD (Gradin, Kumar, Waiter, et al., 2011; Kumar, Waiter, Ahearn, et al., 2008). The origin and persistence of core symptoms of MDD, such as anhedonia, helplessness, rumination and cognitive biases can be explained as arising from biased internal processing; i.e. a biased evaluation of internal states and biased cognitions (Huys and Renz, 2017; Huys, Daw, and Dayan, 2015). Such a decision-theoretic approach allows quantitative coupling of valuation and action which is a central aspect of emotion (Dolan, 2002). A behavioural meta-analysis found evidence for reduced primary reward value sensitivity in depression (Huys, Pizzagalli, Bogdan, and Dayan, 2013) and other recent reviews have argued for blunted reward valuation in anxiety and depression (Bishop and Gagne, 2018; Rizvi, Pizzagalli, Sproule, and Kennedy, 2016) modulated by stress vulnerability (Pizzagalli, 2014). This conceptualisation of MDD is consistent with the National Institute of Mental Health (NIMH), Research Domain Criteria (RDoC, Cuthbert and Insel (2013)) framework, implying a blunted positive valence system, increased sensitivity of the negative valence system and cognitive biases in line with both (Johnston, Tolomeo, Gradin, et al., 2015).

Model-based functional magnetic resonance imaging (fMRI) can be used to determine brain region encoding of signals derived from a computational model such as estimated value or reward prediction error (RPE) (O'Doherty, Hampton, and Kim, 2007). Meta-analyses have highlighted the importance of the striatum and ventromedial prefrontal cortex (vmPFC) as regions encoding value (Bartra, McGuire, and Kable, 2013; Chase, Kumar, Eickhoff, and Dombrovski, 2015). Using

model-based fMRI with an instrumental task, we reported blunted encoding of expected reward value in chronically medicated patients with treatment-resistant MDD and schizophrenia (Gradin, Kumar, Waiter, et al., 2011); however, the effect of medication on these results was unclear. A recent meta-analysis of fMRI and electroencephalography studies found converging evidence for blunted striatal activation and feedback-related negativity responses to reward in depression which may precede the first episode of illness (Keren, O'Callaghan, Vidal-Ribas, et al., 2018). Very recently, we reported behavioural evidence for impairments in both the learning and decision-making phases of a novel Pavlovian conditioning task using computational modelling (Rupprechter, Stankevicius, Huys, Steele, et al., 2018). Here we extend that behavioural analysis to identify the neural substrates of these abnormalities.

Although a number of studies have reported RPE abnormalities (e.g. most recently, Kumar, Goer, Murray, et al., 2018), to our knowledge only a few have tested for expected reward value encoding abnormalities using fMRI with a computational model in MDD patients: we reported blunted reward value encoding (Gradin, Kumar, Waiter, et al., 2011) and reduced reward value signals have been reported in elderly depressed patients with a history of suicide attempts (Dombrovski, Szanto, Clark, et al., 2013). In addition, Greenberg et al. reported that healthy subjects but not unipolar unmedicated depressed patients showed the expected theoretical inverse relationship between prediction error and reward expectancy, mediated by anhedonia (Greenberg, Chase, Almeida, et al., 2015) with similar observations in medicated depressed patients with MDD or bipolar disorder (Chase, Nusslock, Almeida, et al., 2013). Notably though, Greenberg et al. did not find evidence for blunted reward value or RPE signals in unmedicated unipolar depression (Greenberg, Fournier, Sisitsky, et al., 2015).

Here we tested the following four hypotheses: (a) is it possible to replicate previous findings of blunted striatal reward response signals in MDD (Keren, O'Callaghan, Vidal-Ribas, et al., 2018), (b) do unmedicated subjects with MDD exhibit abnormal brain encoding of learned Pavlovian reward values during decision making, (c) are there correlations between aberrant brain encoding and illness severity and (d) is there evidence for abnormal event-related connectivity in MDD for brain regions identified as exhibiting abnormal encoding of reward values.

4.2 Methods and Materials

4.2.1 Participants

The study was approved by the East of Scotland Research Ethics Committee (REC reference 13/ES/0043) and written informed consent obtained from all subjects. Thirty-nine subjects comprising 19 satisfying DSM-IV criteria for MDD not receiving antidepressant medication and 20 healthy controls matched on age, sex and IQ

(NART; Nelson and Willison, 1991) were recruited. Diagnosis was made according to MINI Plus v5.0 structured diagnostic criteria (Sheehan, Lecrubier, Sheehan, et al., 1998). Demographics and illness severity (Beck Depression Inventory, BDI; Beck, Steer, Ball, and Ranieri, 1996) scores are summarised in Table 4.1 with more details in Supplementary Materials. Exclusion criteria were claustrophobia, serious physical illness, pre-existing cerebrovascular or other neurological disease, previous history of significant head injury and receipt of medication likely to affect brain function. Subjects were recruited using the University of Dundee advertisement system HERMES and compensated for participation (£20) with up to £10 extra depending on task performance. One MDD subject and four controls were excluded due to problems with fMRI data acquisition, so data from 18 MDD subjects and 16 controls were analysed. Power estimation in fMRI is recognised as difficult because of the complexity of the analyses and not possible in this instance as no previous similar data existed to allow such an estimate. We did however know on the basis of previous work that the behavioural data, acquired in the same experimental session, showed a significant abnormality (Rupprechter, Stankevicius, Huys, Steele, et al., 2018).

Group	**N**	**Age range**	**Sex (F/M)**	**BDI**	**NART**
Patients	18	18 – 33	15 / 3	25.9 ± 12.9	45.8 ± 4.5
Controls	16	17 – 41	10 / 6	5.4 ± 5.6	47.3 ± 3.6
Comparison		$z = -1.27$ $p = 0.205$	$z = 1.37$ $p = 0.169$	$z = 4.22$ $p < 0.0001$	$z = -1.01$ $p = 0.313$

TABLE 4.1: Clinical characteristics of subjects Group. BDI, Beck Depression Inventory; NART, National Adult Reading Test. Data are displayed as n or mean $\pm$ standard deviation. For more details see online Supplementary materials.

4.2.2 Paradigm

The task was adapted from our earlier work (Stankevicius, Huys, Kalra, and Seriès, 2014) and described in detail in Supplementary Materials. Subjects passively observed a series of different fractals; each fractal was always followed by either a reward symbol (£) indicating "value" or a blank screen indicating "no value". Each fractal was observed on four occasions. Participants had to form an internal estimate of the value (reward probability) associated with each fractal (i.e. number of observed rewards divided by total number of observations). The fractal then appeared at a later time in a single decision trial where subjects were asked to choose the higher reward probability, which required comparison of their internally estimated value for the fractal with a displayed numeric value. Participants made a choice by pressing one of two available buttons ("choose fractal" and "choose explicit probability"). Either option could have a value 10, 20 or 30% higher than

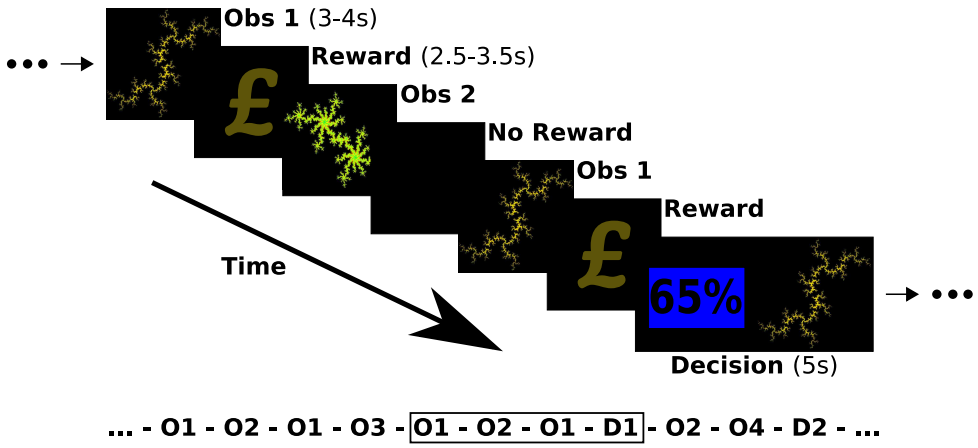

FIGURE 4.1: Pavlovian learning paradigm. Participants passively observed different fractals followed by reward or no reward. From these observations they estimated the probability of reward for each fractal then choose the higher of their estimated fractal value or an explicitly presented value.

the other or be of equal value. Either option could have a value 10, 20 or 30% higher than the other or be of equal value. This means a total of 240 fractals (60×4) were observed with 60 decisions being made. The sequence of observations and decisions were interleaved in a pseudo-random order and identical for all subjects. The study was divided into four sessions of 15 min each, between which there were periods where participants could briefly rest. Each session was split into three blocks and during each block participants made five decisions after having observed 5×4 fractals. Participants did not receive feedback during the task but were told their performance scores would be converted into money they would receive at the end of the experiment. The task is summarised in Figure 4.1.

4.2.3 Computational Modelling of Behaviour

To measure individuals' performance, their psychometric response curves were plotted as the percentage of times a fractal option was chosen as a function of the difference between the probabilities associated with each option with curves fitted with a sigmoid function (Rupprechter, Stankevicius, Huys, Steele, et al., 2018). The slopes of the sigmoid curves were significantly steeper for controls compared to MDD ($p = 0.025$) and detailed computational analyses indicated that MDD was associated with impaired value learning. Details on these behavioural analyses are summarised in the Supplementary Materials and have been published elsewhere (Rupprechter, Stankevicius, Huys, Steele, et al., 2018).

Briefly, to reveal which decision-making components explained the performance difference, three different families of models were compared, reflecting distinct hypotheses about how participants make decisions. All models assumed participants internally estimated a value for each observed fractal then compared this

estimate to the explicitly presented value when making a decision. For model fitting, parameters were estimated using maximum a posteriori estimates incorporating an empirical prior estimated from behavioural data initialised using maximum likelihood estimates. Thereafter, expectation–maximisation was used to iteratively improve the value estimates and the model that best fitted the behavioural data, taking into account model complexity, was identified using the integrated Bayesian information criterion (Huys, Pizzagalli, Bogdan, and Dayan, 2013; Rupprechter, Stankevicius, Huys, Steele, et al., 2018). Here we focus on the best model identified from that work (Rupprechter, Stankevicius, Huys, Steele, et al., 2018) as this was used for model-based fMRI analyses.

The model that best described observed behaviour was termed "Leaky" and included a retrospective discounting factor or memory loss parameter (Rupprechter, Stankevicius, Huys, Steele, et al., 2018). Internal value estimates were assumed to be updated after observing fractal i and associated reward r occurring at time t as

$$V_i^{t+1} = A \times V_i^t + r_i^t, \tag{4.1}$$

where A is a memory parameter (range $0-1$) and smaller A reflected increased forgetting or retrospective discounting, r was unity if a £ reward symbol was observed and zero otherwise. The probability of choosing fractal i was calculated using a softmax function

$$p(\text{choose fractal i}) = \sigma(\beta \times (f(V_i) - \phi_i)) = \frac{1}{1 + \exp(-\beta \times (f(V_i) - \phi_i))}, \tag{4.2}$$

incorporating estimated value (V) and explicitly presented value (ϕ) where $f(x) = x/4$ is a transformation of the internal value estimate compared to the explicitly displayed reward probability of the alternative choice. The inverse temperature β determined the ability of participants to use internal value estimations to make decisions. Smaller values of β indicated a more variable use of internal values.

4.2.4 Image Acquisition and Pre-processing

Functional whole brain images were acquired using a 3T Siemens Magnetom Tim Trio scanner using an echo-planar imaging sequence with the following parameters: repetition time = 2500 ms, echo time = 30 ms, flip angle = 90°, field of view = 224 mm, matrix = 64×64, 37 slices, voxel size $3.5 \times 3.5 \times 3.5$ mm. The first four blood oxygen level-dependent volumes were discarded as standard because of transient effects. Data were pre-processed using Statistical Parametric Mapping 12 (SPM12[1]) with functional images realigned to the first image, unwarped and co-registered

[1] https://www.fil.ion.ucl.ac.uk/spm/

to the segmented T1 weighted structural image. An estimated deformation field was used to spatially normalise the images and an 8 mm Gaussian kernel used to smooth the functional images.

Random-effects, event-related designs were used for analyses. Three event times were of particular interest: (a) when participants observed a fractal stimulus and may have retrieved their previously estimated value for that fractal, (b) when participants observed a rewarding Pavlovian association (£ symbol) indicating reward value or alternatively a blank screen in the case of zero value, this being the trial "outcome event" and (c) when participants were prompted to choose between the estimated value of an observed fractal and an explicit probability value this being the "decision event". For first level analyses, events were modelled as truncated delta functions and convolved with the SPM12 canonical haemodynamic response function without time or dispersion derivatives. Vectors representing these events were entered into first level analyses for each subject and six rigid body motion realignment parameters estimated during pre-processing included as covariates of no interest. Activation at these event times was investigated using both model-based and standard fMRI strategies, testing for significant activations across and between groups and for correlations of activity with illness severity scores.

Given strong evidence for blunted striatal responses to rewards in depression, we used the results of an automated meta-analysis of fMRI studies on healthy subjects ("Neurosynth", Yarkoni, Poldrack, Nichols, et al., 2011) with the search term "reward" which identified 922 studies. We then chose voxels with the global maximum z-score in left and right hemisphere located in left (-12, 10, -8) and right (12, 10, -8) nucleus accumbens (NAc). For each participant in our study we extracted median beta values from the reward contrast maps from a 5 mm sphere centred at these co-ordinates, then tested for significant group differences using Welch's t test.

For model-based fMRI, the Leaky model was used to calculate the value of each fractal on each trial. The estimated value was used as a first level analysis parametric modulator at the time when the fractal stimulus was presented. Additionally, the difference between the internally estimated fractal probability value and the displayed explicit probability value was calculated and used as a parametric modulator at the decision time. The value difference was defined as $V_{chosen} - V_{alternative}$, i.e. the value of the chosen option minus the value of the alternative option. Notably, our model uses the value difference to assign probabilities for choosing each option at the decision time. We therefore expected to observe a value difference encoding signal in regions identified as being active at the decision time.

Event-related functional connectivity between brain regions activated during the task was calculated using the generalised psychophysiological interaction (gPPI) method (McLaren, Ries, Xu, and Johnson, 2012), which tested the hypothesis that value-based decision making involves a distributed network and MDD is associated

with abnormal connectivity in that network. Specifically, we assessed how the "decision event" (the psychological state) modulated activity within brain networks that included our anterior mid-cingulate cortex (aMCC, Tolomeo, Christmas, Jentzsch, et al., 2016) seed region. For each participant, we calculated the contrast at the first (i.e. subject) level (connectivity at decision time > implicit baseline) and then took these contrasts to a standard second (i.e. group) level analysis using SPM12.

For all calculations, activity was corrected for multiple comparisons using a Monte Carlo method (Slotnick, Moo, Segal, and Hart Jr, 2003) with simultaneous requirement for a cluster extent threshold of 108 contiguous resampled voxels and a voxel threshold of $p < 0.05$, resulting in a whole brain corrected cluster threshold of $p < 0.01$. This threshold was enforced for all contrasts. With the exception of the NAc ROI-selection as described above, inference was performed on a whole-brain level and follow-up ROI analyses were based on local maxima of these whole-brain activations.

4.3 Results

There was no significant difference between MDD and control groups in the number of (missed) behavioural responses from subjects during the paradigm: two group t test $p = 0.728$. Since behavioural responses were matched and subjects were not given feedback during the task, all events were matched between groups.

4.3.1 Striatal Reward Response

Given strong evidence for blunted striatal reward response in depression (Gradin, Kumar, Waiter, et al., 2011; Johnston, Tolomeo, Gradin, et al., 2015; Steele, Kumar, and Ebmeier, 2007), we performed both a whole-brain analysis as well as a region of interest (see Section 4.2.4) analysis. The outcome event time was associated with strong activations in regions including the bilateral striatum (10, 12, -4), (-10, 18, 0), aMCC (-10, 10, 48) and bilateral dorsolateral cortex (-46, 8, 24), (44, 6, 32). Consistent with our first hypothesis using the Region of Interest (ROI) approach, striatal activation to reward symbols were significantly blunted in unmedicated MDD in right NAc (12, 10, -8), $t(25.54) = 2.907$, $p = 0.007$ with a trend for left NAc (-12, 10, -8), $t(22.80) = 1.953$, $p = 0.063$ (Figure 4.2a). Using voxel-based methods not confined to the NAc, we found significantly blunted activation in left (-22, 14, -16) and right striatum (12, 4, -4), (22, 26, 10) (Figure 4.2b). This is consistent with our independent studies of chronically medicated patients with treatment-resistant MDD (Gradin, Kumar, Waiter, et al., 2011; Johnston, Tolomeo, Gradin, et al., 2015; Steele, Kumar, and Ebmeier, 2007) and other reports from independent groups (e.g. Keren, O'Callaghan, Vidal-Ribas, et al., 2018).

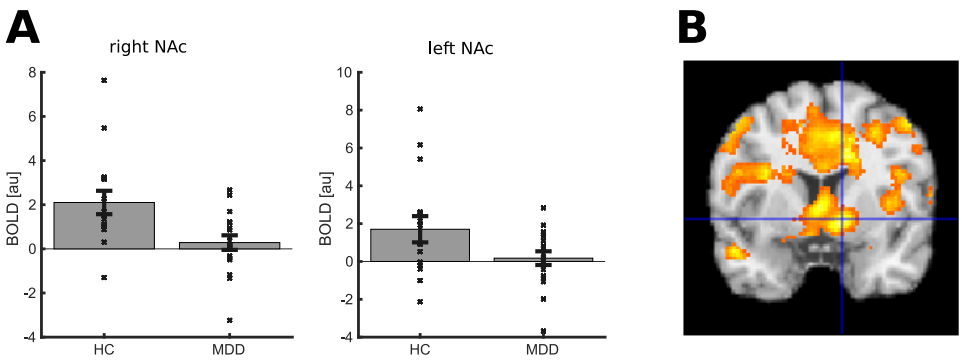

FIGURE 4.2: Reward events. (a) Reward activation in NAc ROIs, (b) decreased reward activation in MDD participants compared to healthy controls (HC) in the striatum. All regions significant at $p < 0.01$ whole-brain corrected.

4.3.2 Reward Value Encoding

At the fractal presentation time, the estimated value of the presented fractal was used as a parametric modulator at the first level. Single group second level analyses showed positive encoding of reward value (activation) in controls (Figure 4.3a) in areas including hippocampus (-38, -28, 0), (46, -26, -2) and rostral ACC (rACC) (14, 50, -2) and negative encoding (deactivation) of reward value in MDD subjects (Figure 4.3b) in hippocampus (-30, -30, -2), (36, -26, -2) and rACC (14, 50, -10). A subsequent two-group comparison revealed significantly larger positive value encoding in controls compared to MDD participants (Figure 4.3c, d) in hippocampus (-36, -32, 2), (48, -26, 4) and rACC (14, 50, -8). Having observed these positive and negative value encodings within the hippocampus, we extracted estimated contrast-beta values from the maximum difference voxel (-36,-32,2) and illustrate it split by group in Figure 4.3d. Note that this post-hoc analysis was primarily performed for more detailed visualisation rather than inference purposes. We then predicted that encoding signals in the two regions showing group differences (rACC and hippocampus) would also be related to depression severity; i.e. variation in depression severity within the depressed group might similarly be related to a change in value encoding. To test this we again extracted contrast-betas from local-maxima voxels and ran regression analyses. Within MDD subjects only, there was a significant negative correlation of BDI illness severity with extracted contrast-betas from the rACC ($r = -0.59, p = 0.009$; (14,50,-8); Figure 4.3e) but not hippocampus ($r = -0.02$, $p = 0.931$; (-36,-32,2)).

In addition to classical statistical inference it is important to test for individual patient predictive accuracy (Steele and Paulus, 2019). Logistic regression with leave-one-out cross-validation was used to classify participants as MDD or controls using median beta values of the value encoding contrast at rACC and left hippocampal ROIs. The classifier achieved an individual subject accuracy of 79% (area under the

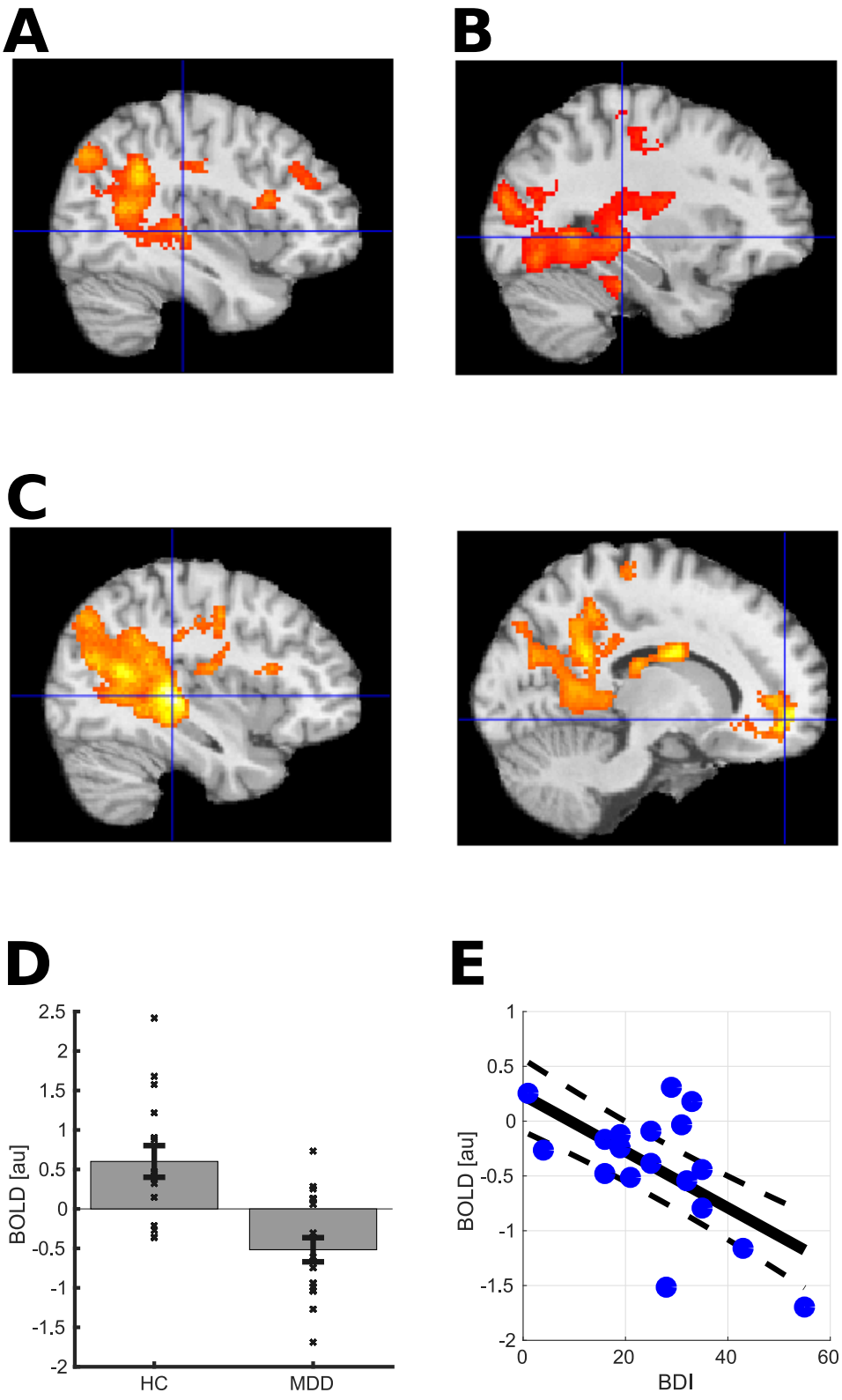

FIGURE 4.3: Reward value encoding at fractal presentation time. (a) Positive value encoding within healthy controls. (b) Negative value encoding in depressed participants. (c) Larger value encoding in healthy controls (HC) compared to MDD participants in hippocampus and rostral ACC. All regions significant at $p < 0.01$ whole-brain corrected. (d) Group comparison of value encoding in hippocampal ROI (-36,-32,2). (e) Within MDD subjects negative correlation between BDI illness severity and rAC (14,50,-8) value encoding ($r = -0.59$, $p = 0.009$).

Receiver Operating Characteristic (ROC) curve Area Under Curve (AUC) = 0.86; see Supplementary Materials).

4.3.3 Decision Making

The decision event time was associated with strong activation in regions including the aMCC (-2, 14, 50) and bilateral anterior insula (-28, 22, -2), (32, 26, -6) across both groups (Figure 4.4a), a pattern consistent with activation of cognitive control processes as identified in a large meta-analysis (Shackman, Salomons, Slagter, et al., 2011). Bilateral insula, subgenual anterior cingulate cortex (-2, 28, -2) and aMCC (-12, 20, 32) (22, 28, 42) activity was significantly increased in MDD subjects compared to controls (Figure 4.4b), with the aMCC region (-6, 26, 36) correlating positively with BDI illness severity scores within the MDD group alone.

The difference between the value of the chosen option and the value of the alternative option was used as a parametric modulator at the first level. In the softmax decision rule, the value difference is used together with the beta inverse temperature parameter to calculate choice probabilities. Across participants, we observed a significant negative correlation of value difference encoding in regions including the aMCC region (-14, 16, 48), (12, 24, 28) (Figure 4.4c). In addition, a negatively correlated absolute value difference encoding signal was also observed in regions including aMCC (-4, 24, 46), (10, 10, 46) (Figure 4.4d) and a positively correlated absolute value difference signal was observed in regions including the rACC (-16, 42, 8), (-4, 50, -14), (24, 38, 4) (Figure 4.4e). Mean value difference and mean absolute value difference were weakly correlated across participants ($r = 0.36$, $p = 0.037$). We did not identify a significant difference between groups for either value encoding parameter within these dorsal and rostral cingulate regions (see Supplementary Materials).

4.3.4 Event-related Connectivity

The aMCC region from the decision event time activation across groups was used as a seed region for a gPPI analysis, to test whether this region exhibited abnormal event-related connectivity in MDD compared to controls. Significantly weaker connectivity at the decision time between the dACC and posterior, mid and rostral cingulate cortex regions (-12, 42, 4), (8, 50, 8) in MDD was identified as shown in Figure 4.4f.

4.3.5 Post-hoc Correction for Grey Matter Variation

Because there is evidence for hippocampal volume reductions in recurrent depression (Schmaal, Veltman, Erp, et al., 2016; Schmaal, Hibar, Sämann, et al., 2017) an additional analysis was done (see also Supplementary Materials) to test for the effect of grey matter variation on fMRI findings. For every participant the estimated

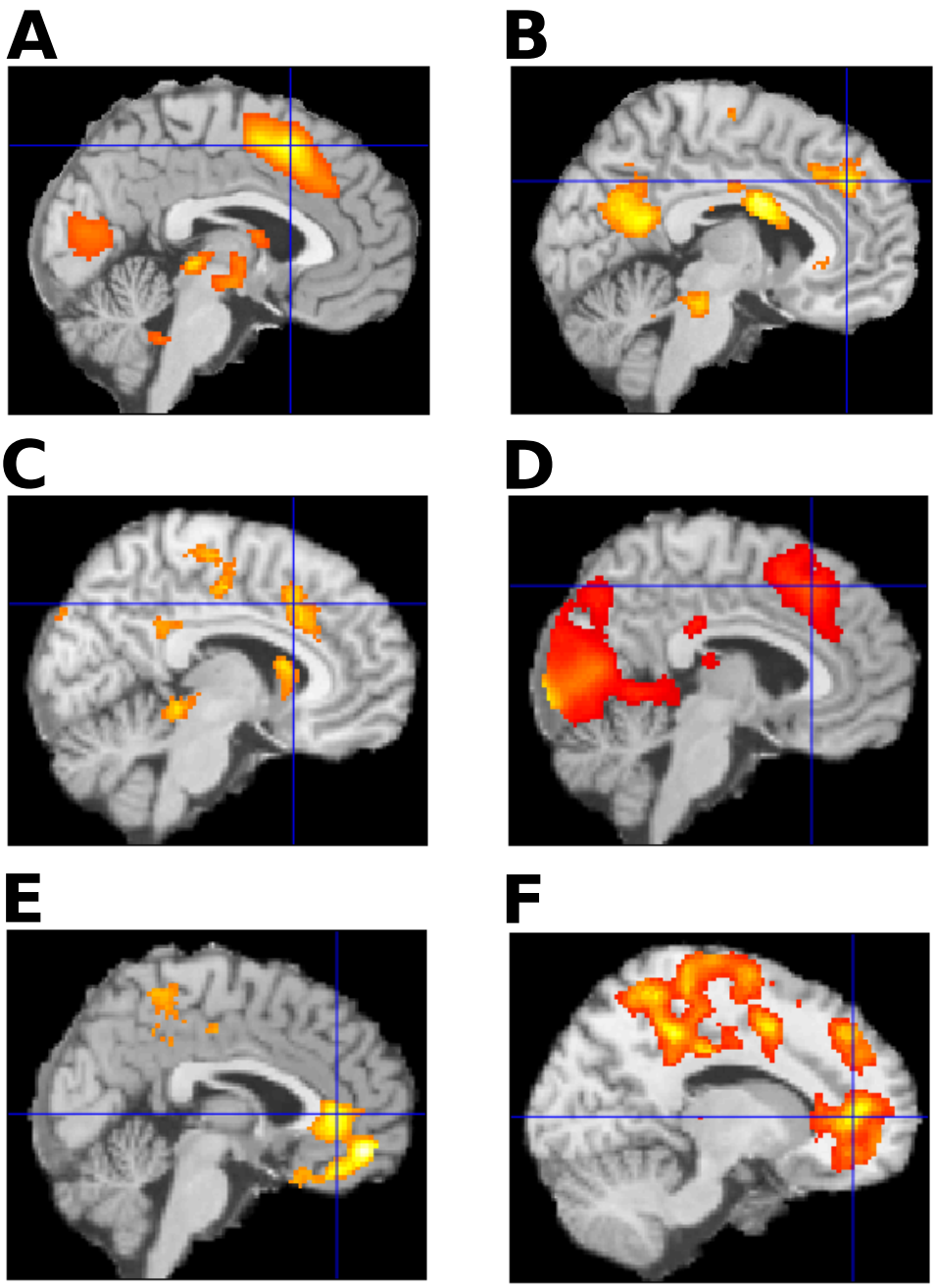

FIGURE 4.4: Activation during decision making. (a) Activation across all participants ($p < 0.05$ FWE threshold). (b) Larger activations in MDD compared to controls. (c) Negative value difference encoding signal across participants. (d) Negative absolute value difference encoding signal across participants. (e) Positive absolute value difference encoding signal across participants. (f) Decreased event-related connectivity in depression between dorsal cingulate region and other cingulate regions. All regions significant at $p < 0.01$ whole-brain corrected.

forward deformation field was used to normalise the grey matter probability image, thereby obtaining for each resampled voxel an estimate of the probability that a voxel was grey matter. Beta values in the hippocampal and rostral anterior cingulate of the fMRI contrast images were then multiplied by these grey matter probabilities and two group t tests used to test for differences. The results still showed significant fMRI group differences: left hippocampus $t(21.36) = 3.313$, $p = 0.003$; right hippocampus $t(31.03) = 2.501$, $p = 0.018$; rACC $t(31.19) = 2.890$, $p = 0.007$.

4.4 Discussion

To our knowledge, this is the first study to test hypotheses about abnormal reward value encoding and event-related connectivity in patients with unmedicated MDD. In our previous detailed behavioural analyses (Rupprechter, Stankevicius, Huys, Steele, et al., 2018) we reported impaired behavioural performance in MDD caused by impairments in both value learning and decision phases of our Pavlovian task; MDD subjects also showed lower memory of observed reward and had an impaired ability to use internal value estimations to guide decision making (Rupprechter, Stankevicius, Huys, Steele, et al., 2018). Here we sought to identify the neural substrates of these behavioural abnormalities.

Consistent with our first hypothesis, we found that the striatal reward activation was blunted as was the reward signal in an independently defined NAc ROI of unmedicated MDD subjects. This is consistent with our previous independent studies on chronically medicated treatment-resistant MDD (Gradin, Kumar, Waiter, et al., 2011; Johnston, Tolomeo, Gradin, et al., 2015; Steele, Kumar, and Ebmeier, 2007) and reports by independent groups (Keren, O'Callaghan, Vidal-Ribas, et al., 2018; Zhang, Chang, Guo, et al., 2013). Whilst the region is often referred to generically in the literature as the "striatum", which includes the NAc and caudate, the region of significantly blunted reward activation during our Pavlovian task also prominently included the region between the two NAc (Figure 4.2b) which is the septum (Mai, Majtanik, and Paxinos, 2015). This structure is part of the septo-hippocampal system which is strongly implicated in anxiety and in the action of antidepressant and anxiolytic medication (Gray and McNaughton, 2000). Notably, using a very different instrumental task to study an independent group of treatment-resistant medicated patients with MDD, we also observed septal reward signal blunting and similarly asymmetric blunting of the NAc (Figure 4.3b; Johnston, Tolomeo, Gradin, et al., 2015). Further study of septal reward response blunting in MDD is indicated.

Consistent with our second hypothesis, we found brain regions with decreased reward value signal encoding in MDD, in particular hippocampus and rACC. We have previously reported decreased reward value encoding in the hippocampus of an independent group of chronically medicated patients with treatment-resistant

MDD using an instrumental learning task (Gradin, Kumar, Waiter, et al., 2011) and as noted above, there is strong evidence for hippocampal abnormalities in treatment-resistant and recurrent MDD (Johnston, Tolomeo, Gradin, et al., 2015; Schmaal, Veltman, Erp, et al., 2016). Here, using a novel Pavlovian reward task with unmedicated MDD subjects, we report positive reward value encoding in the hippocampus of controls and negative reward value encoding of reward value in MDD. Interestingly, a recent Pavlovian study using aversive stimulus learning reported positive encoding of an aversive conditioned stimulus signal in the habenula of controls and negative encoding in MDD (Lawson, Nord, Seymour, et al., 2017).

Recent meta-analyses and reviews have provided substantial evidence for the involvement of regions in the PFC including the rACC in the encoding of reward value (Bartra, McGuire, and Kable, 2013; Chase, Kumar, Eickhoff, and Dombrovski, 2015). The ventromedial PFC (vmPFC) is thought to be a key region involved in value-based decision making (Gläscher, Hampton, and O'doherty, 2008; Treadway, Bossaller, Shelton, and Zald, 2012). Notably, Glaescher and colleagues reported that the vmPFC encoded value signals from a computational model in addition to the amygdala-hippocampal complex, although these value signals were related to actions and expected outcomes (Gläscher, Hampton, and O'doherty, 2008). Reduced expected reward value signals have previously been reported in the vmPFC of suicide attempters (Dombrovski, Szanto, Clark, et al., 2013). Importantly and consistent with our third hypothesis, we found a significant negative correlation between illness severity and rACC value encoding within MDD subjects alone. Consequently, there is considerable evidence for reward value encoding in the hippocampus and vmPFC of healthy subjects, and in addition to the present study, evidence for blunted reward value encoding in two independent studies: on MDD (Gradin, Kumar, Waiter, et al., 2011) and attempted suicide (Dombrovski, Szanto, Clark, et al., 2013). This suggests these two regions are part of the neural substrates of impaired value learning observed in our behavioural analyses (Rupprechter, Stankevicius, Huys, Steele, et al., 2018).

The aMCC has been highlighted as crucial for decision making in a large meta-analysis of healthy subjects (Shackman, Salomons, Slagter, et al., 2011), and it has been suggested that abnormalities of anterior cingulate reward-linked computational function and connectivity could explain core symptoms in a variety of disorders including MDD (Holroyd and Umemoto, 2016). Consistent with this, we have reported decision-making abnormalities in treatment-resistant MDD patients receiving aMCC therapeutic lesions (Tolomeo, Christmas, Jentzsch, et al., 2016) and evidence for electro-convulsive therapy therapeutically altering aMCC connectivity in an independent group of patients with treatment-resistant MDD (Perrin, Merz, Bennett, et al., 2012). Also consistent with our second hypothesis, in the present study we found abnormally increased activation in MDD and encoding of a value difference signal in the aMCC region at the decision time, linking our

behavioural model (Rupprechter, Stankevicius, Huys, Steele, et al., 2018) to localised brain function. Consistent with our fourth hypothesis, event-related connectivity analysis at the decision time revealed reduced connectivity between the aMCC and more rostral ACC regions, in MDD compared to controls. An influential theory of aMCC function linking cognitive control, valuation and motivation, proposes that the underlying function of the aMCC is to determine how much control to allocate (Shenhav, Botvinick, and Cohen, 2013). Consistent with our interpretation, the theory posits that the aMCC receives value-representation inputs from regions such as the vmPFC which are used to monitor outcomes and adjust the level of control. There is evidence that abnormal anterior cingulate cortex maturation during adolescence contributes to the development of MDD reflected by inflexible aMCC connectivity (Ho, Sacchet, Connolly, et al., 2017). The present work suggests this could be related to impairment in the communication of value estimates from the rACC to the aMCC where these estimates are used to guide decision making.

A large meta-analysis of subcortical regions found decreased hippocampal volume in recurrent depression (Schmaal, Veltman, Erp, et al., 2016) and a later meta-analysis reported a range of cortical structural abnormalities including the rACC (Schmaal, Hibar, Sämann, et al., 2017) although see Shen, Reus, Cox, et al. (2017). We therefore did additional analyses addressing the possibility of structural differences influencing our results (*Results* section and Supplementary Materials). The value encoding signals remained significantly different between groups and our conclusions are unaltered. Reward and loss have different value functions with overlapping but different neural substrates which are relevant for MDD (Johnston, Tolomeo, Gradin, et al., 2015) but we could not address this using our current paradigm, although see Lawson, Nord, Seymour, et al. (2017). A possible limitation of our analyses is that the voxel threshold $p < 0.05$ was within the permitted range but not the ideal range. We therefore repeated the analyses using a more stringent voxel threshold $p < 0.01$ and found the results analogous with the exception of the encoding of negative value difference across subjects which was not significant (see Supplementary Materials).

4.5 Conclusions

A close link between emotional experience and valuation has previously been proposed (Dolan, 2002). Diverse symptoms of MDD can be explained within a decision-theoretic framework in which abnormal valuation plays a central role (Huys, Daw, and Dayan, 2015; Huys and Renz, 2017). We reported behavioural evidence for abnormal reward value learning and decision making in depression (Chapter 3, Rupprechter, Stankevicius, Huys, Steele, et al., 2018) and here we identified the neural substrates of these abnormalities as being the striatum, septo-hippocampal system and anterior cingulate, with both reward value encoding and event-related

connectivity being abnormal. This supports the theory that abnormally biased neural valuation plays a central role in MDD, and suggests there is impaired communication between the neural substrates of valuation and decision making in depression.

To the extent that emotion reflects valuation, abnormal valuation could explain abnormal emotional experience in MDD, reflect a core pathophysiological process and be a target of treatment. Finally, MDD may not be the only common psychiatric illness associated with abnormal neural valuation, as there is also evidence for schizophrenia (Gradin, Kumar, Waiter, et al., 2011) and addiction (Redish, 2004; Redish, Jensen, and Johnson, 2008), implying different psychiatric disorders may reflect different disorders of neural valuation.

Chapter 5

Blunted Medial Prefrontal Cortico-Limbic Reward-Related Effective Connectivity and Depression

This chapter consists of a slightly modified version of a published journal article: S. Rupprechter, L. Romaniuk, P. Seriès, et al. (2020). "Blunted Medial Prefrontal Cortico-Limbic Reward-Related Effective Connectivity and Depression". In: *Brain (accepted). Supplementary Materials for this chapter are included in Appendix C.*

My contributions

This work is part of a larger Scotland-wide research project called *STratifying Resilience and Depression Longitudinally (STRADL)* with the goal of "subtyping major depressive disorder (MDD) on the basis of its aetiology, using detailed clinical, cognitive, and brain imaging assessments" (Navrady, Wolters, MacIntyre, et al., 2017; Habota, Sandu, Waiter, et al., 2019).

I performed the computational modelling analysis, processed the fMRI data and ran the activation and connectivity analyses. I was critically involved in the planning of the analysis strategy and proposed and implemented the specific testable hypotheses relevant to the existing literature after discussion with coauthors. I interpreted the results in the context of existing translational neuroscience research which was discussed with coauthors. I created the figures and wrote the initial version of the manuscript. My collaborators made critical contributions to the planning of the project, the analysis strategy, the interpretation of results, and the writing of the manuscript.

Blunted Medial Prefrontal Cortico-Limbic Reward-Related Effective Connectivity and Depression

Samuel Rupprechter[1], *Liana Romaniuk*[2], *Peggy Seriès*[1], *Yoriko Hirose*[2], *Emma Hawkins*[2], *Anca-Larisa Sandu*[3], *Gordon D. Waiter*[3], *Christopher J. McNeil*[3], *Xueyi Shen*[2], *Mathew A. Harris*[2], *Archie Campbell*[4], *David Porteous*[4], *Jennifer A. Macfarlane*[5], *Stephen Lawrie*[2], *Alison D. Murray*[3], *Mauricio R. Delgado*[6], *Andrew M. McIntosh*[2], *Heather C. Whalley*[2*], *J. Douglas Steele*[5*]

[1]School of Informatics, University of Edinburgh, UK; [2]Division of Psychiatry, University of Edinburgh; [3]Biomedical Imaging Centre, University of Aberdeen; [4]Centre for Genomic and Experimental Medicine, University of Edinburgh; [5]Division of Imaging Science and Technology, Medical School, University of Dundee; [6]Department of Psychology, Rutgers University. *joint last authors

Abstract

Major Depressive Disorder is a leading cause of disability and significant mortality yet mechanistic understanding remains limited. Over the past decade evidence has accumulated from case-control studies that depressive illness is associated with blunted reward activation in the basal ganglia and other regions such as the medial prefrontal cortex. However it is unclear whether this finding can be replicated in a large number of subjects. The functional anatomy of the medial prefrontal cortex and basal ganglia has been extensively studied and the former has excitatory glutamatergic projections to the latter. Reduced effect of glutamatergic projections from the prefrontal cortex to the nucleus accumbens has been argued to underlie motivational disorders such as depression, and many prominent theories of Major Depressive Disorder propose a role for abnormal cortico-limbic connectivity. However, it is unclear whether there is abnormal reward-linked effective connectivity between the medial prefrontal cortex and basal ganglia related to depression. Whilst resting-state connectivity abnormalities have been frequently reported in depression, it has not been possible to directly link these findings to reward-learning studies. Here we tested two main hypotheses. First, mood symptoms are associated with blunted striatal reward prediction error signals in a large community-based sample of recovered and currently ill patients, similar to reports from a number of studies. Second, event-related directed medial prefrontal cortex to basal ganglia effective connectivity is abnormally increased or decreased related to the severity of mood symptoms. Using an RDoC approach, data were acquired from a large community-based sample of subjects who participated in a probabilistic reward learning task during event-related fMRI. Computational modelling of behaviour,

model-free and model-based fMRI, and effective connectivity dynamic causal modelling analyses were used to test hypotheses. Increased depressive symptom severity was related to decreased reward signals in areas which included the nucleus accumbens in 475 participants. Decreased reward-related effective connectivity from the medial prefrontal cortex to striatum was associated with increased depressive symptom severity in 165 participants. Decreased striatal activity may have been due to decreased cortical to striatal connectivity consistent with glutamatergic and cortical-limbic related theories of depression and resulted in reduced direct pathway basal ganglia output. Further study of basal ganglia pathophysiology is required to better understand these abnormalities in patients with depressive symptoms and syndromes.

5.1 Introduction

Major Depressive Disorder (MDD) is a leading cause of disability worldwide and a cause of significant mortality, yet there is wide agreement that its treatment has not changed fundamentally in over half a century (Steele and Paulus, 2019). However, there is now substantial evidence from a series of independent neuroimaging studies acquired over more than a decade, that MDD is associated with blunted reward signals in the medial prefrontal cortex and particularly in the basal ganglia (Forbes, Christopher May, Siegle, et al., 2006; Steele, Kumar, and Ebmeier, 2007; Kumar, Waiter, Ahearn, et al., 2008; Pizzagalli, Holmes, Dillon, et al., 2009; Eshel and Roiser, 2010; Gradin, Kumar, Waiter, et al., 2011; Zhang, Chang, Guo, et al., 2013; Pizzagalli, 2014; Johnston, Tolomeo, Gradin, et al., 2015; Stringaris, Vidal-Ribas Belil, Artiges, et al., 2015; Rothkirch, Tonn, Köhler, and Sterzer, 2017; Keren, O'Callaghan, Vidal-Ribas, et al., 2018; Kumar, Goer, Murray, et al., 2018), consistent with earlier large behavioural decision making studies (Forbes, Shaw, and Dahl, 2007) and the conclusions of a large behavioural meta-analysis on decision making in depression (Huys, Pizzagalli, Bogdan, and Dayan, 2013).

In addition to studies on task-based reward processing, there are now many studies of resting state connectivity in major depressive disorder (Kaiser, Andrews-Hanna, Wager, and Pizzagalli, 2015; Kaiser, Whitfield-Gabrieli, Dillon, et al., 2016); however, the link between blunted reward signals in task-based reward learning studies and possible event-related connectivity abnormalities in MDD remains unclear. Functional connectivity abnormalities present during a resting-state study may be different from event-related effective connectivity abnormalities during reinforcement learning studies involving valenced (reward or punishment) feedback. Recognition of different types of connectivity is important, because a number of prominent theories propose a role for abnormal connectivity in depression (Mayberg, Lozano, Voon, et al., 2005; Disner, Beevers, Haigh, and Beck, 2011; Roiser,

Elliott, and Sahakian, 2012; Russo and Nestler, 2013; Pizzagalli, 2014) without distinguishing different types of connectivity. Whilst most MDD neuroimaging studies have focused on resting state undirected functional connectivity, a recent exception reported blunted striatal reward prediction error signals and blunted reward-linked ventral tegmental (VTA) area to striatal event-related connectivity (Kumar, Goer, Murray, et al., 2018). The VTA projection is dopaminergic, has been extensively studied in animals and is part of the classical basal ganglia thalamocortical circuit (Alexander and Crutcher, 1990; Alexander, Crutcher, and DeLong, 1991).

Event-related fMRI studies of reward learning tasks in humans report consistent activation of the basal ganglia and rostral-subgenual medial prefrontal cortex (e.g. Kim, Shimojo, and O'Doherty, 2011; Johnston, Tolomeo, Gradin, et al., 2015) which are prominent parts of the limbic basal ganglia thalamocortical circuits. The medial prefrontal cortex to basal ganglia projection has been studied in animals and is glutamatergic (Alexander and Crutcher, 1990; Alexander, Crutcher, and DeLong, 1991). We were particularly interested in whether the effective connectivity for this medial prefrontal projection was abnormal in volunteers with increased depressive symptoms and decreased brain reward responses. The rostral cingulate is important as influential Positron Emission Tomography (PET) imaging studies reported abnormal metabolic activity in MDD (Drevets, Price, Simpson Jr, et al., 1997; Mayberg, Lozano, Voon, et al., 2005) which motivated a subgenual deep brain stimulation international treatment trial (Holtzheimer, Husain, Lisanby, et al., 2017).

Here we analysed behaviour and fMRI data from a large community-based sample of volunteers. A dimensional approach was chosen because the Research Domain Criteria (RDoC, Insel, Cuthbert, Garvey, et al., 2010) approach aims to explore the "full range of variation from normal to abnormal", recognising current diagnostic systems "do not adequately reflect relevant neurobiological and behavioural systems — impeding not only research on aetiology and pathophysiology but also the development of new treatments" (Cuthbert and Insel, 2013). Our behavioural task included an aspect of control, as there have been reports that reward processing may be affected by whether an individual values making their own choices and in our previous work (Romaniuk, Sandu, Waiter, et al., 2019), we found evidence for an association between the inherent value of choice and activation in MDD-related regions including striatum and medial prefrontal cortex.

Two primary hypotheses were tested: (a) mood symptoms are associated with abnormally blunted reward and/or reward prediction error signals, similar to reports from a number of clinical studies, and (b) there is abnormal (increased or decreased) event-related, directed rostral anterior cingulate to basal ganglia effective connectivity, linked to the severity of mood symptoms. In addition motivated by our previous work (Romaniuk, Sandu, Waiter, et al., 2019), we also tested the hypothesis that (c) individuals learned differently from outcomes depending on whether they had control over decisions, related to the presence of mood symptoms.

5.2 Materials and methods

5.2.1 Participants

Subjects were recruited via the Stratifying Resilience and Depression Longitudinally (STRADL) study (Navrady, Wolters, MacIntyre, et al., 2017; Habota, Sandu, Waiter, et al., 2019). The STRADL clinical cohort is a subset of the Generation Scotland Scottish Family Health Study who were originally recruited in Scotland 2006–2011, aged over 18 at the time (Smith, Campbell, Linksted, et al., 2012). Generation Scotland participants residing in north east Scotland (Grampian and Tayside areas) were invited to attend a clinic in Aberdeen or Dundee for MRI scanning, other testing and sample collection.

5.2.2 Clinical Interview and Questionnaire Data

All participants were assessed for a lifetime history of MDD using the Structured Clinical Interview for DSM-IV disorders (SCID, First, Spitzer, Gibbon, Williams, et al., 2002). Diagnostic criteria were based on the Diagnostic and Statistical Manual of Mental Disorders (DSM-IV-TR). Participants also completed a series of questionnaires which included The Quick Inventory of Depressive Symptomatology (QIDS, Rush, Trivedi, Ibrahim, et al., 2003) which is sixteen-item inventory designed to assess the severity of depression symptoms, and the Hospital Anxiety and Depression Scale (HADS, Zigmond and Snaith, 1983) anxiety subscale (seven items) which was used to assess symptoms of anxiety (Habota, Sandu, Waiter, et al., 2019).

5.2.3 Participant Selection and Analyses

Computational modelling of behaviour and event-related fMRI analyses were performed on 475 participants which included twenty subjects with a current Major Depressive Episode (MDE) (Table 5.1). For Dynamic Causal Modelling (DCM) 165 subjects were selected who had sufficiently strong fMRI signals in the regions of interest. Sufficiently strong signals are required for DCM to be valid, despite depressive symptoms being associated with blunting of signal strength in clinical studies. Data selection is summarised in Fig. S9 and further described in the Supplementary material which contains additional analyses, showing that varying the inclusion criteria did not significantly influence the DCM results. Importantly, included and excluded subjects did not differ significantly with respect to QIDS depression severity scores.

5.2.4 Scanning and Behavioural Paradigms

T1 weighted images and fMRI data were acquired at Dundee and Aberdeen Universities. For fMRI acquisition in Dundee, a 3T Siemens PRISMA was used with TR 1.56 sec, TE 22 ms, FA 70 degrees, FOV 217 mm, matrix 64×64, 32 axial slices; in

	Healthy participants	**Past MDD**	**Current MDE**
Number of subjects	345	110	20
Age (range, mean ± sd)	28–78 60 ± 8.8	27–72 57 ± 8.4	37–65 56 ± 8.7
Sex (F/M)	177 / 168	78 / 32	16 / 4
QIDS–SR (range, mean ± sd)	0–12 3.39 ± 2.08	1–22 5.41 ± 3.84	9–21 14.55 ± 3.79
HADS–A (range, mean ± sd)	0–12 3.13 ± 2.44	0–17 5.04 ± 3.35	6–20 10.65 ± 3.62

TABLE 5.1: Demographic and clinicals details. QIDS = Quick Inventory of Depressive Symptomatology–Self Report; HADS = Hospital Anxiety and Depression Scale; GHQ = General Health Questionnaire; sd = standard deviation

Aberdeen a 3T Philips ACHIEVA was used with TR 1.56 sec, TE 26 ms, FA 70 degrees, FOV 217 mm, matrix 64×64, 32 axial slices. Subjects completed 66 trials of a probabilistic reward learning task (Romaniuk, Sandu, Waiter, et al., 2019) which involved choosing one of two stimuli (yellow or blue squares). Participants were not told that the stimuli were associated with different reward probabilities (80% for the yellow square, 20% for the blue square) and feedback on their choices was provided by display of a number of points: 100 points for a "win" or reward, 0 points for "no win" or no reward. During the first phase of each trial a cue indicated whether participants would be allowed to freely make a choice between the two squares or whether the computer would choose for them and they had to follow that choice. Phases were jittered, allowing for disambiguation. The number of trials was split into 33 "choice" and 33 "no choice" trials with the task being summarised in Figure 5.1.

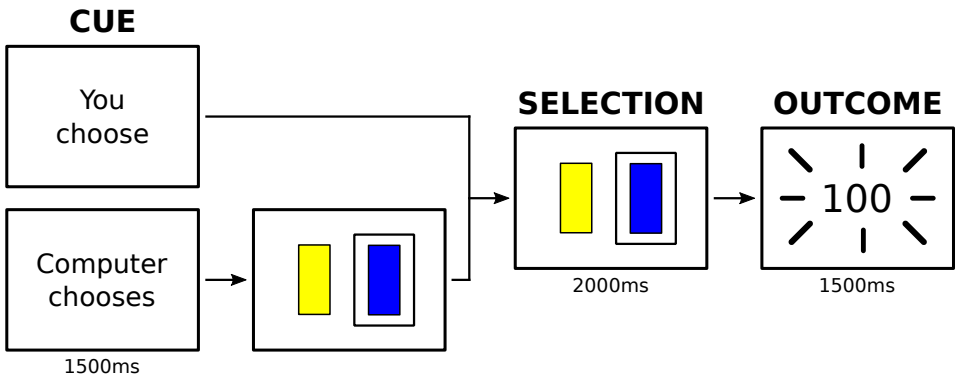

FIGURE 5.1: Probabilistic reward learning task. Subjects completed trials of a probabilistic reward learning task which involved choosing one of two stimuli. During the first phase of each trial a cue indicated whether participants would be allowed to freely make a choice between the two squares or whether the computer would choose for them and they had to follow that choice. During the second phase a choice was made or confirmed. During the third phase an outcome ("no reward" or "reward") was presented.

5.2.5 Computational modelling of behaviour

Five reinforcement learning models represented distinct hypotheses about how subjects learned during the task (Table S1). The aims of the modelling were to (a) correlate model parameter estimates with depressive symptom severity scores, (b) estimate reward prediction error (RPE) signals for use in model-based fMRI analyses and (c) compare learning during choice vs. no-choice trials. Model 1 assumed participants only learned from choice outcomes and ignored no-choice outcomes, model 2 assumed participants learned equally well during both choice and no-choice trials, model 3 assumed participants learned at different rates on choice vs no-choice trials, model 4 assumed reward outcomes were experienced differently depending on the choice vs. no-choice condition (i.e. different "reward sensitivity" parameters) and model 5 assumed both learning and outcomes were experienced differently (different learning rates and reward sensitivity parameters). Fitted parameters were maximum a posteriori estimates and models were compared using the integrated Bayesian Information Criterion (iBIC, Huys, Pizzagalli, Bogdan, and Dayan, 2013) (Supplementary material).

5.2.6 Image pre-processing and GLM voxel based fMRI analyses

SPM12 was used for analyses with functional images realigned to the first image, unwarped and slice time corrected. The T1 weighted structural image was segmented and functional images were co-registered to the bias corrected T1 image. Images were spatially normalised and smoothed using an 8mm Gaussian kernel. Additional details are presented in the Supplementary material.

An event-related design was used for the first-level analysis. A first level general linear model (GLM) design matrix included two columns for onsets of choice or no-choice cues, four columns of possible outcomes (reward or no-reward during choice or no-choice trials), two columns for responses (button-press) during choice/no-choice trials, and one column for nuisance regressors (response time-out or incorrect response during no-choice trials). Six rigid body motion realignment parameters estimated during pre-processing were included as covariates of no interest. For model-based fMRI analyses, the four outcome columns were replaced by a single column of all outcome events and a column of the parametric modulator: reward/no-reward outcome coded as 1 or 0, or the estimated Reward Prediction Error (RPE) signal. Events were modelled as truncated delta-functions and convolved with the SPM12 canonical haemodynamic response function without time or dispersion derivatives.

Contrast estimates from each subject's first level analysis were taken to the second level. Of interest was (a) the reward activations and RPE encoding signals across all participants calculated using contrasts for the corresponding parametric modulator (as expected a contrast of reward(choice + no-choice) outcome >

no-reward(choice + no-choice) outcome in the GLM matrix not using parametric modulators gave similar results), (b) reward response during choice conditions compared to reward response during no-choice conditions (reward(choice) outcome > reward(no-choice) outcome), and (c) correlations with depressive symptom scores across participants.

Multiple comparisons of effects linked to depressive symptom severity were corrected using a whole brain cluster corrected threshold of $p < 0.001$, comprising a simultaneous requirement for a $p < 0.05$ voxel threshold and >131 contiguous supra-threshold voxels, this being estimated using Monte Carlo simulations (Supplementary Materials, Slotnick, Moo, Segal, and Hart Jr, 2003).

5.2.7 Dynamic Causal Modelling of Event-Related Effective Connectivity

DCM (Friston, Ashburner, Kiebel, et al., 2007) was used to investigate how the severity of depressive symptoms was associated with a small network of three brain regions active during the task. Our connectivity hypotheses concerned between-subject level inferences, meaning we tested for an association between QIDS scores and the general task-independent connectivity (DCM "A" matrix).

Brain regions were selected to test the hypotheses of a mood linked change in effective connectivity between regions involved in the brain's reward network. The left ventral striatum (VS) centred at MNI (-12,10,-14) (local reward activation maximum; see results and Table S2) was selected because there is extensive evidence for blunted activation in MDD (Steele, Kumar, and Ebmeier, 2007; Kumar, Waiter, Ahearn, et al., 2008; Pizzagalli, Holmes, Dillon, et al., 2009; Eshel and Roiser, 2010; Gradin, Kumar, Waiter, et al., 2011; Zhang, Chang, Guo, et al., 2013; Pizzagalli, 2014; Johnston, Tolomeo, Gradin, et al., 2015; Rothkirch, Tonn, Köhler, and Sterzer, 2017; Keren, O'Callaghan, Vidal-Ribas, et al., 2018; Kumar, Goer, Murray, et al., 2018). A medial prefrontal cortex (mPC) region was selected centred at (-2,52,18) (local maximum of reward-choice activation; Figure 5.2C, Table S4) because this region usually co-activates with the VS on reward delivery (O'Doherty, Dayan, Schultz, et al., 2004; Gradin, Baldacchino, Balfour, et al., 2014; Johnston, Tolomeo, Gradin, et al., 2015) and the mPC has direct projections to the striatum (Alexander and Crutcher, 1990; Alexander, Crutcher, and DeLong, 1991). In addition, a visual cortex region centred at (-8,-88,-4) (local maximum during reward outcome display; Table S2) was chosen as the brain region receiving experimentally-controlled inputs. This visual region and VS were also constrained anatomically using the pericalcarine and accumbens Freesurfer masks (Reuter, Schmansky, Rosas, and Fischl, 2012). For each participant we extracted the first principal component of the time series of 12mm spheres which were centred at the above MNI coordinates, but importantly were further constrained by liberal individual activation thresholds as well as the

above mentioned anatomical masks, meaning signals were only extracted from a subset of the voxels contained in the spherical regions of interest.

A bilinear DCM with one state per region and no stochastic effects was assumed and a fully connected model of 9 connections including inhibitory self-connections was fitted. There are known direct excitatory glutamatergic projections from the anterior cingulate to the striatum (Alexander and Crutcher, 1990; Alexander, Crutcher, and DeLong, 1991) and the possible effects of depression symptoms on this direct top-down connection were of particular interest. All other connections were assumed to be indirect. Four outcome types ("reward" [choice + no-choice trials], "no-reward" [choice + no-choice], "choice" [reward + no-reward], "no-choice" [reward + no-reward]) were used as driving inputs to the visual cortex ("outcome display"); see Supplementary material for control analyses using an alternative input specification. It was assumed that each of these four outcome conditions could also modulate each of the intrinsic (endogenous, task-invariant) connections. The display of choice / no-choice cues served as additional inputs to the visual area and responses (choice / no-choice condition button presses) drove activity in any region. Inputs were mean-centred so that parameters of the endogenous ("A" matrix) connectivity specified the average effective connectivity between regions and the modulations ("B" matrix) added or subtracted from this average.

For each participant, the full DCM was fitted to the data and the percentage of the variance explained was calculated. As recommended in the SPM documentation and online SPM discussion groups (Zeidman, 2019), we only included participants for which the variance explained by the model was at least 10% (Supplementary material). The Parametric Empirical Bayes (PEB) framework (Friston, Litvak, Oswal, et al., 2016) was used to model commonalities and differences across participants. The group-level between-subject PEB design matrix included a column of ones, corresponding to the mean connectivity across participants, and a zero-mean centred column of our covariate of interest (QIDS depression scores). Five additional mean-centred covariates included HADS anxiety scores, age, sex, collection site and current MDE diagnosis (see Supplementary material for additional analyses without these covariates). The group-level within-subject design matrix was defined as the identity matrix, which means we assumed the covariates could potentially have an effect on every within-subject DCM parameter. The full PEB model was inverted to obtain parameter estimates and the model's "free energy".

Bayesian Model Reduction (Friston, Litvak, Oswal, et al., 2016) was employed to rapidly estimate different reduced PEB models within which certain parameters were "switched off". An automatic "greedy" search procedure was used to iteratively prune parameters that did not contribute to the free energy. The models identified at the final iteration were combined using Bayesian Model Averaging (Figure 5.4A) (Penny, Mattout, and Trujillo-Barreto, 2006). Our main analysis focussed on a PEB

model including 9 DCM ("A" matrix) parameters (see Supplementary material for additional analyses).

To increase confidence in our results, a large number of control analyses were performed (Supplementary material). Most notably, during these analyses different variance-explained thresholds were used, and different covariates were included in the second level design matrix (e.g., only QIDS was included as covariate). Additional control analyses also included an analysis of individual symptoms (as opposed to the QIDS sum of individual symptom scores) to address both a skew in overall QIDS scores and the possibility of correlation effects being influenced by a group-level (i.e. never-depressed healthy participants versus MDE subjects) effect. This is described in detail in the Supplementary material. Bootstrap split-sample replication was used to test the effective connectivity hypothesis.

5.3 Results

5.3.1 Behavioural analyses

There was no significant Spearman's correlation between QIDS depression score and number of rewards gained (Spearman's $\rho(475) = 0.064$, $p = 0.164$) on the task, or between QIDS score and number of missed trials (Spearman's $\rho(475) = 0.064$, $p = 0.164$), facilitating interpretation of the imaging results. Formal model comparison identified model 3, which assumed subjects learned at different rates from choice and no-choice outcomes, as the most parsimonious description of decision making behaviour (Supplementary material). Learning rates for choice trials were larger than learning rates for no-choice trials for most (440 of 475, 93%) participants. These results indicate that whilst participants learned from all outcomes, they learned most from outcomes over which they had more control. However there were no significant Spearman's correlations between parameter estimates and mood scores (Supplementary material). We repeated this correlation analysis using a "default" Bayesian hypothesis test and found strong evidence for the absence of a correlation between depressive symptom severity scores and each of the three parameters ($1/30 < BF10 < 1/10$, (Wetzels and Wagenmakers, 2012)) (Supplementary material).

5.3.2 GLM voxel based fMRI analyses

As expected, across all 475 participants, significant reward activations were identified in areas including the VS (-12,10,-14) (10,8,-10), ventromedial prefrontal cortex (-4,52,-10), orbitofrontal cortex (-24,34,-20) (30,34,-16) and mPC (-10,28,0), as well as activations in the occipital lobe visual areas (10,-86,-6) (-10,-88,-8). As hypothesised, significant negative correlations between reward activation magnitude and mood symptom (QIDS) scores were found in areas including the striatum (8,10,16)

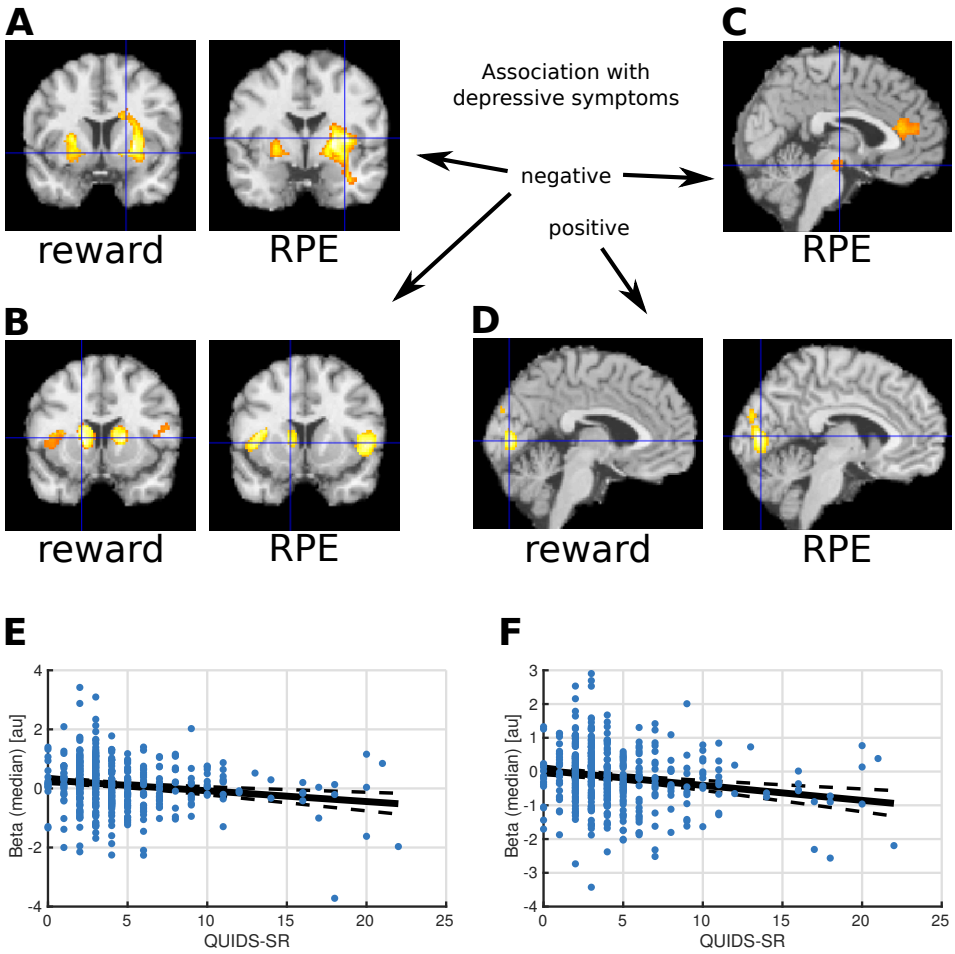

FIGURE 5.2: Correlations between depressive symptom scores and reward signal encoding. Higher depressive symptoms were associated with lower striatal reward response. (A) decreased reward activation / RPE encoding signal in putamen / ventral striatum, (B) increased deactivation / negative RPE encoding signal in caudate and insula, (C) decreased RPE encoding signal in midbrain, (D) increased reward activation / RPE encoding in occipital lobe, with regions significant at $p < 0.001$ whole-brain corrected. (E) Negative correlation of QIDS scores with striatal activity (26,4,0) (Spearman's $\rho = -0.16$, $p < .001$). (F) Negative correlation of QIDS scores with striatal activity (-16,10,6) (Spearman's $\rho = -0.20$, $p < .001$).

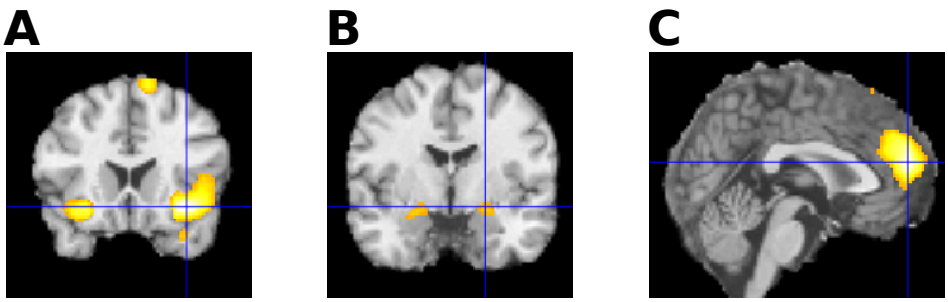

FIGURE 5.3: Activations comparing choice with no-choice conditions. Activated regions during reward outcomes during choice compared to reward outcomes during no-choice conditions: (A) insula, (B) amygdala, (C) medial prefrontal cortex. Regions significant at $p < 0.001$ whole-brain corrected.

(-10,8,22) (-16,12,4), and also in the insula (-34,18,-12) (30,16,-16) and dorsomedial prefrontal cortex (-4,30,50). Additionally, a positive correlation with QIDS scores was found in the occipital lobe (10,-86,20) (-8,-90,10).

A conjunction analysis of correlations with group-level activations and deactivations was done revealing that higher depressive symptoms were associated with decreased activation in the ventral striatum, and increased deactivation in caudate / dorsal striatum, anterior insula and dorsomedial prefrontal cortex. Results of RPE signal encoding correlations were as expected very similar (Supplementary material), due to a correlation between the RPE signal and simple binary reward outcome signals. Notably though, higher depressive symptoms were associated with decreased RPE signal encoding (only) in two additional areas: midbrain / ventral tegmental area (VTA) (-2,-16,-16) and mPC (-2,34,14). These results are shown in Figure 5.2. Figures 5.2A-D show the results of the initial whole-brain analyses, while Figures 5.2E-F show subsequent ROI analyses. For the ROI analyses we extracted local maxima voxels from the estimated contrast-beta values (see also Table S10). The primary purpose of these follow-up ROI analyses was not to show the significance of the results (which was always done on a whole-brain level), but to depict the correlation results and the distribution of the individual beta and QIDS values in more detail.

Across participants, reward activations were significantly larger during choice compared to no-choice conditions in regions including mPC (0,52,16), insula (36,18,-12) (-28,18,-14) and amygdala (-22,-6,-14) (22,-4,-12) (Figure 5.3). Higher depressive symptoms were also associated with decreased choice vs. no-choice response difference in regions including the precuneus (0,-46,36) and increased response difference in regions including left insula (-36,16,0) and subgenual ACC (4,28,0). Additional results are presented in the Supplementary Materials.

5.3.3 Dynamic causal modelling of event-related effective connectivity

The mean of the explained variance across the 165 participants with sufficiently strong fMRI signals was 21.90%. There were no statistically significant differences in mean QIDS scores between the 165 participants with explained variance greater than 10% (mean QIDS $= 4.6$) and excluded (mean QIDS $= 4.4$) participants (Welch's t-test: $p = 0.618$). Additional analyses showed that alternative variance thresholds led to similar DCM results (Supplementary material).

At the group level and consistent with known anatomy, there was insufficient evidence for effective connectivity from V1 to VS and from VS to mPC, but all other connections had a high probability. Details about group-commonalities are presented in the Supplementary material; here we focus on associations with QIDS mood symptoms. Of particular interest was the directed influence (connectivity) from the mPC to the VS. This was found to be negatively correlated with mood symptom scores (Figure 5.4B); higher depression scores were related to a decreased top-down mPC to VS influence. Notably, we did not find this association with anxiety scores (Supplementary material). The analyses also revealed complicated indirect interactions between the visual cortex and both cortical and subcortical regions. Specifically, higher depressive symptoms were negatively associated with the connection from the accumbens and positively associated with the connection to the mPC.

Additional control analyses were done to verify that our results did not depend on the exact specifications of the model, covariates and variance threshold criteria. The negative association between depressive symptom severity and directed influence from the mPC to VS was found for each analysis strategy (Supplementary material).

We investigated the association of connection strengths with individual symptoms assessed with QIDS (rather than the sum-of-scores) and also performed this analysis after excluding current and past MDE participants. This exploratory analysis revealed a more specific negative association between symptoms of "concentration or decision making difficulties" and the top-down connection from mPC to VS and this result was replicated after a stepwise exclusion of current MDE and past MDE participants (Supplementary material).

5.3.4 Bootstrap split-sample replication of mPC to VS effective connectivity correlation

The dataset was randomly split into two halves repeatedly and the second level PEB model (without BMR) estimated for each half. Figure 5.5 shows the histogram of results for 100 splits (200 second level models) of the association between QIDS and mPC to VS effective connectivity. The association was negative in 98% of cases, showing the QIDS blunted effective connectivity result can be replicated on a split-sample basis.

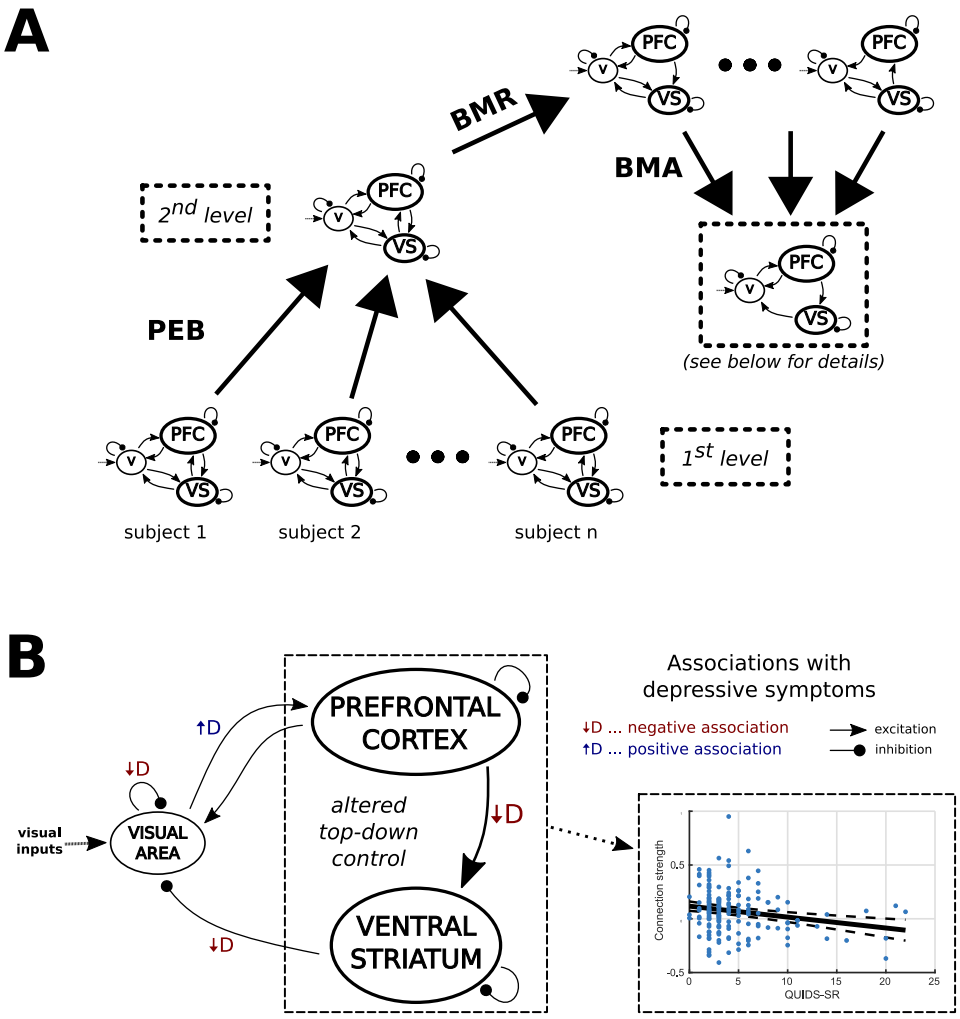

FIGURE 5.4: Effective connectivity analyses. (A) Individual DCMs were taken to the second level where BMR was performed to "prune" connections. BMA was then used to average the DCMs, weighted by their probabilities. (B) Top-down control of the prefrontal cortex over the ventral striatum was decreased with increasing depression symptom severity.

5.4 Discussion

Data from a large community-based study was used to test hypotheses that mood symptoms were associated with blunted reward signal. Increased depressive symptoms were indeed found to be negatively correlated with reward-linked signals in the striatum, consistent with many independent studies (Forbes, Christopher May, Siegle, et al., 2006; Steele, Kumar, and Ebmeier, 2007; Kumar, Waiter, Ahearn, et al., 2008; Pizzagalli, Holmes, Dillon, et al., 2009; Eshel and Roiser, 2010; Gradin, Kumar, Waiter, et al., 2011; Zhang, Chang, Guo, et al., 2013; Pizzagalli, 2014; Johnston, Tolomeo, Gradin, et al., 2015; Rothkirch, Tonn, Köhler, and Sterzer, 2017; Keren, O'Callaghan, Vidal-Ribas, et al., 2018; Kumar, Goer, Murray, et al., 2018) and a large

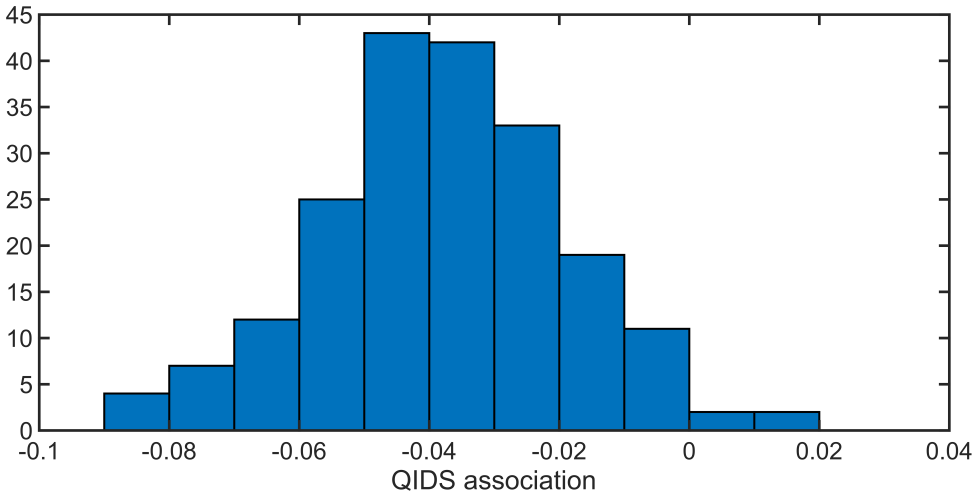

FIGURE 5.5: Association between QIDS and mPC to VS effective connectivity. Histogram after 100 random splits in the total data.

community-based studies which used reward anticipation during a Monetary Incentive Delay task which did not include a decision making component (Stringaris, Vidal-Ribas Belil, Artiges, et al., 2015; Pornpattananangkul, Leibenluft, Pine, and Stringaris, 2019). We also tested whether individuals learned differently from outcomes depending on whether they had control over decisions. Subjects did learn differently from outcomes depending on whether they had control over their decisions that lead to the outcomes; however, we did not find a clear influence of depressive symptoms. Matched behaviour but differences in brain function might indicate a compensatory mechanism. Future studies should consider the possibility that depression might also alter the interaction between cortico-limbic connectivity and task-related events such as choice vs. no-choice reward outcomes.

Previous independent clinical studies have reported RPE abnormalities in MDD (Kumar, Waiter, Ahearn, et al., 2008; Gradin, Kumar, Waiter, et al., 2011; Dombrovski, Szanto, Clark, et al., 2013; Kumar, Goer, Murray, et al., 2018). Here we found decreased RPE signal encoding in many of the same striatal areas as decreased reward responses. It is difficult to disentangle RPE encoding from a binary reward signal (Chowdhury, Guitart-Masip, Lambert, et al., 2013) in our task as the signals are correlated which is common. However, we also found the VTA was associated with an RPE (but not binary) signal which was negatively correlated with mood score, consistent with an independent study on treatment-resistant depression (Gradin, Kumar, Waiter, et al., 2011). The VTA is strongly implicated in the brain's reward system and RPE signals (Schultz, Dayan, and Montague, 1997) and is a source of dopaminergic projections to the VS and frontal cortex (Alexander and Crutcher, 1990; Alexander, Crutcher, and DeLong, 1991). Reduced reward-linked effective connectivity from the VTA to striatum has been reported (Kumar, Goer, Murray, et al., 2018).

There is substantial evidence for resting-state connectivity abnormalities in MDD (Kaiser, Andrews-Hanna, Wager, and Pizzagalli, 2015; Kaiser, Whitfield-Gabrieli, Dillon, et al., 2016), indicating that this illness is not only associated with abnormalities in isolated brain regions but also interactions between these brain regions. Recent reviews and meta-analyses point towards widespread network dysfunction in MDD but much of the work has focused on undirected functional connectivity or connectivity measured during the resting state. Notably, a recent functional connectivity study using resting-state fMRI data reported decreased cingulo-striatal connectivity in children related to anhedonia (Pornpattananangkul, Leibenluft, Pine, and Stringaris, 2019).

Here we identified significant directed medial prefrontal cortex to striatal reward-linked effective connectivity. This projection has been reported to consist of excitatory glutamatergic neurons from studies on animals(Alexander and Crutcher, 1990; Alexander, Crutcher, and DeLong, 1991). A glutamatergic hypothesis of depression has been proposed (Sanacora, Treccani, and Popoli, 2012) and reduced glutamatergic projections from the prefrontal cortex to the striatum have been argued to underlie motivational disorders such as addiction (Kalivas, 2009) and depression (Russo and Nestler, 2013). Indeed, many prominent theories of MDD propose a role for abnormal cortical-limbic connectivity such as Beck's cognitive model (Disner, Beevers, Haigh, and Beck, 2011), Mayberg's cortical-limbic dysregulation model (Mayberg, 1997), Pizzagalli's stress interaction model (Pizzagalli, 2014) and Roiser's neuropsychological model (Roiser, Elliott, and Sahakian, 2012). Different abnormalities have been reported for the medial prefrontal cortical region. Mayberg's deep brain stimulation was applied to the subgenual cingulate Brodmann area 25 which they found overactive in depression using long timescale PET imaging (Mayberg, Lozano, Voon, et al., 2005), whilst reward-related activity in the medial prefrontal region used in our connectivity model has been reported decreased using short timescale event-related fMRI (e.g., Johnston, Tolomeo, Gradin, et al. (2015)).

We also found evidence for changes in effective connectivity between the visual processing area and both nucleus accumbens and cingulate cortex. Alterations in these indirect connections are more difficult to interpret and we did not have strong a priori hypotheses about them. As these connections are likely indirect it is unclear if associations with depression exist between only some or all of the intermediate regions. It is notable that the connection from nucleus accumbens to visual region may occur via the amygdala (Dolan, 2002; Amaral, Behniea, and Kelly, 2003), a region strongly implicated in depression, so it is possible that the back projection from the amygdala to early visual areas is affected by depression. Areas in the occipital lobe have been shown to have a much wider range of function than typically assumed and might play a role in mood and anxiety disorders (Li, Zhang, Zhang, et al., 2020). Abnormal activity and connectivity involving the occipital

cortex in anxiety might underlie increased perception of threatening or feared stimuli (Bruehl, Delsignore, Komossa, and Weidt, 2014; Yang, Liu, Meng, et al., 2019). Although altered occipital lobe function has sometimes been reported in depression (Fitzgerald, Laird, Maller, and Daskalakis, 2008), results are inconsistent and likely depend on experimental context (Müller, Cieslik, Serbanescu, et al., 2017).

Decreased accumbens activity may be due to decreased cortical to striatal connectivity, consistent with prominent theories of depression. Most (95%) accumbens neurons are GABAergic medium spiney neurons, so a decrease in blood oxygen level dependent (BOLD) activity during fMRI may reflect a change in the inhibitory output from the accumbens, with opposite effects for D1-type direct pathway versus D2-type indirect pathway neurons (Russo and Nestler, 2013). Reward-gain tasks are controlled by activation of the D1-type direct pathway and punishment-avoidance tasks by inactivation of the D2-type indirect pathway (Nakanishi, Hikida, and Yawata, 2014). Here the task was reward-gain similar to our previous independent clinical case-control studies (Steele, Kumar, and Ebmeier, 2007; Gradin, Kumar, Waiter, et al., 2011; Johnston, Tolomeo, Gradin, et al., 2015) although we have also reported punishment-avoidance accumbens abnormalities in treatment-resistant MDD (Johnston, Tolomeo, Gradin, et al., 2015). Striatal BOLD activation in the present study may therefore predominately have reflected activation of D1-type direct pathway medium spiney neurons, and blunting of this signal with depressive symptoms impairment of the direct pathway.

The strengths of this work are between-study replication of blunted reward-linked striatal signals in a large community based sample and the novel finding of blunted medial prefrontal cortex to striatal event-related connectivity which was replicated on a split-sample within-study basis. There are however some limitations as potential avenues for future work. During both computational and imaging analyses a common model was assumed for all participants although in principle models could differ between subjects (Stephan, Penny, Daunizeau, et al., 2009). DCM is a region of interest approach and we chose our regions to test for hypothesised differences between activated regions. Future studies should consider tasks which activate additional regions such as the amygdala and hippocampus (Mayberg, 1997; Drevets, Price, and Furey, 2008; Roiser, Elliott, and Sahakian, 2012; Pizzagalli, 2014; Johnston, Tolomeo, Gradin, et al., 2015; Schmaal, Veltman, Erp, et al., 2016) and explore trans-diagnostic (Cuthbert and Insel, 2013) constructs such as anhedonia. We did not have a hypothesis about abnormal connectivity in one hemisphere compared to another. To maximise the number of included subjects we focused on the hemisphere which had the strongest signals across subjects. Exploration of possible covariates was done to determine whether our conclusions about a significant negative association could be confounded by such effects, not because we had specific hypotheses about these. Our conclusions were unchanged (Supplementary

Material). To make an unbiased estimate of cortico-limbic connectivity it was necessary to include subjects who had sufficient signals to allow valid estimation, despite depression being associated with reward-signal blunting. When this was done a significant negative association with depression severity was found, which was not dependent on the precise criteria used for selecting data. Including all subjects, even those with the weakest signals, resulted in connectivity estimates being dominated by noise, although a non-significant negative trend remained (Figure S8). Importantly, none of the analyses suggested significantly increased cortico-limbic connectivity (Supplementary Material). We did not have a specific hypothesis about which sub-symptom of depression would be associated with altered cortical to subcortical connectivity and note that our finding of an association with concentration or decision making difficulties will need to be independently replicated.

In conclusion, using an RDoC positive valence system approach with a large community-based sample, we found evidence that depressive symptom severity was related to blunting of reward-linked striatal activity, consistent with a series of previous studies on MDD. Decreased striatal activity may be due to decreased cortical to striatal event-related effective connectivity consistent with prominent theories of depression, and here have resulted in decreased direct pathway basal ganglia output. Further study of basal ganglia pathophysiology is required to better understand these abnormalities and develop new treatments.

Future work

As in Chapter 3, I was not involved in the design of this study. This section briefly explores a few things that could have been done differently and/or might be fruitful avenues for future work with regard to the study design.

As mentioned previously, the connectivity results should be viewed as implicitly conditioned on the experimental (reward learning) context. Future work will need to address whether depression severity is also associated with a change in top-down connectivity during other contexts. A study could include multiple contexts, such as a reward and a punishment or stress context, in which case it could be tested if depression severity is associated with endogenous connectivity and/or with modulation of that connection by the experimental context.

We had to exclude a sizeable number of participants because their estimated DCMs "flatlined", meaning there was not enough evidence from the data to support a deviation from the zero-centred prior. I suspect that this was, at least in part, due to the limited number of trials in this study. As discussed in Chapter 3, fMRI imposes certain requirements on study design, one of them being trial length of several seconds which limits the overall number of trials within a study. Nevertheless, future work should consider increasing the overall length of the experiment and the number of trials. In an ideal world simulations during the design of a study could help to reliably estimate the minimum amount of data needed for good DCM estimability, but at the moment it is not entirely clear how such simulations could be performed.

The current study included an element of controllability. In half of the trials participants were allowed to choose freely but instead had to accept the computer's choice. Being able to make choices and exerting control over one's environment has inherent value and affects reward processing (Romaniuk, Sandu, Waiter, et al., 2019). The theory of learned helplessness posits that prolonged and continues perception of a lack of control over the environment can lead to depressed behaviour (Chapter 2). The value of personal choice and its association with depressive symptoms was previously studied in more detail within a subset of the current data (Romaniuk, Sandu, Waiter, et al., 2019). They reported striatal activation during the anticipation of choice, which was decreased with higher depression symptom severity, suggesting decreased value of choice. Here we found that participants learned more from outcomes following their own choices compared to outcomes following the computer's choices, but we found no association with depression symptom severity.

It would be interesting to extend the current paradigm to allow for a more direct measurement of the value of control. For example, in some of the trials participants might be allowed to "pay" a certain amount of points in order to be allowed to make their own choice. However, the amount they would be willing to pay would presumably depend on various things, including their value of control but also

the expected outcome which in turn would be influenced by their internal value estimation and their belief about the predictability of the outcomes.

A different variation of the paradigm might allow to improve on this by having the computer offer the participant a number of points to take away the control from them (and make a random choice) after a learning period. If current reward contingencies were kept the same (20% or 80% probability of 100 points) and participants had learned them perfectly, the expected value of their own choice would be 80 points, while the expected value of the computer's choice would be 50 points. This means the subject should accept any offer over 30 points if making their own choice did not have any inherent value. Computational modelling could be used to infer their estimated internal values of the stimuli and estimated expected value of their choice. Simulations could be used to estimate the type and amount of data (i.e. number of trials, reward contingencies, etc.) required for reliable estimates of these internal values. It might therefore be possible to estimate how much a participant values having a choice in terms of number of points by combining information about their acceptance or refusal of various amounts of points with their internal value estimation.

The paradigm could also be translated into the punishment or loss domain by simply making the good option be an outcome of zero points and the alternative be a loss of points. The inherent value of control might not be the same during reward and punishment processing and/or this asymmetry could be increased in depression (Chen, Takahashi, Nakagawa, et al., 2015).

Chapter 6

A generative embedding approach to detecting lifetime depression

This chapter consists of a "proof-of-concept" study which shows how a "generative embedding" approach, combining a generative dynamic causal model (Chapter 5) with a discriminative support vector machine model, can be used for classification of lifetime depression using functional MRI data.

Supplementary Materials for this chapter are included in Appendix D.

6.1 Introduction

The search for biomarkers of psychiatric disorders is a central goal of computational psychiatry (Adams, Huys, and Roiser, 2016; Huys, Maia, and Frank, 2016). Imaging biomarkers might be especially promising, but clinically useful biomarkers have yet to be found, with unreliable diagnoses and too few replicated imaging findings posing challenges for precision medicine in psychiatry (Abi-Dargham and Horga, 2016).

Huys, Maia, and Frank (2016) argued that there exist at least two complementary approaches to computational psychiatry. So far in this thesis I have mainly described "theory-driven" approaches. I used prior knowledge from previous research to inform hypotheses about disease mechanisms. Models at multiple levels of abstraction, including behaviour, neural activation and functional and effective connectivity, incorporated this prior knowledge and were then used to test predictions. Alternative "data-driven" approaches do not generally incorporate knowledge about possible mechanisms (Huys, Maia, and Frank, 2016). Instead, (supervised) machine-learning methods are trained on the raw data and then used for regression or classification. This could, for example, be used to predict the outcome of a specific pharmacotherapy treatment without knowing anything about the underlying mechanism of the drug (Huys, Maia, and Frank, 2016).

Using a large sample, Chekroud, Zotti, Shehzad, et al. (2016) showed that a classifier could be used to predict pharmacological treatment response of MDD patients. A large number of features from several psychiatric questionnaires as well as information about demographics, previous depressive episodes and medication were included. After training these predictors were ranked based on their weights to obtain features predictive of remission (e.g. currently being employed, total years of education) and non-remission (e.g. baseline QIDS-SR severity). However, only few objective features were available and many of the top 25 predictors were subjective self-report features.

Mwangi, Ebmeier, Matthews, and Steele (2012) trained a machine learning classifier on structural MRI scans to classify (carefully defined treatment-resistant) MDD patients versus healthy controls with high accuracy. Costafreda, Chu, Ashburner, and Fu (2009) found that structural neuroanatomy could be used to predict treatment response to antidepressant medication but not CBT. Structural imaging data has several advantages over functional MRI data. It is usually cheaper and quicker to acquire and does not depend on a specific paradigm as well as participants' comprehension and cooperation (Mwangi, Ebmeier, Matthews, and Steele, 2012). However, a patient's brain may appear normal in terms of structure (at least at the resolution of MRI) with typical abnormalities only appearing when the brain is "at work" (Abi-Dargham and Horga, 2016). Studies based on functional MRI have shown potential for classification of healthy controls versus MDD (Fu, Mourao-Miranda, Costafreda, et al., 2008) or treatment-resistant MDD (Johnston, Tolomeo, Gradin, et al., 2015) patients and prediction of treatment response to antidepressant medication (Mourão-Miranda, Hardoon, Hahn, et al., 2011).

While theory-driven approaches are often used when mechanistic insights are pursued, and machine-learning approaches are generally used when the development of clinically useful applications is the main goal (Huys, Maia, and Frank, 2016), the combination of the two approaches might be especially powerful (Huys, Maia, and Frank, 2016; Brodersen, Schofield, Leff, et al., 2011). A theory-based generative model can be used to project the raw data into a lower-dimensional space which can increase efficiency and reliability, while also aiding interpretability, of a subsequently trained classifier (Huys, Maia, and Frank, 2016; Brodersen, Schofield, Leff, et al., 2011).

An early study employing such a "generative embedding" strategy has shown great promise for its use in psychiatric disease identification. A dynamic causal model was fitted to fMRI time-series data and a classifier was then trained on the DCM parameters, achieving near-perfect classification accuracy (Brodersen, Schofield, Leff, et al., 2011). More recently, Queirazza, Fouragnan, Steele, et al. (2019) showed that generative embedding, relying on previous knowledge about reinforcement learning impairments in depression, has the potential to predict CBT treatment response. A model-based fMRI approach was used to calculate contrasts encoding

reward prediction errors which were then used as features for classification. Notably, this generative embedding can lead to the discovery of "mechanistic biomarkers" which might provide important insights into key pathophysiological processes (Queirazza, Fouragnan, Steele, et al., 2019).

In previous work (Chapter 5) an association between depression symptom severity and top-down connectivity from the medial prefrontal cortex to the ventral striatum was found. Here I extended this work using a generative embedding approach to test the hypothesis that effective connectivity parameter estimates can be used to classify never-depressed healthy subjects versus participants with lifetime MDD. Notably, the main goal of this approach was to determine whether there was enough information contained *solely* within estimated connectivity parameters to identify an individual's depression status with good accuracy. This means that while achieving high accuracy was important, the goal was not to build a classifier which maximises predictive accuracy which could probably be improved by including additional features such as age, sex, and questionnaire scores. Indeed, in clinical practice such a classifier would most likely be useless as most clinicians would not be interested in whether a patient is ill (why else would they be here?), but how to best help them.

6.2 Materials and methods

Participants and their estimated DCM parameters from earlier work (Chapter 5) were selected (n=165) and split into two groups of never-depressed healthy subjects (n=112) and lifetime-depression subjects (n=53, of which 12 subjects suffered from current MDD and 41 participants were identified as having had at least one past major depressive episode). The Python library *scikit-learn* (v0.22.1) was used (Pedregosa, Varoquaux, Gramfort, et al., 2011) to implement the classification task.

6.2.1 Classifier

A soft-margin linear support vector machine (SVM) with elastic net regularisation was chosen to perform the multivariate classification. An implementation with stochastic gradient descent learning was used. The maximum number of iterations was set to 5000 as larger numbers did not change performance. Two hyper-parameters were optimised: A regularisation parameter, α, which multiplied the (elastic net) regularisation term and an elastic net mixing parameter, ρ, which controlled the combination of L1 and L2 penalty.

6.2.2 Cross-validation and performance measures

A nested cross-validation (CV) scheme (Figure 6.1) was used which consisted of an "inner loop" using repeated *under-sampled* 5-fold CV and an "outer loop" using

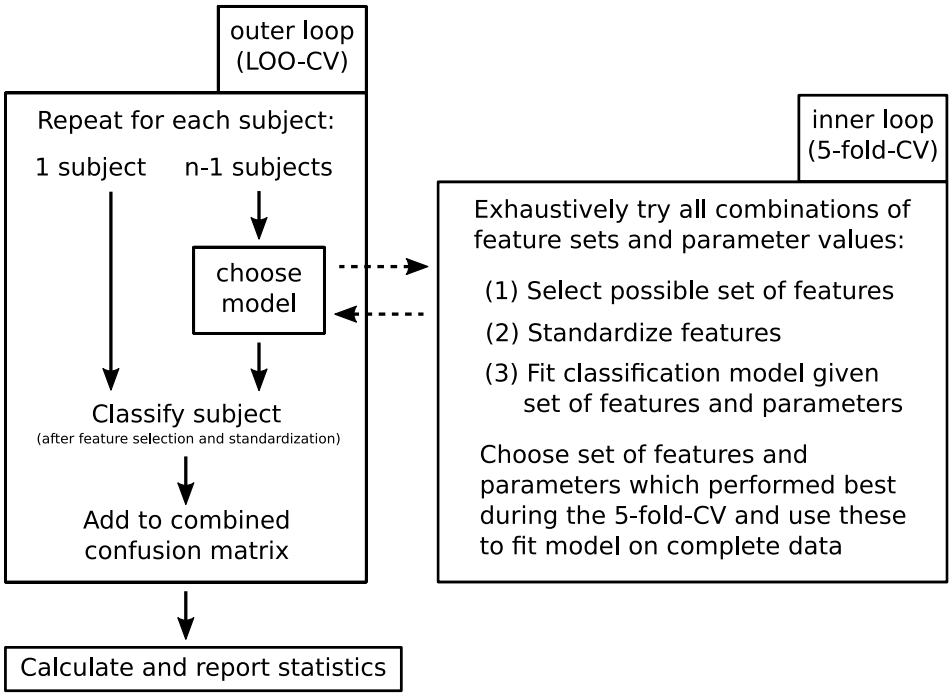

FIGURE 6.1: The nested cross-validation scheme. The outer loop is used to estimate the generalisation performance of the whole pipeline. Feature (and hyper-parameter) selection, and training is performed in an inner cross-validated loop.

leave-one-out (LOO) CV to estimate generalisation performance.

Before each of the 10 repetitions within the inner CV, the majority class (never-depressed healthy controls) was randomly down-sampled to the same number as the minority class (lifetime MDD subjects) due to the slightly imbalanced classes. Further analysis showed that a repeated *stratified* 5-fold CV inner loop performed very similarly (see Supplementary Materials). The inner loop used area under the receiver operating characteristic curve (ROC-AUC) as the scoring function to optimise. Selection and standardisation of features and optimisation of hyper-parameters were performed within the inner loop to avoid leaking knowledge from the testing data into the training process.

The outer loop used LOO-CV to maximise the number of subjects during training. For each left-out subject the whole "pipeline" of feature-selection, feature-scaling, and classification was estimated using (inner) cross-validation on N-1 subjects and then applied to the left-out subject. This means we estimated the generalisation performance of the whole pipeline and for each (left-out) subject we estimated a whole new (cross-validated) classifier.

The main measures of interest were (balanced) accuracy, sensitivity (the proportion of actual lifetime MDD cases correctly identified as such) and specificity (the proportion of never-depressed participants correctly identified as such) as well as

positive and negative predictive value. In addition, the ROC curve for each of the N classifiers (one per left-out subject) was calculated (on its training data).

We compared the accuracy of our classification with the expected distribution of accuracies of a random classifier without any features. This classifier was assumed to know the true frequency of the two classes and a sample was classified as class C with probability $n(C)/N$, where $n(C)$ is the number of samples in class C and N is the total number of samples. After all samples were "classified", the accuracy of the whole sample was computed. This procedure was repeated 10^8 times to obtain the expected distribution of accuracies. The accuracy obtained from the SVM classifier was then compared to this distribution to quantify the proportion of random classifiers it outperformed.

6.2.3 Features

Mean estimates of posterior expectations of dynamic causal modelling parameters of the single fitted *full model* for each participant were used as features. Possible features included (mean) estimates of the intrinsic connectivity (DCM "A" matrix), modulations (DCM "B" matrix) and inputs (DCM "C" matrix). Importantly, these estimates were not constrained by the hierarchical group PEB model and therefore no information about the association with depression severity (or other covariates) was leaked (see also discussion).

Within the inner loop a (cross validated) grid search over combinations of features (A only, A+B, A+C, A+B+C) was performed. The addition of estimated variance of A and B parameters as additional features was explored to test the possibility that lifetime MDD is associated with a change in precision of estimated connectivity parameters.

Data were included from two different collection sites using two different scanners (see Chapter 5) because such a multi-centre approach can improve the generalisability of results. Accuracy performance measures are reported separately for each location because the number of participants were not balanced across them. For additional analysis a collection-site-indicator was included as possible feature to test if explicit information about the site would improve classification performance.

To identify the most important features for classification the weights for each feature from each classifier were extracted. For each feature the median absolute value of its weight across classifiers was then calculated (setting a weight of zero when the feature was not included) and features were then ranked according to these weights.

6.2.4 Alternative classifiers

A linear SVM has the advantage of allowing a straightforward ranking and interpretation of feature weights. During further analysis a radial basis function (RBF) kernel

SVM was employed to see if a non-linear kernel would lead to increased accuracy, essentially trading off interpretability for performance. Finally, a logistic regression classifier was also tested.

6.3 Results

Using DCM features and a leave-one-out nested CV scheme, a regularised soft-margin linear SVM classifier achieved a balanced accuracy of 72% (accuracy 70%, PPV 53%, NPV 85%). The accuracy of 70% was higher than 99.99% of all simulated accuracies of a random classifier. 76 of 112 (68%) never-depressed healthy subjects and 40 of 53 (75%) subjects with lifetime depression were classified correctly. Further inspection showed that 9 of 12 (75%) current MDD subjects and 31 of 41 (76%) past MDD subjects were classified correctly. ROC curves are shown in Figure 6.2. The mean ROC-AUC was 0.85.

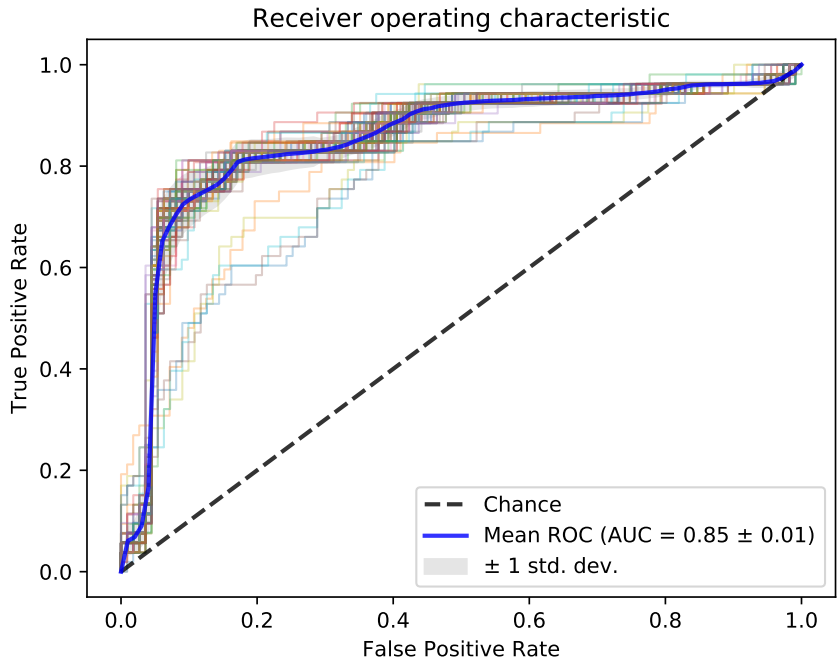

FIGURE 6.2: Receiver Operating Characteristic (ROC) curves for each training data set; i.e. a curve is displayed for each trained model after one subject was left-out. The area under the mean curve was 0.85.

On average, based on the median values of weights, 33 features were used by the classifier to make predictions (Table 6.1). Interestingly, the only intrinsic (A matrix) connectivity estimate not included was the connection from the medial prefrontal cortex to the ventral striatum which is the connection which was found to be associated with depressive severity.

The accuracies differed between sites with 74% (N=107) and 64% (N=58). The addition of explicit information about the collection site decreased the accuracy to 67%. Adding information about estimated parameter variance did not change the results as selected features did not differ from the original classifier. Performance of an alternative classifier using an RBF kernel performed was almost identical to the classifier with a linear kernel, while a logistic regression classifier performed worse (see Supplementary Materials).

6.3.1 Predictive accuracy

It is likely that predictive accuracy could have been increased by including additional features and/or exploring the use of different classifiers. Indeed, exploratory analysis revealed that simply by including questionnaire scores (QIDS-SR, HADS-A, and neuroticism), age, and sex as additional features the cross-validated balanced accuracy increased to 76% (accuracy 81%, sensitivity 60%, specificity 91%). However, it should be noted again that the goal of this work was not to just maximise accuracy by any means possible but rather to show that estimated connectivity parameters contain sufficient information about depression status so that a prediction would be feasible.

6.4 Discussion

A generative embedding approach, combining DCM parameter estimates and a support vector machine classifier, was shown to be able to predict diagnosis of 53 lifetime depression participants versus 112 never-depressed healthy controls with a balanced accuracy of 72%. Data were collected at two separate collection sites. Participants performed a probabilistic reward learning task during fMRI scanning and a DCM was fitted to their behaviour and neuronal data (Chapter 5). Estimated parameters were used as features to train a machine learning classifier which resulted in good cross-validated predictive accuracy (70%), sensitivity (75%), and specificity (68%). The results show that estimated effective connectivity parameters contain information about depression status.

The identification of reliable and clinically useful biomarkers for objective diagnoses is an important goal in the field of computational psychiatry (Adams, Huys, and Roiser, 2016; Huys, Maia, and Frank, 2016). Neuroimaging has a lot of potential in this regard (Abi-Dargham and Horga, 2016; Stephan, Iglesias, Heinzle, and Diaconescu, 2015), and the current generative embedding work provides a proof-of-concept of how task-based fMRI data could be used for objective diagnosis.

In a clinical setting, it would arguably be most practical to use T_1-weighted structural scans for prediction. They are very quick to acquire (<5 minutes), do not require cooperation or understanding from the participant (other than not moving) and the necessary equipment and trained staff are already in place at sites with an

MRI scanner (Steele and Paulus, 2019). Using structural MRI scans, Costafreda, Chu, Ashburner, and Fu (2009) reported a diagnostic accuracy of 68% for 37 depressed patients versus 37 healthy controls. Predicting remission or non-remission after eight weeks of treatment of 18 patients who received antidepressant medication was possible with 89% accuracy. Prediction of CBT treatment outcome of 12 patients was however not possible (Costafreda, Chu, Ashburner, and Fu, 2009). A study including 23 refractory depressive disorder, 23 non-refractory depressive disorder, and 23 healthy control participants reported accuracies between 67% and 76% for the three between-groups classifiers (Gong, Wu, Scarpazza, et al., 2011). Using structural scans from two different sites, trained machine learning models were able to distinguish between 30 MDD patients and 32 controls with 90% accuracy (Mwangi, Ebmeier, Matthews, and Steele, 2012), and were able predict the patients' illness severity well (Mwangi, Matthews, and Steele, 2011). Johnston, Steele, Tolomeo, et al. (2015) reported 85% accuracy for the classification of 20 participants with lifetime depression versus 21 never-depressed controls using structural MRI.

Although these studies show there is promise in this approach, Abi-Dargham and Horga (2016) argued that many pathological features of psychiatric disorders may be elusive and not detectable using current neuroimaging techniques. While a diseased brain may appear typical at rest it may display abnormalities while performing a task (Abi-Dargham and Horga, 2016)—for example, effective connectivity may play an important role in depression (Chapter 5).

Task-based fMRI studies using whole brain functional images as features for machine learning have shown potential for diagnostic classification. An early study using the brain activity pattern during a sad-faces processing achieved 86% accuracy in the classification of 19 MDD patients versus 19 controls (Fu, Mourao-Miranda, Costafreda, et al., 2008), and in a subset of the data it was shown that 7 patients who responded to CBT could be distinguished from 7 non-responders with 79% accuracy (Costafreda, Khanna, Mourao-Miranda, and Fu, 2009). A later study included 19 treatment-resistant MDD patients and 21 healthy controls performing an instrumental reinforcement learning task (Johnston, Tolomeo, Gradin, et al., 2015). They showed that diagnostic classification based on fMRI contrast images of both win and loss events was possible with 84% and 97% accuracy respectively. A recent study by Bürger, Redlich, Grotegerd, et al. (2017) included 36 bipolar and 36 unipolar depressed patients and 36 healthy controls who performed an emotional face matching task. Classifiers based on contrast images achieved between 63% and 72% accuracy in distinguishing unipolar depressed participants from depressed bipolar patients or healthy controls (Bürger, Redlich, Grotegerd, et al., 2017).

It is worth noting that small studies often include homogeneous patient groups and confidence in the accuracy of the diagnosis can be high. Studies including large samples will usually include more heterogeneous groups which can increase generalisability to real world data even though accuracy will often be lower (Schnack

and Kahn, 2016). However, it is also worth emphasising that quality control is crucial which might sometimes be neglected in large studies (Johnston, Mwangi, Matthews, et al., 2013). While a routinely collected image may be acceptable for radiologists, small artefacts in the image, which can be caused by a participant's movement or non-optimal scanner setup, can have large effects on machine learning classifiers. Artefacts can increase inter-subject variance and might not be balanced between groups (Johnston, Mwangi, Matthews, et al., 2013).

The current study included a far greater number of participants than most previous studies and the data was collected at two different sites, making the results potentially more generalisable than previous work. It focused on the identification of lifetime (past or current) MDD rather than just current depression and highlighted that differences in effective connectivity may be a an important feature of depressive illness; perhaps indicating that abnormal connectivity is either a vulnerability factor or a (permanent) consequence of the disease. As the mean age of our sample was almost sixty (Table 5.1), and the typical age of onset of depression is much younger (Kessler and Bromet, 2013), it is tempting to conjecture that almost all lifetime MDD cases have already materialised.

To assess the importance of individual features we inspected the weights the classifier assigned to them. Results showed that a large number of network parameters were important for the diagnostic classification. A linear relationship between depression symptoms severity and the task-independent top-down connectivity from prefrontal cortex to ventral striatum was found using a hierarchical DCM approach (Chapter 5). Here, feature ranking indicated that this connection was not important for the prediction of lifetime depression. This might be surprising as both remitted and currently depressed patients usually report higher depressive severity, but notably, the correlation found in Chapter 5 was found to not just be an effect of group and the results in this chapter further support this notion.

Although the number of current-MDD patients was limited, we found that predictive accuracy was very similar for patients who were currently depressed and subjects who had previously experienced depression. This indicated it was not "easier" for the classifier to predict MDD (or greater severity of depression symptoms) and feature weights likely represent a more fundamental difference between never-depressed healthy participants and lifetime sufferers. Changes in connectivity might be related to greater susceptibility to depression or a consequence of the illness, but with the available data it is not possible to distinguish between these possibilities. Notably, compared to other clinical studies the severity of depression in our sample was mild and very few volunteers were long term patients. For example, Mwangi, Ebmeier, Matthews, and Steele (2012) only recruited treatment-resistant MDD patients with severe and enduring illness, making (identification of) brain structure abnormalities (c.f. Schmaal, Veltman, Erp, et al., 2016; Schmaal,

Hibar, Sämann, et al., 2017) more likely and therefore perhaps more applicable for automatic classification.

It is important to point out that the DCM region selection was performed using a combination of individual activation and brain anatomy but also whole group activation. This means left-out data influenced the region selection and therefore (indirectly) DCM parameter estimation of the training data. To get a completely unbiased estimate it would have been necessary to repeat region selection and DCM estimation for each left-out participant, which would have resulted in the estimation of $165^2 = 27225$ models. Given our large sample, the substantial computational time required (≈ 15 minutes to fit a single model), and the likely very small influence every individual participant had on region selection we did not go down this route. Importantly, the whole brain contrasts used for region selection were activations and not QIDS correlations and therefore did not include any information about depression severity or status. In Chapter 5 we included information about depression at the second level. For each participant we first estimated a single full DCM which included parameters for all the connections and modulations. We then took these parameter estimates to the group level where we included information about depression severity. QIDS was included as covariate and model comparison (and model reduction) was performed *on the second level*, meaning models with and without associations of connections with depression severity were compared. In the current chapter we only used the estimated DCM parameters from the full DCM of each participant without going to the group level.

We could have also incorporated a group model into the current work by first estimating a group model (with or without additional covariates such as QIDS) for each training fold and then using individual estimates constrained by this group prior as features for the classification. For each left out subject we would then first apply the group prior to re-estimate their DCM before using the parameters as features. This might be a fruitful path for future studies including less data. It should be noted that this makes the assumption that subjects are sampled from a single population distribution.

A fundamental challenge to the development of clinically useful biomarkers for psychiatry is the lack of gold standards for diagnoses (Abi-Dargham and Horga, 2016). In our case this issue might be further compounded by the fact that past or remitted MDD are even more difficult to diagnose accurately. Mourão-Miranda, Hardoon, Hahn, et al. (2011) showed how one approach to this might be to use a one-class approach in which patients are modelled as "outliers", although this does not provide any information about the specific diagnosis. Possibly the most promising approach for future work might be to include multiple groups displaying different pathological phenotypes.

Increasing evidence points towards connectivity abnormalities in the brain in depression (Chapter 5). Our work indicates that information about an individual's connectivity profile during a reward-based decision-making task could be used to predict their diagnosis with high accuracy. Importantly, it provides additional evidence for the importance of connectivity in the disease and highlights the potential of currently available data-driven approaches (see also Steele and Paulus, 2019). It also indicates that a patient's connectivity profile might contain other vital information related to their depression, for example which therapy would best be suited for them. Although that question would be of much greater interest to clinicians, the current data can not help answer it. However, the novel generative embedding approach incorporating effective connectivity parameters could readily be applied to a suitable data set. A longitudinal study might be a good way to approach this. Data collected at different time points, for example before the start of (different types of) treatments and a year later, could be used to train a model to predict an individual's probability of recovery given a specific treatment. Ethical concerns aside, this could then be used in a randomised doubly blinded control trial in which clinicians and the model prescribe treatment for different sets of patients to compare outcomes.

In conclusion, we found support for our hypothesis that a generative embedding approach to detecting lifetime depression is viable. A generative model (DCM) was fitted to fMRI data and its parameters were then used for diagnostic classification. Results showed that for best performance a large number of connectivity estimates were included during feature selection, indicating that lifetime depression is related to a large number of changes in whole-brain connectivity. Generative embedding approaches, combining effective connectivity models with machine learning models, might be promising not only for diagnosis but also prognosis of treatment outcomes.

Rank	Weight (median)	Feature
1	0.39	B(VA to VA, no-choice)
2	0.34	A(VA to VA)
3	-0.33	B(mPC to mPC, no-choice)
4	-0.32	B(VS to mPC, choice)
5	0.30	A(VA to mPC)
6	-0.24	B(VA to mPC, no-reward)
7	-0.24	B(VS to mPC, reward)
8	-0.24	A(VS to VA)
9	0.21	B(VA to VA, reward)
10	-0.20	B(mPC to mPC, no-reward)
11	0.19	B(VA to VS, no-choice)
12	-0.18	A(mPC to VA)
13	0.18	B(VS to mPC, no-choice)
14	0.16	B(VA to mPC, reward)
15	0.15	A(mPC to mPC)
16	-0.14	B(VA to VS, choice)
17	0.13	B(mPC to VS, choice)
18	-0.12	B(mPC to VA, reward)
19	-0.12	B(mPC to VA, no-choice)
20	-0.11	A(VA to VS)
21	0.10	B(VA to VA, no-reward)
22	-0.10	B(VA to VS, no-reward)
23	-0.08	B(VS to VA, no-choice)
24	0.08	B(VA to VA, choice)
25	-0.07	A(VS to mPC)
26	0.06	B(VA to mPC, choice)
27	-0.06	B(VA to mPC, no-choice)
28	-0.05	B(VS to VA, reward)
29	-0.04	B(VS to VS, reward)
30	-0.04	A(VS to VS)
31	0.04	B(VA to VS, reward)
32	0.03	B(VS to VS, no-reward)
33	0.03	B(mPC to mPC, choice)

TABLE 6.1: Ranking of features. Median weights were calculated across classifiers and features were then ranked according to the absolute weight. Features not included in this table had a median weight of zero.

Chapter 7

Discussion

In this thesis I described my contributions towards improving the scientific understanding of depression. A computational approach was used, employing mathematical models to describe decision making behaviour and neuronal activity. Evidence was reported supporting the notion that depressive symptomatology is associated with individual differences in behaviour and brain function.

Chapter 2 reviewed the literature from a computational perspective, aiming to be accessible for students. Major depression, its symptoms and diagnosis, and theories about biological bases were described. Previous studies incorporating computational models, including neural network, drift diffusion, and reinforcement learning models, were then reviewed. A case study, relating reward learning to the core depression symptom anhedonia, was described in detail.

Chapters 3-4 described the investigation of value-based decision-making abnormalities in major depressive disorder. A novel experimental task was performed by a group of unmedicated patients suffering from major depressive disorder and a group of matched healthy control participants during fMRI scanning. Fractal images were displayed, followed by a binary outcome picture indicating "reward" or "no-reward". Based on four observations for each type of fractal, subjects were asked to estimate the probability of reward. For example, if a fractal was followed by reward three times and followed by no-reward once, they were expected to estimate the probability of reward as $3/4 = 75\%$. During intermittent decision trials a choice (in favour of the higher number) between this estimated probability and an explicit probability, for example 65%, had to be made. In Chapter 3 the behavioural and computational modelling analysis was described. Multiple models, representing distinct hypotheses about participants' learning, were fitted to the data and the best model was chosen using formal model comparison. Results indicated that the patient group was characterised by behavioural impairments during both the passive observation (value estimation) phases and the active decision making trials. Depressed subjects displayed lower memory or increased discounting of previous value estimations and their ability to use their value estimations to make decisions appeared diminished.

The following Chapter 4 was devoted to the analysis of the neuronal basis of the groups' behaviour. Model-free fMRI analysis was used to replicate results of previous studies showing blunted reward activation in the striatum in depression. At decision time a mid-cingulate cortex (aMCC) region, an area crucial for decision making, showed increased activity in depression. The best-fitting computational model of behaviour was simulated, given the estimated parameters of individuals, to generate value signals for use in model-based fMRI analysis. Positive value encoding was larger in controls compared to patients in areas notably including (para-)hippocampus and rostral anterior cingulate (rACC). Within the latter region there was a significant negative correlation between patients' illness severity and the strength of their value encoding signal. A logistic regression classifier was able to correctly predict diagnostic status of 27 out of 34 (79%) participants just from the encoding signal strength of the two regions. Importantly, there is compelling evidence for the involvement of prefrontal regions in internal value representation in healthy subjects (Gläscher, Hampton, and O'doherty, 2008; Bartra, McGuire, and Kable, 2013). Decisions were modelled, as is common, by assuming that a choice between two options depended on the difference between the values of the two options. This was formalised by applying a softmax decision function, including a steepness of temperature parameter, to the difference of individuals' estimated fractal value and the alternative explicit numeric probability value. Further linking the behavioural model to localised brain function, there were significant value difference encoding signals in aMCC and rACC across participants. MDD patients displayed reduced connectivity between aMCC and rACC regions, suggesting impairments in the communication and use of reward value estimates related to these rostral and dorsal prefrontal regions in depression.

Hence Chapters 3 and 4 provided support for the hypotheses of abnormal reward learning function in major depressive disorder. Behaviour and fMRI revealed group differences which were related to abnormal reward valuation in MDD. A number of brain regions were highlighted, prominently including ventral striatum and ventral and dorsal prefrontal cortex regions.

Chapter 5 included data from a large community-based sample of individuals who performed a novel reward-based learning task. In each trial participants had to choose between a yellow and a blue square stimulus which were associated with different reward probabilities. However, subjects were only allowed to choose for themselves in half of the trials and had to follow the computer's choice otherwise. A dimensional approach was chosen for the analysis, in line with recommendations from the Research Domain Criteria (RDoC; Insel, Cuthbert, Garvey, et al., 2010), looking at variation across different levels of illness severity. Replicating a number of previous studies, it was found that increased mood symptoms were associated with decreased reward signals in regions including the striatum. Results of a Dynamic Causal Modelling (DCM) analysis showed that effective connectivity between basal

ganglia and prefrontal cortex was related to mood symptoms. Specifically, increased depression symptom severity was associated with decreased top-down medial prefrontal cortex to ventral striatum connectivity. Importantly, various theories about depression have proposed that abnormal cortical-limbic connectivity plays an important role and these results provided important supporting evidence using an effective connectivity analysis based on a community-based sample.

Chapter 6 presented a novel generative embedding approach to detecting lifetime depression. Estimated DCM parameters were used as features for a support vector machine classifier which achieved a balanced accuracy of 72%. The proof-of-concept study showed how combining a theory-driven model with machine learning methods may allow for accurate prediction of diagnoses. Furthermore, it also provided novel support for the supposition that major depression is related to (information contained within) effective connectivity. The identification of objective biomarkers is an important goal of computational psychiatry and neuroimaging based biomarkers are especially promising in a clinical setting (Abi-Dargham and Horga, 2016). It is conceivable that parameters of computational models of behaviour showing abnormalities in MDD (c.f. Chapter 3) might be especially useful in other settings. For example, automated assessment or screening to decide who should come into the clinic for further assessment.

It is worth highlighting a few shared limitations. Depression comes in many shapes, forms and severities. Two MDD patients could experience almost entirely different sets of symptoms owing to the fact that a standard diagnosis is mostly based on clinical consensus without good understanding of the biological basis (Chapter 2). While mild depression can be difficult to distinguish from normal everyday mood swings, patients with moderate to severe depression will display more symptoms with higher impact than what is required as minimum for diagnosis. It is crucial to study the full range of emotions as is emphasised by approaches such as RDoC and it is also important to realise that severe and/or treatment-resistant depression might be more than just "mild depression but slightly more extreme". There might be similar differences between mild and severe depression as there are between healthy and mild-moderate depression (Otte, Gold, Penninx, et al., 2016) and there are discussions about the possibility that treatment-resistant MDD might be a unique subtype of depression (Fagiolini and Kupfer, 2003). While both pharmacotherapy and psychotherapy are recommended treatment options for mild and moderate depression, only medication treatment might be effective and is recommended for patients with severe depression (Otte, Gold, Penninx, et al., 2016; National Institute for Health and Care Excellence (NICE), 2010). It is therefore worth emphasising that the results in this thesis are based on moderate depression (Chapters 3-4) and mild/subthreshold depression symptoms (Chapters 5-6).

Severely depressed patients are especially hard to recruit into studies because they are less common and by definition very unmotivated. In addition they are

usually medicated and it would be unethical to stop the therapy, and comorbidity is likely (Otte, Gold, Penninx, et al., 2016). This means studies including treatment-resistant severely depressed patients (e.g. Steele, Kumar, and Ebmeier, 2007; Mwangi, Ebmeier, Matthews, and Steele, 2012) necessarily include smaller samples but confidence in diagnosis is increased and the group will be much more homogeneous. The likelihood of detectable brain function and structure abnormalities is also higher which might be a partial explanation for higher diagnostic accuracy (e.g. Mwangi, Ebmeier, Matthews, and Steele, 2012) in smaller machine learning studies (Schnack and Kahn, 2016). However, larger machine learning studies such as the one described in Chapter 6 which included a relatively heterogeneous[1] sample will have larger generalisability at the cost of lower accuracy (Schnack and Kahn, 2016; see also discussion in Chapter 6).

The analysis of fMRI relied on many underlying assumptions and parameter settings. For example, it was assumed that BOLD signal reflects cognition and that the general linear modelling approach is sensible. Parameter settings affect a variety of things such as the amount of spatial smoothing or which brain template to use for spatial normalisation. In this thesis standard SPM settings (and its subjacent assumptions about neurophysiology and analysis strategy) were used as much as possible and it is reassuring that when alternative settings were explored they usually yielded very similar results. Regarding the computational modelling of behaviour we made the assumptions that all participants' parameters were sampled from the same group prior which was empirically estimated (see Chapter 3 and Appendix A for details). One big advantage of this approach is that it can improve parameter estimation and suppress outliers. However, it would also be reasonable to assume that, for example, patients and controls would be better modelled using separate prior distributions. In principle this would be straightforward to address using formal model comparison (i.e. comparing a model using a single prior versus a model using two separate priors). In practice this raises questions whether there should be also be different priors for individual parameters (as opposed to the whole set of parameters) and how to address the co-variance of parameters across different priors. In addition, studies, such as the one described in Chapter 5, might include participants which would not clearly fall into either a patient or a control group.

This thesis was written within the context of the brain's positive reinforcement or reward system. As discussed in Chapter 2, depression is strongly associated with abnormalities in reward processing and its sub-domains. However, there is good evidence that aversive processing is also impaired in depressive illness. Although an omission of an expected reward may be felt as punishing, reward and punishment processing likely involve different neuronal bases (Chen, Takahashi, Nakagawa, et al., 2015). It has been suggested that in addition to decreased reward

[1] The study included subjects with a range of depression symptom severities but was still homogeneous in the sense that it primarily included "old, white, Scottish" participants.

processing depression is also characterised by increased aversive processing (Chen, Takahashi, Nakagawa, et al., 2015; Johnston, Tolomeo, Gradin, et al., 2015). Indeed, most initial major depressive episodes follow a major negative life event (Pizzagalli, 2014). The most common antidepressants work by altering serotonin levels in the brain (Eshel and Roiser, 2010) and the neurotransmitter has long been implicated in aversive processing (Deakin, 2013). The presented results should therefore be seen as implicitly conditioned on a reward processing context. For example, the DCM analysis focused on "task-independent" connectivity, as opposed to the "task-dependent" driving inputs and modulations, but although the DCM framework (attempts to) divide connectivity in this way, the results are still dependent on the context of the task.

In the case study (Chapter 2) I described how the absence of expected reward could be perceived as punishment. Huys, Pizzagalli, Bogdan, and Dayan (2013) included this in one of their models by adjusting the reward prediction error depending on presence or absence of reward. The model included two separate sensitivity parameters scaling reward and no-reward outcomes. Similarly, Chapter 3 included models which tested whether learning was different following reward versus no-reward ("punishment"). Two different learning rate parameters were included which scaled the prediction error depending on the outcome. These experiments could potentially be translated into the punishment domain in a straightforward way, by changing the outcome to zero points (positive outcome) or a loss of points (negative outcome).

Depression seems to be characterised by an abnormal response to negative feedback (Eshel and Roiser, 2010). This reaction can either be a hypersensitivity or a "catastrophic response" to failure (Beats, Sahakian, and Levy, 1996; Tavares, Clark, Furey, et al., 2008), or it could indicate a difficulty to learn from negative outcomes (Eshel and Roiser, 2010), depending on the context or type of punishment. However, associations between increased decision-making performance during tasks with the goal of punishment minimisation have also been reported (Beevers, Worthy, Gorlick, et al., 2013). Katz, Matanky, Aviram, and Yovel (2020) reported meta-analytic evidence for enhanced punishment sensitivity in both depression and anxiety, but altered reward sensitivity only in depression. Depression and anxiety are highly comorbid (Watson, 2009), and anxiety is especially common in more severe depression (Kessler, Chiu, Demler, and Walters, 2005). The two disorders also represent risk factors of each other, and share some symptoms and basic mechanisms (Katz, Matanky, Aviram, and Yovel, 2020).

As discussed in Chapter 1, analysis of the brain can be done at different levels of analyses. Although largely ignored in this thesis, biophysical computational models of major depression do exist (Mäki-Marttunen, Kaufmann, Elvsåshagen, et al., 2019). For example, Ramirez-Mahaluf, Roxin, Mayberg, and Compte (2017) showed how a

change in neurotransmitter uptake could cause aberrant activity in cortical regions, and how simulated clinical treatments could counteract this.

Other environmental conditions and lifestyle factors not discussed in this thesis have been shown to influence (and be influenced by) depression symptoms. For example, sleep, diet, and exercise play important roles in the development, progression and treatment of depression (Lopresti, Hood, and Drummond, 2013). Treatment of insomnia may prevent the development of depression (Alvaro, Roberts, and Harris, 2013). Depression symptoms have been shown to be associated negatively with Mediterranean diet and positively with the high consumption of sweets, fast food, and processed pastries (Lopresti, Hood, and Drummond, 2013). Although inconclusive, there is some evidence for the efficacy of exercise as therapy for depression (Cooney, Dwan, Greig, et al., 2013).

In this thesis variations of a "two-alternative forced choice" task were used, in combination with reinforcement learning, to study decision making. Participants were presented with two options and had to choose one of them within a small time frame. An outcome was then presented from which subjects could learn. An association between major depression and behavioural differences in one of the tasks was found (Chapter 3), but there did not appear to be an association between depression symptom severity and performance during a different task (Chapter 5). Notably, a number of previous fMRI studies reporting significant differences in brain activity did not find behavioural differences between groups of MDD patients and healthy controls (Gradin, Kumar, Waiter, et al., 2011; Johnston, Tolomeo, Gradin, et al., 2015). Differences in brain function in the absence of (statistically significant) behavioural effects might indicate compensatory mechanisms but it is unclear when and how exactly such mechanisms work—and why sometimes they do not. Furthermore it is not always obvious how behaviour during studies within an artificial experimental environment maps onto behaviour in the real world. This artificial nature of tasks might be especially pronounced during fMRI scanning where subjects are put into a tight, uncomfortable tube, commonly with their head fixed and are asked to lie very still (Muehlhan, Lueken, Wittchen, and Kirschbaum, 2011). It is also possible that the effects of such an aversive environment are greater for MDD patients compared to healthy participants.

It will be important to study depression in ecologically valid environments. A recent study utilised smartphones to collect data during real world activities and showed how this data may be used to predict changes in users' depression symptom severity (Canzian and Musolesi, 2015). Smartphone applications have great potential for disease screening, monitoring and managing (BinDhim, Shaman, Trevena, et al., 2015) although in their review about mobile apps offering support for depressed users Huguet, Rao, McGrath, et al. (2016) found that current efficacy is questionable. Further studies about how to improve effectiveness and usability while increasing participants' engagement and minimising dropout are needed.

Ultimately one of the most important goals of depression research is to develop effective treatments but better understanding of the disease is needed. Neural substrates and associated abnormalities need to be reliably identified in patients so they can be translated to animal models. These can then be used to screen novel antidepressants. The computational psychiatry approach promises to lead to many new insights into neurobehavioural mechanisms and aid in the discovery of novel therapeutic targets. While applied computational psychiatry and drug discovery will likely still require many years of research, it has been argued that currently available neuroscience techniques can and should be used today (McGuire, Sato, Mechelli, et al., 2015; Steele and Paulus, 2019). This requires additional training for psychiatrists and a collaborative effort with stakeholders, politicians and funding agencies and a general cultural change (Steele and Paulus, 2019; McGuire, Sato, Mechelli, et al., 2015). Importantly, this also means that NHS psychiatric services need to routinely collect quantitative data from individual patients (Steele and Paulus, 2019). Objective clinically useful predictions for individual patients are possible using machine learning techniques (Steele and Paulus, 2019) and they, maybe for the first time in over half a century, give hope for tangible clinical progress.

And so I will end this thesis the same way it began; with a quote from William Styron. But this time it endows us with hope. The hope that depression is not the end. The hope that restoration is possible. The hope of a return to the shining world.

> *"For those who have dwelt in depression's dark wood, and known its inexplicable agony, their return from the abyss is not unlike the ascent of the poet, trudging upward and upward out of hell's black depths and at last emerging into what he saw as 'the shining world.' There, whoever has been restored to health has almost always been restored to the capacity for serenity and joy, and this may be indemnity enough for having endured the despair beyond despair.*
>
> E quindi uscimmo a riveder le stelle.
> And so we came forth, and once again beheld the stars."
>
> — William Styron, Darkness Visible: A Memoir of Madness

Appendix A

Supplementary Materials for Chapter 3

This chapter contains the Supplementary Materials for Chapter 3 which was published as S. Rupprechter, A. Stankevicius, Q. J. M. Huys, J. D. Steele, et al. (2018). "Major Depression Impairs the Use of Reward Values for Decision-Making". In: *Scientific Reports* 8.13798.

Supplement

Major depression impairs the use of reward values for decision-making

S. Rupprechter, A. Stankevicius, Q. J. M. Huys, J. D. Steele, P. Seriès

Experiment Details

First, personality and clinical questionnaires were filled out and an interview was conducted, which lasted approximately one hour. This was followed by a training session lasting between 10 and 20 minutes. Final 15 minutes of preparation included subjects changing and a safety check by the NHS personnel. Scanning lasted approximately 50 minutes and the experiment ended with a 5 minutes debriefing session and monetary reimbursement. Every participant was paid £20. Their scores were converted into a percentage and rounded up. Performance-dependent bonus was defined as that percentage number divided by ten, so for example if they correctly responded in 66% of trials, they would receive an additional £7.

The 60 trials were divided into 4 periods, which again were split into three blocks each. After each period (every 15 minutes), there was a brief rest period. In each block, participants observed five different fractals exactly four times and made 5 decisions. Fractals were presented for 3 to 4 seconds and outcomes for 2.5 to 3.5 seconds. Decisions had to be made within 5 seconds. Null events (blank screens without interaction) and decisions (responding to a simple response prompt) were sometimes displayed (between 1.25 and 7.5 seconds) to obtain a baseline of brain activity.

Other modifications from the original task of Stankevicius et al. (6) included the display of the reward as a pound symbol instead of a treasure chest and simplified instructions that were more accessible to people suffering from depressive symptoms.

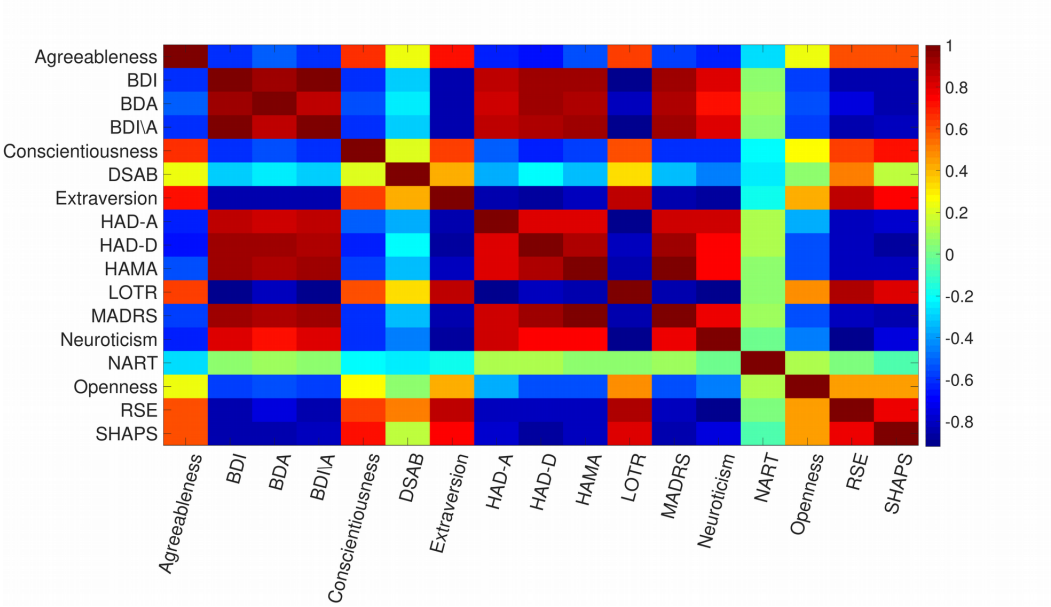

Figure S1. Correlation matrix of questionnaire scores of the fMRI dataset. As expected, questionnaire scores are often correlated with on another. See the section about additional analysis details below for more information about correlations between beta, neuroticism and other questionnaire scores.

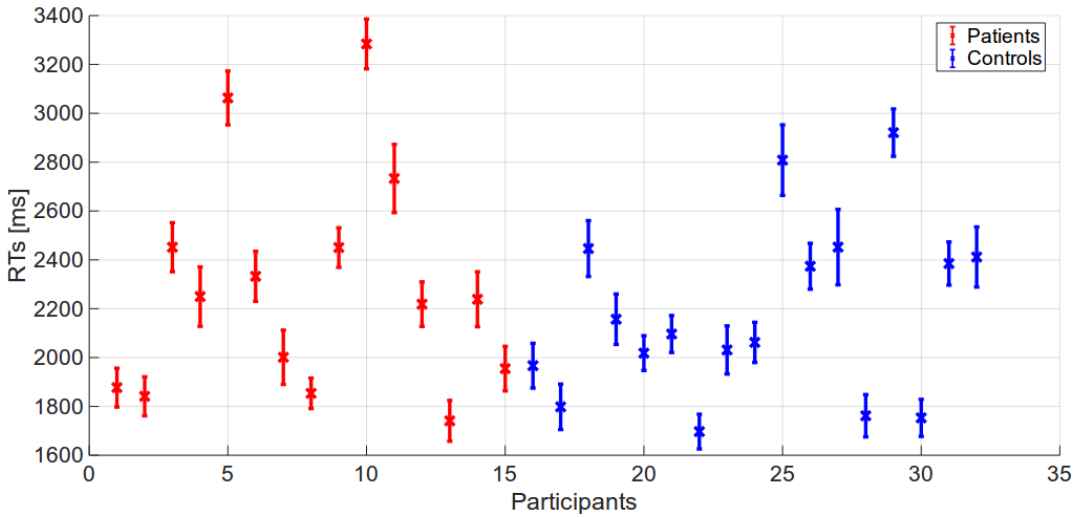

Figure S2. Average reaction times of participants in the fMRI dataset. Error bars represent standard errors. Mean response times were not significantly different between groups (Welch's t-test; t(26.6) = 0.692, p = .495).

Questionnaire	**Patients**	**Controls**	**Score Range**	**p-value**
fMRI dataset				
BDI	24.7 ± 13.1	4.2 ± 5.6	0 – 63	< 0.001
BDA	4.8 ± 2.9	0.5 ± 0.9	0 – 12	< 0.001
BDI\A	19.9 ± 10.8	3.7 ± 4.8	0 – 51	< 0.001
DSAB	15.0 ± 4.0	18.1 ± 2.7	0 – 24	0.013
HAD-A	12.3 ± 5.2	4.2 ± 2.3	0 – 21	< 0.001
HAD-D	8.6 ± 4.8	1.4 ± 2.1	0 – 21	< 0.001
HAMA	17.3 ± 7.0	1.4 ± 2.6	0 – 56	< 0.001
LOT-R	9.1 ± 5.5	18.4 ± 3.1	0 – 24	< 0.001
MADRS	17.7 ± 6.6	1.4 ± 2.6	0 – 60	< 0.001
NART	46.8 ± 4.2	46.6 ± 3.2	0 – 50	0.873
RSE	13.5 ± 6.9	24.5 ± 4.9	0 – 30	< 0.001
SHAPS	37.8 ± 8.5	49.6 ± 6.0	14 – 56	< 0.001
Agreeableness	39.5 ± 7.2	46.7 ± 5.9	12 – 60	0.004
Conscientiousness	36.3 ± 10.5	45.1 ± 7.0	12 – 60	0.008
Extraversion	30.5 ± 8.1	44.5 ± 5.2	12 – 60	< 0.001
Neuroticism	46.3 ± 7.1	29.8 ± 8.0	12 – 60	< 0.001
Openness	41.1 ± 5.1	46.5 ± 4.4	12 – 60	0.003
Pilot dataset				
BDI	27.7	10.1 ± 12.2	0 – 63	-
DSAB	13.7	14.8 ± 3.9	0 – 24	-
HAD-A	9.0	11.1 ± 3.5	0 – 21	-
HAD-D	7.3	8.4 ± 1.5	0 – 21	-
HAMA	18.0	5.1 ± 7.1	0 – 56	-
LOT-R	9.3	14.5 ± 5.5	0 – 24	-
MADRS	18.0	5.1 ± 7.1	0 – 60	-
NART	45.3	44.0 ± 11.3	0 – 50	-
RSE	18.7	9.5 ± 6.6	0 – 30	-
SHAPS	7.7	7.0 ± 1.1	14 – 56	-
Agreeableness	43.0	45.0 ± 5.8	12 – 60	-
Conscientiousness	32.0	43.3 ± 8.2	12 – 60	-
Extraversion	27.7	41.6 ± 6.9	12 – 60	-
Neuroticism	50.7	34.4 ± 11.5	12 – 60	-
Openness	46.7	46.2 ± 6.3	12 – 60	-

Table S1. Summary of questionnaire scores of participant groups and p-values for Welch's t-tests (fMRI dataset). Due the small number of patients included in the Pilot dataset, we did not calculate standard deviations for them and did not perform t-tests. BDI = Beck Depression Inventory; DSAB = Digit Score Part B; HAD = Hospital Anxiety and Depression Scale; HAMA = Hamilton Anxiety Rating Scale; LOT-R = Life Orientation Test – Revised; MADRS = Montgomery-Åsberg Depression Rating Scale; NART = National Adult Reading Test; RSE = Rosenberg Self-Esteem Scale; SHAPS = Snaith-Hamilton Pleasure Scale; Scores displayed as mean ± std.

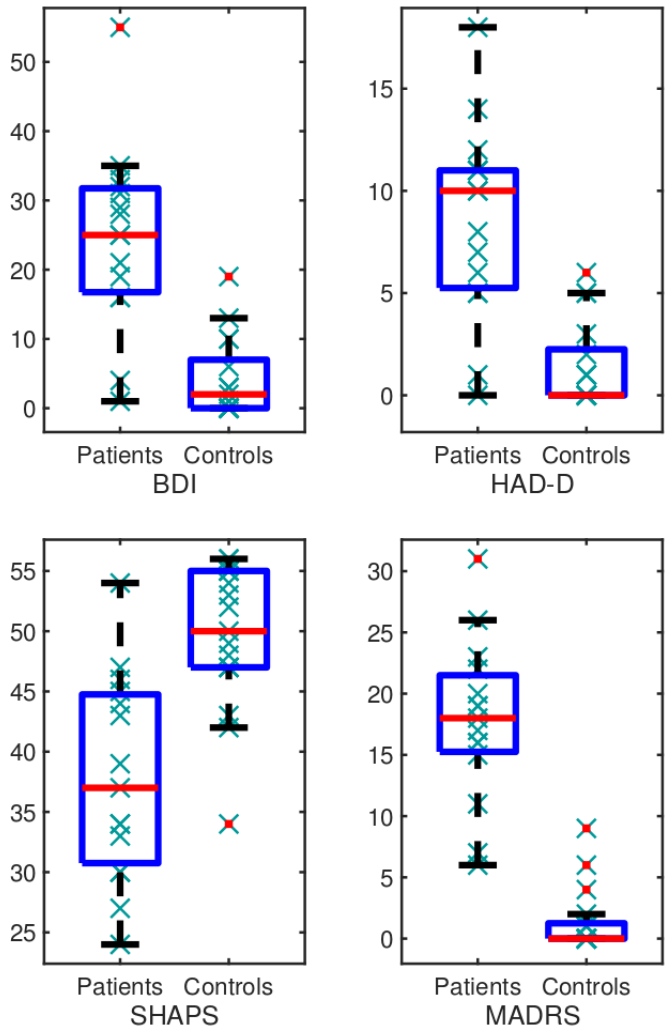

Figure S3. Boxplots of four questionnaires assessing depressive symptom severity (fMRI dataset). Patients had significantly higher scores than controls on the three scales measuring depressive severity (BDI, HAD-D, MADRS) and significantly lower scores on SHAPS, which measures pleasure (see Table S1).

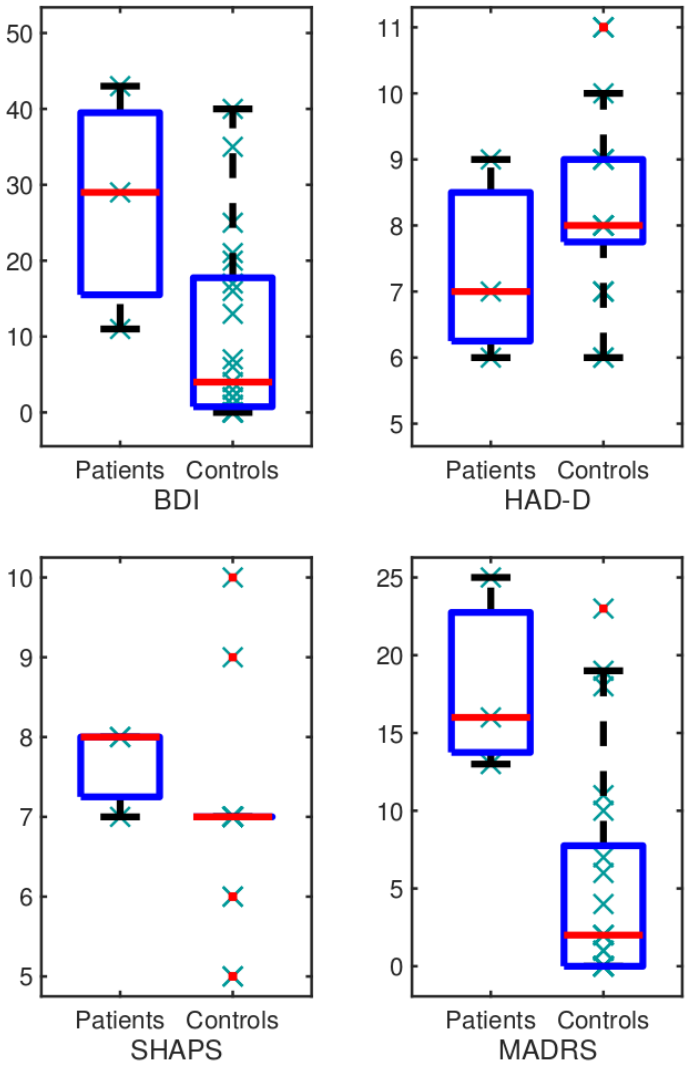

Figure S4. Boxplots of four questionnaires assessing depressive symptom severity (Pilot dataset). Note that the Snaith-Hamilton Pleasure Scale (SHAPS) was scored differently here: Each answer was scored either as zero (for two of the four possible answer options) or one (two alternative options), instead of scoring it one through four.

Additional Analyses Details

For our winning model we also tested whether our groups were better described using a shared population prior or separate priors for each group. Our data (fMRI dataset) was best described using a single population prior (ΔiBIC = 13.5).

Estimated model parameters were compared between groups using a Wilcoxon rank sum test which does not require an assumption of normality. (We used MATLAB's jbtest and lillietest to test for normality. In both cases the tests rejected the null hypothesis that the data comes from a normal distribution for the memory parameter for one of the groups, but not for the beta parameter. Using Welch's t-test instead gave us an almost identical result in terms of p value for the beta parameter.) Pearson correlation analysis across groups was performed, for which we reported classical p values. Below, we additionally used a Bayesian hypothesis test (1). A Bayes factor (BF10) larger than 3 indicates substantial evidence in favour of the alternative hypothesis (presence of a correlation). Classical p values may overestimate the evidence against the null hypothesis (2), but are also reported. All analyses were performed in MATLAB (R) R2017a (The MathWorks, Inc., Natick, MA).

Additional correlations with beta

Neuroticism was significantly negatively correlated with the inverse temperature parameter (r = -0.491, p = .004) across groups in the fMRI dataset (Figure S5). Because it is possible that this correlation is a function of group differences, we performed additional analyses taking into account group and also included our Pilot dataset after separately fitting the Leaky model. After controlling for group in the fMRI dataset, there was a non-significant but trending negative relationship between beta and neuroticism (r=-0.301, p=.100). This is unsurprising because the majority of our controls scored low in neuroticism, while most of our patients scored high. After controlling for group in the Pilot dataset, there was a significant negative correlation between beta and neuroticism (r=-0.433, p=0.039). Note that this dataset includes several control participants who scored high on neuroticism. In the pooled data, we again found a significant negative relationship between beta and neuroticism (t=-2.986, p=.004) after controlling for group and dataset version. Similarly, there was a significant negative relationship between beta and neuroticism (t(35)=-2.679, p=.011) combining only the control participants of both datasets, controlling for dataset version (reported in the main text). There was no significant correlation within the combined patients after correcting for dataset version (t(15)=-1.082, p=.297).

In the fMRI dataset (but not the Pilot dataset) there were also (weaker) positive correlations between β and extraversion (r = 0.423, BF10 = 2.46, p = .016), RSE (r = 0.410, BF10 = 2.01, p = .020), and LOT-R (r = 0.382, BF10 = 1.38, p = .031) scores, with this being at an "anecdotal" level of evidence (BF10 < 3). Since these scores were negatively correlated with neuroticism (Figure S1), we performed additional analyses to check whether neuroticism was the driving factor in these correlations and concluded that it was indeed so:

We fitted an additional general linear regression model (using MATLAB's fitglm) including coefficients for neuroticism, extraversion, RSE, LOT-R, group membership and dataset version to the combined dataset. None of the coefficients were significant, but the p-value for neuroticism shows a trend (t=-1.826, p=.074), while all other coefficients were non-significant (p > 0.6), indicating that neuroticism should be the variable of interest (Table S2).

Model 1: `Beta ~ 1 + Neuroticism + Extraversion + RSE + LOTR + Group + Dataset`

We then created a linear regression model by stepwise regression (stepwiseglm), starting from the above Model 1, using the differences in the deviances of models as the criterion. Predictors where removed (stepwise) if the deviance was greater than 0.05 and only neuroticism remained in the final model (t=-3.286, p=.002):

Model 2: `Beta ~ 1 + Neuroticism`

This shows that indeed neuroticism is the variable of interest and was the driving factor for the correlations between the other variables and beta in the fMRI dataset and suggests a possible link between participants' neuroticism and their difficulty in making decisions based on their internal value estimations across groups.

Coefficient	**t**	**p**
Neuroticism	-1.826	**0.074**
Extraversion	-0.321	0.749
RSE	-0.290	0.772
LOT-R	0.367	0.715
Group	-0.437	0.664
Dataset Version	-0.510	0.612

Table S2. Results of t-tests on individual coefficients of Model 1.

Optimism and previous results

The original Life Orientation Test (LOT) was revised (3) to the current form (LOT-R) after criticism that LOT scores could not be distinguished from neuroticism scores and correlations with optimism disappeared when controlled for neuroticism (4). However, it has been shown that even these LOT-R scores are not independent from neuroticism scores (5). After re-analysing the published data from Stankevicius et al. (6) using the methods described here (see Model Fitting Procedure), we were not only able to confirm that LOT-R scores corresponded to a prior belief about rewards ($r = .524$, $p < 0.001$), but also found that neuroticism was similarly related to a (negative) prior belief ($r = -.327$, $p = 0.019$).

In the present fMRI data, the prior mean did not significantly correlate with LOT-R ($r=-0.255$, $p=.159$) nor with neuroticism ($r=0.322$, $p=.072$), nor with the first principal component of our questionnaires measuring depression severity ($r=0.115$, $p=.532$), nor with any of the individual depression questionnaire scores (BDI, HAD-D, MADRS, SHAPS), suggesting that neither optimism, nor neuroticism, nor depression biased participants towards choosing a certain option.

We do not know for certain why we were unable to directly replicate previous results, but we have several hypotheses and are planning to address this in future work. Overall, we think that we introduced too many important changes from the original experiment and so the tasks are not directly comparable any more: In our Pilot and fMRI experiments, trials lasted a lot longer than in the published task (several seconds instead of fractions of a second). This was necessary to be able to capture the BOLD response during scanning, but initially made the task too easy. We tried to compensate for that by reducing the space of possible differences between the probability of reward associated with the two targets (-30% to 30% instead of -100% to 100%), which introduced much more uncertainty in the decisions. It is likely that the scanner induced additional uncertainty and pressure and so overall the task was very hard.

There were other differences as well: Each fractal was observed a variable number of times in the published data, while in the novel tasks each fractal was observed exactly four times. While participants only performed a short trial version of the task in the original version, here we trained our subjects extensively (between 10 and 20 minutes) before the main experiment. In addition, (a) there might be trait-cohorts interactions, (b) we might not have enough participants to reliably find the effect, (c) the saliency of the rewards might have been different (empty or full treasure chest versus a pound symbol or empty screen), and (d) the performance-related monetary reward the participants received after the experiments was different and likely led to differences in motivations.

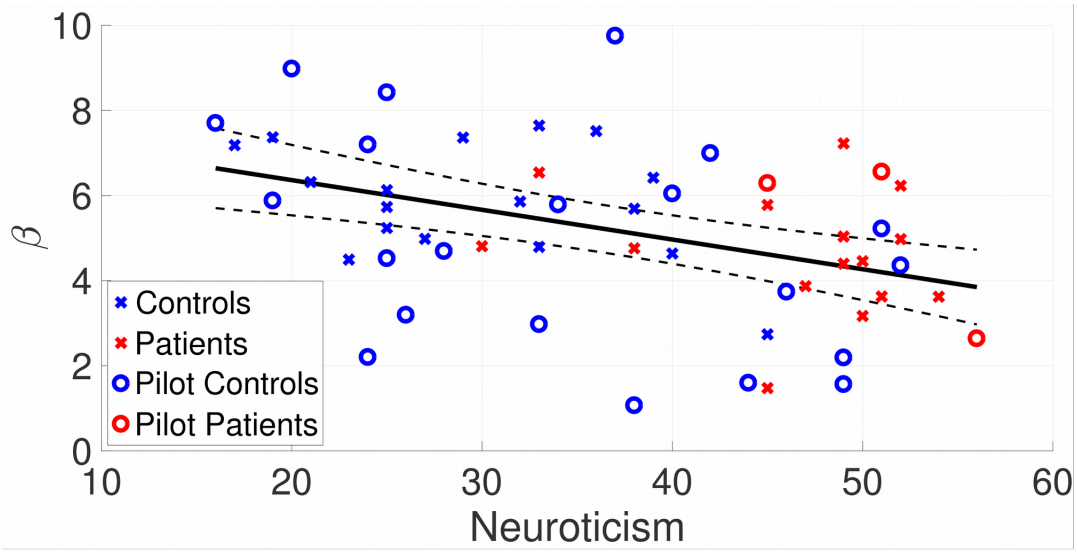

Figure S5. A scatter plot of neuroticism and β, a parameter in our best fitting Leaky model capturing participants' ability to follow internal value estimations, and their correlation across patients and control subjects of both datasets (shown without controlling for group or dataset version: r=-0.408, p=.002; regression line with 95% confidence interval; after controlling for both group and dataset version: t=-2.986, p=.004).

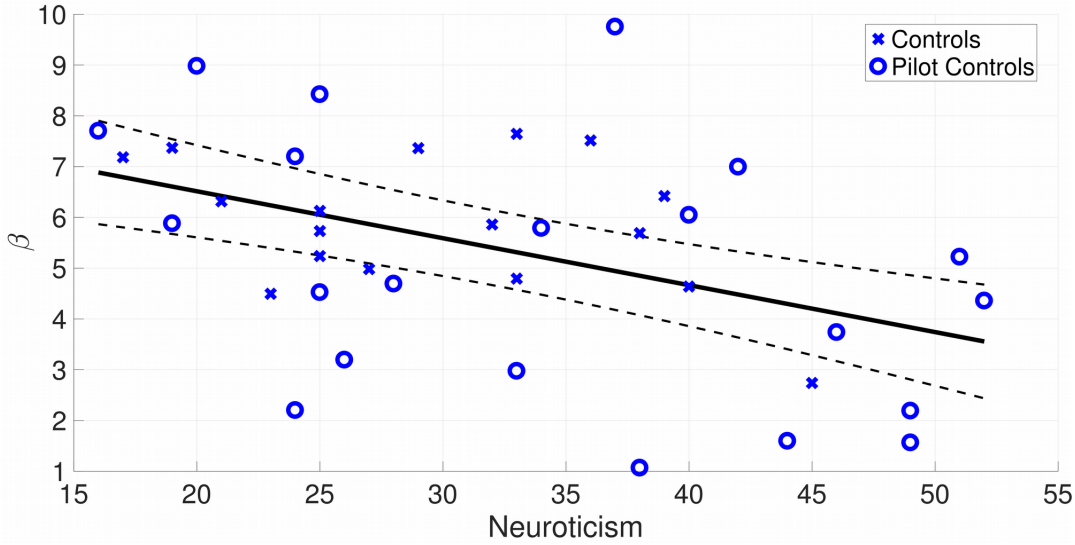

Figure S6. A scatter plot of neuroticism and β, a parameter in our best fitting Leaky model capturing participants' ability to follow internal value estimations, and their correlation across control subjects of both datasets (without controlling for dataset version; regression line with 95% confidence interval).

Bayesian model

The Bayesian model was introduced in detail by Stankevicius et al. (6). We briefly describe it here for completeness:

At each decision point, participants are assumed to know how often the fractal *i* used in the decision was shown (N_i) and how often it was followed by reward (n_i). It is further assumed that subjects behave as Bayesian observers and use Bayes rule to compute a posterior, from which they extract the mean to make decisions. The prior is modelled as a Beta distribution, which is conjugate to the binomial distribution. It can be shown that the posterior mean takes on the following form:

$$m_i = \frac{n_i+\alpha}{N_i+\alpha+\beta}$$

where alpha and beta control the shape of the Beta distribution. The mean is then plugged into a softmax function to obtain the probability of choosing fractal *i* as in the other models:

$$\sigma(\gamma(m_i - \phi_i))$$

Reward Sensitivity

In previous work (12), the inverse temperature parameter has also been interpreted as reward sensitivity and it has been argued that in some cases it can be substituted exactly for a reward sensitivity parameter (9) in a RL model. This however only holds when all options in the softmax are estimated from observed rewards, which is not the case here, as we show in an example:

In our model, on the first timestep we will have $V^{(1)} = \rho r^1$. After the second timestep we will have $V^{(2)} = A V^{(1)} + \rho r^{(2)}$ which we can rewrite as $V^{(2)} = \rho \left(A r^{(1)} + r^{(2)} \right)$. In general, after each step we will have a V value that is a combination of A and r scaled by ρ . Within the softmax function there is a subtraction term $x - y$ which is multiplied by β . This can be rewritten as $\beta x - \beta y$, which means that the β parameter scales both x and y , just as ρ would scale each of the variables *if they are both estimated on a trial-by-trial basis*. However, if one of these values is instead fixed (as is the case for our explicit probability), ρ will only scale one of the variables, while β will still scale both of them, which makes the parameters distinguishable.

Our beta parameter should therefore not be interpreted as being equivalent to a reward sensitivity parameter. In our model, a high inverse temperature likely indicates that participants were able to perform better in the highly uncertain environment and put more trust in their own estimations. Lower beta values indicate that participants put less trust in their estimations and chose more randomly. It is perfectly possible (and given previous research it is indeed likely) that patients were less reward sensitive than controls, and some of this difference may be captured by the beta parameter. It is, for example, possible that patients put less trust in their estimations because they were less sensitive to the rewards in the first place, but this is not explicitly modelled here. To reliably distinguish beta from reward sensitivity, we would need an additional reward sensitivity parameter, which we included in one of our models (Leaky-rho). However, model comparison did not reveal this to be the most parsimonious model and so we did not pursue this further.

Model Simulations

We provide additional mesh plots where we simulated data using the model while we systematically varied both parameters (Figure S7). The plots show that variations in the two parameters lead to different effects: While the number of correct responses alone can not be used to distinguish

between the parameters, the effects are very different when separately looking at trials on which a fractal response was correct and trials on which an explicit probability response was correct.

There is a clear positive correlation between the beta value and the (average) number of correct responses on trials on which the explicit option was correct. Variations in the memory parameter have little effect in that case. However, the memory parameter is important on trials on which the fractal was the correct choice and higher values lead to more correct choices. The beta parameter modulates this relationship between memory and number of correct choices. High beta values results in a large effect of memory on the number of correct responses, while low beta values flatten out this effect.

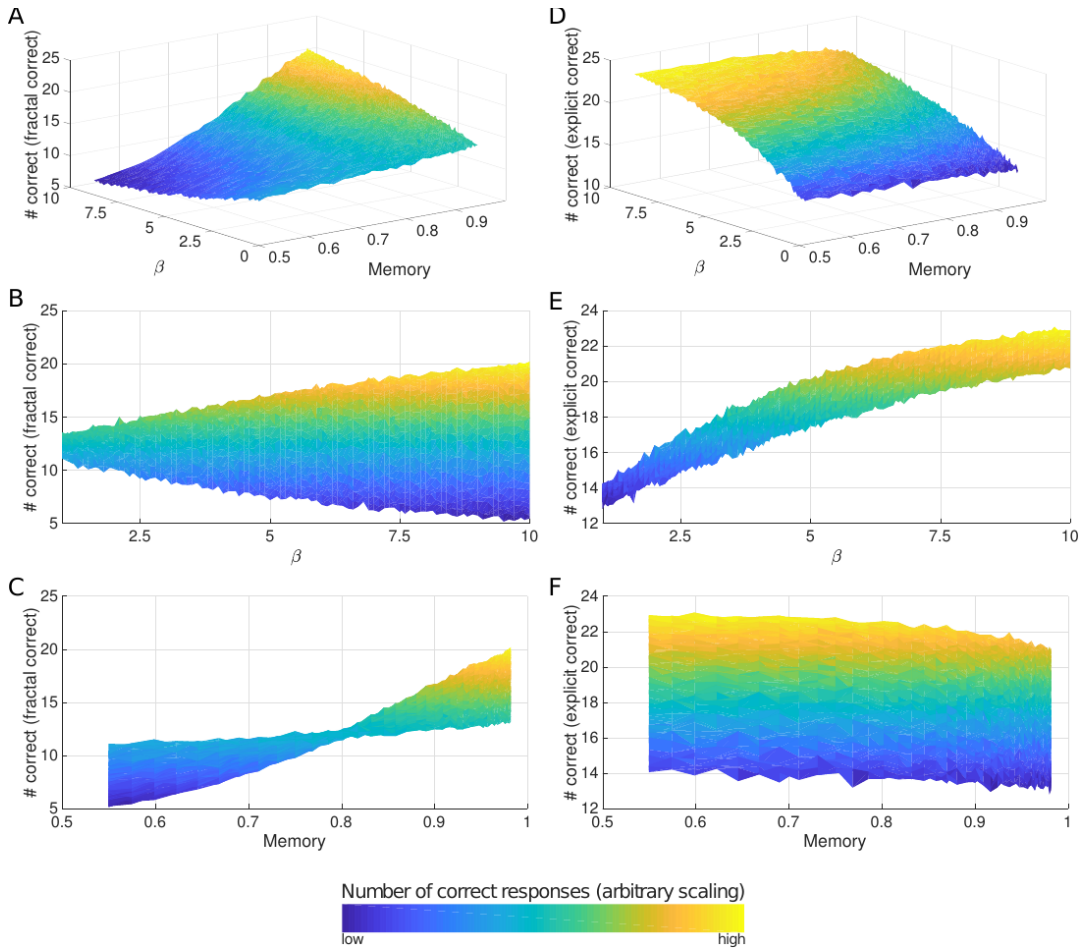

Figure S7. Simulations of our model using different parameter values for memory (discount parameter A) and β. The number of correct responses averaged over 100 simulations is shown. The left column (A-C) shows the number of correct choices on trials for which 'fractal' was the correct response as a function of the two parameters from different viewpoints of the grid. The right column (D-F) shows the same for the number of correct choices on trials for which the explicit probability was the correct response.

Model Fitting Procedure

We used model fitting and comparison procedures that have been used previously by Huys et al. (7, 8, 9). For completeness, we will describe them here in detail.

The goal of the model fitting procedure is to find estimates of the parameter vector θ_i for each participant *i*. This can be done by maximizing the probability that the observed choice data C_i came from the distribution governed by this θ:

$$\theta_i^{ML} = \underset{\theta}{\operatorname{argmax}}\, p(\mathcal{C}_i|\theta).$$

Repeating this procedure for each participant separately without any constraints can however lead to poor estimates and ignores the fact that we would expect parameters of different individuals to be comparable (e.g. to be of the same order of magnitude). One simple way to deal with this would be to enforce hard constraints on the parameter estimates, but a more principled way is to use a maximum a posteriori estimate and add a prior with information about the likely range of parameter values (10):

$$\theta_i^{MAP} = \underset{\theta}{\operatorname{argmax}}\, p(\mathcal{C}_i|\theta)\; p(\theta).$$

One option for such a prior is to estimate it from the data. Making the random effects assumption that parameters of individuals are samples from an overall group distribution and that this distribution is a Normal distribution with mean μ and variance Σ, we can use Expectation-Maximisation to simultaneously estimate group and individual parameters (7, 8, 9).

In the E-step (kth iteration) a Laplace approximation (mean mu and variance V) is used to estimate the parameters of individuals:

$$\begin{aligned} p(\theta|\mathcal{C}_i) &\approx \mathcal{N}(\boldsymbol{m}_i^{(k)}, \boldsymbol{V_i}^{(k)}) \\ \boldsymbol{m}_i^{(k)} &= \underset{\boldsymbol{m}}{\operatorname{argmax}}\; p(\mathcal{C}_i|\boldsymbol{m})\; p(\theta_i|\boldsymbol{\mu}^{(k-1)}, \boldsymbol{\Sigma}^{(k-1)}), \end{aligned}$$

In the M-step the population parameters are updated, taking into account the uncertainty of parameter estimations of individuals (weighted mean vector and covariance matrix):

$$\begin{aligned} \boldsymbol{\mu}^{(k)} &= \Big(\sum_{i=1}^{N} \boldsymbol{V_i}^{-1}\Big)^{-1}\Big(\sum_{i=1}^{N} \boldsymbol{V_i}^{-1}\boldsymbol{m}_i\Big) \\ \boldsymbol{\Sigma}^{(k)} &= \frac{1}{N-1}\sum_{i=1}^{N}(\boldsymbol{m}_i - \boldsymbol{\mu})(\boldsymbol{m}_i - \boldsymbol{\mu})^{\intercal} + \boldsymbol{V_i} \end{aligned}$$

To enforce constraints, parameters were transformed through non-linear functions with support on the real line. To avoid falling into local minima, multiple random initialisations were used. The procedure proved to be quite stable over multiple runs, repeatedly estimating very similar parameters.

Model Comparison Procedure

Having fitted our models, we want to find out which model has the highest probability of being the correct model given our data (11). This means that for some model M we are interested in finding its posterior probability

$$P(\mathcal{M}|\mathcal{C}) = \frac{P(\mathcal{C}|\mathcal{M})\ P(\mathcal{M})}{P(\mathcal{C})}.$$

The probability of the choice data P(C) will be the same under all models and since we have no prior preference for any of the models, P(M) will also be equal for all models, which means that when we take the ratio of posterior model probabilities they will both cancel out. The model evidence remains and can be rewritten as

$$P(\mathcal{C}|\mathcal{M}) = \int d\boldsymbol{\theta}\ P(\mathcal{C}|\boldsymbol{\theta},\mathcal{M})\ P(\boldsymbol{\theta}|\mathcal{M}),$$

which we then approximate (7, 8, 9) with

$$\log(P(\mathcal{C}|\mathcal{M})) \approx \log(P(\mathcal{C}|\hat{\theta},\mathcal{M})) - \frac{1}{2}|\mathcal{M}|\log(|\mathcal{C}|) = -\frac{1}{2}\mathrm{iBIC},$$

where |M| is the number of fitted prior parameters, |C| is the overall number of choices and the difference in iBIC values of two models will be an approximation to the log Bayes Factor (9). The "i" in front of BIC stands for "integrated", because to compute log(p(C|θ, M)) we integrate over parameters so that

$$\log(p(\mathcal{C}|\hat{\boldsymbol{\theta}},\mathcal{M})) = \sum_{i=1}^{N}\log(P(\mathcal{C}_i|\hat{\boldsymbol{\theta}},\mathcal{M})) = \sum_{i=1}^{N}\log\Big(\int d\boldsymbol{h}\ P(\mathcal{C}_i|\boldsymbol{h},\mathcal{M})\ P(\boldsymbol{h}|\hat{\boldsymbol{\theta}},\mathcal{M})\Big).$$

This can be approximated by sampling from our estimate prior and averaging over those samples (7, 8, 9):

$$\begin{aligned}\boldsymbol{h}^{(s)} &\sim p(\boldsymbol{h}|\hat{\boldsymbol{\theta}},\mathcal{M})\\ \log(p(\mathcal{C}|\hat{\boldsymbol{\theta}},\mathcal{M})) &\approx \sum_{i=1}^{N}\log\Big(\frac{1}{S}\sum_{s=1}^{S}p(\mathcal{C}_i|\boldsymbol{h}^{(s)},\mathcal{M})\Big)\end{aligned}$$

For our winning model we also tested whether our groups were better described using a shared population prior or separate priors for each group. For this, iBIC values of the fits of separate group

priors were added and compared to the iBIC value of a single population prior. Our data was best described using a single population prior (ΔiBIC = 13.5).

Simulations

It is important to check that models can be recovered given the available data and so we performed model recovery simulations. Models were simulated to produce the same amount of actually available data (32 subjects, 60 decisions) and then the generating model and an alternative model were fit to the data and standard model comparison was used to decide which model produced the better fit.

These simulations showed that Leaky and Leaky-ρ could not reliably be distinguished with the amount of data we have and Leaky was often selected as best model even when Leaky-ρ produced the data. Importantly, however, our second and third best-fitting reinforcement learning models could reliably be recovered from data they generated in most simulations as shown in Table S3.

Bayesian	**RL-basic**	**RL-learning**	**RL-unbiased**	**RL-learning-unbiased**
12/15	12/15	15/15	14/15	15/15

Table S3. Model recovery table showing how often each model was recovered from data they had generated (15 simulations) against the Leaky model. Leaky always had the lower iBIC value (15/15 against all models) when fitted to data it had generated.

To check whether the model fitting procedure is actually able to recover parameters given the amount of data available to us, we simulated 32 participants with 60 decisions each from known parameters. To get sensible parameter values, we randomly sampled from the estimated group prior. Errors were consistently lower for our procedure than standard maximum likelihood estimations and our procedure also avoids outliers sometimes produced by MLE by pushing estimations towards the group mean. Figures S8 and S9 show a first example of the recovery of memory A and inverse temperature β parameters for the model Leaky, while Figures S10 and S11 show the same for a second example and Figures S12 and S13 for a third example. Simulations of other models showed similar parameter recovery.

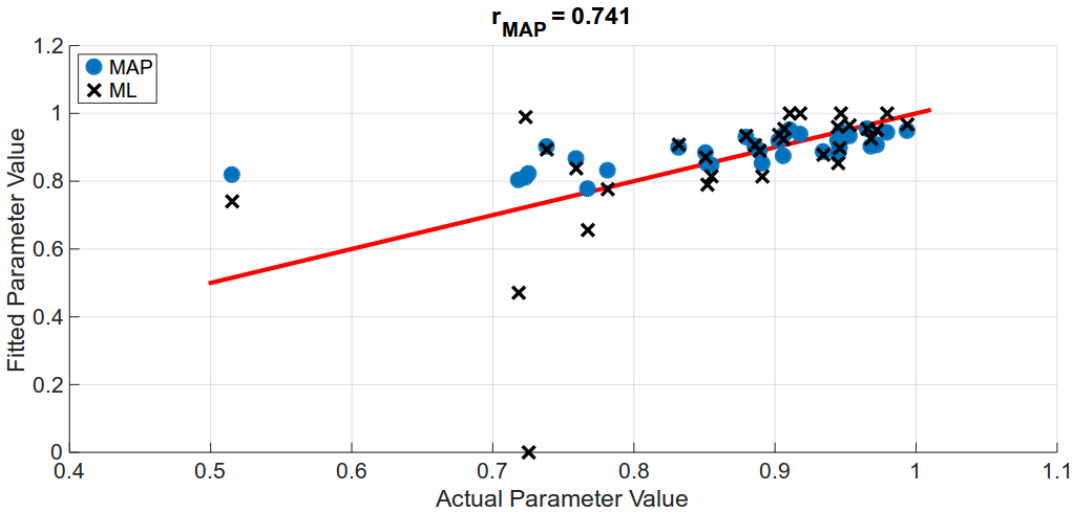

Figure S8. Example 1 (A): Parameter recovery simulation of the memory parameter A using a group prior (MAP) and simple maximum likelihood (ML). The red line shows the values with which the data was actually generated. Note how MAP estimation leads to improvements over ML estimation, in particular by eliminating the outlier lying on the zero boundary.

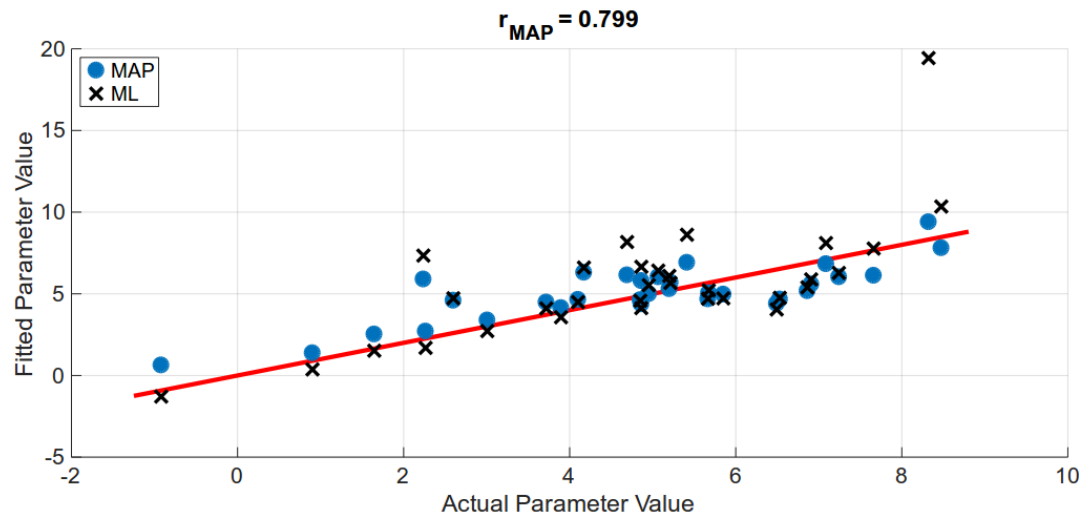

Figure S9. Example 1 (β): Parameter recovery simulation of the inverse temperature parameter β using a group prior (MAP) and simple maximum likelihood (ML). The red line shows the values with which the data was actually generated.

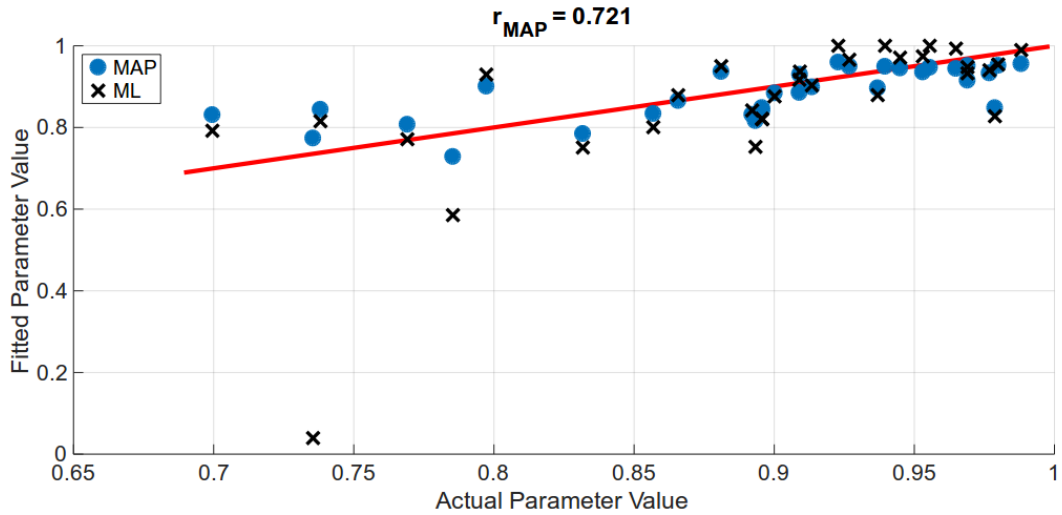

Figure S10. Example 2 (A): Parameter recovery simulation of the memory parameter A using a group prior (MAP) and simple maximum likelihood (ML). The red line shows the values with which the data was actually generated.

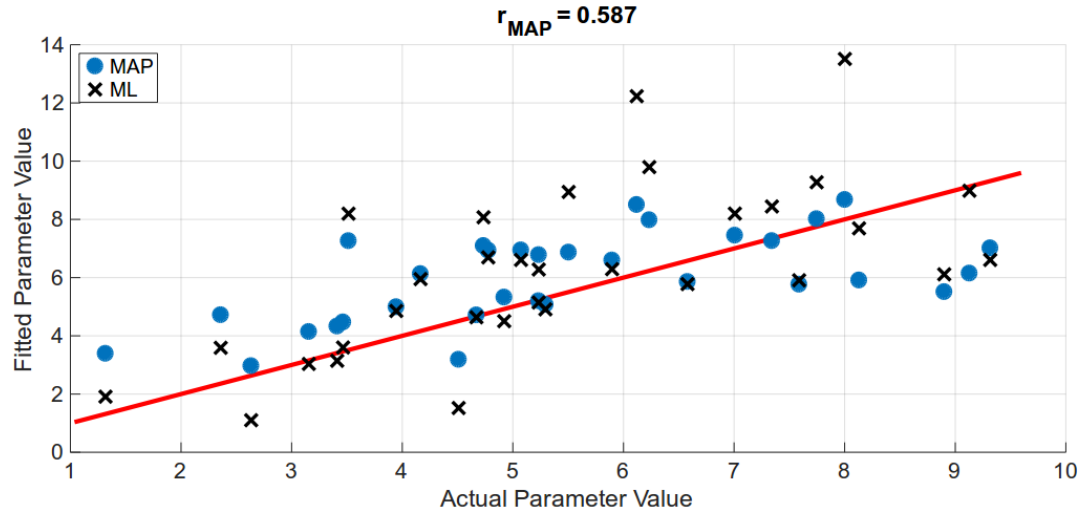

Figure S11. Example 2 (β): Parameter recovery simulation of the inverse temperature parameter β using a group prior (MAP) and simple maximum likelihood (ML). The red line shows the values with which the data was actually generated.

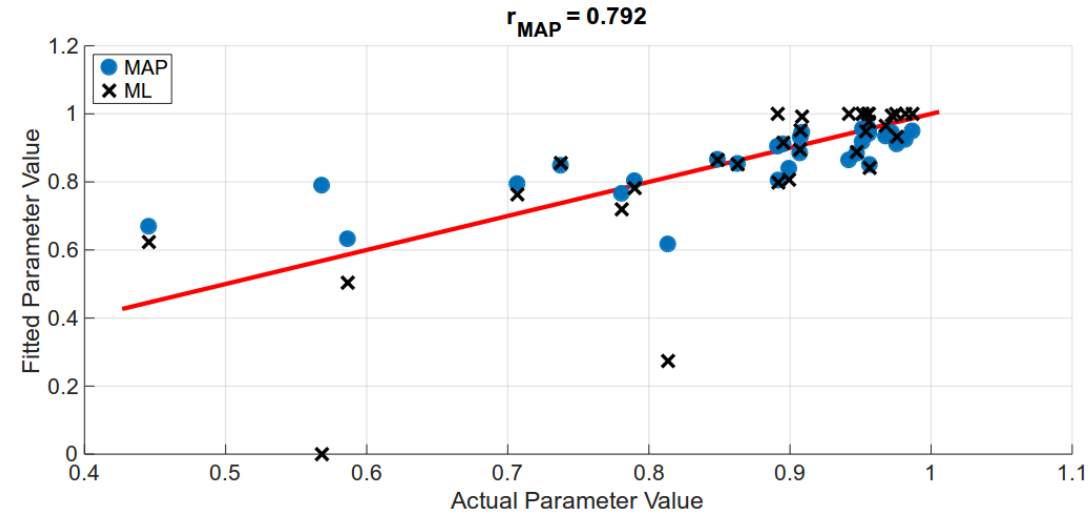

Figure S12. Example 3 (A): Parameter recovery simulation of the memory parameter A using a group prior (MAP) and simple maximum likelihood (ML). The red line shows the values with which the data was actually generated.

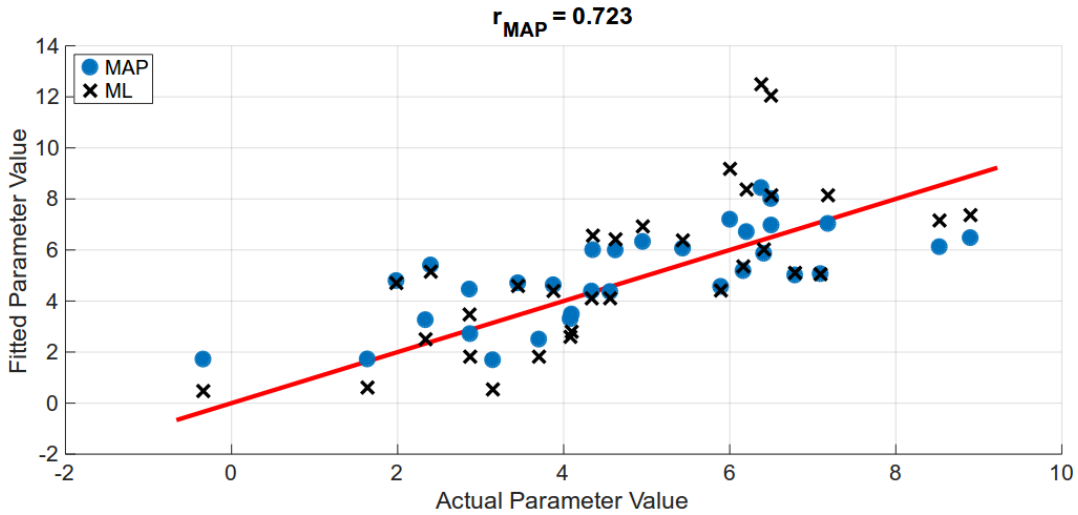

Figure S13. Example 3 (β): Parameter recovery simulation of the inverse temperature parameter β using a group prior (MAP) and simple maximum likelihood (ML). The red line shows the values with which the data was actually generated.

Parameter correlation

There was a trend suggesting a correlation between parameter estimates (r = 0.349, BF10 = 0.91, p = .051). We performed additional parameter recovery simulations (Figures S14, S15, S16) in which we systematically varied parameters to further convince ourselves that parameter correlations did not systematically influence the fitting of parameters. We simulated individual participants, with one of the values fixed to be the same for everybody (e.g. setting the memory $A=0.9$) while varying the other parameter across participants (e.g. have participants with betas in the range of 4 until 9). Most importantly, for the beta parameter we did not find that different realistic values of the memory parameter had a systematic influence on the quality of the parameter recovery (Figure S14).

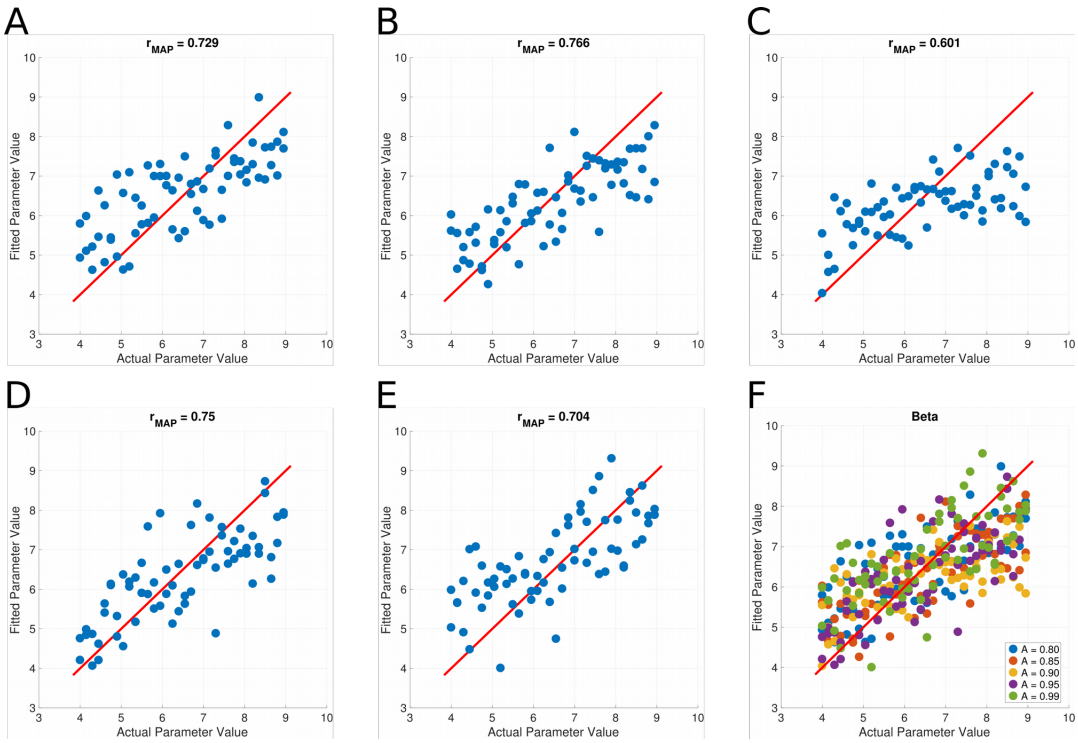

Figure S14. Recovery of the beta parameter, while fixing the memory parameter *A* to certain realistic values: (A) *A*=0.80, (B) *A*=0.85, (C) *A*=0.90, (D) *A*=0.95, (E) *A*=0.99. Subfigure (F) shows (A-E) combined. For each recovery plot, 68 participants were simulated, making 120 decisions. It can be seen that the parameter recovery of the beta parameter is not systematically influenced by the setting of the memory parameter.

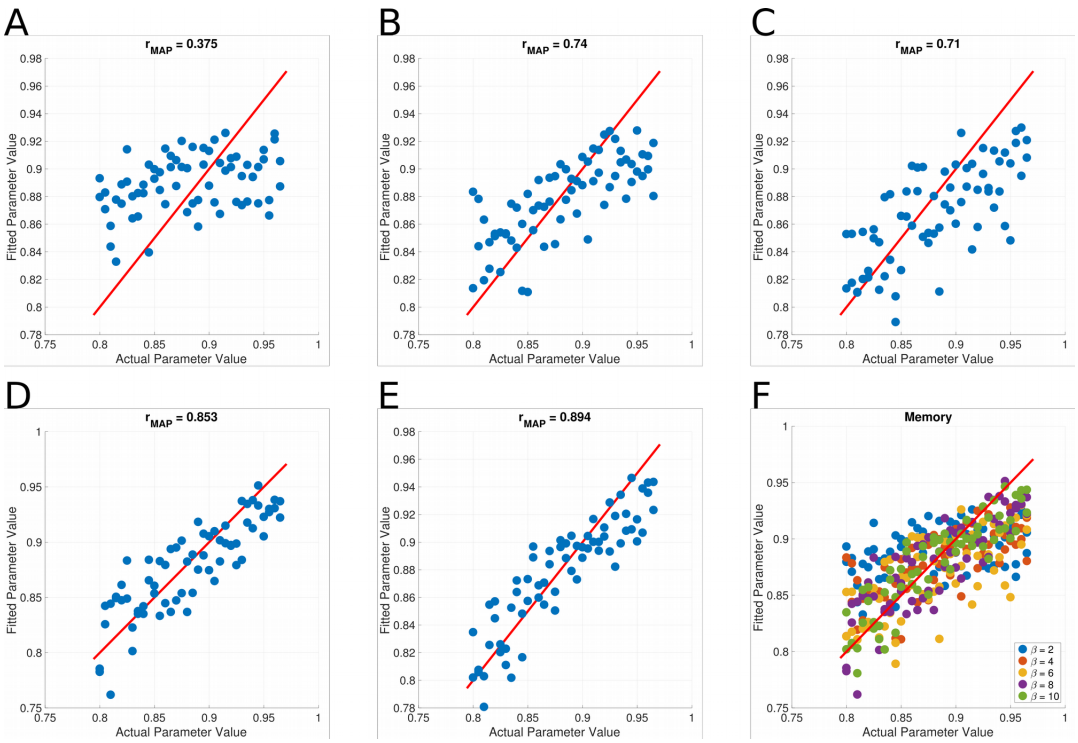

Figure S15. Recovery of the memory (*A*) parameter, while fixing the inverse temperature parameter β to certain values: (A) β=2, (B) β=4, (C) β=6, (D) β=8, (E) β=10. Subfigure (F) shows (A-E) combined. For each recovery plot, 68 participants were simulated, making 120 decisions. For very low (and probably mostly unrealistic) β values, the recovery of the memory parameter was noticeably worse than for all the other more realistic values of 4 and above.

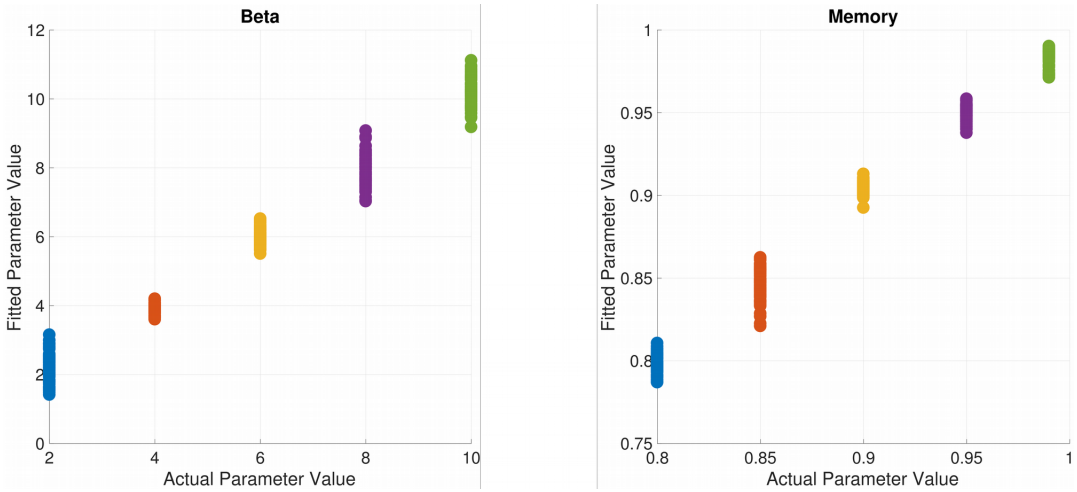

Figure S16. Recovery of the fixed parameters. (Left) Beta parameters were fixed at values 2, 4, 6, 8, and 10 and recovered well. The corresponding recoveries of the systematically varying memory parameters are shown in Figure S14. (Right) Memory parameters were fixed at values 0.80, 0.85, 0.90, 0.95, and 0.99 and recovered well. The corresponding recoveries of the systematically varying beta parameters are shown in Figure S15.

Supplementary References

[1] R. Wetzels and E.-J. Wagenmakers, “A default Bayesian hypothesis test for correlations and partial correlations,” Psychonomic bulletin & review, vol. 19, no. 6, pp. 1057–1064, 2012.

[2] J. O. Berger and T. Sellke, “Testing a point null hypothesis: The irreconcilability of p values and evidence,” Journal of the American statistical Association, vol. 82, no. 397, pp. 112–122, 1987.

[3] M. F. Scheier, C. S. Carver, and M. W. Bridges, “Distinguishing optimism from neuroticism (and trait anxiety, self-mastery, and self-esteem): a reevaluation of the life orientation test.,” Journal of personality and social psychology, vol. 67, no. 6, p. 1063, 1994.

[4] T. W. Smith, M. K. Pope, F. Rhodewalt, and J. L. Poulton, “Optimism, neuroticism, coping, and symptom reports: An alternative interpretation of the life orientation test.,” Journal of Personality and Social Psychology, vol. 56, no. 4, p. 640, 1989.

[5] D. K. Kennedy and B. M. Hughes, “The optimism-neuroticism question: An evaluation based on cardiovascular reactivity in female college students,” The psychological record, vol. 54, no. 3, p. 373, 2004.

[6] Stankevicius, A., Huys, Q. J., Kalra, A., and Seriès, P. (2014). Optimism as a prior belief about the probability of future reward. PLoS Computational Biology, 10(5):e1003605.

[7] Huys, Q. J., Cools, R., Gölzer, M., Friedel, E., Heinz, A., Dolan, R. J., and Dayan, P. (2011). Disentangling the roles of approach, activation and valence in instrumental and Pavlovian responding. PloS Computational Biology, 7(4):e1002028.

[8] Huys, Q. J., Eshel, N., O’Nions, E., Sheridan, L., Dayan, P., and Roiser, J. P. (2012). Bonsai trees in your head: how the pavlovian system sculpts goal-directed choices by pruning decision trees. PloS Computational Biology, 8(3):e1002410.

[9] Huys, Q. J., Pizzagalli, D. A., Bogdan, R., and Dayan, P. (2013). Mapping anhedonia onto reinforcement learning: a behavioural meta-analysis. Biology of mood & anxiety disorders, 3(1):12.

[10] Daw, N. D. (2011). Trial-by-trial data analysis using computational models. Decision making, affect, and learning: Attention and performance XXIII, 23:3–38.

[11] MacKay, D. J. (2003). Information theory, inference and learning algorithms. Cambridge University Press.

[12] Huys, Q. J., Vogelstein, J. T., Dayan, P. & Bottou, L. Psychiatry: Insights into depression through normative decision-making models. In NIPS, 729–736 (2008).

Appendix B

Supplementary Materials for Chapter 4

This chapter contains the Supplementary Materials for Chapter 4 which was published as S. Rupprechter, A. Stankevicius, Q. J. M. Huys, P. Series, et al. (2020). "Abnormal reward valuation and event-related connectivity in unmedicated major depressive disorder". In: *Psychological Medicine*, pp. 1–9.

Supplementary Materials

Abnormal Reward Valuation and Event-Related Connectivity in Unmedicated Major Depressive Disorder

Experiment Details

Written informed consent was obtained then, questionnaires and an interview conducted which lasted an hour, then task training for 10-20 minutes followed by 50 minutes scanning then debriefing lasting 5 minutes. Participants were paid £20 plus a performance dependent bonus of up to £10. Final scores were converted into a percentage.

Subjects passively observed fractals; each was always followed by either a reward symbol (£) indicating 'value' or a blank screen indicating 'no value'. After each fractal was observed on four occasions it appeared, at some later time, in a single decision trial where subjects were asked to choose the higher reward probability; their internally estimated value for the fractal or an explicit numeric value. Either option could have a value 10% 20% or 30% higher than the other or equal value. This means a total of 240 fractals (60x4) were observed with 60 decisions being made. Fractals were presented for 3 to 4 seconds. Outcomes were presented for 2.5 to 3.5 seconds. Decisions had to be made within a 5 second response window. Null events (blank screens) and null decisions (requiring a button press in response to a cross in the centre of the screen) were randomly interspersed throughout the experiment. The sequence of observations and decisions were interleaved in a pseudo-random order and identical for all subjects. The study was divided into 4 sessions of 15 min each between which there were periods where participants could briefly rest. Each session was split into 3 blocks and during each block participants made 5 decisions. Participants did not receive feedback during the task but were told their performance scores would be converted into money they would receive at the end of the experiment. The task is summarised in Figure 1 (main text).

Behavioural modelling

We recently published a detailed computational modelling analysis of participants' behaviour on the task (Rupprechter *et al*., 2018). Here we summarise the approach and main findings. We fitted seven different models, representing distinct hypotheses about participants' decision-making, to the data. All models assume that participants estimate an internal value for each fractal stimulus and compare this internal value to the explicit value at decision time. To model the probability of choosing an action, the value difference was passed into a standard softmax function, which also

included an inverse temperature parameter β. Higher values of β lead to more deterministic decision-making. The parameter can be interpreted as an individual's ability to use their internal value estimations to make decisions.

Four different variations of reinforcement learning (RL) models were defined. These models incorporate trial-by-trial prediction errors and learning rate parameters. After an outcome is observed, the expected value of the fractal that was displayed is updated by adding the prediction error (difference between expected value and reward outcome coded as 1 or 0) scaled by the learning rate. The initial value was either set to a fitted initial value parameter (in two of the RL models) or fixed at 0.5 corresponding to a prior belief that reward was equally likely from either option. Two models included separate learning rates for separate reward outcomes, aiming to test whether learning would be different following rewards versus no-rewards. We also fitted the winning model of the original study by Stankevicius *et al*. (2014) which tested the Bayesian observer hypothesis. This model assumed that participants would count the number of times each fractal was followed by reward and combine this evidence with a prior belief about the probability of rewards associated with fractals. The model does not explicitly model the observation phase of the experiment and instead assumed at the decision time perfect counting had occurred. To overcome these limitations, we fitted two additional models ('Leaky' and 'Leaky-ρ') which also assumed participants would count the number of times a fractal was followed by reward, but this was modelled on a trial-by-trial basis. In addition, a memory or discounting parameter was included, which assumed that subjects forgot about some of the previously observed values.

Model fitting was based on maximum *a posteriori* estimates, which included an empirical Gaussian prior estimated from the data. Parameters were initialised with maximum likelihood estimates and then an expectation-maximization procedure applied to iteratively update these estimates until convergence. The integrated Bayesian Information Criterion (iBIC) was used to identify the model that best fit the data while also penalizing for model complexity.

The best fitting model according to iBIC was the *Leaky* model, which updated the value for fractal *i* on trial *t* as where *A* is a memory parameter and smaller *A* reflected increased forgetting or retrospective discounting, and r was unity if a £ reward symbol was observed and zero otherwise.

$$V_i^{t+1} = A \times V_i^t + r_i^t,$$

As above, the probability of choosing a fractal *i* was calculated using a softmax function incorporating estimated value (*V*) and explicitly presented values (*phi*)

$$p(\text{choose fractal i}) = \sigma(\beta \times (f(V_i) - \phi_i)) = \frac{1}{1 + \exp(-\beta \times (f(V_i) - \phi_i))},$$

where *f(x) = x/4* is a transformation of the internal value estimate comparable to the explicitly displayed reward probability.

We identified differences between the groups in both memory parameter (z = −2.15, p = 0.031; A patients μ ± σ =0.90 ± 0.04, median = 0.91; A controls μ ± σ = 0.92 ± 0.09, median = 0.96) and softmax β parameter (z = −2.34, p = 0.019; β patients μ ± σ = 4.67 ± 1.45, β controls μ ± σ = 5.89 ± 1.33). This indicates MDD patients discounted more of their estimated values and found it harder to follow their internal value estimations.

Logistic Regression

Logistic regression models were fitted using *glmfit* in MATLAB to the data of all participants except one, which was then used to predict the group of the left-out participant (using *glmval* and a threshold of *0.5*). This was repeated all participants. Overall, we were able to classify 27 participants (14 patients, 13 controls) correctly, which corresponds to an accuracy of 79% (27 out of 34, precision=76%, recall=81%). The area under the ROC curve, for which the p threshold was varied between 0 and 1 and true and false positive rates were calculated, was approximately 0.86 (Figure S5).

Value difference signal encoding: Group comparison

Beta values were extracted from the first level contrast images of each participant and then compared between two groups. We did not find a group difference with betas extracted from a 5mm sphere within the aMCC region identified as being active during decision making (-2,14,50) for value difference (t(29.09)=-0.30, p=0.764) or absolute value difference (t(29.28)=-0.990, p=0.330) signal encoding. We also did not find a group difference of value difference encoding in slightly different aMCC ROIs ([-14,16,48]: t(23.47)=-1.33, p=0.197; [12,24,28]: t(24.32)=0.42, p=0.682). Neither did we find a group difference of absolute value difference encoding in different aMCC ([-4,24,46]: t(23.92)=-0.69, p=0.498; [10,10,46]: t(28.49)=-1.55, p=0.132) or rACC ([-16,42,8]: t(29.72)=-1.21, p=0.237; [-4,50,-14]: t(29.04)=-1.86, p=0.074) regions of interest.

Connectivity analysis

The conditions included in the gPPI analysis were outcome time, fractal presentation time, decision prompt time, button press time, and null events. Event-related connectivity methods are not as well established as some other areas of neuroimaging, so we also explored beta series correlation analysis (BASCO toolbox; Göttlich et al. 2015), as an additional method to infer event-related functional connectivity between a dACC seed region and other brain regions. Encouragingly, we obtained a similar result as gPPI, with controls showing stronger connectivity between dACC and rACC than patients at the decision-time (Figure S6).

Structural differences

To address the possibility of structural differences influencing our results (see discussion in main text), we performed additional analyses. For every participant, we obtained a grey matter probability image (*c1*.nii in SPM*) during preprocessing of the T1 structural image and an estimated forward deformation field image (*y_*.nii in SPM*) used to normalise the functional images. The deformation field was used to normalise the grey matter probability image, including a resampling of voxels in the same way as was done for the functional scans; giving for each resampled voxel, an estimate of the probability that a voxel was grey matter. We then multiplied beta values in the hippocampal and rACC ROIs (5mm) of contrast images for value encoding at fractal presentation time by these grey matter weights. From each ROI the mean values were calculated and between group Welch's t-tests done. The results still showed significant group differences after these adjustments (L hippocampus (-36,-32,2) $t(21.36)=3.313$, $p=0.003$; R hippocampus (48,-26,4) $t(31.03)=2.501$, $p=0.018$; rACC (14,50,-10) $t(31.19)=2.890$, $p=0.007$)

Interpretation of Results

We were cautious in interpreting our results: i) At a behavioural level we found decreased 'value memory' and at an imaging level we found decreased 'value encoding' in the brain. Theories of decision making posit that value estimations are used as the basis of decision making. Therefore, altered value encoding could have been the cause of the observed behavioural abnormalities. However, as both behaviour and brain encoding were abnormal we were cautions about a possible circular argument in interpreting our data further than we have in the main text. ii) Regarding abnormalities in decision-making, we made the prediction that we would find both an activation across participants and a group difference in cortical signals at the decision time. We further hypothesized a signal encoding 'value difference' because in our behavioural model, this is

the variable which enters at the decision event time. Importantly though, these variables are related. While it would be possible to test for a direct correlation between the signal encoding and estimated inverse temperature parameters at the second level, interpretation with our data would be difficult.

Control analyses

We repeated our analysis using a decreased individual voxel threshold ($p<0.01$) for multiple comparison corrections and reproduced the figures from the main text (Figures S1-S4). Results were broadly similar, with the exception of negative value difference encoding signal across participants which was not significant (Figure S4). Additional Monte Carlo simulations showed that with an assumed individual voxel type 1 error of $p=0.01$ a smaller cluster size of $k=102$ would be needed to correct for multiple comparisons at the same cluster correction threshold of $p<0.01$. The script (cluster_threshold_beta.m) can be found on the author's webpage (https://www2.bc.edu/sd-slotnick/scripts.htm).

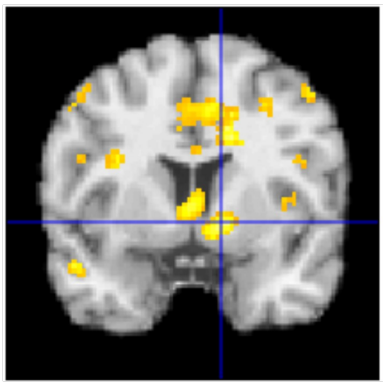

Figure S1. *Decreased reward activation in MDD participants compared to healthy controls in the striatum. Display threshold $p<0.01$ and $k=108$; c.f. Figure 2B.*

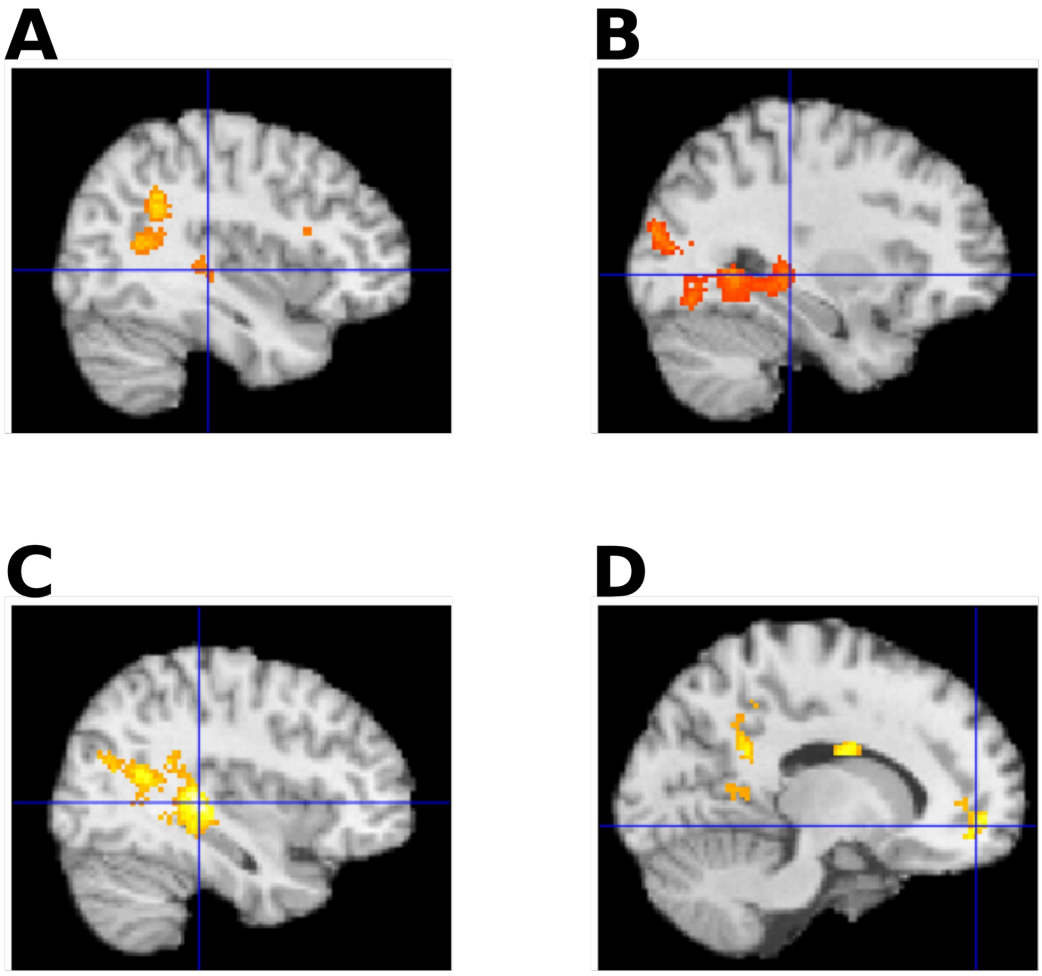

Figure S2. *Reward value encoding at fractal presentation time. (A) Positive value encoding within healthy controls. Note that the cluster size here is k=66; c.f. Figure 3A. (B) Negative value encoding in depressed participants. Display threshold p<0.01 and k=108; c.f. Figure 3B. (C) Larger value encoding in healthy controls compared to MDD participants in hippocampus. Display threshold p<0.01 and k=108; c.f. Figure 3B – left. (D) Larger value encoding in healthy controls compared to MDD participants in rostral ACC. Note that the cluster size here is k=91; c.f. Figure 3B – right.*

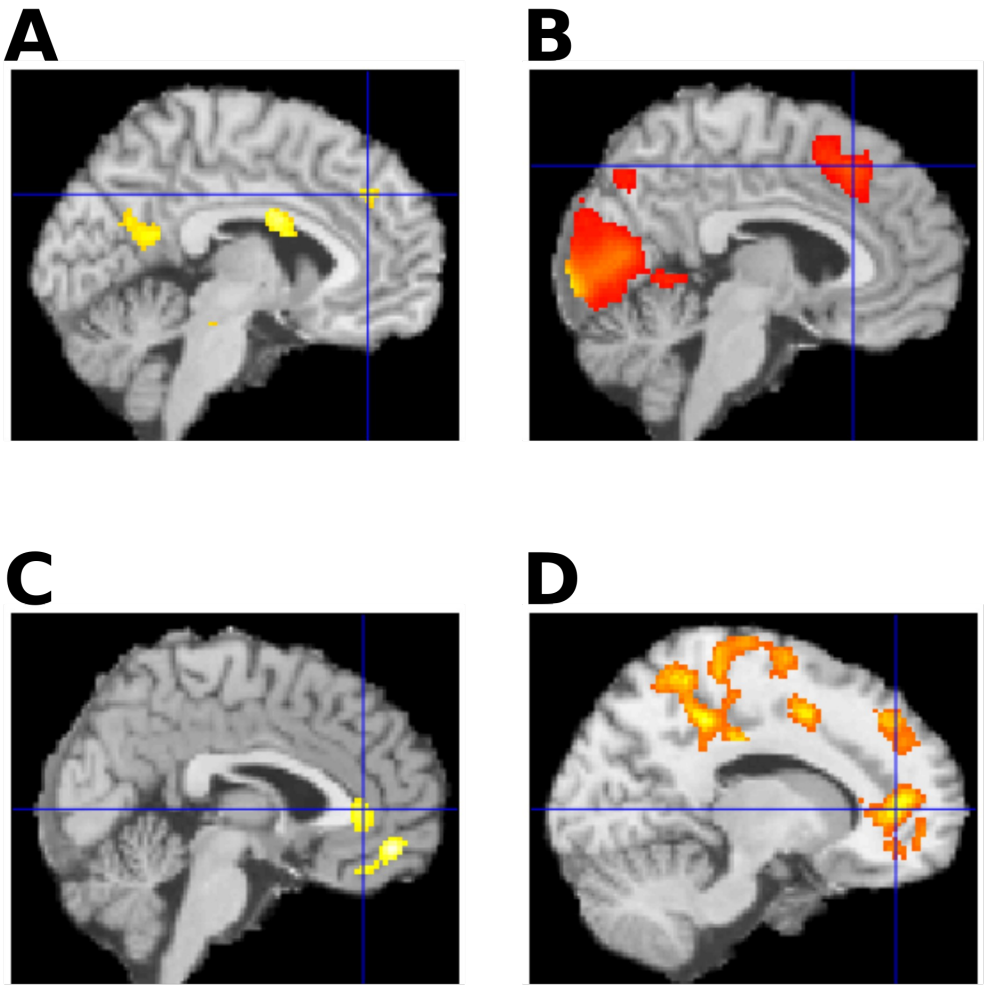

Figure S3. *Activation during decision making. (A) Larger activations in MDD compared to controls. Note that the cluster size here is k=103; c.f. Figure 4B. (B) Negative absolute value difference encoding signal across participants. Display threshold p<0.01 and k=108; c.f. Figure 4D. (C) Positive absolute value difference encoding signal across participants. Note that the cluster size here is k=97 and the cluster size for the second cluster further down (ventral) is k=144; c.f. Figure 4E. (D) Decreased event-related connectivity in depression between dorsal cingulate region and other cingulate regions. Display threshold p<0.01 and k=108; c.f. Figure 4F.*

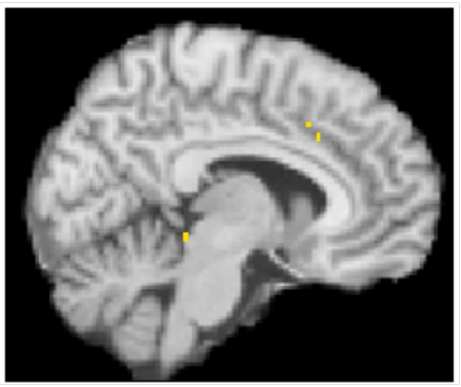

Figure S4. *Negative value difference encoding signal across participants was not significant in the anterior mid-cingulate region at an individual voxel threshold of p<0.01; c.f. Figure 4C.*

Figures

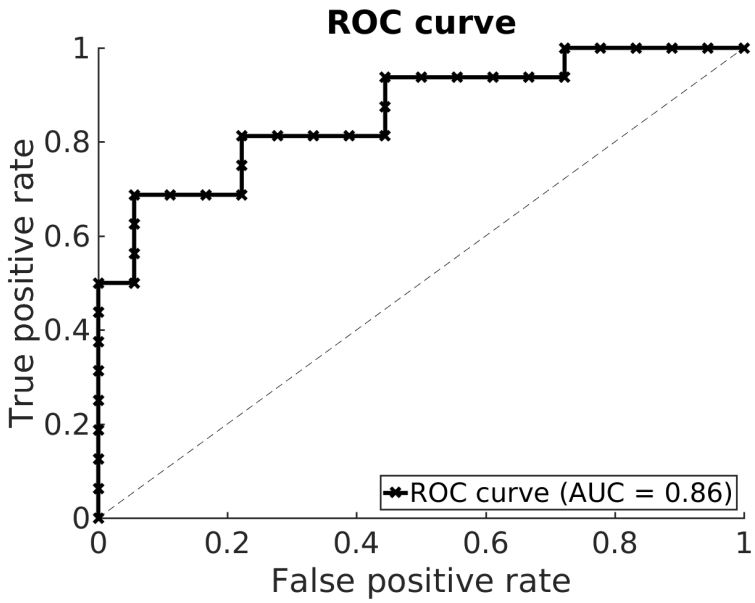

Figure S5. *The ROC curve (AUC = 0.86) of our logistic regression classifier.*

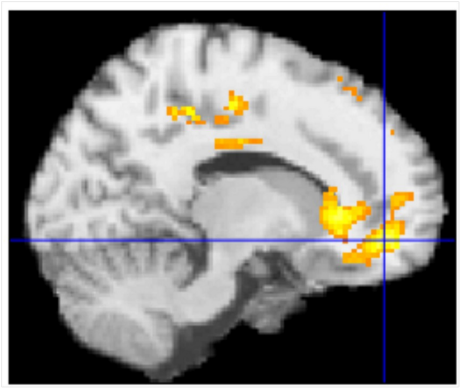

Figure S6. *Functional connectivity. Significantly higher functional connectivity in HC compared to MDD subjects between a dACC seed region with rostral ACC and PCC, obtained using beta series correlations (Göttlich* et al., *2015).*

Tables

Questionnaire	Patients	Controls
BDI	25.9 ± 12.9	5.4 ± 5.6
DSAB	15.1 ± 4.0	16.9 ± 2.4
HAD-A	12.7 ± 5.1	4.3 ± 2.5
HAD-D	8.6 ± 4.6	1.8 ± 2.0
HAMA	18.8 ± 6.9	1.8 ± 2.7
LOT-R	9.0 ± 5.1	18.4 ± 3.1
MADRS	18.8 ± 6.9	1.8 ± 2.7
NART	45.8 ± 4.5	47.3 ± 3.6
RSE	13.3 ± 6.9	23.7 ± 4.6
SHAPS	38.6 ± 8.7	49.2 ± 5.9
Agreeableness	39.6 ± 6.5	45.6 ± 5.7
Conscientiousness	36.4 ± 10.0	44.8 ± 7.2
Extraversion	31.2 ± 7.6	43.3 ± 4.2
Neuroticism	46.9 ± 7.1	31.4 ± 6.9
Openness	41.5 ± 5.4	45.8 ± 5.3

Table S1. Clinical characteristics of participants. BDI = Beck Depression Inventory; DSAB = Digit Score Part B; HAD = Hospital Anxiety and Depression Scale; HAMA = Hamilton Anxiety Rating Scale; LOT-R = Life Orientation Test – Revised; MADRS = Montgomery-Åsberg Depression Rating Scale; NART = National Adult Reading Test; RSE = Rosenberg Self-Esteem Scale; SHAPS = Snaith-Hamilton Pleasure Scale; Scores displayed as mean ± std.

Reward response

Regions	t	z	MNI coordinates [mm]			Voxels in cluster
			x	y	z	
Controls + Patients						
striatum, midcingulate, dorsolateral cortex, occipital lobe	12.19	7.39	-14	-90	2	94077
	4.89	4.20	10	12	-4	
	4.44	3.89	-10	18	0	
	8.28	6.01	-10	10	48	
	8.25	6.00	-46	8	24	
	7.14	5.48	44	6	32	
Controls > Patients						
Striatum, nucleus accumbens	4.58	3.99	22	26	10	27510
	4.48	3.92	-22	14	-16	
	4.45	3.9	-48	-36	30	
Cerebellum	4.44	3.89	-30	-52	-42	1691
	2.9	2.71	8	-70	-28	
	2.83	2.65	-28	-64	-52	
thalamus	3.4	3.12	2	-32	2	357
	2.31	2.21	10	-24	-2	
	2.31	2.21	20	-18	-2	
Cerebellum	3.05	2.84	36	-52	-44	461
	2.55	2.42	4	-58	-48	
	2.51	2.38	40	-58	-48	
FFA	3.03	2.82	48	-60	-18	229
	2.48	2.36	46	-52	-22	
	2.28	2.18	46	-70	-16	
Auditory cortex / insula	3.01	2.8	-38	-18	4	127

Value encoding

Regions	t	z	MNI coordinates [mm]			Voxels in cluster
			x	y	z	
Controls (activations)						
Occipital lobe	6.29	4.34	-16	-102	4	748
Precuneus, L hippocampus, caudate, prefrontal cortex	5.7	4.1	8	-58	40	16096
	5.62	4.06	-8	-54	52	
	5.58	4.04	0	-52	48	
	4.19	3.36	26	-96	-4	337
Occipital lobe	2.91	2.55	34	-94	4	
	2.74	2.43	10	-88	-6	
Supramarginal gyrus	3.98	3.24	58	-44	32	645
	3.27	2.8	48	-46	36	
	2.3	2.09	40	-52	32	
R Supp motor area	3.66	3.04	16	-2	56	183
	2.41	2.19	16	-6	68	
R temporal gyrus, R hippocampus	3.61	3.02	66	-20	-4	744
	3.51	2.95	34	-50	10	
	3.06	2.65	66	-10	0	
	2.36	2.14	10	-38	-46	160
brainstem	2.32	2.11	0	-32	-54	
	2.16	1.99	0	-20	-36	
Patients (deactivations)						
Occipital lobe, hippocampus	8.38	5.21	18	-88	18	20400
	8.07	5.11	38	-68	-8	
	5.47	4.1	-2	-86	-6	
Medial prefrontal cortex, rostral ACC	4.16	3.41	14	50	-10	1035
	3.3	2.86	2	34	-18	
	3.01	2.66	2	24	-22	
Motor cortex	3.68	3.11	-38	-8	36	730
	3.09	2.72	-4	-16	54	
	2.7	2.43	-48	-8	34	
Motor cortex	3.6	3.06	16	-26	68	898
	3.51	3	20	-30	54	
	3	2.65	4	-26	70	
R amygdala	3.55	3.03	30	8	-18	213
	1.95	1.83	30	-2	-16	

Brainstem	3.2	2.79	6	-16	-42	108
	2.42	2.22	-2	-18	-36	
Brainstem	2.64	2.38	2	-38	-48	119
Corpus callosum	2.57	2.33	8	-2	28	115
	2.01	1.88	-4	-6	26	
Controls > Patients						
Hippocampus, precuneus	4.88	4.19	-36	-32	2	18480
	4.57	3.98	50	-4	18	
	4.4	3.86	-32	-68	16	
Medial prefrontal cortex, rostral ACC, R anterior insula	3.73	3.37	14	50	-8	2169
	3.61	3.28	28	12	44	
	3.41	3.12	28	20	12	
Precuneus	2.92	2.73	-10	-58	48	161
	2.06	1.98	4	-64	54	
	2.03	1.96	-4	-66	56	
Brainstem	2.84	2.66	0	-20	-38	122
L anterior insula	2.65	2.5	-28	12	16	109
	2.33	2.23	-36	18	16	
	2.17	2.09	-30	26	18	
Brainstem	2.63	2.49	4	-38	-48	108

Decision making

Regions	t	z	MNI coordinates [mm]			Voxels in cluster
			x	y	z	
Controls + Patients						
Anterior insula, dorsal ACC (aMCC), striatum	16.68	Inf	32	26	-6	111774
	14.21	Inf	16	0	-6	
	14.07	Inf	-28	22	-2	
	14.74	Inf	26	-66	-4	
	14.61	Inf	-16	-68	12	
	14.02	Inf	-26	-62	-8	
	12.91	7.59	-2	14	50	
Patients > Controls						
Insula	4.21	3.73	8	0	26	1185
	3.26	3.01	34	-22	24	
	2.89	2.7	-8	-4	22	
sgACC	4.06	3.62	-2	28	-2	176
Occipital lobe	3.44	3.15	-34	-88	24	384
	2.94	2.74	-48	-74	26	
	2.44	2.32	-36	-76	44	
insula	3.3	3.04	-38	-8	20	675
	3.23	2.99	-36	-26	22	
	3.14	2.91	-44	-24	20	
(para)hippocampus, brainstem	3.25	3	-20	-28	-18	950
	3.19	2.95	14	-36	-20	
	3.19	2.95	12	-22	-16	
dACC	3.21	2.97	22	28	42	741
	3.11	2.88	-12	20	32	
	3.01	2.81	6	38	34	
PCC	3.14	2.91	-2	-56	28	1651
	2.93	2.74	6	-52	18	
	2.9	2.71	2	-60	22	
Supp motor area	3.09	2.87	-8	-18	62	157
	1.96	1.9	4	-12	64	
Temporal lobe, hippocampus	3.07	2.86	-22	-34	4	154
	2.05	1.98	-12	-32	12	
Temporal lobe, hippocampus	3.06	2.85	42	-34	4	534
	2.84	2.66	40	-52	-6	
	2.56	2.42	28	-36	0	

Occipital lobe	2.92	2.73	42	-60	28	113
	2.76	2.6	-40	-70	2	266
Occipital lobe	2.39	2.28	-34	-76	-4	
	1.93	1.87	-40	-58	-12	
	2.72	2.57	54	24	32	245
Prefrontal cortex	2.38	2.26	36	6	34	
	2.16	2.08	52	14	40	
	2.68	2.52	-42	-34	-4	456
Temporal lobe	2.67	2.52	-36	-44	-14	
	2.24	2.15	-38	-46	-6	
Occipital lobe	2.6	2.46	36	-70	-10	121

References

Göttlich M., Beyer F., Krämer U. BASCO: a toolbox for task-related functional connectivity. *Frontiers in systems neuroscience*, *Frontiers*, 2015;*9*.

Rupprechter S, Stankevicius A, Huys Q, Steele JD, Series P. Major Depression Impairs the Use of Reward Values for Decision-Making. *Scientific Reports*. 2018;(in press).

Stankevicius A, Huys Q, Kalra A, Series P. Optimism as a prior belief about the probability of future reward. *PLoS Computational Biology*. 2014;10.

Appendix C

Supplementary Materials for Chapter 5

This chapter contains the Supplementary Materials for Chapter 5 which was published as S. Rupprechter, L. Romaniuk, P. Seriès, et al. (2020). "Blunted Medial Prefrontal Cortico-Limbic Reward-Related Effective Connectivity and Depression". In: *Brain (accepted)*.

Tables B1-B24 show the results of the DCM BMA analyses which included individual QIDS symptoms (listed at the end). See Tables S11-S21 for legends.

Supplementary Material

Blunted Medial Prefrontal Cortico-Limbic Reward-Related Effective Connectivity and Depression

Samuel Rupprechter[1], Liana Romaniuk[2], Peggy Series[1], Yoriko Hirose[2], Emma Hawkins[2], Anca-Larisa Sandu[3], Gordon D. Waiter[3], Christopher J. McNeil[3], Xueyi Shen[2], Mathew A. Harris[2], Archie Campbell[4], David Porteous[4], Jennifer A. Macfarlane[5], Stephen M. Lawrie[2], Alison D. Murray,[3] Mauricio R. Delgado[6], Andrew M. McIntosh[2], Heather C. Whalley[2]*, J. Douglas Steele[5]*

[1]School of Informatics, University of Edinburgh, UK; [2]Division of Psychiatry, University of Edinburgh; [3]Biomedical Imaging Centre, University of Aberdeen; [4]Centre for Genomic and Experimental Medicine, University of Edinburgh, [5]Division of Imaging Science and Technology, Medical School, University of Dundee, [6]Department of Psychology, Rutgers University. *joint last authors

Participant Details

Table 1 (in the main text) and Table S23 contain details about participants' demographics and clinical information. Diagnostic screening showed that our sample included 20 participants satisfying criteria for MDD, 110 participants matching remitted MDD, and 345 never-depressed subjects. Dynamic Causal Modelling (DCM) of event-related connectivity was done with data from an initial 301 participants (after excluding participants with insufficient signal in our regions of interest, 19 MDE remained, who were further filtered to include subjects for whom the explained variance of the full DCM for each subject exceeded variable minimum thresholds (see DCM section below). This is summarised in Figure S11.

QIDS scores covered a wide range (0 to 23), although the distribution was skewed (Figure S1). Additional non-parametric Spearman's rank correlation tests were used to test for the relationship between QIDS and reward signals to minimize the risk of outliers affecting our mass-univariate GLM results (see below). Figure S2 shows a histogram of the number of missed trials.

Figure S1. Histogram of participants' QIDS scores.

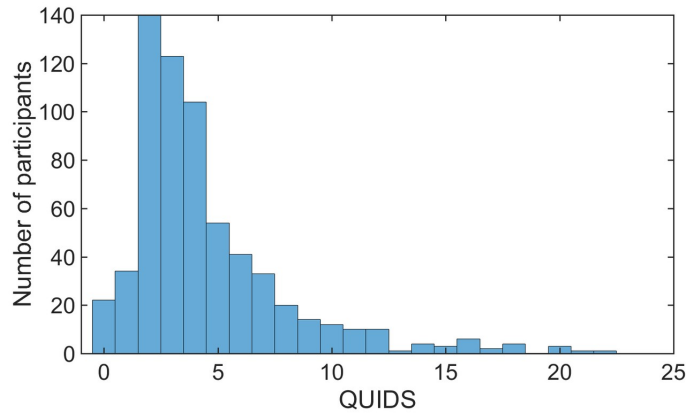

Figure S2. Histogram of number of missed trials.

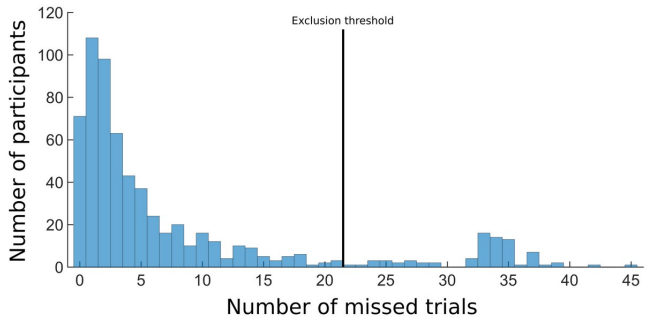

Participants with more than 21 missed trials were excluded (77 participants).

Computational modelling

Table S1. Model specification.

Name	Description	Value update: $V^{(t+1)}$	Parameters
M1	only learn from choice condition	$V^{(t)} + \varepsilon_c \times \left(r^{(t)} - V^{(t)}\right)$	ε_c, β
M2	learn equally from choice/no-choice conditions	$V^{(t)} + \varepsilon \times \left(r^{(t)} - V^{(t)}\right)$	ε, β
M3	learn differently from choice/no-choice conditions	$V^{(t)} + \varepsilon_D^{(t)} \times \left(r^{(t)} - V^{(t)}\right)$	ε_c, ε_n, β
M4	experience reward differently during choice/no-choice conditions	$V^{(t)} + \varepsilon \times \left(\rho_D^{(t)} \times r^{(t)} - V^{(t)}\right)$	ε, ρ_c, ρ_n
M5	learn and experience reward differently during choice/no-choice conditions	$V^{(t)} + \varepsilon_D^{(t)} \times \left(\rho_D^{(t)} \times r^{(t)} - V^{(t)}\right)$	ε_c, ε_n, ρ_c, ρ_n

The third column shows how internal values are updated after observing an outcome r in trial t. Choices were modelled probabilistically by passing the value difference to a logistic sigmoid function: p(choose V_1) = 1 / (1 + e^(-β (V_1 – V_2))). ε is the learning rate with c and n being indicators for separate choice/no-choice learning rates; β is the inverse temperature parameter; ρ is the reward sensitivity parameter with c and n being indicators for separate choice/no-choice parameters.

Model-fitting and model comparison

Parameter estimation (for each model) followed a hierarchical procedure. For each participant, we first estimated maximum likelihood (ML) estimates and then combined these into a group prior (normal distribution). The prior was then used to estimate maximum *a posteriori* (MAP) parameter values for each participant. These estimates were again combined into a single group prior and the procedure was iterated until convergence. We used the integrated Bayesian information criteria (iBIC) to perform model comparison. Sampling was used to estimate an integral over parameters, which was used to approximate the model evidence. iBIC scores were computed for each model and compared to choose the most parsimonious model. More details are available (Supplements of Huys et al. 2013 and Rupprechter et al. 2018).

Computational modelling results

Model comparison identified *Model 3* as the most parsimonious model (Figure S3) and subsequent analyses only focussed on this model. For each participant we calculated the asymptotic internal value estimations for the two stimuli as the average over the last 10 trials. The results are depicted in Figure S4, which shows that participants' value estimations are close to the actual probabilities of the two stimuli. The two estimated learning rate parameters of the winning model were highly correlated across participants (Pearson's r=0.883, $p<10^{-10}$) but parameter recovery simulations showed they could both be recovered. Spearman's correlations were calculated between QIDS scores and each the three model parameters. No correlation was significant (choice learning rate: Spearman's ρ=0.046, p=0.316; no-choice learning rate: Spearman's ρ=0.056, p=0.226; inverse temperature parameter: Spearman's ρ=0.076, p=0.098). We then performed a "default Bayesian hypothesis test" (Wetzels & Wagenmakers, 2012) which allowed us to quantify evidence *for* the null hypothesis of no correlation. This relies on estimated Pearson correlations which were all similar to the Spearman's correlations and non-significant (choice learning rate: r=0.032, p=0.487; no-choice learning rate: r=0.047, p=0.302; inverse temperature parameter: r=0.017, p=0.704). The estimate Bayes factors were: choice learning rate: BF10=0.047, no-choice learning rate: BF10=0.062, inverse temperature parameter: BF10=0.039. These values can be interpreted as "strong" evidence in favour of the null (Wetzels & Wagenmakers, 2012).

Whilst Huys et al. (2013) found meta-analytic evidence for an association of depressive symptom scores (specifically anhedonia) and a "reward sensitivity" model parameter, which is closely related to our "inverse temperature" model parameter, we did not find this effect. Differences between studies could account for this. It is important to note that we used an overall depressive symptoms score instead of a specific

anhedonia score. Additionally the signal detection task used by Huys et al. involves many more trials and the influence of reward sensitivity on behaviour might only become apparent after many trials.

Figure S3. Model comparison results.

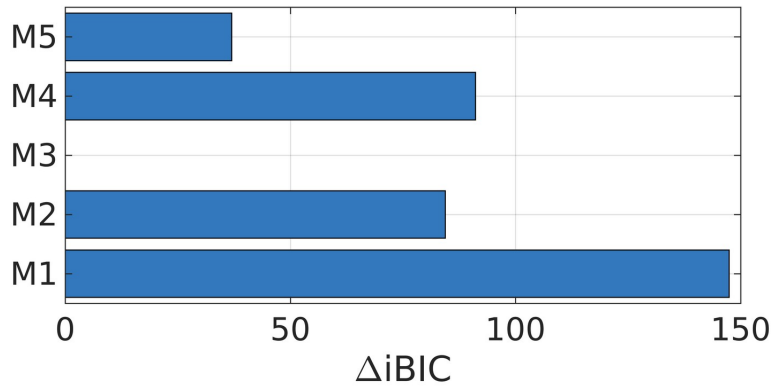

iBIC scores relative to the lowest (i.e. best) iBIC score are shown. M3 which includes different learning rates depending on choice or no-choice condition was the most parsimonious model. M1 assumed participants did not learn from no-choice trials. M2 assumed participants learned equally well from both conditions (same learning rate parameter). M4 assumed that it was reward responsiveness that was dependent on condition but not learning rate (one learning rate parameter, two reward sensitivity parameters). M5 assumed both learning rate and reward sensitivity were dependent on condition.

Figure S4. Asymptotic internal value estimations.

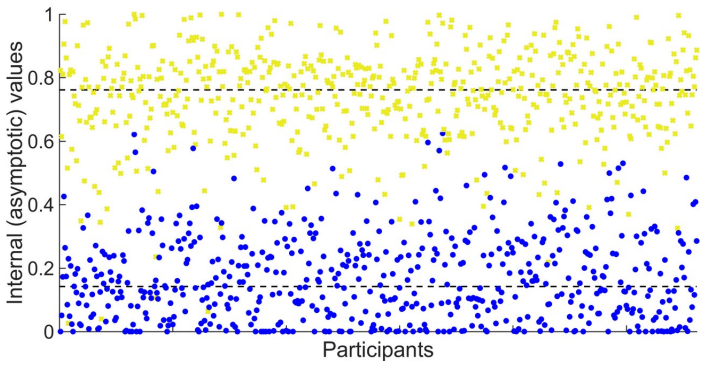

Yellow dots are asymptotic value estimations for the yellow stimulus (80% reward probability) and blue dots are asymptotic value estimations for the blue stimulus (20% reward probability). The black dotted lines show the average asymptotic value estimations across participants for the two stimuli, which are close to the true reward probabilities.

Neuroimaging analyses

Pre-processing details

SPM12 (version 7487) was used for analyses. Functional images were manually checked for artefacts before pre-processing. The first six blood oxygen level-dependent volumes were discarded as standard because of transient effects. Functional images were realigned to the first image using a rigid body spatial transformation (6 parameters) and unwarped. The estimated movement parameters were plotted and manually inspected for excessive motion. If such excessive motion was identified, the corresponding functional images were inspected and participants were excluded if there were noticeable excessive movement. Slice timing correction was performed with the middle slice as the reference slice. (We therefore did not use the additional slice timing correction model included as part of DCM.) The T1 weighted structural image was segmented using SPM12 tissue probability maps and the ICBM space template for European brains and functional images were co-registered to the bias corrected T1 image. The estimated deformation field was then used to spatially normalise the images and an 8 mm FWHM Gaussian kernel was used to smooth the normalised images. The registration was inspected manually using SPM's checkreg tool and participants were excluded if the registration quality was judged insufficient.

Freesurfer ROIs

Raw T1 images were segmented and parcellated using FreeSurfer version 5.3 (Dale et al., 1999; Fischl et al., 1999; Fischl et al., 2004) and the Desikan-Killany atlas (Desikan et al., 2006). FreeSurfer output was visually quality checked, major errors were excluded and minor errors were corrected manually. To create ROI masks, FreeSurfer parcellations were reoriented to the original image and converted back to NIfTI format. Using FSL 5.0 (Smith et al., 2004; Woolrich et al., 2009; Jenkinson et al., 2012), these images were thresholded to isolate each ROI and then binarised to create a mask. ROIs were normalised in the same way as functional images using the estimated deformation field.

Multiple comparisons correction

To correct for multiple comparisons we used Monte Carlo simulations (Slotnick & Schacter, 2004) to establish a cluster extent threshold. This relies on the fact that the larger a cluster the less likely it is that each individual voxel in the cluster shows spurious activity and survives an individual voxel threshold. The script we used can be downloaded from the author's website (https://www2.bc.edu/sd-slotnick/scripts.htm) who also defended this method in subsequent publications (Slotnick, 2017). The parameters we used are as follows: x_matrix=64; y_matrix=64; slices=32; dim_xy=3.4; dim_z=4.5; mask_name='none'; mask_bytes=0; mask_plot=0; FWHM=8; dim_resampled=2; iterations=5000; p_corrected=0.001; p_voxel=0.05. Note that in Tables S2-S9 we usually list a small number of local maxima at least 8mm apart but we focus on interpreting clusters of activity rather than individual voxels.

Signal dropout

For group level analyses, SPM only includes voxels which are included in the mask of every individual. Signal dropout of voxels within a single participant therefore excludes those voxels from further analyses for all participants, which can become a problem when a large number of participants are involved. For first level analyses the masking threshold was therefore lowered to 0.4 to increase the included area. An explicit mask was used to constrain analysis to voxels within the brain (SPM's intracranial volume mask; mask_ICV.nii). Nevertheless, a few areas were excluded due to signal dropout (Figure S5), including parts of the right VS and a region in the PFC including subgenual ACC and OFC.

Figure S5. Group-level signal dropout.

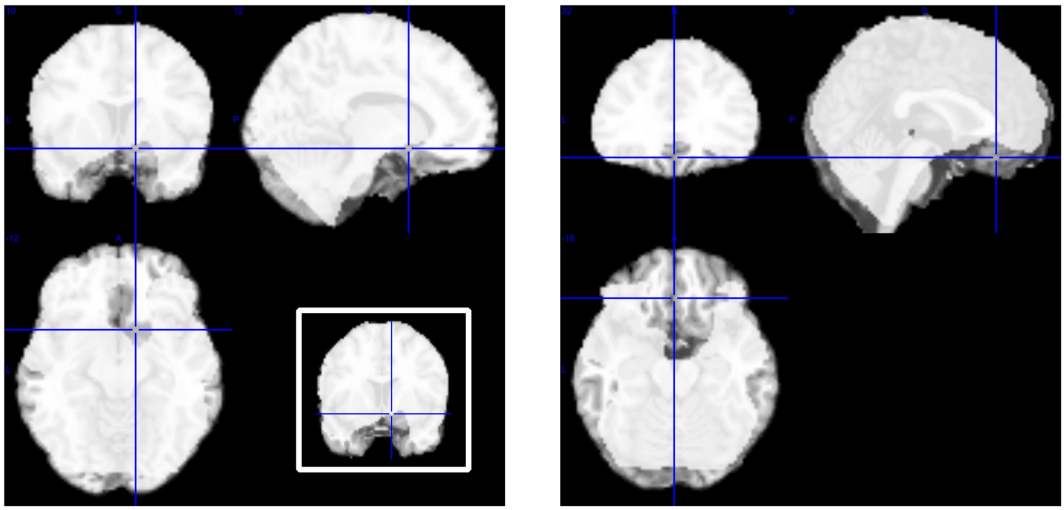

The second level mask (white) is shown as overlay on a Colin brain. **Left**: Dropout in the right VS (12,10,-12); the inset of the bottom right shows a small part of the right VS which is included in the mask (10,8,-10). **Right**: Dropout in the subgenual ACC and OFC (0,32,-18).

fMRI results tables

Table S2. Reward activation across participants.

***Reward* > *No-reward* (p<0.05 FWE correction)**					
k	T	x	y	z	
19270	40.05	10	-86	-6	Occipital lobe
	38.91	-20	-80	-14	
	38.43	-10	-88	-8	
710	15.38	-52	0	48	Premotor cortex L
	6.77	-40	-2	62	
426	12.12	-16	44	50	dPFC
	5.89	-32	34	48	
	5.47	-22	22	64	
1311	10.97	-58	-8	-12	Temporal gyrus L
	9.66	-58	-30	0	
	7.97	-50	-40	2	
3036	10.61	-12	10	-14	Ventral striatum, vmPFC
	9.95	-4	54	-10	
	9.87	-6	66	16	
237	9.18	-22	-30	-2	Hippocampus L
117	7.91	54	38	6	PFC
	6.76	52	42	-2	
	5.80	56	34	16	
48	7.80	22	42	50	PFC
	6.23	14	50	46	
177	7.62	-26	-56	52	Parietal lobe L
97	7.04	24	-56	52	Parietal lobe R
73	6.56	24	-28	-2	Hippocampus R
122	5.91	-28	-8	2	Putamen L
82	5.68	-28	-8	-22	Hippocampus L
79	5.47	62	0	-14	Temporal lobe R
	5.33	58	-6	-18	
3	5.32	46	50	2	PFC
3	4.97	16	38	58	PFC
19	4.96	-22	-42	-48	Cerebellum
3	4.93	6	58	38	
2	4.86	-4	54	42	
3	4.75	20	16	22	
3	4.75	28	48	36	
4	4.72	62	18	26	
1	4.66	58	8	-18	
1	4.63	32	36	48	
1	4.58	-24	14	-24	
1	4.57	-26	18	-24	

Table S3. Reward deactivation across participants.

***No-reward > Reward* (p<0.05 FWE correction)**

k	T	x	y	z	
4938	13.22	42	-72	42	Angular gyrus R
	13.00	58	-56	34	
	6.82	64	-52	-8	
6654	12.54	0	22	50	SMA, dPFC / MCC
	11.99	12	16	62	
	10.40	42	14	46	
1156	11.39	46	16	0	Insula R
	9.65	34	22	0	
2925	10.17	-58	-62	28	Angular gyrus L
	9.59	-58	-50	44	
	9.56	-62	-46	38	
787	9.92	-40	18	2	Insula L
	9.28	-30	22	-8	
1347	8.62	4	-62	48	Precuneus
	7.72	8	-66	64	
192	7.36	-12	6	6	Caudate L
333	7.23	22	54	18	PFC
	6.29	32	52	8	
153	6.73	-32	-58	-32	Cerebellum
	5.75	-24	-72	-32	
	4.85	-14	-78	-30	
87	6.28	14	6	6	Caudate R
159	6.18	-30	52	16	PFC
16	5.41	-44	-60	-46	cerebellum
15	5.15	48	-4	-36	Temporal lobe R

Table S4. Effects of choice reward outcomes.

***Reward (choice) > Reward (no-choice)* (p<0.05 FWE correction)**

k	T	x	y	z	
1290	8.76	36	18	-12	Insula R
	7.43	46	26	-2	
	5.41	34	20	-28	
2394	8.50	0	52	16	mPFC / rostral ACC
	6.96	4	42	26	
	6.46	18	58	28	
259	6.83	-28	18	-14	Insula L
165	6.20	-32	-92	6	Occipital lobe
65	5.33	-22	-6	-14	Amygdala L
142	5.32	-34	-82	-10	Occipital lobe
	4.97	-30	-74	-14	
74	5.26	22	-4	-12	Amygdala R
	5.13	22	6	-8	
5	4.75	-12	4	-10	VS L

Table S5. Negative association between depressive severity and reward outcome signals in areas of reward activation across participants.

Conjunction analysis (each p<0.001 whole brain cluster corrected):
(1) negative association of reward outcome signal with QIDS
(2) *activation* across participants during reward outcome

k	T	x	y	z	
3580	3.50	26	4	0	Putamen R + L, OFC
	3.20	32	-2	6	
	2.99	-26	18	-20	
168	2.51	-6	-60	-32	Cerebellum
	2.37	-6	-52	-34	
	2.13	-16	-44	-40	

Table S6. Negative association between depressive severity and reward outcome signals in areas of reward deactivation across participants.

Conjunction analysis (each p<0.001 whole brain cluster corrected):
(1) negative association of reward outcome signal with QIDS
(2) *deactivation* across participants during reward outcome

k	T	x	y	z	
1629	4.01	-16	10	6	Caudate L, insula L
	4.00	-34	18	-10	
	3.65	-14	8	16	
478	3.84	18	8	6	Caudate R
1727	3.38	-4	30	50	dmPFC, ACC
	3.23	10	32	48	
	2.57	24	56	20	
162	3.22	-36	22	46	PFC L
	2.00	-34	16	36	
260	3.17	-42	-62	-48	Cerebellum
	2.79	-38	-62	-36	
860	2.74	-58	-46	34	Angular gyrus L
	2.40	-60	-58	18	
	2.28	-52	-56	30	
459	2.47	28	24	-6	Insula R
	2.30	28	20	10	
	2.27	54	6	14	
198	2.38	42	24	44	PFC R
	2.12	36	20	40	
	2.05	32	14	30	

Table S7. Positive association between depressive severity and reward outcome signals in areas of reward activation across participants.

Conjunction analysis (each p<0.001 whole brain cluster corrected): **(1) positive association of reward outcome signal with QIDS** **(2) *activation* across participants during reward outcome**					
k	T	x	y	z	
1403	3.13	10	-86	20	Occipital lobe
	2.92	4	-82	2	
	2.84	-8	-90	10	

Table S8. Negative association between depressive severity and reward prediction error signals in areas of positive RPE signals across participants.

Conjunction analysis (each p<0.001 whole brain cluster corrected): **(1) negative association of RPE signal with QIDS** **(2) *positive RPE signal encoding* across participants**					
k	T	x	y	z	
3304	3.98	32	-2	6	Putamen R + L, pallidum R + L, OFC R,
	3.87	22	-2	2	midbrain / VTA
	3.30	32	-14	4	
	2.26	8	-16	-10	
327	3.10	-42	12	-30	Temporal lobe L
	2.40	-34	4	-30	
	2.23	-36	6	-22	
198	2.89	-28	-62	-46	Cerebellum L
	2.16	-38	-64	-46	
	1.71	-38	-62	-38	
872	2.58	16	36	10	ACC
	2.55	-10	38	22	
	2.40	14	42	24	
161	2.53	-34	22	-16	OFC L
	2.47	-26	20	-20	
	1.88	-50	28	-16	

Table S9. Negative association between depressive severity and reward prediction error signals in areas of negative RPE signals across participants.

Conjunction analysis (each p<0.001 whole brain cluster corrected):
(1) negative association of RPE signal with QIDS
(2) *negative RPE signal encoding* across participants

k	T	x	y	z	
632	3.14	46	14	-2	Insula R
	2.94	46	12	6	
	2.83	56	6	6	
384	2.86	-34	12	12	Insula L
	2.69	-42	10	2	
	2.39	-38	16	-4	
160	2.72	-12	10	2	Caudate L
	2.02	-16	20	2	
143	2.58	-40	-62	14	
324	2.54	-4	28	52	dmPFC
	2.39	10	32	48	
	2.28	-4	38	48	
165	2.28	-52	-56	32	Parietal lobe
	2.10	-54	-58	42	

Control analyses

We repeated our correlation analyses using a GLM with additional covariates “site”, “sex”, and “age” (mean-centred). We also performed additional control analysis excluding 103 participants who were related to another participant (372 remaining). The results of these analyses were very similar to the results in Tables S2-S9 and here we only show that the negative association between depressive severity and reward signals in the striatum (Figure S6).

Figure S6. Correlations with depressive symptom scores.

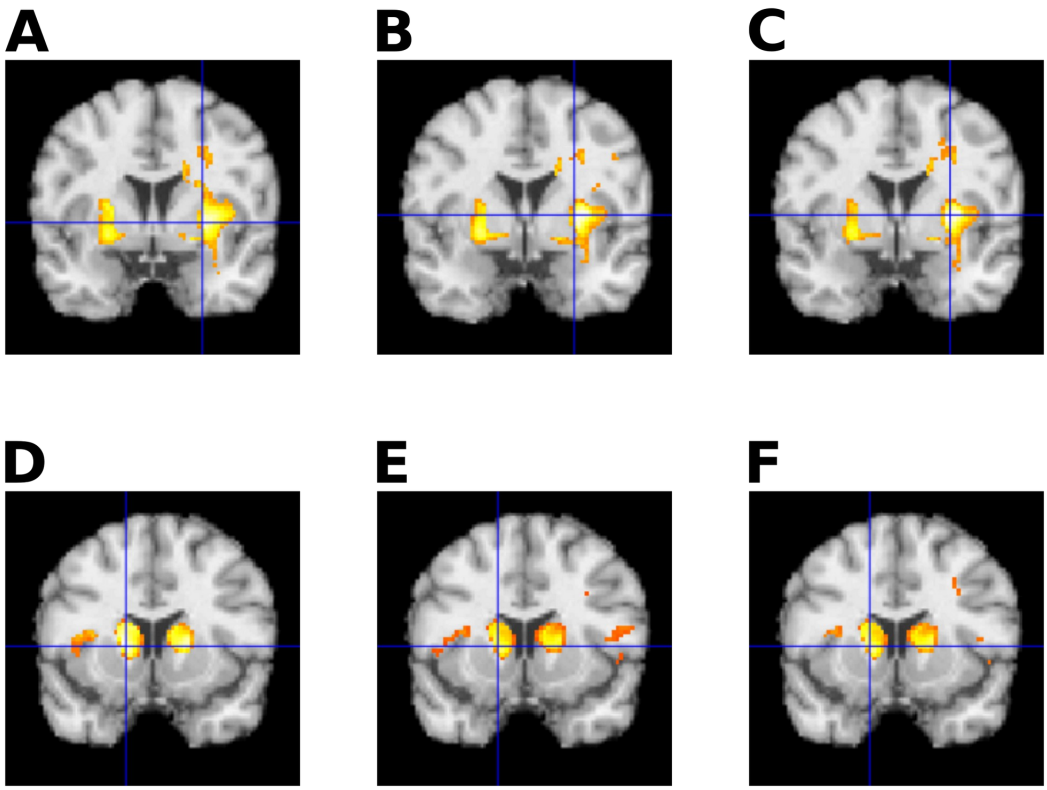

This shows the results of conjunction analyses of activation or deactivation across participants and negative association with depressive symptoms (see also Figure 2 in the main text). (A and D) Results following the inclusion of additional covariates site, sex and age. (B and E) Results following the exclusion of related participants. (C and F) Results following exclusion of related participants and inclusion of additional covariates.

Non-parametric correlations

Additional non-parametric Spearman correlation tests were performed between QIDS scores and median contrast (*reward > baseline*) beta values extracted of 4mm spheres centred around local maxima of the GLM analyses (Table S10). The results agree with the previous analysis, with the exception that the positive association between depressive symptoms scores and reward signal encoding in the occipital lobe was not significant.

Table S10. Spearman rank correlation analysis between reward signals and QIDS scores.

x	y	z	Spearman's ρ	p	
18	8	6	-0.150	0.001	basal ganglia
26	4	0	-0.159	0.0005	putamen
32	-2	6	-0.127	0.005	putamen
-24	6	6	-0.152	0.0009	putamen
20	6	-6	-0.127	0.006	ventral striatum
-12	10	2	-0.121	0.008	ventral striatum
-16	10	6	-0.198	1.34e-05	caudate
-4	30	50	-0.156	0.0006	medial PFC
16	36	10	-0.127	0.006	rostral ACC
-34	18	-10	-0.183	6.15e-05	insula
4	-82	2	0.089	0.054	occipital lobe
10	-86	20	0.071	0.124	occipital lobe
-8	-90	10	0.044	0.337	occipital lobe

The median estimated beta values from individuals' contrast files were extracted from voxels within 4mm spheres centred around coordinates of significant reward signals. Correlations were calculated between these beta values and depressive severity scores and results are presented here.

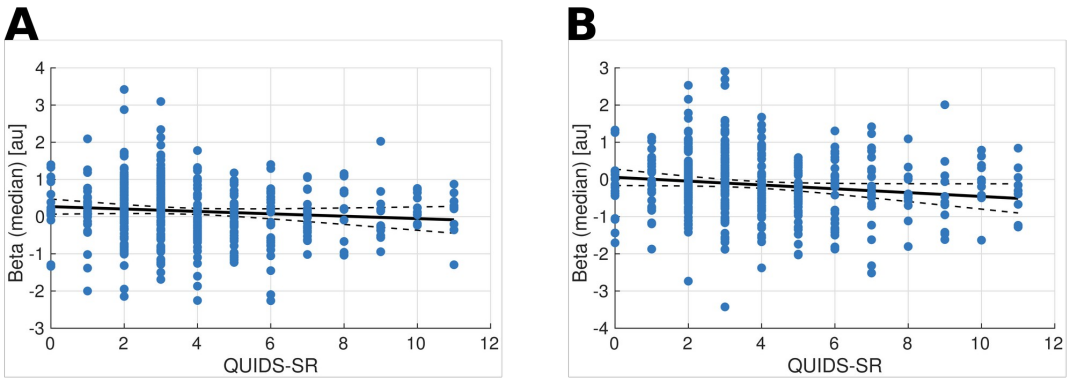

Figure S7. Scatter plot of QIDS scores and median reward-contrast beta estimates.
Participants with QIDS scores larger than 11 were excluded and correlations remained significant after these exclusions. (A) 4mm spheres centred at (26,4,0); Spearman's ρ=-0.140, p=.003. (B) 4mm sphere centred at (-16,10,6); Spearman's ρ=-0.180, p<.001.

DCM Analysis

Dynamic causal modelling (DCM12.5; Friston et al. 2003) was used to test for effective (directed) interactions between brain regions. DCM treats the brain as a deterministic non-linear dynamic system which receives inputs and then produces outputs. The unknown (arbitrary) function describing the evolution of the neuronal states is parameterised using a bilinear approximation, which reduces the parameters to three important sets: (a) the interaction between neuronal systems in the absence of input ("A" matrix), (b) the change of this interaction induced by (experimentally-controlled) inputs ("B" matrix), (c) extrinsic experimentally-controlled inputs ("C" matrix). A haemodynamic model (containing additional parameters which are usually not of interest) is used to map the underlying neuronal state changes to the haemodynamic response (i.e. the observed BOLD signal).

Time-series extraction

For the time-series extraction a GLM was used containing columns for outcomes, reward outcomes, choice outcomes, choice cues, no-choice cues, choice responses, no-choice responses and nuisance regressors, and an "effects of interest" F contrast was computed (including all effects except nuisance regressors). ROIs were defined as a combination (logical AND) of the following ROIs: (a) 12mm spheres centred around coordinates of (group-level) local maxima (see main-text), (b) subject-specific whole brain mask (*mask.nii* from first level analysis), (c) thresholded SPM mask using a liberal threshold ($p<0.15$; note that this was used to exclude noisy voxels and was not used to infer statistical significance) for the *reward* (visual area and VS) or choice (mPC) contrast, (d) anatomical FreeSurfer masks for the visual area (pericalcarine) and VS (striatum). Time-series were extracted from each of these (combined) ROIs, adjusted for the effects of interest. We were not able to extract time-series from all three regions for 174 participants (because in at least one region there were no voxels in the combined mask).

Variance thresholds

We used a script included with SPM (spm_dcm_fmri_check.m) to calculate the proportion of explained signal by the model. As suggested in the function's documentation and the SPM mailing-list (https://www.jiscmail.ac.uk/cgi-bin/webadmin?A0=SPM), we set an *a priori* threshold at 10% and excluded participants below this threshold. Examples of models with low variance explained were inspected manually and many of these models seemed to have "flat-lined", meaning estimates did not converge from their prior mean.

Control analyses

We performed several control analyses to verify that our results did not depend on the exact specification of the model. First, we increased the threshold of the minimum explained variance to 15% and repeated the PEB analysis with the remaining 99 participants (mean variance explained 28.31%). Similarly, we reduced the threshold to 7.5% and repeated the analysis with 208 participants (mean variance explained 19.20%) and also computed the top-down connection strength as a function of the threshold (see *Variance threshold* section below). Second, we repeated the analysis without including covariates and with including only anxiety (HADS-A) as covariate. Third, we estimated a single PEB model for both "A" and "B" DCM matrices (54 parameters; only using QIDS and site as covariates to limit the dilution of evidence). Last, we re-defined the experimentally-controlled inputs as outcome(choice, reward), outcome(choice, no reward), outcome(no-choice, reward), outcome(no-choice, no-reward) in addition to the (unchanged) inputs cue(choice), cue(no choice), response(choice) and response(no choice). It was again assumed that each of the four outcome conditions could modulate each of the endogenous connections.

Results of control analyses are displayed in Tables S12-S17. Although the exact values of estimated parameters varied and automatic pruning did not always identify the exact same connections as important,

there was generally a large overlap between the individual results. Importantly, the negative association between QIDS depressive severity and intrinsic connectivity strength from mPC to VS remained for *every* single analysis strategy. Note that any parameter not pruned during the automatic search is important and useful in that it contributes to the free energy, even if the posterior probability is less than 95%.

PEB-BMA results: intrinsic connections (A matrix)

Tables S11-S17 list posterior probabilities and effect sizes of intrinsic connections related to commonalities and differences across participants. Results for different variance thresholds are shown and with various covariates included. The connection from mPC to VS is highlighted in all tables. It is the only connection that has non-zero probability of there being an effect of QIDS for every single analysis strategy.

Table S11. BMA results of intrinsic connections.

	P(common)	P(QIDS)	P(HADS-A)	P(site)	P(age)	P(sex)	P(MDD)
A(1,1)	1	1	0	1	0.72	0	0
A(2,1)	1	1	0	0.62	0	0	0
A(3,1)	0	0	0	0.51	0	0	1
A(1,2)	1	0	0	0.56	0	0	0
A(2,2)	1	0	1	0	1	0	0
A(3,2)	1	1	0	1	0	1	0
A(1,3)	1	1	0.73	0.8	0.63	0	0
A(2,3)	0	0	0	1	0	1	0
A(3,3)	1	0	1	0	0	0.66	0

	E(common)	E(QIDS)	E(HADS-A)	E(site)	E(age)	E(sex)	E(MDD)
A(1,1)	0.480	-0.019	0.000	0.152	-0.006	0.000	0.000
A(2,1)	0.121	0.013	0.000	0.021	0.000	0.000	0.000
A(3,1)	0.000	0.000	0.000	0.013	0.000	0.000	0.145
A(1,2)	0.450	0.000	0.000	-0.032	0.000	0.000	0.000
A(2,2)	-0.369	0.000	0.031	0.000	0.006	0.000	0.000
A(3,2)	0.065	-0.011	0.000	-0.048	0.000	0.086	0.000
A(1,3)	-0.232	-0.030	-0.017	0.060	0.004	0.000	0.000
A(2,3)	0.000	0.000	0.000	-0.095	0.000	0.135	0.000
A(3,3)	-0.245	0.000	-0.013	0.000	0.000	-0.054	0.000

165 participants; 10% variance threshold; P(x) shows the posterior probability of the estimates (E(x)) being non-zero. The first column identifies the connection as A(TO, FROM), where 1=visual area, 2=mPC, 3=VS; e.g. A(1,2) is the connection from mPC to visual area

Table S12. BMA results of intrinsic connections using an increased quality threshold.

	P(common)	P(QIDS)	P(HADS-A)	P(site)	P(age)	P(sex)	P(MDD)
A(1,1)	1	1	0	1	0.54	0	1
A(2,1)	1	1	0	0.71	0	0	0
A(3,1)	0.73	0.71	1	1	0	1	0.7
A(1,2)	1	0	0	1	0.53	0	0
A(2,2)	1	1	0	0	0	0	0
A(3,2)	1	1	0	1	0	1	0
A(1,3)	1	0.77	1	1	0	0	0
A(2,3)	1	0	0	0.77	0	1	0
A(3,3)	1	0	1	0	1	1	0

	E(common)	E(QIDS)	E(HADS-A)	E(site)	E(age)	E(sex)	E(MDD)
A(1,1)	0.424	-0.032	0.000	0.122	-0.003	0.000	0.596
A(2,1)	0.135	0.017	0.000	0.028	0.000	0.000	0.000
A(3,1)	-0.024	0.009	-0.016	0.059	0.000	-0.077	0.107
A(1,2)	0.429	0.000	0.000	-0.085	0.003	0.000	0.000
A(2,2)	-0.316	0.022	0.000	0.000	0.000	0.000	0.000
A(3,2)	0.068	-0.010	0.000	-0.082	0.000	0.109	0.000
A(1,3)	-0.179	-0.018	-0.033	0.088	0.000	0.000	0.000
A(2,3)	0.114	0.000	0.000	-0.052	0.000	0.178	0.000
A(3,3)	-0.311	0.000	-0.020	0.000	0.006	-0.169	0.000

99 participants; 15% variance threshold; P(x) shows the posterior probability of the estimates (E(x)) being non-zero. The first column identifies the connection as A(TO, FROM), where 1=visual area, 2=mPC, 3=VS; e.g. A(1,2) is the connection from mPC to visual area.

Table S13. BMA results of intrinsic connections using a decreased quality threshold.

	P(common)	P(QIDS)	P(HADS-A)	P(site)	P(age)	P(sex)	P(MDD)
A(1,1)	1	1	0	1	0	0	0
A(2,1)	1	1	0	0	0	0	0
A(3,1)	0.73	0	0	0.51	0	0	1
A(1,2)	1	0.63	0	0.56	0	0	0
A(2,2)	1	0	1	0	1	0	0
A(3,2)	1	1	0	1	0	0	0
A(1,3)	1	1	0.76	0.59	0.51	0	0
A(2,3)	0	0	0	1	0	0.65	0
A(3,3)	1	0	1	0	0	1	0

	E(common)	E(QIDS)	E(HADS-A)	E(site)	E(age)	E(sex)	E(MDD)
A(1,1)	0.539	-0.021	0.000	0.157	0.000	0.000	0.000
A(2,1)	0.104	0.010	0.000	0.000	0.000	0.000	0.000
A(3,1)	-0.021	0.000	0.000	0.012	0.000	0.000	0.153
A(1,2)	0.436	-0.009	0.000	-0.031	0.000	0.000	0.000
A(2,2)	-0.361	0.000	0.033	0.000	0.005	0.000	0.000
A(3,2)	0.058	-0.010	0.000	-0.039	0.000	0.000	0.000
A(1,3)	-0.247	-0.027	-0.018	0.034	0.003	0.000	0.000
A(2,3)	0.000	0.000	0.000	-0.082	0.000	0.066	0.000
A(3,3)	-0.243	0.000	-0.012	0.000	0.000	-0.110	0.000

208 participants; 7.5% variance threshold; P(x) shows the posterior probability of the estimates (E(x)) being non-zero. The first column identifies the connection as A(TO, FROM), where 1=visual area, 2=mPC, 3=VS; e.g. A(1,2) is the connection from mPC to visual area.

Table S14. BMA results of intrinsic connections using a PEB matrix without covariates.

	P(common)	P(QIDS)	E(common)	E(QIDS)
A(1,1)	1	0.96	0.471	-0.023
A(2,1)	1	0.98	0.121	0.012
A(3,1)	0	0	0.000	0.000
A(1,2)	1	0	0.447	0.000
A(2,2)	1	1	-0.366	0.023
A(3,2)	1	0.76	0.069	-0.007
A(1,3)	1	1	-0.237	-0.042
A(2,3)	0	0	0.000	0.000
A(3,3)	1	0	-0.244	0.000

165 participants; 10% variance threshold; P(common) and P(QIDS) show the posterior probability of the estimates (E) being non-zero. The first column identifies the connection as A(TO, FROM), where 1=visual area, 2=mPC, 3=VS; e.g. A(1,2) is the connection from mPC to visual area.

Table S15. BMA results of intrinsic connections using a PEB matrix with a single covariate (anxiety).

	P(common)	P(QIDS)	P(HADS-A)	E(common)	E(QIDS)	E(HADS-A)
A(1,1)	1	0.95	0	0.475	-0.023	0.000
A(2,1)	1	0.97	0	0.120	0.012	0.000
A(3,1)	0	0	0	0.000	0.000	0.000
A(1,2)	1	0	0	0.449	0.000	0.000
A(2,2)	1	0	1	-0.366	0.000	0.031
A(3,2)	1	0.78	0	0.069	-0.008	0.000
A(1,3)	1	0.92	0.82	-0.236	-0.027	-0.022
A(2,3)	0	0	0	0.000	0.000	0.000
A(3,3)	1	0	0.7	-0.245	0.000	-0.008

165 participants; 10% variance threshold; P(common), P(QIDS), and P(HADS-A) show the posterior probability of the estimates (E) being non-zero. The first column identifies the connection as A(TO, FROM), where 1=visual area, 2=mPC, 3=VS; e.g. A(1,2) is the connection from mPC to visual area.

Table S16. BMA results of intrinsic connections using an alternative input specification.

	P(common)	P(QIDS)	E(common)	E(QIDS)
A(1,1)	1	0	0.674	0.000
A(2,1)	0.98	0	0.050	0.000
A(3,1)	0.62	0.93	-0.015	0.010
A(1,2)	1	0	0.453	0.000
A(2,2)	1	0	-0.402	0.000
A(3,2)	1	0.98	0.071	-0.014
A(1,3)	0	0	0.000	0.000
A(2,3)	0.7	0	0.042	0.000
A(3,3)	1	0	-0.396	0.000

141 participants; 10% variance threshold; common variance explained = 19.89%; P(common) and P(QIDS) show the posterior probability of the estimates (E) being non-zero. The first column identifies the connection as A(TO, FROM), where 1=visual area, 2=mPC, 3=VS; e.g. A(1,2) is the connection from mPC to visual area. See Control analyses section for input specification.

Table S17. BMA results of intrinsic connections using an alternative input specification and anxiety as covariate.

	P(common)	P(QIDS)	P(HADS-A)	E(common)	E(QIDS)	E(HADS-A)
A(1,1)	1	0	0.62	0.677	0.000	0.012
A(2,1)	0.98	0	0	0.051	0.000	0.000
A(3,1)	0.64	1	0.46	-0.016	0.012	-0.004
A(1,2)	1	0	0.93	0.457	0.000	0.023
A(2,2)	1	0.66	1	-0.401	-0.013	0.024
A(3,2)	1	1	0	0.072	-0.015	0.000
A(1,3)	0	0	0	0.000	0.000	0.000
A(2,3)	0.71	0	0	0.046	0.000	0.000
A(3,3)	1	0	0.57	-0.397	0.000	-0.008

141 participants; 10% variance threshold; mean variance explained = 19.89%; P(common), P(QIDS) and P(HADS-A) show the posterior probability of the estimates (E) being non-zero. The first column identifies the connection as A(TO, FROM), where 1=visual area, 2=mPC, 3=VS; e.g. A(1,2) is the connection from mPC to visual area.

PEB results: modulations (B matrix)

Tables S18-S21 list posterior probabilities and effect sizes of modulations of connections related to commonalities and differences (QIDS) across participants. Table S21 lists posterior probabilities and effect sizes of a control analysis for which a single PEB model was defined for both intrinsic connectivity and modulations.

Table S18. BMA results of modulations by reward outcome conditions.

	P(common)	P(QIDS)	E(common)	E(QIDS)
B(1,1)	1	0	-1.346	0.000
B(2,1)	0	0	0.000	0.000
B(3,1)	0	0	0.000	0.000
B(1,2)	0	0.82	0.000	-0.069
B(2,2)	0.98	0.88	-0.579	-0.068
B(3,2)	0	0	0.000	0.000
B(1,3)	0	0	0.000	0.000
B(2,3)	0.62	0	0.185	0.000
B(3,3)	1	0	-0.775	0.000

P(common) and P(QIDS) show the posterior probability of the estimates (E) being non-zero. The first column identifies the modulation of connection as B(TO, FROM), where 1=visual area, 2=mPC, 3=VS; e.g. B(1,2) is the modulation of the connection from mPC to visual area.

Table S19. BMA results of modulations by reward omission conditions.

	P(common)	P(QIDS)	E(common)	E(QIDS)
B(1,1)	0	0	0.000	0.000
B(2,1)	0	0	0.000	0.000
B(3,1)	0	0	0.000	0.000
B(1,2)	0	0	0.000	0.000
B(2,2)	1	0	-0.957	0.000
B(3,2)	0	0	0.000	0.000
B(1,3)	0.88	0.99	0.492	0.187
B(2,3)	0	0	0.000	0.000
B(3,3)	1	0	-1.223	0.000

P(common) and P(QIDS) show the posterior probability of the estimates (E) being non-zero. The first column identifies the modulation of connection as B(TO, FROM), where 1=visual area, 2=mPC, 3=VS; e.g. B(1,2) is the modulation of the connection from mPC to visual area.

Table S20. BMA results of modulations by choice outcome conditions.

	P(common)	P(QIDS)	E(common)	E(QIDS)
B(1,1)	1	0	-0.626	0.000
B(2,1)	1	0	-0.238	0.000
B(3,1)	1	0	0.251	0.000
B(1,2)	0.99	0	-0.519	0.000
B(2,2)	0.98	0	-0.615	0.000
B(3,2)	0	0	0.000	0.000
B(1,3)	0	0	0.000	0.000
B(2,3)	0	0	0.000	0.000
B(3,3)	1	1	-0.959	0.114

Bayesian model average results. P(common) and P(QIDS) show the posterior probability of the estimates (E) being non-zero. The first column identifies the modulation of connection as B(TO, FROM), where 1=visual area, 2=mPC, 3=VS; e.g. B(1,2) is the modulation of the connection from mPC to visual area.

Table S21. BMA results of modulations by no-choice outcome conditions.

	P(common)	P(QIDS)	E(common)	E(QIDS)
B(1,1)	1	0	-0.527	0.000
B(2,1)	1	0	-0.180	0.000
B(3,1)	1	0	0.147	0.000
B(1,2)	1	0	-0.660	0.000
B(2,2)	1	0	-0.916	0.000
B(3,2)	0	0	0.000	0.000
B(1,3)	0	0	0.000	0.000
B(2,3)	0	0	0.000	0.000
B(3,3)	1	0	-1.050	0.000

P(common) and P(QIDS) show the posterior probability of the estimates (E) being non-zero. The first column identifies the modulation of connection as B(TO, FROM), where 1=visual area, 2=mPC, 3=VS; e.g. B(1,2) is the modulation of the connection from mPC to visual area.

Table S22. Control analysis BMA results of intrinsic connections and modulations

		P(mean)	P(QIDS)	P(site)	E(mean)	E(QIDS)	E(site)
	A(1,1)	1	0.71	1	0.441	-0.011	0.147
	A(2,1)	1	1	0	0.123	0.012	0.000
	A(3,1)	1	0	0.58	-0.033	0.000	0.014
	A(1,2)	1	0	0.55	0.443	0.000	-0.030
	A(2,2)	1	1	0	-0.457	0.027	0.000
	A(3,2)	1	0.72	1	0.069	-0.006	-0.045
	A(1,3)	1	1	1	-0.230	-0.039	0.092
	A(2,3)	0	0	1	0.000	0.000	-0.091
	A(3,3)	1	0	0	-0.376	0.000	0.000
	B(1,1)	1	0	1	-1.115	0.000	-0.361
	B(2,1)	0	0	0	0.000	0.000	0.000
	B(3,1)	0	0	0	0.000	0.000	0.000
	B(1,2)	0	1	1	0.000	-0.098	-0.381
reward	B(2,2)	1	0	1	-1.166	0.000	0.417
	B(3,2)	0	0	1	0.000	0.000	0.177
	B(1,3)	0	0	0	0.000	0.000	0.000
	B(2,3)	0	0	0	0.000	0.000	0.000
	B(3,3)	1	0	1	-1.179	0.000	0.383
	B(1,1)	0.52	1	0	-0.169	0.074	0.000
	B(2,1)	0	0	0	0.000	0.000	0.000
	B(3,1)	0	0	0	0.000	0.000	0.000
	B(1,2)	0	0	0	0.000	0.000	0.000
reward omission	B(2,2)	1	0	1	-1.155	0.000	0.463
	B(3,2)	0	0	0	0.000	0.000	0.000
	B(1,3)	0	1	1	0.000	0.216	0.487
	B(2,3)	0	0	0	0.000	0.000	0.000
	B(3,3)	1	0	0	-1.340	0.000	0.000
	B(1,1)	1	0	0	-0.906	0.000	0.000
	B(2,1)	1	0	0	-0.122	0.000	0.000
	B(3,1)	1	0	0	0.106	0.000	0.000
	B(1,2)	0	0	0	0.000	0.000	0.000
choice	B(2,2)	1	0	0	-1.175	0.000	0.000
	B(3,2)	0	0	0	0.000	0.000	0.000
	B(1,3)	0	0	0	0.000	0.000	0.000
	B(2,3)	0	0	0	0.000	0.000	0.000
	B(3,3)	1	1	0	-1.210	0.087	0.000
	B(1,1)	1	0	0.62	-0.845	0.000	-0.122
	B(2,1)	1	0	0	-0.105	0.000	0.000
	B(3,1)	0.52	0	0	0.038	0.000	0.000
	B(1,2)	1	0	0	-0.309	0.000	0.000
no-choice	B(2,2)	1	0	0	-1.174	0.000	0.000
	B(3,2)	0	0	0	0.000	0.000	0.000
	B(1,3)	0	0	0	0.000	0.000	0.000
	B(2,3)	0	0	0	0.000	0.000	0.000
	B(3,3)	1	0.59	0	-1.297	-0.038	0.000

(See Tables S12 and S21 for legends.)

Summary of main DCM results

Modulation of connectivity

On average across subjects, reward outcomes modulated visual area, mPC and VS self-connectivity. Self-inhibition was decreased during reward outcomes leading to increased overall activation in these regions (as observed during model-free GLM analysis). No difference in modulation was associated with QIDS scores. Similarly, no-reward outcomes modulated self-connectivity of mPC and VS. Self-inhibition was decreased leading to overall increased activation. Both mPC and VS showed stronger negative modulation during no-reward than during reward outcomes (leading to decreased inhibition and therefore stronger activation during no-choice outcomes). In addition, differences in the no-reward modulation of the VS to the visual area (inhibitory) connection were positively associated with QIDS scores. This means higher depressive symptoms were associated with increased excitation / decreased inhibition from VS to the visual area.

Outcomes during both choice and no-choice conditions modulated the following connections: visual area→visual area, visual area→mPC, visual area→VS, mPC→visual area, mPC→mPC, VS→VS. Self-inhibition was decreased for all regions, leading to increased activation. Self-inhibition of the visual area was stronger and self-inhibition of VS and mPC was weaker during choice outcomes compared to no-choice outcomes. Visual area to VS connectivity was increased during both choice and no-choice outcomes, and higher during choice compared to no-choice outcomes. Choice and no-choice outcome conditions decreased the connectivity from the visual area and mPC and from mPC to the visual area. Compared to choice outcomes, no-choice outcomes had a weaker negative modulation effect on the visual area→mPC connection, but a stronger negative modulation effect on the mPC→visual area connection. Higher depressive symptom scores were associated with increased modulation of VS self-inhibition during choice outcomes only. This means that while outcomes from participants' own choice overall led to an increase in VS activity (through decreased inhibition), in participants with higher depressive symptoms this increase was reduced.

Summary of DCM results organised by region

Visual area: There was evidence for effective (excitatory) endogenous connectivity to mPC, which was increased with higher depressive symptoms. The region's self-inhibition was weaker in participants with higher depressive symptoms. The medial PFC region had an excitatory influence on the visual area, while VS had an inhibitory influence and the connection strength was negatively associated with depressive symptoms. Choice and no-choice outcomes were associated with increased influence on VS. Self-inhibition was weaker (resulting in increased activity) during all outcomes except no-reward outcomes. Both choice and no-choice conditions decreased the connectivity to and from mPC. Higher depressive symptoms were associated with decreased inhibition from VS during no-reward outcomes.
mPC: There was evidence for excitatory endogenous connections to and from the visual area and to VS. The excitation from the visual area and the mPC self-inhibition increased with higher depressive symptoms. The influence of mPC on VS decreased with higher depressive symptoms. Self-inhibition was weaker during all outcomes compared to baseline. Both choice and no-choice outcomes decreased the connectivity to and from the visual area.
VS: Received excitatory input from mPC and its activity exerted inhibitory influence on the visual area. The influence from mPC was decreased with higher depressive symptoms. The connection strength to the visual area was negatively associated with depressive symptoms. Self-inhibition was weaker during all outcomes compared to baseline. Choice and no-choice outcomes were associated with increased influence of the visual area, with stronger modulation during choice than no-choice outcomes. Higher depressive symptoms were associated with increased influence on the visual area during no-reward outcomes and stronger self-inhibition during choice outcomes.

Variance threshold

In Figure S8 we plot the association of QIDS with VS to VS connectivity as a function of the variance threshold. It shows the expected values (c.f. E(QIDS) of A(3,2) in previous tables) of the second level PEB model (without BMR). Covariates included (zero-mean centred) QIDS, HADS anxiety, site age and sex. As expected, it roughly follows an inverted U shape. At low thresholds noise suppresses the association and at high thresholds too few participants remain.

Figure S8. Association of fop-down connection strength with QIDS as a function of variance threshold.

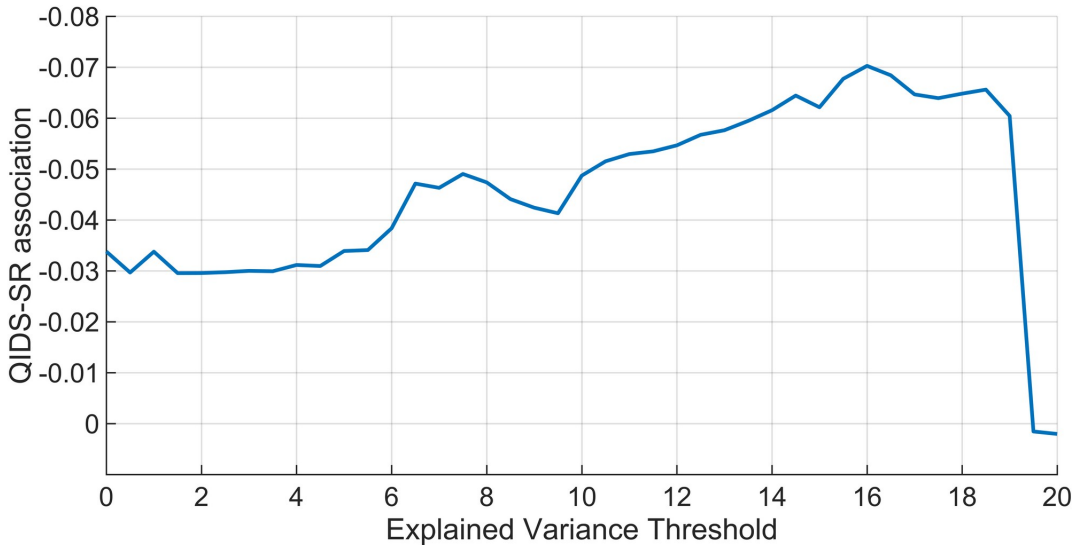

The association of the covariate of interest (QIDS) with the connection from VS to accumbens as a function of the variance threshold in the estimated PEB model. As described earlier, our a priori chosen threshold was 10%.

To make an unbiased estimate of connectivity it was necessary to include data from subjects who had sufficient signals. To convince ourselves of the validity of our findings we performed a large number of control analyses. Importantly, there was no significant difference in depression symptom severity between included and excluded participants, making it extremely unlikely that exclusions biased our main results.

We varied the DCM threshold criterion, including up to 301 participants (see Table S23), and observed exactly what we predicted (Figure S8): at very low thresholds the reward activation signals are so low that noise dominates which suppresses the negative association, although a non-significant negative trend remains when all subjects were included. (At very high thresholds so few subjects were included that the statistical power was affected and the association was not significant). In Tables S12-13 we show the results of another two full BMA analyses using higher and lower thresholds with very similar results to the main text analysis. Finally, we show that the negative association also holds within random splits of the data (Figure 5).

Consequently we believe it is extremely unlikely that the exact number of inclusions biased our main result, which is the association between depression symptom severity and effective cortico-limbic connectivity. Rather than lowering the variance threshold post-hoc, which would have allowed us to include more participants, we chose to be consistent with DCM recommendations on signal threshold to allow valid inferences, so used additional control analyses to provide an unbiased estimate of abnormal connectivity.

In summary, when we used data with sufficient signals to make valid inferences we found a significant negative association between cortico-limbic connectivity and depressive symptoms, when there was insufficiently strong signals we couldn't draw conclusions, and none of the analyses suggested a significant positive relationship between cortico-limbic connectivity and depressive symptoms.

Analyses of individual depression symptoms

There are some potential issues of the correlation analysis we performed so far. QIDS scores are skewed and correlation results might be affected by the heteroscedasticity. Closely related to this, we performed the analysis across groups and since the MDD group naturally displayed higher depressive symptom scores, it is possible our results related more closely to a group effect rather than an effect of increasing symptom severity (although we did try to account for that by including an additional group-indicator covariate). Finally, the sum of the 16 individual symptom scores of our depression questionnaire might hide additional variation related to individual symptoms (Fried & Nesse, 2015).

To begin to address these potential concerns, we performed additional analyses for which we included each individual QIDS symptom (i.e. question) in the PEB design matrix. In the questionnaire each question was coded as a number from 0 to 3 with increasing severity. For the design matrix columns were transformed to code absence (score=0) or presence (score>0) of the symptom and not mean centered so that the mean column corresponded to a participant without any symptoms and each symptom column coded the additive effect of having the symptom. Other covariates (anxiety, age, sex, site) were again zero-mean centered. This means we essentially performed a list of 'group comparisons' of 'participants reporting a specific symptom' (e.g. concentration/decision-making difficulties) versus 'participants who did not report this symptom'.

We also repeated this analysis after excluding current MDD participants and then again after excluding both current MDD and remitted MDD participants. Results are shown in the additional Supplement Tables document). The top-down connection from the prefrontal cortex to the accumbens was related to the presence of a number of symptoms, most notably "concentration or decision making difficulties" which was found in a variety of different analyses strategies including the analysis which did not include past or present MDD participants. This means participants reporting changes in their usual capacity to concentrate or make decisions had a decreased top-down connectivity. We also found evidence for decreased top-down control in participants displaying changes in their general interest, a substantial sub-part of "anhedonia", but this was only true when all participants were included. Importantly however, only 4 never-depressed participants reported "general interest" symptoms, but 18 reported "concentration or decision making difficulties". We note that these are exploratory analyses and we did not have strong hypotheses about which symptoms would be most associated with the connection from VS to VS.

As a final remark, it is worth mentioning that the symptom of decreased energy (one of the three core symptoms of a major depressive episode as defined in ICD-10 and also related to "motivation") was associated with increased VS (self-)inhibition which would also lead to decreased activation as observed in many previous fMRI studies. In this study blunted reward response associated with *overall* depressive symptoms severity was mainly found in caudate and putamen. This might mean that blunting in different parts of the striatum could be related to (severity of) different depression symptoms.

Figure S11. Project overview and analysis workflow.

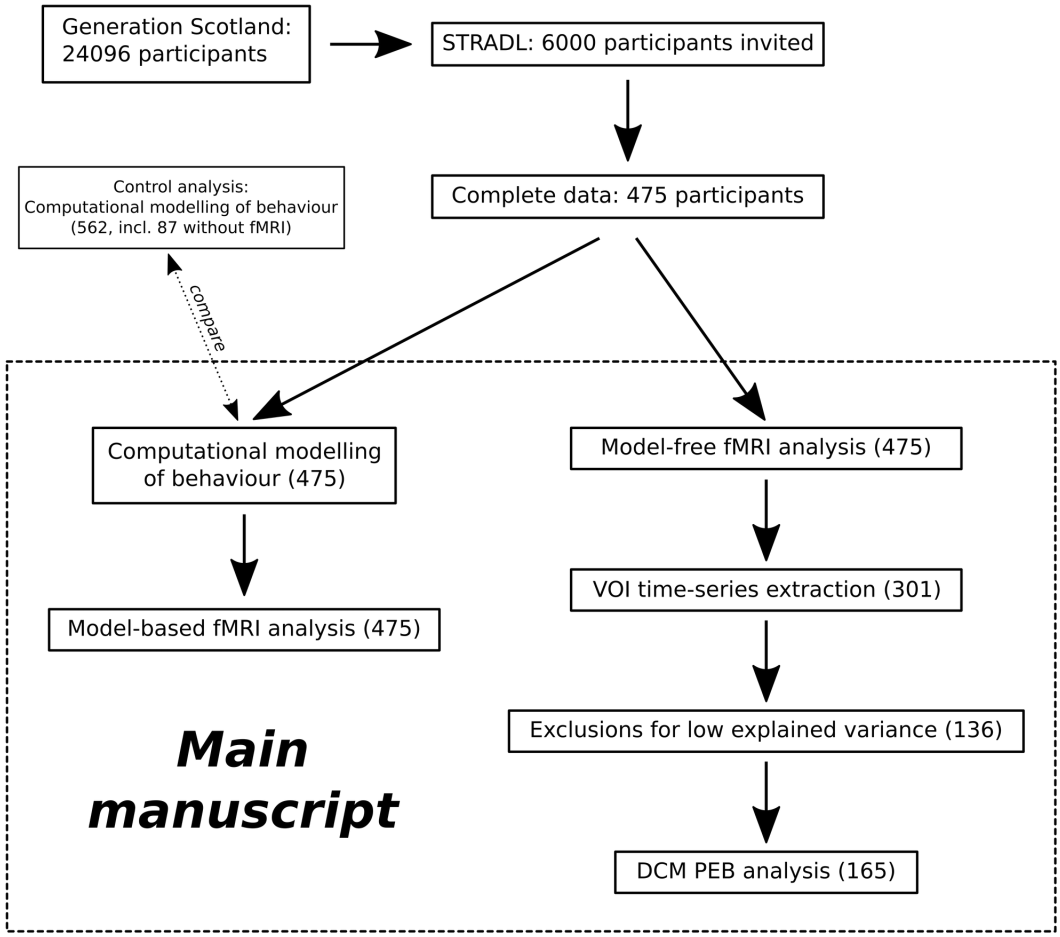

Table S23. Demographic and clinical details after exclusions (c.f. Figure S11)

		Controls	Past MDD	Current MDD
652 participants (excluding 3 of unknown group)	Number of subjects	463	156	30
	QIDS (range, mean ± std)	0 – 14, 3.59 ± 2.24	1 – 22, 5.42 ± 3.84	7 – 21, 13.9 ± 3.53
	HADS-A (range, mean ± std)	3.24 ± 2.53	5.17 ± 3.58	11.13 ± 3.83
475 participants	Number of subjects	407	129	26
	QIDS (range, mean ± std)	0 -14, 3.52 ± 2.23	1 – 22, 5.33 ± 3.77	7 – 21, 14.12 ± 3.78
	HADS-A (range, mean ± std)	0 – 15, 3.20 ± 2.56	0 – 17, 5.15 ± 3.55	6 – 20, 11.15 ± 3.82
475 participants (c.f. Table 1)	Number of subjects	345	110	20
	QIDS (range, mean ± std)	0 – 12, 3.39 ± 2.08	1 – 22, 5.41 ± 3.84	9 – 21, 14.55 ± 3.79
	HADS-A (range, mean ± std)	0 – 12, 3.13 ± 2.44	0 – 17, 5.04 ± 3.35	6 – 20, 10.65 ± 3.62
301 participants	Number of subjects	214	68	19
	QIDS (range, mean ± std)	0 – 12, 3.36 ± 2.07	1 – 22, 5.43 ± 3.85	9 – 21, 14.47 ± 3.88
	HADS-A (range, mean ± std)	0 – 12, 3.09 ± 2.51	0 – 17, 5.37 ± 3.46	6 – 20, 10.42 ± 3.56
165 participants	Number of subjects	112	41	12
	QIDS (range, mean ± std)	0 – 10, 3.21 ± 1.86	1 – 22, 5.73 ± 4.35	10 – 21, 14.00 ± 3.95
	HADS-A (range, mean ± std)	0 – 12, 3.08 ± 2.55	0 – 17, 5.32 ± 3.73	6 – 20, 11.50 ± 3.90

QIDS = Quick Inventory of Depressive Symptomatology (Self Report;) HADS = Hospital Anxiety and Depression Scale

Additional computational modelling

It was possible to fit our computational models to the behaviour of 562 participants as some participants were excluded for fMRI pre-processing reasons (see Figure S11). In our hierarchical fitting approach every included participant can potentially influence every other participant (by changing the empirical group prior) and model comparison might also be affected. We therefore repeated our model fitting and model comparison including all 562 participants. The winning model remained the same. For each approach we extracted the estimated parameters from the winning model for the included participants. All three parameters were nearly identical for all participants (Pearson's r>.99 for each parameter). We note that for model-based fMRI we used the estimated parameters (and simulated hidden variables) from the model which was fitted to all participants.

Model recovery simulations

To assess the strength of our model comparison results, we performed model recovery simulations by simulating data from one of the models and then fitting each model to the simulated data. Model comparison was then used to see if it correctly identified the model which simulated the data as "best-fitting" model. Each model was simulated 20 times using 562 participants and 66 trials to match our experimental data. Table S24 shows the results of these model recovery simulations. It can be seen that while simple models (including our winning model) were recovered well, there was too little data (per individual) to reliably support the recovery of the more complicated models against their simpler versions. Given the similarity of models 3 (our winning model) and 5 (which also includes separate reward sensitivity parameters), we ran additional analysis to compare these two models and see if our result of increased learning with increased control was also reproducible using a more complicated version of our winning model. There was a large significant correlation between the instrumental learning rates (Spearman's ρ=0.553, $p<10^{-10}$) and between the Pavlovian learning rates (Spearman's ρ=0.601, $p<10^{-10}$) of the two models. As in our winning model, analysis of the alternative model 5 showed that the large majority of participants had a higher learning rate for choice trials than for no-choice trials (553 of 562, 98%; model 3: 499 of 562 or 89%). We repeated these model recovery simulations with only the included 475 participants which again gave us very similar results (Table S25) and we also repeated the correlation analysis between QIDS and model parameters which led us to the same conclusions.

Table S24. Model recovery (475 participants)

		Best-fitting model				
		M1	**M2**	**M3**	**M4**	**M5**
Simulating model	**M1**	20	0	0	0	0
	M2	0	20	0	0	0
	M3	0	2	18	0	0
	M4	0	7	1	8	4
	M5	0	0	9	7	4

Table S25. Model recovery (475 participants)

		Best-fitting model				
		M1	**M2**	**M3**	**M4**	**M5**
Simulating model	**M1**	20	0	0	0	0
	M2	0	20	0	0	0
	M3	0	0	20	0	0
	M4	0	13	0	7	0
	M5	0	0	16	1	3

Supplementary References

Dale, A. M., Fischl, B., & Sereno, M. I. (1999). Cortical surface-based analysis: I. Segmentation and surface reconstruction. *Neuroimage*, *9*(2), 179-194.
Desikan, R. S., Ségonne, F., Fischl, B., Quinn, B. T., Dickerson, B. C., Blacker, D., ... & Albert, M. S. (2006). An automated labeling system for subdividing the human cerebral cortex on MRI scans into gyral based regions of interest. *Neuroimage*, 31(3), 968-980.
Fischl, B., Sereno, M. I., & Dale, A. M. (1999). Cortical surface-based analysis: II: inflation, flattening, and a surface-based coordinate system. *Neuroimage*, *9*(2), 195-207.
Fischl, B., Van Der Kouwe, A., Destrieux, C., Halgren, E., Ségonne, F., Salat, D. H., ... & Caviness, V. (2004). Automatically parcellating the human cerebral cortex. *Cerebral cortex*, 14(1), 11-22.
Fried, E. I., & Nesse, R. M. (2015). Depression sum-scores don't add up: why analyzing specific depression symptoms is essential. *BMC medicine*, 13(1), 72.
Friston, K. J., Harrison, L., & Penny, W. (2003). Dynamic causal modelling. *Neuroimage*, *19*(4), 1273-1302.
Huys, Q. J., Pizzagalli, D. A., Bogdan, R., & Dayan, P. (2013). Mapping anhedonia onto reinforcement learning: a behavioural meta-analysis. *Biology of mood & anxiety disorders*, *3*(1), 12.
Jenkinson, M., Beckmann, C. F., Behrens, T. E., Woolrich, M. W., & Smith, S. M. (2012). Fsl. *Neuroimage*, 62(2), 782-790.
Rupprechter, S., Stankevicius, A., Huys, Q. J., Steele, J. D., & Seriès, P. (2018). Major Depression Impairs the Use of Reward Values for Decision-Making. *Scientific reports*, *8*(1), 13798.
Slotnick, S. D., & Schacter, D. L. (2004). A sensory signature that distinguishes true from false memories. *Nature neuroscience*, 7(6), 664.
Slotnick, S. D. (2017). Cluster success: fMRI inferences for spatial extent have acceptable false-positive rates. *Cognitive neuroscience*, 8(3), 150-155.
Smith, S. M., Jenkinson, M., Woolrich, M. W., Beckmann, C. F., Behrens, T. E., Johansen-Berg, H., ... & Niazy, R. K. (2004). Advances in functional and structural MR image analysis and implementation as FSL. *Neuroimage*, 23, S208-S219.
Wetzels, R., & Wagenmakers, E. J. (2012). A default Bayesian hypothesis test for correlations and partial correlations. *Psychonomic bulletin & review*, 19(6), 1057-1064.
Woolrich, M. W., Jbabdi, S., Patenaude, B., Chappell, M., Makni, S., Behrens, T., ... & Smith, S. M. (2009). Bayesian analysis of neuroimaging data in FSL. *Neuroimage*, 45(1), S173-S186.

Tables B1-B6 include (zero-mean centered) HADS anxiety, site, age and sex covariates of no interest

Table B1: All 165 participants: BMA Expectations

Nr	Pname	mean	HADS	site	age	sex	QIDS1	QIDS2	QIDS3	QIDS4	QIDS5	QIDS6	QIDS7	QIDS8	QIDS9	QIDS10	QIDS11	QIDS12	QIDS13	QIDS14	QIDS15	QIDS16
1	A(1,1)	0.35	0.00	0.16	-0.08	0.00	0.00	0.19	0.00	0.00	0.00	0.00	0.00	0.00	0.00	0.00	0.00	0.00	-0.25	0.00	0.00	0.00
2	A(2,1)	0.00	0.00	0.04	0.00	0.00	0.00	0.08	0.08	0.00	0.00	0.00	0.00	0.00	0.00	0.05	0.00	0.00	0.00	0.00	0.10	0.00
3	A(3,1)	0.00	0.00	0.00	0.00	0.00	0.00	0.00	0.00	-0.08	0.00	0.00	0.00	0.00	0.00	0.00	0.00	0.00	0.05	0.00	0.00	0.00
4	A(1,2)	0.33	0.00	0.00	0.00	0.00	0.00	0.17	0.00	0.00	0.00	0.00	0.00	0.00	-0.09	0.00	0.00	0.23	0.00	-0.28	0.00	0.00
5	A(2,2)	-0.38	0.13	0.00	0.00	0.00	0.00	0.00	0.00	0.00	0.00	0.00	0.00	0.00	-0.15	0.07	0.12	-0.32	0.00	0.00	0.29	-0.15
6	A(3,2)	0.09	0.00	-0.04	0.00	0.02	-0.04	0.00	0.00	0.09	0.00	0.12	0.00	0.00	0.00	-0.09	0.00	0.00	-0.08	0.00	0.00	0.00
7	A(1,3)	0.00	-0.12	0.06	0.09	0.00	0.00	-0.17	-0.19	0.00	0.00	0.00	0.21	0.00	0.00	0.00	0.00	0.00	0.00	-0.19	0.00	0.00
8	A(2,3)	0.00	0.00	-0.10	0.00	0.07	0.10	0.00	0.00	0.00	0.00	0.00	0.00	0.00	0.00	0.00	0.00	0.00	0.09	0.00	-0.13	0.00	0.00
9	A(3,3)	-0.20	0.00	0.00	0.00	-0.06	-0.14	0.00	0.00	-0.20	0.13	0.23	0.00	0.00	0.00	0.00	0.00	0.00	-0.31	-0.23	0.21	0.00	0.00

Table B2: All 165 participants: BMA Probabilities

Nr	Pname	mean	HADS	site	age	sex	QIDS1	QIDS2	QIDS3	QIDS4	QIDS5	QIDS6	QIDS7	QIDS8	QIDS9	QIDS10	QIDS11	QIDS12	QIDS13	QIDS14	QIDS15	QIDS16
1	A(1,1)	1.00	0.00	1.00	1.00	0.00	0.00	1.00	0.00	0.00	0.00	0.00	0.00	0.00	0.00	0.00	0.00	0.00	1.00	0.00	0.00	0.00
2	A(2,1)	0.00	0.00	1.00	0.00	0.00	0.00	1.00	1.00	0.00	0.00	0.00	0.00	0.00	0.00	0.54	0.00	0.00	0.00	0.00	1.00	0.00
3	A(3,1)	0.00	0.00	0.00	0.00	0.00	0.00	0.00	0.00	1.00	0.00	0.00	0.00	0.00	0.00	0.00	0.00	0.00	0.54	0.00	0.00	0.00
4	A(1,2)	1.00	0.00	0.00	0.00	0.00	0.00	1.00	0.00	0.00	0.00	0.00	0.00	0.00	0.62	0.00	0.00	1.00	0.00	1.00	0.00	0.00
5	A(2,2)	1.00	1.00	0.00	0.00	0.00	0.00	0.00	0.00	0.00	0.00	0.00	0.00	0.00	1.00	0.59	1.00	1.00	0.00	0.00	1.00	1.00
6	A(3,2)	1.00	0.00	1.00	0.00	0.66	0.68	0.00	0.00	1.00	0.00	1.00	0.00	0.00	0.00	1.00	0.00	0.00	0.67	0.00	0.00	0.00
7	A(1,3)	0.00	1.00	1.00	1.00	0.00	0.00	1.00	1.00	0.00	0.00	0.00	1.00	0.00	0.00	0.00	0.00	0.00	0.00	1.00	0.00	0.00
8	A(2,3)	0.00	0.00	1.00	0.00	1.00	1.00	0.00	0.00	0.00	0.00	0.00	0.00	0.00	0.00	0.00	0.00	0.00	0.56	0.00	1.00	0.00	0.00
9	A(3,3)	1.00	0.00	0.00	0.00	1.00	1.00	0.00	0.00	1.00	1.00	1.00	0.00	0.00	0.00	0.00	0.00	0.00	1.00	1.00	1.00	0.00	0.00

Table B3: HC+rMDD (MDD excluded) participants: BMA Expectations

Nr	Pname	mean	HADS	site	age	sex	QIDS1	QIDS2	QIDS3	QIDS4	QIDS5	QIDS6	QIDS7	QIDS8	QIDS9	QIDS10	QIDS11	QIDS12	QIDS13	QIDS14	QIDS15	QIDS16
1	A(1,1)	0.38	0.00	0.17	-0.09	0.00	0.00	0.16	0.00	0.00	0.00	0.00	0.00	0.00	0.00	0.00	0.00	0.00	-0.40	0.00	0.00	0.00
2	A(2,1)	0.00	0.00	0.02	0.00	0.00	0.00	0.08	0.09	0.00	0.00	0.00	0.00	0.00	0.00	0.00	0.00	0.00	0.00	0.00	0.12	0.00
3	A(3,1)	0.00	0.00	0.00	0.00	0.00	0.00	0.00	0.00	-0.06	0.00	0.00	0.00	0.00	-0.07	0.00	0.00	0.00	0.00	0.00	0.00	0.00
4	A(1,2)	0.34	0.00	0.00	0.00	0.00	0.00	0.17	0.00	0.00	0.00	0.00	0.32	0.26	-0.20	0.00	0.00	0.15	0.00	-0.35	0.00	0.00
5	A(2,2)	-0.34	0.14	0.00	0.03	-0.02	-0.08	0.00	0.00	-0.10	0.00	0.00	0.00	-0.12	0.00	0.13	-0.41	0.00	0.00	0.00	0.39	-0.26
6	A(3,2)	0.08	0.00	-0.04	0.00	0.04	0.00	0.00	0.00	0.05	0.00	0.14	0.00	0.00	0.00	-0.10	0.00	0.00	0.00	0.00	0.00	0.00
7	A(1,3)	0.00	-0.12	0.07	0.07	0.00	0.13	-0.19	-0.21	0.00	0.00	0.00	0.28	0.00	0.00	0.00	-0.14	0.00	0.00	-0.23	0.00	0.00
8	A(2,3)	0.11	0.00	-0.12	0.00	0.08	0.07	-0.11	0.00	0.00	0.00	0.00	0.00	0.00	-0.08	0.00	0.00	0.00	0.00	0.00	0.00	0.00
9	A(3,3)	-0.20	0.00	0.00	0.00	-0.06	-0.13	0.00	0.00	-0.22	0.12	0.23	0.20	0.00	0.00	-0.12	0.00	0.00	-0.33	0.18	0.00	0.00

Table B4: HC+rMDD (MDD excluded) participants: BMA Probabilities

Nr	Pname	mean	HADS	site	age	sex	QIDS1	QIDS2	QIDS3	QIDS4	QIDS5	QIDS6	QIDS7	QIDS8	QIDS9	QIDS10	QIDS11	QIDS12	QIDS13	QIDS14	QIDS15	QIDS16
1	A(1,1)	1.00	0.00	1.00	1.00	0.00	0.00	1.00	0.00	0.00	0.00	0.00	0.00	0.00	0.00	0.00	0.00	0.00	1.00	0.00	0.00	0.00
2	A(2,1)	0.00	0.00	0.63	0.00	0.00	0.00	1.00	1.00	0.00	0.00	0.00	0.00	0.00	0.00	0.00	0.00	0.00	0.00	0.00	1.00	0.00
3	A(3,1)	0.00	0.00	0.00	0.00	0.00	0.00	0.00	0.00	1.00	0.00	0.00	0.00	0.00	0.00	1.00	0.00	0.00	0.00	0.00	0.00	0.00
4	A(1,2)	1.00	0.00	0.00	0.00	0.00	0.00	1.00	0.00	0.00	0.00	0.00	1.00	1.00	1.00	0.00	0.00	0.64	0.00	1.00	0.00	0.00
5	A(2,2)	1.00	1.00	0.00	0.66	0.52	1.00	0.00	0.00	1.00	0.00	0.00	0.00	0.00	1.00	0.00	1.00	1.00	0.00	0.00	1.00	1.00
6	A(3,2)	1.00	0.00	1.00	0.00	1.00	0.00	0.00	0.00	0.65	0.00	1.00	0.00	0.00	0.00	1.00	0.00	0.00	0.00	0.00	0.00	0.00
7	A(1,3)	0.00	1.00	1.00	1.00	0.00	1.00	1.00	1.00	0.00	0.00	0.00	1.00	0.00	0.00	0.00	0.59	0.00	0.00	1.00	0.00	0.00
8	A(2,3)	1.00	0.00	1.00	0.00	1.00	0.66	1.00	0.00	0.00	0.00	0.00	0.00	0.00	0.00	0.60	0.00	0.00	0.00	0.00	0.00	0.00
9	A(3,3)	1.00	0.00	0.00	0.00	1.00	1.00	0.00	0.00	1.00	1.00	1.00	1.00	0.00	0.00	1.00	0.00	0.00	1.00	1.00	0.00	0.00

Table B5: HC (rMDD + MDD excluded) participants: BMA Expectations

Nr	Pname	mean	HADS	site	age	sex	QIDS1	QIDS2	QIDS3	QIDS4	QIDS5	QIDS6	QIDS7	QIDS8	QIDS9	QIDS10	QIDS11	QIDS12	QIDS13	QIDS14	QIDS15	QIDS16
1	A(1,1)	0.48	0.00	0.16	0.00	0.00	0.00	0.00	0.00	0.00	0.00	0.00	0.00	0.00	0.00	0.00	0.00	0.16	-0.14	0.00	0.00	0.00
2	A(2,1)	0.00	0.05	0.05	0.00	0.00	0.00	0.10	0.09	0.00	-0.12	0.00	0.00	0.00	0.00	0.14	-0.14	0.44	0.00	0.00	0.00	0.00
3	A(3,1)	0.00	0.00	0.04	0.00	-0.03	0.00	0.00	0.00	-0.06	0.00	0.00	0.00	0.00	0.00	0.00	0.00	0.00	0.00	0.00	0.00	0.00
4	A(1,2)	0.33	0.00	0.00	0.00	0.00	0.00	0.15	0.00	0.00	0.00	0.51	0.65	-0.23	0.00	0.00	0.65	0.00	-0.18	-0.11	0.00	0.00
5	A(2,2)	-0.48	0.10	0.00	0.02	0.00	0.00	0.00	0.00	0.00	0.00	0.27	0.00	0.00	0.21	0.00	0.00	0.00	0.00	0.00	0.00	-0.24
6	A(3,2)	0.09	0.00	-0.06	0.00	0.04	0.00	0.00	0.00	0.00	0.00	0.09	0.00	0.00	0.00	-0.09	0.00	0.00	0.00	0.00	0.00	0.00
7	A(1,3)	0.00	-0.16	0.00	0.04	0.00	0.00	-0.21	-0.07	0.00	0.00	0.00	0.00	0.00	0.00	0.00	0.00	0.00	0.56	0.00	-0.35	0.35
8	A(2,3)	0.00	-0.06	-0.12	0.00	0.06	0.17	0.00	-0.12	0.00	0.00	0.44	-0.25	0.00	0.00	0.24	0.00	0.00	0.00	-0.25	0.00	0.00
9	A(3,3)	-0.21	0.06	0.00	0.00	-0.05	0.00	0.00	0.00	-0.25	0.00	0.00	0.00	0.00	0.00	-0.22	-0.29	0.00	-0.35	0.24	0.00	-0.17

Table B6: HC (rMDD + MDD excluded) participants: BMA Probabilities

Nr	Pname	mean	HADS	site	age	sex	QIDS1	QIDS2	QIDS3	QIDS4	QIDS5	QIDS6	QIDS7	QIDS8	QIDS9	QIDS10	QIDS11	QIDS12	QIDS13	QIDS14	QIDS15	QIDS16
1	A(1,1)	1.00	0.00	1.00	0.00	0.00	0.00	0.00	0.00	0.00	0.00	0.00	0.00	0.00	0.00	0.00	0.00	0.51	0.52	0.00	0.00	0.00
2	A(2,1)	0.00	1.00	1.00	0.00	0.00	0.00	1.00	1.00	0.00	1.00	0.00	0.00	0.00	0.00	1.00	1.00	1.00	0.00	0.00	0.00	0.00
3	A(3,1)	0.00	0.00	1.00	0.00	1.00	0.00	0.00	0.00	1.00	0.00	0.00	0.00	0.00	0.00	0.00	0.00	0.00	0.00	0.00	0.00	0.00
4	A(1,2)	1.00	0.00	0.00	0.00	0.00	0.00	1.00	0.00	0.00	0.00	1.00	1.00	1.00	0.00	0.00	1.00	0.00	0.58	0.65	0.00	0.00
5	A(2,2)	1.00	1.00	0.00	0.53	0.00	0.00	0.00	0.00	0.00	0.00	1.00	0.00	0.00	1.00	0.00	0.00	0.00	0.00	0.00	0.00	1.00
6	A(3,2)	1.00	0.00	1.00	0.00	1.00	0.00	0.00	0.00	0.00	0.00	0.60	0.00	0.00	0.00	1.00	0.00	0.00	0.00	0.00	0.00	0.00
7	A(1,3)	0.00	1.00	0.00	0.63	0.00	0.00	1.00	0.60	0.00	0.00	0.00	0.00	0.00	0.00	0.00	0.00	0.00	1.00	0.00	1.00	1.00
8	A(2,3)	0.00	1.00	1.00	0.00	1.00	1.00	0.00	1.00	0.00	0.00	1.00	1.00	0.00	0.00	1.00	0.00	0.00	0.00	1.00	0.00	0.00
9	A(3,3)	1.00	1.00	0.00	0.00	1.00	0.00	0.00	0.00	1.00	0.00	0.00	0.00	0.00	0.00	1.00	1.00	0.00	1.00	1.00	0.00	1.00

Tables B7-B12 do not include additional covariates of no interest

Table B7: All 165 participants: BMA Expectations

Nr	Pname	mean	QIDS1	QIDS2	QIDS3	QIDS4	QIDS5	QIDS6	QIDS7	QIDS8	QIDS9	QIDS10	QIDS11	QIDS12	QIDS13	QIDS14	QIDS15	QIDS16
1	A(1,1)	0.42	0.00	0.15	0.00	-0.15	0.00	0.00	0.00	0.00	0.00	0.00	0.00	0.00	-0.26	0.00	0.00	0.00
2	A(2,1)	0.00	0.00	0.09	0.08	0.00	0.00	0.00	0.00	0.00	0.00	0.00	0.00	0.00	0.00	0.05	0.00	0.00
3	A(3,1)	0.00	0.00	0.00	0.00	-0.07	0.00	0.00	0.00	0.00	-0.07	0.00	0.00	0.00	0.00	0.04	0.00	0.00
4	A(1,2)	0.31	0.00	0.17	0.05	0.00	0.00	0.00	0.00	-0.06	0.00	0.00	0.23	0.00	-0.31	0.00	0.00	0.00
5	A(2,2)	-0.40	0.00	0.00	0.00	0.00	0.00	0.00	0.00	-0.17	0.00	0.06	0.00	0.00	0.00	0.00	0.28	0.00
6	A(3,2)	0.09	-0.08	0.00	0.04	0.11	0.00	0.15	0.00	0.00	0.00	-0.09	0.00	0.00	-0.12	0.00	0.00	0.00
7	A(1,3)	0.00	0.00	-0.12	-0.19	0.00	0.00	0.00	0.00	0.00	0.00	0.00	-0.32	0.00	0.00	-0.17	0.00	0.00
8	A(2,3)	0.00	0.00	0.00	0.00	0.00	0.00	0.19	0.00	0.00	0.00	0.00	0.00	0.08	0.00	-0.04	0.00	0.00
9	A(3,3)	-0.23	-0.11	0.00	0.00	-0.18	0.18	0.19	0.00	0.00	0.00	0.00	0.00	-0.36	-0.20	0.23	0.00	0.00

Table B8: All 165 participants: BMA Probabilities

Nr	Pname	mean	QIDS1	QIDS2	QIDS3	QIDS4	QIDS5	QIDS6	QIDS7	QIDS8	QIDS9	QIDS10	QIDS11	QIDS12	QIDS13	QIDS14	QIDS15	QIDS16
1	A(1,1)	1.00	0.00	1.00	0.00	1.00	0.00	0.00	0.00	0.00	0.00	0.00	0.00	0.00	1.00	0.00	0.00	0.00
2	A(2,1)	0.00	0.00	1.00	1.00	0.00	0.00	0.00	0.00	0.00	0.00	0.00	0.00	0.00	0.00	0.62	0.00	0.00
3	A(3,1)	0.00	0.00	0.00	0.00	1.00	0.00	0.00	0.00	0.00	1.00	0.00	0.00	0.00	0.00	0.66	0.00	0.00
4	A(1,2)	1.00	0.00	1.00	0.54	0.00	0.00	0.00	0.00	0.55	0.00	0.00	1.00	0.00	1.00	0.00	0.00	0.00
5	A(2,2)	1.00	0.00	0.00	0.00	0.00	0.00	0.00	0.00	1.00	0.00	0.55	0.00	0.00	0.00	0.00	1.00	0.00
6	A(3,2)	1.00	1.00	0.00	0.59	1.00	0.00	1.00	0.00	0.00	0.00	1.00	0.00	0.00	1.00	0.00	0.00	0.00
7	A(1,3)	0.00	0.00	1.00	1.00	0.00	0.00	0.00	0.00	0.00	0.00	0.00	1.00	0.00	0.00	1.00	0.00	0.00
8	A(2,3)	0.00	0.00	0.00	0.00	0.00	0.00	1.00	0.00	0.00	0.00	0.00	0.00	0.53	0.00	0.48	0.00	0.00
9	A(3,3)	1.00	1.00	0.00	0.00	1.00	1.00	1.00	0.00	0.00	0.00	0.00	0.00	1.00	1.00	1.00	0.00	0.00

Table B9: HC+rMDD (MDD excluded) participants: BMA Expectations

Nr	Pname	mean	QIDS1	QIDS2	QIDS3	QIDS4	QIDS5	QIDS6	QIDS7	QIDS8	QIDS9	QIDS10	QIDS11	QIDS12	QIDS13	QIDS14	QIDS15	QIDS16
1	A(1,1)	0.49	0.00	0.07	0.00	-0.18	0.00	-0.16	0.00	0.00	0.00	0.00	0.00	0.00	-0.40	0.00	0.00	0.00
2	A(2,1)	0.00	0.00	0.08	0.09	0.00	0.00	0.00	0.00	0.00	0.00	0.00	0.00	0.00	0.00	0.00	0.11	0.00
3	A(3,1)	0.00	0.00	0.00	0.00	-0.07	0.00	0.00	0.00	0.00	-0.08	0.00	0.00	0.00	0.00	0.00	0.00	0.00
4	A(1,2)	0.33	0.00	0.17	0.00	0.00	0.00	0.34	0.29	-0.20	0.00	0.00	0.26	0.00	-0.37	0.00	-0.08	0.00
5	A(2,2)	-0.43	0.00	0.00	0.00	0.00	0.00	0.21	0.00	-0.17	0.00	0.17	-0.24	0.00	0.00	0.00	0.33	-0.08
6	A(3,2)	0.10	-0.07	0.00	0.00	0.09	0.00	0.18	0.00	0.00	0.00	-0.09	0.00	0.00	0.00	0.00	0.00	0.00
7	A(1,3)	0.00	0.08	-0.14	-0.21	0.00	0.00	0.00	0.00	0.00	0.00	0.00	-0.42	0.00	0.00	-0.17	0.00	0.00
8	A(2,3)	0.00	0.03	0.00	0.00	0.00	0.00	0.26	0.00	0.00	0.00	0.00	0.00	0.00	-0.10	0.00	0.00	0.00
9	A(3,3)	-0.21	-0.11	0.00	0.00	-0.21	0.11	0.16	0.19	0.00	0.00	-0.07	0.00	0.00	-0.30	0.19	0.00	0.00

Table B10: HC+rMDD (MDD excluded) participants: BMA Probabilities

Nr	Pname	mean	QIDS1	QIDS2	QIDS3	QIDS4	QIDS5	QIDS6	QIDS7	QIDS8	QIDS9	QIDS10	QIDS11	QIDS12	QIDS13	QIDS14	QIDS15	QIDS16
1	A(1,1)	1.00	0.00	0.62	0.00	1.00	0.00	0.64	0.00	0.00	0.00	0.00	0.00	0.00	1.00	0.00	0.00	0.00
2	A(2,1)	0.00	0.00	1.00	1.00	0.00	0.00	0.00	0.00	0.00	0.00	0.00	0.00	0.00	0.00	0.00	1.00	0.00
3	A(3,1)	0.00	0.00	0.00	0.00	1.00	0.00	0.00	0.00	0.00	1.00	0.00	0.00	0.00	0.00	0.00	0.00	0.00
4	A(1,2)	1.00	0.00	1.00	0.00	0.00	0.00	1.00	1.00	1.00	0.00	0.00	1.00	0.00	1.00	0.00	0.51	0.00
5	A(2,2)	1.00	0.00	0.00	0.00	0.00	0.00	1.00	0.00	1.00	0.00	1.00	1.00	0.00	0.00	0.00	1.00	0.65
6	A(3,2)	1.00	1.00	0.00	0.00	1.00	0.00	1.00	0.00	0.00	0.00	1.00	0.00	0.00	0.00	0.00	0.00	0.00
7	A(1,3)	0.00	0.65	1.00	1.00	0.00	0.00	0.00	0.00	0.00	0.00	0.00	1.00	0.00	0.00	1.00	0.00	0.00
8	A(2,3)	0.00	0.48	0.00	0.00	0.00	0.00	1.00	0.00	0.00	0.00	0.00	0.00	0.00	0.55	0.00	0.00	0.00
9	A(3,3)	1.00	1.00	0.00	0.00	1.00	1.00	1.00	1.00	0.00	0.00	0.67	0.00	0.00	1.00	1.00	0.00	0.00

Table B11: HC (rMDD + MDD excluded) participants: BMA Expectations

Nr	Pname	mean	QIDS1	QIDS2	QIDS3	QIDS4	QIDS5	QIDS6	QIDS7	QIDS8	QIDS9	QIDS10	QIDS11	QIDS12	QIDS13	QIDS14	QIDS15	QIDS16
1	A(1,1)	0.49	0.00	0.00	0.00	-0.16	0.00	0.00	0.00	0.00	0.00	0.00	0.00	0.18	0.00	0.00	0.00	0.00
2	A(2,1)	0.00	0.00	0.06	0.12	0.00	0.00	0.00	0.00	0.00	0.00	-0.06	0.32	0.00	0.00	0.00	0.22	0.00
3	A(3,1)	0.00	0.00	0.00	0.00	-0.08	0.00	0.00	0.00	0.00	0.00	0.00	0.00	0.00	0.00	0.00	0.00	0.00
4	A(1,2)	0.33	0.00	0.15	0.00	0.00	0.00	0.51	0.68	-0.23	0.00	0.00	0.66	0.00	-0.22	-0.11	0.00	0.00
5	A(2,2)	-0.50	0.00	0.00	0.00	0.00	0.00	0.41	0.00	-0.09	0.20	0.12	0.00	0.00	0.00	-0.06	0.00	0.00
6	A(3,2)	0.10	-0.07	0.00	0.00	0.09	0.00	0.17	0.00	0.00	0.00	-0.09	0.00	0.00	0.00	0.00	0.00	0.00
7	A(1,3)	0.00	0.00	-0.15	-0.18	0.00	0.00	0.00	0.00	0.00	0.00	0.00	-0.17	0.00	0.45	0.00	0.00	0.00
8	A(2,3)	0.03	0.14	0.00	-0.13	0.00	0.00	0.46	-0.25	0.00	0.00	0.20	0.00	0.00	0.00	-0.28	0.00	0.00
9	A(3,3)	-0.23	0.00	0.00	0.00	-0.24	0.00	0.00	0.00	0.00	0.00	-0.21	0.00	0.00	-0.36	0.22	0.00	0.00

Table B12: HC (rMDD + MDD excluded) participants: BMA Probabilities

Nr	Pname	mean	QIDS1	QIDS2	QIDS3	QIDS4	QIDS5	QIDS6	QIDS7	QIDS8	QIDS9	QIDS10	QIDS11	QIDS12	QIDS13	QIDS14	QIDS15	QIDS16
1	A(1,1)	1.00	0.00	0.00	0.00	1.00	0.00	0.00	0.00	0.00	0.00	0.00	0.00	0.54	0.00	0.00	0.00	0.00
2	A(2,1)	0.00	0.00	1.00	1.00	0.00	0.00	0.00	0.00	0.00	0.00	0.68	1.00	0.00	0.00	0.00	1.00	0.00
3	A(3,1)	0.00	0.00	0.00	0.00	1.00	0.00	0.00	0.00	0.00	0.00	0.00	0.00	0.00	0.00	0.00	0.00	0.00
4	A(1,2)	1.00	0.00	1.00	0.00	0.00	0.00	1.00	1.00	1.00	0.00	0.00	1.00	0.00	0.64	0.66	0.00	0.00
5	A(2,2)	1.00	0.00	0.00	0.00	0.00	0.00	1.00	0.00	0.69	1.00	1.00	0.00	0.00	0.00	0.51	0.00	0.00
6	A(3,2)	1.00	1.00	0.00	0.00	1.00	0.00	1.00	0.00	0.00	0.00	1.00	0.00	0.00	0.00	0.00	0.00	0.00
7	A(1,3)	0.00	0.00	1.00	1.00	0.00	0.00	0.00	0.00	0.00	0.00	0.00	0.53	0.00	1.00	0.00	0.00	0.00
8	A(2,3)	0.52	1.00	0.00	1.00	0.00	0.00	1.00	1.00	0.00	0.00	1.00	0.00	0.00	0.00	1.00	0.00	0.00
9	A(3,3)	1.00	0.00	0.00	0.00	1.00	0.00	0.00	0.00	0.00	0.00	1.00	0.00	0.00	1.00	1.00	0.00	0.00

Tables B13-B18 only include a single symptom (concentration / decision making difficulties)

Table B13: All 165 participants: BMA Expectations

Nr	Pname	mean	QIDS10
1	A(1,1)	0.48	0.00
2	A(2,1)	0.12	0.00
3	A(3,1)	0.00	0.00
4	A(1,2)	0.45	0.00
5	A(2,2)	-0.42	0.20
6	A(3,2)	0.09	-0.09
7	A(1,3)	-0.17	-0.26
8	A(2,3)	0.00	0.00
9	A(3,3)	-0.25	0.00

Table B14: All 165 participants: BMA Probabilities

Nr	Pname	mean	QIDS10
1	A(1,1)	1.00	0.00
2	A(2,1)	1.00	0.00
3	A(3,1)	0.00	0.00
4	A(1,2)	1.00	0.00
5	A(2,2)	1.00	0.99
6	A(3,2)	1.00	0.93
7	A(1,3)	1.00	1.00
8	A(2,3)	0.00	0.00
9	A(3,3)	1.00	0.00

Table B15: HC+rMDD (MDD excluded) participants: BMA Expectations

Nr	Pname	mean	QIDS10
1	A(1,1)	0.48	0.00
2	A(2,1)	0.11	0.00
3	A(3,1)	-0.03	0.00
4	A(1,2)	0.46	0.00
5	A(2,2)	-0.43	0.18
6	A(3,2)	0.09	-0.07
7	A(1,3)	-0.16	-0.23
8	A(2,3)	0.00	0.00
9	A(3,3)	-0.26	0.00

Table B16: HC+rMDD (MDD excluded) participants: BMA Probabilities

Nr	Pname	mean	QIDS10
1	A(1,1)	1.00	0.00
2	A(2,1)	1.00	0.00
3	A(3,1)	0.87	0.00
4	A(1,2)	1.00	0.00
5	A(2,2)	1.00	0.97
6	A(3,2)	1.00	0.75
7	A(1,3)	1.00	0.97
8	A(2,3)	0.00	0.00
9	A(3,3)	1.00	0.00

Table B17: HC (rMDD + MDD excluded) participants: BMA Expectations

Nr	Pname	mean	QIDS10
1	A(1,1)	0.46	0.00
2	A(2,1)	0.10	0.00
3	A(3,1)	0.00	0.00
4	A(1,2)	0.46	0.00
5	A(2,2)	-0.45	0.00
6	A(3,2)	0.09	-0.07
7	A(1,3)	-0.16	0.00
8	A(2,3)	0.00	0.00
9	A(3,3)	-0.24	-0.23

Table B18: HC (rMDD + MDD excluded) participants: BMA Probabilities

Nr	Pname	mean	QIDS10
1	A(1,1)	1.00	0.00
2	A(2,1)	1.00	0.00
3	A(3,1)	0.00	0.00
4	A(1,2)	1.00	0.00
5	A(2,2)	1.00	0.00
6	A(3,2)	1.00	0.71
7	A(1,3)	1.00	0.00
8	A(2,3)	0.00	0.00
9	A(3,3)	1.00	1.00

Tables B19-B24 include a single symptom (concentration / decision making difficulties) and additional covariates of no interest (HADS anxiety, site, age, sex)

Table B19: All 165 participants: BMA Expectations

Nr	Pname	mean	HADS	site	age	sex	QIDS10
1	A(1,1)	0.48	0.00	0.16	-0.04	0.00	0.00
2	A(2,1)	0.12	0.03	0.00	0.00	0.00	0.00
3	A(3,1)	0.00	0.00	0.00	0.00	0.00	0.00
4	A(1,2)	0.45	0.00	-0.03	0.00	0.00	0.00
5	A(2,2)	-0.41	0.08	0.00	0.06	0.00	0.15
6	A(3,2)	0.09	0.00	-0.04	0.00	0.04	-0.11
7	A(1,3)	-0.23	-0.15	0.07	0.04	0.00	0.00
8	A(2,3)	0.00	0.00	-0.09	0.00	0.06	0.00
9	A(3,3)	-0.25	-0.05	0.00	0.00	-0.03	0.00

Table B20: All 165 participants: BMA Probabilities

Nr	Pname	mean	HADS	site	age	sex	QIDS10
1	A(1,1)	1.00	0.00	1.00	0.67	0.00	0.00
2	A(2,1)	1.00	0.70	0.00	0.00	0.00	0.00
3	A(3,1)	0.00	0.00	0.00	0.00	0.00	0.00
4	A(1,2)	1.00	0.00	0.55	0.00	0.00	0.00
5	A(2,2)	1.00	1.00	0.00	1.00	0.00	1.00
6	A(3,2)	1.00	0.00	1.00	0.00	0.86	1.00
7	A(1,3)	1.00	1.00	0.85	0.64	0.00	0.00
8	A(2,3)	0.00	0.00	1.00	0.00	0.89	0.00
9	A(3,3)	1.00	1.00	0.00	0.00	0.65	0.00

Table B21: HC+rMDD (MDD excluded) participants: BMA Expectations

Nr	Pname	mean	HADS	site	age	sex	QIDS10
1	A(1,1)	0.49	0.00	0.17	-0.08	0.00	0.00
2	A(2,1)	0.11	0.02	0.00	0.00	0.00	0.00
3	A(3,1)	-0.03	0.00	0.02	0.00	0.00	0.00
4	A(1,2)	0.46	0.00	0.00	0.00	0.00	0.00
5	A(2,2)	-0.42	0.08	0.00	0.06	0.00	0.14
6	A(3,2)	0.10	0.00	-0.05	0.00	0.04	-0.08
7	A(1,3)	-0.20	-0.15	0.07	0.00	0.00	0.00
8	A(2,3)	0.00	0.00	-0.10	0.00	0.08	0.00
9	A(3,3)	-0.25	0.00	0.00	0.00	0.00	0.00

Table B22: HC+rMDD (MDD excluded) participants: BMA Probabilities

Nr	Pname	mean	HADS	site	age	sex	QIDS10
1	A(1,1)	1.00	0.00	1.00	0.92	0.00	0.00
2	A(2,1)	1.00	0.57	0.00	0.00	0.00	0.00
3	A(3,1)	0.87	0.00	0.60	0.00	0.00	0.00
4	A(1,2)	1.00	0.00	0.00	0.00	0.00	0.00
5	A(2,2)	1.00	1.00	0.00	1.00	0.00	0.97
6	A(3,2)	1.00	0.00	1.00	0.00	0.94	0.85
7	A(1,3)	1.00	1.00	0.87	0.00	0.00	0.00
8	A(2,3)	0.00	0.00	1.00	0.00	1.00	0.00
9	A(3,3)	1.00	0.00	0.00	0.00	0.00	0.00

Table B23: HC (rMDD + MDD excluded) participants: BMA Expectations

Nr	Pname	mean	HADS	site	age	sex	QIDS10
1	A(1,1)	0.47	0.00	0.16	0.00	0.00	0.00
2	A(2,1)	0.11	0.05	0.02	0.00	0.00	-0.05
3	A(3,1)	0.00	0.00	0.04	0.00	-0.02	0.00
4	A(1,2)	0.46	0.00	0.00	0.00	0.00	0.00
5	A(2,2)	-0.45	0.07	0.00	0.03	0.00	0.00
6	A(3,2)	0.09	0.00	-0.06	0.00	0.05	-0.09
7	A(1,3)	-0.16	-0.13	0.00	0.00	0.00	0.00
8	A(2,3)	0.00	0.00	-0.14	0.00	0.05	0.00
9	A(3,3)	-0.25	0.00	0.00	0.00	0.00	-0.22

Table B24: HC (rMDD + MDD excluded) participants: BMA Probabilities

Nr	Pname	mean	HADS	site	age	sex	QIDS10
1	A(1,1)	1.00	0.00	1.00	0.00	0.00	0.00
2	A(2,1)	1.00	0.95	0.58	0.00	0.00	0.52
3	A(3,1)	0.00	0.00	1.00	0.00	0.70	0.00
4	A(1,2)	1.00	0.00	0.00	0.00	0.00	0.00
5	A(2,2)	1.00	0.98	0.00	0.72	0.00	0.00
6	A(3,2)	1.00	0.00	1.00	0.00	1.00	0.86
7	A(1,3)	1.00	1.00	0.00	0.00	0.00	0.00
8	A(2,3)	0.00	0.00	1.00	0.00	0.80	0.00
9	A(3,3)	1.00	0.00	0.00	0.00	0.00	1.00

QIDS-SR individual symptoms information:

QIDS-16: 1. Falling asleep
QIDS-16: 2. Sleeping during the night
QIDS-16: 3. Waking up too early
QIDS-16: 4. Sleeping too much
QIDS-16: 5. Feeling sad
QIDS-16: 6. Decreased appetite
QIDS-16: 7. Increased appetite
QIDS-16: 8. Decreased weight
QIDS-16: 9. Increased weight
QIDS-16: 10. Concentration/decision making
QIDS-16: 11. View of myself
QIDS-16: 12. Thoughts of suicide or death
QIDS-16: 13. General interest
QIDS-16: 14. Energy level
QIDS-16: 15. Feeling slowed down
QIDS-16: 16. Feeling restless

Appendix D

Supplementary Materials for Chapter 6

Tables D.1-D.18 shows details about the trained classifiers. Each classifier was trained using the nested cross-validation scheme depicted in Figure 6.1. See Table D.1 for the caption relevant for all other tables.

Classifier	Linear SVM	**Accuracy**	70% (72%)
Inner-loop CV	Undersampled k-fold	**Healthy controls**	76/36
		Lifetime MDD	40/13
Features	A, A+B, A+C, A+B+C		

TABLE D.1: Classifier #1 details. Classifier states the inner-loop classifier type. Inner-cross validations were always repeated 10 times. Accuracy shows overall leave-one-out accuracy (and balanced accuracy in parentheses). Healthy controls shows the number of correctly/incorrectly classified controls. Lifetime MDD shows the number of correctly/incorrectly classified lifetime MDD cases. Features lists the possible feature sets (which could be selected in the inner-loop).

Classifier	Linear SVM	**Accuracy**	70% (72%)
Inner-loop CV	Stratified k-fold	**Healthy controls**	76/36
		Lifetime MDD	40/13
Features	A, A+B, A+C, A+B+C		

TABLE D.2: Classifier #2 details.

Classifier	Linear SVM	**Accuracy**	70% (72%)
Inner-loop CV	Undersampled k-fold	**Healthy controls**	87/25
		Lifetime MDD	23/30
Features	A, A+site, A+B, A+B+site, A+B+C, A+B+C+site		

TABLE D.3: Classifier #3 details.

Classifier	Linear SVM	**Accuracy**	65% (65%)
Inner-loop CV	Stratified k-fold	**Healthy controls**	72/40
		Lifetime MDD	35/18
Features	A, A+site, A+B, A+B+site, A+B+C, A+B+C+site		

TABLE D.4: Classifier #4 details.

Classifier	Linear SVM	**Accuracy**	71% (73%)
Inner-loop CV	Undersampled k-fold	**Healthy controls**	76/36
		Lifetime MDD	41/12
Features	A, A+B, A+var(A), A+B+var(A)+var(B)		

TABLE D.5: Classifier #5 details.

Classifier	Linear SVM	**Accuracy**	71% (73%)
Inner-loop CV	Stratified k-fold	**Healthy controls**	76/36
		Lifetime MDD	40/13
Features	A, A+B, A+var(A), A+B+var(A)+var(B)		

TABLE D.6: Classifier #6 details.

Classifier	RBF SVM	**Accuracy**	70% (70%)
Inner-loop CV	Undersampled k-fold	**Healthy controls**	79/33
		Lifetime MDD	37/16
Features	A, A+B, A+C, A+B+C		

TABLE D.7: Classifier #7 details.

Classifier	RBF SVM	**Accuracy**	71% (71%)
Inner-loop CV	Stratified k-fold	**Healthy controls**	79/33
		Lifetime MDD	38/15
Features	A, A+B, A+C, A+B+C		

TABLE D.8: Classifier #8 details.

Classifier	RBF SVM	**Accuracy**	66% (63%)
Inner-loop CV	Undersampled k-fold	**Healthy controls**	81/31
		Lifetime MDD	28/25
Features	A, A+site, A+B, A+B+site, A+B+C, A+B+C+site		

TABLE D.9: Classifier #9 details.

Classifier	RBF SVM	**Accuracy**	64% (61%)
Inner-loop CV	Stratified k-fold	**Healthy controls**	76/36
		Lifetime MDD	29/24
Features	A, A+site, A+B, A+B+site, A+B+C, A+B+C+site		

TABLE D.10: Classifier #10 details.

Classifier	RBF SVM	**Accuracy**	71% (71%)
Inner-loop CV	Repeated k-fold	**Healthy controls**	79/33
		Lifetime MDD	38/15
Features	A, A+B, A+var(A), A+B+var(A)+var(B)		

TABLE D.11: Classifier #11 details.

Classifier	RBF SVM	**Accuracy**	71% (71%)
Inner-loop CV	Stratified k-fold	**Healthy controls**	79/33
		Lifetime MDD	38/15
Features	A, A+B, A+var(A), A+B+var(A)+var(B)		

TABLE D.12: Classifier #12 details.

Classifier	Logistic Regression	**Accuracy**	62% (62%)
Inner-loop CV	Undersampled k-fold	**Healthy controls**	69/43
		Lifetime MDD	33/20
Features	A, A+B, A+C, A+B+C		

TABLE D.13: Classifier #13 details.

Classifier	Logistic Regression	**Accuracy**	63% (63%)
Inner-loop CV	Stratified k-fold	**Healthy controls**	70/42
		Lifetime MDD	34/19
Features	A, A+B, A+C, A+B+C		

TABLE D.14: Classifier #14 details.

Classifier	Logistic Regression	**Accuracy**	63% (60%)
Inner-loop CV	Undersampled k-fold	**Healthy controls**	77/35
		Lifetime MDD	27/26
Features	A, A+site, A+B, A+B+site, A+B+C, A+B+C+site		

TABLE D.15: Classifier #15 details.

Classifier	Logistic Regression	**Accuracy**	65% (63%)
Inner-loop CV	Stratified k-fold	**Healthy controls**	78/34
		Lifetime MDD	30/23
Features	A, A+site, A+B, A+B+site, A+B+C, A+B+C+site		

TABLE D.16: Classifier #16 details.

Classifier	Logistic Regression	**Accuracy**	62% (62%)
Inner-loop CV	Undersampled k-fold	**Healthy controls**	70/42
		Lifetime MDD	33/20
Features	A, A+B, A+var(A), A+B+var(A)+var(B)		

TABLE D.17: Classifier #17 details.

Classifier	Logistic Regression	**Accuracy**	63% (63%)
Inner-loop CV	Stratified k-fold	**Healthy controls**	70/42
		Lifetime MDD	34/19
Features	A, A+B, A+var(A), A+B+var(A)+var(B)		

TABLE D.18: Classifier #18 details.

Bibliography

Abi-Dargham, A. and Horga, G. (2016). "The search for imaging biomarkers in psychiatric disorders". In: *Nature medicine* 22.11, p. 1248.

Abramson, L. Y., Seligman, M. E., and Teasdale, J. D. (1978). "Learned helplessness in humans: Critique and reformulation." In: *Journal of abnormal psychology* 87.1, p. 49.

Adams, R. A., Huys, Q. J., and Roiser, J. P. (2016). "Computational Psychiatry: towards a mathematically informed understanding of mental illness". In: *J Neurol Neurosurg Psychiatry* 87.1, pp. 53–63.

Alexander, G. E. and Crutcher, M. D. (1990). "Functional architecture of basal ganglia circuits: neural substrates of parallel processing". In: *Trends in neurosciences* 13.7, pp. 266–271.

Alexander, G. E., Crutcher, M. D., and DeLong, M. R. (1991). "Basal ganglia-thalamocortical circuits: parallel substrates for motor, oculomotor,"prefrontal" and "limbic" functions". In: *Progress in brain research*. Vol. 85. Elsevier, pp. 119–146.

Alonso, J., Angermeyer, M. C., Bernert, S., Bruffaerts, R., Brugha, T. S., Bryson, H., Girolamo, G. d., Graaf, R. d., Demyttenaere, K., Gasquet, I., et al. (2004). "Prevalence of mental disorders in Europe: results from the European Study of the Epidemiology of Mental Disorders (ESEMeD) project". In: *Acta Psychiatrica Scandinavica* 109.s420, pp. 21–27.

Alvaro, P. K., Roberts, R. M., and Harris, J. K. (2013). "A systematic review assessing bidirectionality between sleep disturbances, anxiety, and depression". In: *Sleep* 36.7, pp. 1059–1068.

Amaral, D. G., Behniea, H., and Kelly, J. (2003). "Topographic organization of projections from the amygdala to the visual cortex in the macaque monkey". In: *Neuroscience* 118.4, pp. 1099–1120.

American Psychiatric Association (2013). *Diagnostic and Statistical Manual of Mental Disorders (5th ed.)* Arlington, VA Washington, D.C: Washington, DC: American Psychiatric Press. ISBN: 9780890425558.

Ashburner, J. (2012). "SPM: a history". In: *Neuroimage* 62.2, pp. 791–800.

Ayuso-Mateos, J. L., Vázquez-Barquero, J. L., Dowrick, C., Lehtinen, V., Dalgard, O. S., Casey, P., Wilkinson, C., Lasa, L., Page, H., Dunn, G., et al. (2001). "Depressive disorders in Europe: prevalence figures from the ODIN study". In: *The British Journal of Psychiatry* 179.4, pp. 308–316.

Bartra, O., McGuire, J. T., and Kable, J. W. (2013). "The valuation system: a coordinate-based meta-analysis of BOLD fMRI experiments examining neural correlates of subjective value". In: *Neuroimage* 76, pp. 412–427.

Beats, B., Sahakian, B. J., and Levy, R. (1996). "Cognitive performance in tests sensitive to frontal lobe dysfunction in the elderly depressed". In: *Psychological medicine* 26.3, pp. 591–603.

Beck, A., Rush, A., Shaw, B., and Emery, G. (1979). *Cognitive Therapy of Depression*. Guilford clinical psychology and psychotherapy series. Guilford Press.

Beck, A. T. (2005). "The current state of cognitive therapy: a 40-year retrospective". In: *Archives of General Psychiatry* 62.9, pp. 953–959.

– (2008). "The evolution of the cognitive model of depression and its neurobiological correlates". In: *American Journal of Psychiatry* 165.8, pp. 969–977.

Beck, A. T. and Steer, R. A. (1988). *Beck Hopelessness Scale*. Psychological Corporation San Antonio, TX.

Beck, A. T., Steer, R. A., Ball, R., and Ranieri, W. F. (1996). "Comparison of Beck Depression Inventories-IA and-II in psychiatric outpatients". In: *Journal of personality assessment* 67.3, pp. 588–597.

Beck, A. T., Ward, C. H., Mendelson, M., Mock, J., and Erbaugh, J. (1961). "An inventory for measuring depression". In: *Archives of general psychiatry* 4.6, pp. 561–571.

Beevers, C. G., Worthy, D. A., Gorlick, M. A., Nix, B., Chotibut, T., and Maddox, W. T. (2013). "Influence of depression symptoms on history-independent reward and punishment processing". In: *Psychiatry research* 207.1, pp. 53–60.

Bickel, W. K., Yi, R., Landes, R. D., Hill, P. F., and Baxter, C. (2011). "Remember the future: working memory training decreases delay discounting among stimulant addicts". In: *Biological psychiatry* 69.3, pp. 260–265.

BinDhim, N. F., Shaman, A. M., Trevena, L., Basyouni, M. H., Pont, L. G., and Alhawassi, T. M. (2015). "Depression screening via a smartphone app: cross-country user characteristics and feasibility". In: *Journal of the American Medical Informatics Association* 22.1, pp. 29–34.

Bishop, S. J. and Gagne, C. (2018). "Anxiety, depression, and decision making: A computational perspective". In: *Annual review of neuroscience* 41, pp. 371–388.

Bogdan, R. and Pizzagalli, D. A. (2006). "Acute stress reduces reward responsiveness: implications for depression". In: *Biological psychiatry* 60.10, pp. 1147–1154.

Borsboom, D. and Cramer, A. O. (2013). "Network analysis: an integrative approach to the structure of psychopathology". In: *Annual review of clinical psychology* 9, pp. 91–121.

Box, G. E. and Draper, N. R. (1987). *Empirical model-building and response surfaces*. John Wiley & Sons.

Brainard, D. H. (1997). "The psychophysics toolbox". In: *Spatial vision* 10, pp. 433–436.

Bright, P., Jaldow, E., and Kopelman, M. D. (2002). "The National Adult Reading Test as a measure of premorbid intelligence: a comparison with estimates derived from demographic variables". In: *Journal of the International Neuropsychological Society* 8.06, pp. 847–854.

Brodersen, K. H., Schofield, T. M., Leff, A. P., Ong, C. S., Lomakina, E. I., Buhmann, J. M., and Stephan, K. E. (2011). "Generative embedding for model-based classification of fMRI data". In: *PLoS computational biology* 7.6.

Bruehl, A. B., Delsignore, A., Komossa, K., and Weidt, S. (2014). "Neuroimaging in social anxiety disorder—a meta-analytic review resulting in a new neurofunctional model". In: *Neuroscience & Biobehavioral Reviews* 47, pp. 260–280.

Bürger, C., Redlich, R., Grotegerd, D., Meinert, S., Dohm, K., Schneider, I., Zaremba, D., Förster, K., Alferink, J., Bölte, J., et al. (2017). "Differential abnormal pattern of anterior cingulate gyrus activation in unipolar and bipolar depression: an fMRI and pattern classification approach". In: *Neuropsychopharmacology* 42.7, pp. 1399–1408.

Butler, A. C., Chapman, J. E., Forman, E. M., and Beck, A. T. (2006). "The empirical status of cognitive-behavioral therapy: a review of meta-analyses". In: *Clinical psychology review* 26.1, pp. 17–31.

Buxton, R. B. (2009). *Introduction to functional magnetic resonance imaging: principles and techniques*. Cambridge university press.

Canzian, L. and Musolesi, M. (2015). "Trajectories of depression: unobtrusive monitoring of depressive states by means of smartphone mobility traces analysis". In: *Proceedings of the 2015 ACM international joint conference on pervasive and ubiquitous computing*, pp. 1293–1304.

Chang, C.-K., Hayes, R. D., Perera, G., Broadbent, M. T., Fernandes, A. C., Lee, W. E., Hotopf, M., and Stewart, R. (2011). "Life expectancy at birth for people with serious mental illness and other major disorders from a secondary mental health care case register in London". In: *PloS one* 6.5, e19590.

Chase, H. W., Kumar, P., Eickhoff, S. B., and Dombrovski, A. Y. (2015). "Reinforcement learning models and their neural correlates: an activation likelihood estimation meta-analysis". In: *Cognitive, affective, & behavioral neuroscience* 15.2, pp. 435–459.

Chase, H. W., Nusslock, R., Almeida, J. R., Forbes, E. E., LaBarbara, E. J., and Phillips, M. L. (2013). "Dissociable patterns of abnormal frontal cortical activation during anticipation of an uncertain reward or loss in bipolar versus major depression". In: *Bipolar disorders* 15.8, pp. 839–854.

Chase, H., Frank, M., Michael, A., Bullmore, E., Sahakian, B., and Robbins, T. (2010). "Approach and avoidance learning in patients with major depression and healthy controls: relation to anhedonia". In: *Psychological medicine* 40.3, pp. 433–440.

Chekroud, A. M., Zotti, R. J., Shehzad, Z., Gueorguieva, R., Johnson, M. K., Trivedi, M. H., Cannon, T. D., Krystal, J. H., and Corlett, P. R. (2016). "Cross-trial prediction

of treatment outcome in depression: a machine learning approach". In: *The Lancet Psychiatry* 3.3, pp. 243–250.

Chen, C., Takahashi, T., Nakagawa, S., Inoue, T., and Kusumi, I. (2015). "Reinforcement learning in depression: a review of computational research". In: *Neuroscience & Biobehavioral Reviews* 55, pp. 247–267.

Chowdhury, R., Guitart-Masip, M., Lambert, C., Dayan, P., Huys, Q., Düzel, E., and Dolan, R. J. (2013). "Dopamine restores reward prediction errors in old age". In: *Nature neuroscience* 16.5, p. 648.

Cléry-Melin, M.-L., Jollant, F., and Gorwood, P. (2018). "Reward systems and cognitions in Major Depressive Disorder". In: *CNS spectrums*, pp. 1–14.

Cléry-Melin, M.-L., Schmidt, L., Lafargue, G., Baup, N., Fossati, P., and Pessiglione, M. (2011). "Why don't you try harder? An investigation of effort production in major depression". In: *PloS one* 6.8, e23178.

Cohen, Z. D. and DeRubeis, R. J. (2018). "Treatment selection in depression". In: *Annual Review of Clinical Psychology* 14.

Collins, A. G., Brown, J. K., Gold, J. M., Waltz, J. A., and Frank, M. J. (2014). "Working memory contributions to reinforcement learning impairments in schizophrenia". In: *Journal of Neuroscience* 34.41, pp. 13747–13756.

Cooney, G. M., Dwan, K., Greig, C. A., Lawlor, D. A., Rimer, J., Waugh, F. R., McMurdo, M., and Mead, G. E. (2013). "Exercise for depression". In: *Cochrane database of systematic reviews* 9.

Costafreda, S. G., Chu, C., Ashburner, J., and Fu, C. H. (2009). "Prognostic and diagnostic potential of the structural neuroanatomy of depression". In: *PloS one* 4.7.

Costafreda, S. G., Khanna, A., Mourao-Miranda, J., and Fu, C. H. (2009). "Neural correlates of sad faces predict clinical remission to cognitive behavioural therapy in depression". In: *Neuroreport* 20.7, pp. 637–641.

Cox, R. W. (1996). "AFNI: software for analysis and visualization of functional magnetic resonance neuroimages". In: *Computers and Biomedical research* 29.3, pp. 162–173.

Cuijpers, P., Straten, A. van, Bohlmeijer, E., Hollon, S., and Andersson, G. (2010). "The effects of psychotherapy for adult depression are overestimated: a meta-analysis of study quality and effect size". In: *Psychological medicine* 40.2, pp. 211–223.

Culpepper, L. (2010). "Why do you need to move beyond first-line therapy for major depression?" In: *The Journal of clinical psychiatry* 71, pp. 4–9.

– (2013). "Improving patient outcomes in depression through guideline-concordant, measurement-based care." In: *The Journal of clinical psychiatry* 74.4, e07–e07.

Cuthbert, B. N. and Insel, T. R. (2013). "Toward the future of psychiatric diagnosis: the seven pillars of RDoC". In: *BMC medicine* 11.1, p. 126.

Deakin, J. W. and Graeff, F. G. (1991). "5-HT and mechanisms of defence". In: *Journal of psychopharmacology* 5.4, pp. 305–315.

Deakin, J. (2013). "The origins of '5-HT and mechanisms of defence'by Deakin and Graeff: a personal perspective". In: *Journal of Psychopharmacology* 27.12, pp. 1084–1089.

DeRubeis, R. J., Hollon, S. D., Amsterdam, J. D., Shelton, R. C., Young, P. R., Salomon, R. M., O'Reardon, J. P., Lovett, M. L., Gladis, M. M., Brown, L. L., et al. (2005). "Cognitive therapy vs medications in the treatment of moderate to severe depression". In: *Archives of general psychiatry* 62.4, pp. 409–416.

Destoop, M., Morrens, M., Coppens, V., and Dom, G. (2019). "Addiction, anhedonia and co-morbid mood disorder. A Narrative review." In: *Frontiers in psychiatry* 10, p. 311.

Dillon, D. G. and Pizzagalli, D. A. (2018). "Mechanisms of Memory Disruption in Depression". In: *Trends in Neurosciences*.

Dillon, D. G., Wiecki, T., Pechtel, P., Webb, C., Goer, F., Murray, L., Trivedi, M., Fava, M., McGrath, P. J., Weissman, M., et al. (2015). "A computational analysis of flanker interference in depression". In: *Psychological medicine* 45.11, pp. 2333–2344.

Disner, S. G., Beevers, C. G., Haigh, E. A., and Beck, A. T. (2011). "Neural mechanisms of the cognitive model of depression". In: *Nature Reviews Neuroscience* 12.8, p. 467.

Dolan, R. J. (2002). "Emotion, cognition, and behavior". In: *science* 298.5596, pp. 1191–1194.

Dombrovski, A. Y., Clark, L., Siegle, G. J., Butters, M. A., Ichikawa, N., Sahakian, B. J., and Szanto, K. (2010). "Reward/punishment reversal learning in older suicide attempters". In: *American Journal of Psychiatry* 167.6, pp. 699–707.

Dombrovski, A. Y., Szanto, K., Clark, L., Reynolds, C. F., and Siegle, G. J. (2013). "Reward signals, attempted suicide, and impulsivity in late-life depression". In: *JAMA psychiatry* 70.10, pp. 1020–1030.

Drevets, W. C., Price, J. L., and Furey, M. L. (2008). "Brain structural and functional abnormalities in mood disorders: implications for neurocircuitry models of depression". In: *Brain structure and function* 213.1-2, pp. 93–118.

Drevets, W. C., Price, J. L., Simpson Jr, J. R., Todd, R. D., Reich, T., Vannier, M., and Raichle, M. E. (1997). "Subgenual prefrontal cortex abnormalities in mood disorders". In: *Nature* 386.6627, p. 824.

Driessen, E., Cuijpers, P., Hollon, S. D., and Dekker, J. J. (2010). "Does pretreatment severity moderate the efficacy of psychological treatment of adult outpatient depression? A meta-analysis." In: *Journal of consulting and clinical psychology* 78.5, p. 668.

Dunlop, B. W. and Nemeroff, C. B. (2007). "The role of dopamine in the pathophysiology of depression". In: *Archives of general psychiatry* 64.3, pp. 327–337.

Dutra, S., Brooks, N., Lempert, K., Guardado, A., Goetz, E., and D, P. (2009). "Reward responsiveness in a remitted depressed sample: Effects of gender and trait negative affect". In: *23rd Annual Meeting of the Society for Research in Psychopathology*.

Ebmeier, K. P., Donaghey, C., and Steele, J. D. (2006). "Recent developments and current controversies in depression". In: *The Lancet* 367.9505, pp. 153–167.

Eldar, E., Roth, C., Dayan, P., and Dolan, R. J. (2018). "Decodability of reward learning signals predicts mood fluctuations". In: *Current Biology* 28.9, pp. 1433–1439.

Eldar, E., Rutledge, R. B., Dolan, R. J., and Niv, Y. (2016). "Mood as representation of momentum". In: *Trends in cognitive sciences* 20.1, pp. 15–24.

Eshel, N. and Roiser, J. P. (2010). "Reward and punishment processing in depression". In: *Biological psychiatry* 68.2, pp. 118–124.

Fagiolini, A. and Kupfer, D. J. (2003). "Is treatment-resistant depression a unique subtype of depression?" In: *Biological psychiatry* 53.8, pp. 640–648.

First, M. B., Spitzer, R. L., Gibbon, M., Williams, J. B., et al. (2002). *Structured clinical interview for DSM-IV-TR axis I disorders, research version, patient edition.* Tech. rep. SCID-I/P New York, NY.

Fitzgerald, P. B., Laird, A. R., Maller, J., and Daskalakis, Z. J. (2008). "A meta-analytic study of changes in brain activation in depression". In: *Human brain mapping* 29.6, pp. 683–695.

Forbes, E. E., Christopher May, J., Siegle, G. J., Ladouceur, C. D., Ryan, N. D., Carter, C. S., Birmaher, B., Axelson, D. A., and Dahl, R. E. (2006). "Reward-related decision-making in pediatric major depressive disorder: an fMRI study". In: *Journal of Child Psychology and Psychiatry* 47.10, pp. 1031–1040.

Forbes, E. E., Shaw, D. S., and Dahl, R. E. (2007). "Alterations in reward-related decision making in boys with recent and future depression". In: *Biological psychiatry* 61.5, pp. 633–639.

Fried, E. I., Nesse, R. M., Zivin, K., Guille, C., and Sen, S. (2014). "Depression is more than the sum score of its parts: individual DSM symptoms have different risk factors". In: *Psychological medicine* 44.10, pp. 2067–2076.

Friston, K. J. (2011). "Functional and effective connectivity: a review". In: *Brain connectivity* 1.1, pp. 13–36.

Friston, K. J., Ashburner, J. T., Kiebel, S. J., Nichols, T. E., and Penny, W. D. (2007). *Statistical parametric mapping: the analysis of functional brain images.* Elsevier, Academic Press. ISBN: 978-0-12-372560-8.

Friston, K. J., Harrison, L., and Penny, W. (2003). "Dynamic causal modelling". In: *Neuroimage* 19.4, pp. 1273–1302.

Friston, K. J., Litvak, V., Oswal, A., Razi, A., Stephan, K. E., Van Wijk, B. C., Ziegler, G., and Zeidman, P. (2016). "Bayesian model reduction and empirical Bayes for group (DCM) studies". In: *Neuroimage* 128, pp. 413–431.

Friston, K. J., Stephan, K. E., Montague, R., and Dolan, R. J. (2014). "Computational psychiatry: the brain as a phantastic organ". In: *The Lancet Psychiatry* 1.2, pp. 148–158.

Fu, C. H., Mourao-Miranda, J., Costafreda, S. G., Khanna, A., Marquand, A. F., Williams, S. C., and Brammer, M. J. (2008). "Pattern classification of sad facial

processing: toward the development of neurobiological markers in depression". In: *Biological psychiatry* 63.7, pp. 656–662.

Gläscher, J., Hampton, A. N., and O'doherty, J. P. (2008). "Determining a role for ventromedial prefrontal cortex in encoding action-based value signals during reward-related decision making". In: *Cerebral cortex* 19.2, pp. 483–495.

Gläscher, J. P. and O'Doherty, J. P. (2010). "Model-based approaches to neuroimaging: combining reinforcement learning theory with fMRI data". In: *Wiley Interdisciplinary Reviews: Cognitive Science* 1.4, pp. 501–510.

Gong, Q., Wu, Q., Scarpazza, C., Lui, S., Jia, Z., Marquand, A., Huang, X., McGuire, P., and Mechelli, A. (2011). "Prognostic prediction of therapeutic response in depression using high-field MR imaging". In: *Neuroimage* 55.4, pp. 1497–1503.

Gotlib, I. H. and Joormann, J. (2010). "Cognition and depression: current status and future directions". In: *Annual review of clinical psychology* 6, pp. 285–312.

Gradin, V. B., Baldacchino, A., Balfour, D., Matthews, K., and Steele, J. D. (2014). "Abnormal brain activity during a reward and loss task in opiate-dependent patients receiving methadone maintenance therapy". In: *Neuropsychopharmacology* 39.4, pp. 885–894.

Gradin, V. B., Kumar, P., Waiter, G., Ahearn, T., Stickle, C., Milders, M., Reid, I., Hall, J., and Steele, J. D. (2011). "Expected value and prediction error abnormalities in depression and schizophrenia". In: *Brain*.

Gradin, V. B. and Pomi, A. (2008). "The role of hippocampal atrophy in depression: a neurocomputational approach". In: *Journal of biological physics* 34.1-2, pp. 107–120.

Gray, J. and McNaughton, N. (2000). "Fundamentals of the septo-hippocampal system". In: *The Neuropsychology of Anxiety: An Enquiry into the Functions of Septo-hippocampal System, 2nd ed. Oxford University Press, Oxford*, pp. 204–232.

Greenberg, P. E., Fournier, A.-A., Sisitsky, T., Pike, C. T., and Kessler, R. C. (2015). "The economic burden of adults with major depressive disorder in the United States (2005 and 2010)". In: *J Clin Psychiatry* 76.2, pp. 155–162.

Greenberg, T., Chase, H. W., Almeida, J. R., Stiffler, R., Zevallos, C. R., Aslam, H. A., Deckersbach, T., Weyandt, S., Cooper, C., Toups, M., et al. (2015). "Moderation of the relationship between reward expectancy and prediction error-related ventral striatal reactivity by anhedonia in unmedicated major depressive disorder: Findings from the EMBARC study". In: *American Journal of Psychiatry* 172.9, pp. 881–891.

Habota, T., Sandu, A.-L., Waiter, G. D., McNeil, C. J., Steele, J. D., Macfarlane, J. A., Whalley, H. C., Valentine, R., Younie, D., Crouch, N., et al. (Nov. 2019). "Cohort profile for the STratifying Resilience and Depression Longitudinally (STRADL) study: A depression-focused investigation of Generation Scotland, using detailed clinical, cognitive, and neuroimaging assessments [version 1; peer review: awaiting peer review]". In: *Wellcome Open Research* 4, p. 185.

Harmer, C. J., Goodwin, G. M., and Cowen, P. J. (2009). "Why do antidepressants take so long to work? A cognitive neuropsychological model of antidepressant drug action". In: *The British Journal of Psychiatry* 195.2, pp. 102–108.

Hitchcock, P., Radulescu, A., Niv, Y., and Sims, C. R. (2017). "Translating a Reinforcement Learning Task into a Computational Psychiatry Assay: Challenges and Strategies". In: *Schizophrenia Research*.

Ho, T. C., Sacchet, M. D., Connolly, C. G., Margulies, D. S., Tymofiyeva, O., Paulus, M. P., Simmons, A. N., Gotlib, I. H., and Yang, T. T. (2017). "Inflexible functional connectivity of the dorsal anterior cingulate cortex in adolescent major depressive disorder". In: *Neuropsychopharmacology* 42.12, p. 2434.

Holroyd, C. B. and Umemoto, A. (2016). "The research domain criteria framework: the case for anterior cingulate cortex". In: *Neuroscience & Biobehavioral Reviews* 71, pp. 418–443.

Holtzheimer, P. E., Husain, M. M., Lisanby, S. H., Taylor, S. F., Whitworth, L. A., McClintock, S., Slavin, K. V., Berman, J., McKhann, G. M., Patil, P. G., et al. (2017). "Subcallosal cingulate deep brain stimulation for treatment-resistant depression: a multisite, randomised, sham-controlled trial". In: *The Lancet Psychiatry* 4.11, pp. 839–849.

Howard, D. M., Adams, M. J., Clarke, T.-K., Hafferty, J. D., Gibson, J., Shirali, M., Coleman, J. R., Hagenaars, S. P., Ward, J., Wigmore, E. M., et al. (2019). "Genome-wide meta-analysis of depression identifies 102 independent variants and highlights the importance of the prefrontal brain regions". In: *Nature neuroscience* 22.3, p. 343.

Huguet, A., Rao, S., McGrath, P. J., Wozney, L., Wheaton, M., Conrod, J., and Rozario, S. (2016). "A systematic review of cognitive behavioral therapy and behavioral activation apps for depression". In: *PloS one* 11.5.

Husain, M. and Roiser, J. P. (2018). "Neuroscience of apathy and anhedonia: a transdiagnostic approach". In: *Nature Reviews Neuroscience*, p. 1.

Huys, Q. J., Cools, R., Gölzer, M., Friedel, E., Heinz, A., Dolan, R. J., and Dayan, P. (2011). "Disentangling the roles of approach, activation and valence in instrumental and pavlovian responding". In: *PLoS computational biology* 7.4.

Huys, Q. J., Daw, N. D., and Dayan, P. (2015). "Depression: a decision-theoretic analysis". In: *Annual review of neuroscience* 38, pp. 1–23.

Huys, Q. J., Maia, T. V., and Frank, M. J. (2016). "Computational psychiatry as a bridge from neuroscience to clinical applications". In: *Nature neuroscience* 19.3, pp. 404–413.

Huys, Q. J., Moutoussis, M., and Williams, J. (2011). "Are computational models of any use to psychiatry?" In: *Neural Networks* 24.6, pp. 544–551.

Huys, Q. J., Pizzagalli, D. A., Bogdan, R., and Dayan, P. (2013). "Mapping anhedonia onto reinforcement learning: a behavioural meta-analysis". In: *Biology of mood & anxiety disorders* 3.1, p. 12.

Huys, Q. J. and Renz, D. (2017). "A formal valuation framework for emotions and their control". In: *Biological psychiatry* 82.6, pp. 413–420.

Huys, Q. J., Vogelstein, J. T., Dayan, P., and Bottou, L. (2008). "Psychiatry: Insights into depression through normative decision-making models." In: *NIPS*, pp. 729–736.

Iglesias, S., Tomiello, S., Schneebeli, M., and Stephan, K. E. (2017). "Models of neuromodulation for computational psychiatry". In: *Wiley Interdisciplinary Reviews: Cognitive Science* 8.3.

Insel, T., Cuthbert, B., Garvey, M., Heinssen, R., Pine, D. S., Quinn, K., Sanislow, C., and Wang, P. (2010). "Research domain criteria (RDoC): toward a new classification framework for research on mental disorders". In: *American Journal of Psychiatry* 167:7.

Jenkinson, M., Beckmann, C. F., Behrens, T. E., Woolrich, M. W., and Smith, S. M. (2012). "FSL". In: *Neuroimage* 62.2, pp. 782–790.

Johnston, B., Mwangi, B., Matthews, K., Coghill, D., and Steele, J. (2013). "Predictive classification of individual magnetic resonance imaging scans from children and adolescents". In: *European child & adolescent psychiatry* 22.12, pp. 733–744.

Johnston, B. A., Steele, J. D., Tolomeo, S., Christmas, D., and Matthews, K. (2015). "Structural MRI-based predictions in patients with treatment-refractory depression (TRD)". In: *PLoS One* 10.7.

Johnston, B. A., Tolomeo, S., Gradin, V., Christmas, D., Matthews, K., and Steele, J. D. (2015). "Failure of hippocampal deactivation during loss events in treatment-resistant depression". In: *Brain* 138.9, pp. 2766–2776.

Joormann, J. and Stanton, C. H. (2016). "Examining emotion regulation in depression: A review and future directions". In: *Behaviour Research and Therapy* 86, pp. 35–49.

Joormann, J. and Vanderlind, W. M. (2014). "Emotion regulation in depression: The role of biased cognition and reduced cognitive control". In: *Clinical Psychological Science* 2.4, pp. 402–421.

Kahan, J. and Foltynie, T. (2013). "Understanding DCM: ten simple rules for the clinician". In: *Neuroimage* 83, pp. 542–549.

Kaiser, R. H., Andrews-Hanna, J. R., Wager, T. D., and Pizzagalli, D. A. (2015). "Large-scale network dysfunction in major depressive disorder: a meta-analysis of resting-state functional connectivity". In: *JAMA psychiatry* 72.6, pp. 603–611.

Kaiser, R. H., Whitfield-Gabrieli, S., Dillon, D. G., Goer, F., Beltzer, M., Minkel, J., Smoski, M., Dichter, G., and Pizzagalli, D. A. (2016). "Dynamic resting-state functional connectivity in major depression". In: *Neuropsychopharmacology* 41.7, p. 1822.

Kalivas, P. W. (2009). "The glutamate homeostasis hypothesis of addiction". In: *Nature Reviews Neuroscience* 10.8, p. 561.

Katz, B. A., Matanky, K., Aviram, G., and Yovel, I. (2020). "Reinforcement sensitivity, depression and anxiety: A meta-analysis and meta-analytic structural equation model". In: *Clinical Psychology Review*, p. 101842.

Kendler, K. S., Kuhn, J., and Prescott, C. A. (2004). "The interrelationship of neuroticism, sex, and stressful life events in the prediction of episodes of major depression". In: *American Journal of Psychiatry* 161.4, pp. 631–636.

Keren, H., O'Callaghan, G., Vidal-Ribas, P., Buzzell, G. A., Brotman, M. A., Leibenluft, E., Pan, P. M., Meffert, L., Kaiser, A., Wolke, S., et al. (2018). "Reward processing in depression: a conceptual and meta-analytic review across fMRI and EEG studies". In: *American Journal of Psychiatry* 175.11, pp. 1111–1120.

Kessler, R. C., Berglund, P., Demler, O., Jin, R., Koretz, D., Merikangas, K. R., Rush, A. J., Walters, E. E., and Wang, P. S. (2003). "The epidemiology of major depressive disorder: results from the National Comorbidity Survey Replication (NCS-R)". In: *Jama* 289.23, pp. 3095–3105.

Kessler, R. C. and Bromet, E. J. (2013). "The epidemiology of depression across cultures". In: *Annual review of public health* 34, pp. 119–138.

Kessler, R. C., Chiu, W. T., Demler, O., and Walters, E. E. (2005). "Prevalence, severity, and comorbidity of 12-month DSM-IV disorders in the National Comorbidity Survey Replication". In: *Archives of general psychiatry* 62.6, pp. 617–627.

Khan, A., Faucett, J., Lichtenberg, P., Kirsch, I., and Brown, W. A. (2012). "A systematic review of comparative efficacy of treatments and controls for depression". In: *PloS one* 7.7, e41778.

Kim, H., Shimojo, S., and O'Doherty, J. P. (2011). "Overlapping responses for the expectation of juice and money rewards in human ventromedial prefrontal cortex". In: *Cerebral cortex* 21.4, pp. 769–776.

Kleiner, M., Brainard, D., Pelli, D., Ingling, A., Murray, R., Broussard, C., et al. (2007). "What's new in Psychtoolbox-3". In: *Perception* 36.14, p. 1.

Kumar, P., Waiter, G., Ahearn, T., Milders, M., Reid, I., and Steele, J. (2008). "Abnormal temporal difference reward-learning signals in major depression". In: *Brain* 131.8, pp. 2084–2093.

Kumar, P., Goer, F., Murray, L., Dillon, D. G., Beltzer, M. L., Cohen, A. L., Brooks, N. H., and Pizzagalli, D. A. (2018). "Impaired reward prediction error encoding and striatal-midbrain connectivity in depression". In: *Neuropsychopharmacology*, p. 1.

Lawson, R., Nord, C., Seymour, B., Thomas, D., Dayan, P., Pilling, S., and Roiser, J. (2017). "Disrupted habenula function in major depression". In: *Molecular psychiatry* 22.2, p. 202.

Li, K., Zhang, M., Zhang, H., Li, X., Zou, F., Wang, Y., Wu, X., and Zhang, H. (2020). "The spontaneous activity and functional network of the occipital cortex is correlated with state anxiety in healthy adults". In: *Neuroscience Letters* 715, p. 134596.

Lilienfeld, S. O. and Treadway, M. T. (2016). "Clashing diagnostic approaches: DSM-ICD versus RDoC". In: *Annual review of clinical psychology* 12, pp. 435–463.

Lopresti, A. L., Hood, S. D., and Drummond, P. D. (2013). "A review of lifestyle factors that contribute to important pathways associated with major depression: diet, sleep and exercise". In: *Journal of affective disorders* 148.1, pp. 12–27.

Mai, J. K., Majtanik, M., and Paxinos, G. (2015). *Atlas of the human brain (4th ed.)* Academic Press.

Maia, T. V. (2015). "Introduction to the series on computational psychiatry". In: *Clinical Psychological Science* 3.3, pp. 374–377.

Maier, S. F. and Seligman, M. E. (1976). "Learned helplessness: Theory and evidence." In: *Journal of experimental psychology: general* 105.1, p. 3.

Mäki-Marttunen, T., Kaufmann, T., Elvsåshagen, T., Devor, A., Djurovic, S., Westlye, L. T., Linne, M.-L., Rietschel, M., Schubert, D., Borgwardt, S., et al. (2019). "Biophysical Psychiatry—How Computational Neuroscience Can Help to Understand the Complex Mechanisms of Mental Disorders". In: *Frontiers in psychiatry* 10.

Marr, D. (1982). *Vision: a computational investigation into the human representation and processing of visual information*. San Francisco: W.H. Freeman. ISBN: 0-7167-1284-9.

Mayberg, H. S. (1997). "Limbic-cortical dysregulation: a proposed model of depression." In: *The Journal of neuropsychiatry and clinical neurosciences*.

– (2009). "Targeted electrode-based modulation of neural circuits for depression". In: *The Journal of clinical investigation* 119.4, pp. 717–725.

Mayberg, H. S., Lozano, A. M., Voon, V., McNeely, H. E., Seminowicz, D., Hamani, C., Schwalb, J. M., and Kennedy, S. H. (2005). "Deep brain stimulation for treatment-resistant depression". In: *Neuron* 45.5, pp. 651–660.

McDermott, L. M. and Ebmeier, K. P. (2009). "A meta-analysis of depression severity and cognitive function". In: *Journal of affective disorders* 119.1, pp. 1–8.

McGuire, P., Sato, J. R., Mechelli, A., Jackowski, A., Bressan, R. A., and Zugman, A. (2015). "Can neuroimaging be used to predict the onset of psychosis?" In: *The lancet Psychiatry* 2.12, pp. 1117–1122.

McIntyre, R. S., Cha, D. S., Soczynska, J. K., Woldeyohannes, H. O., Gallaugher, L. A., Kudlow, P., Alsuwaidan, M., and Baskaran, A. (2013). "Cognitive deficits and functional outcomes in major depressive disorder: determinants, substrates, and treatment interventions". In: *Depression and anxiety* 30.6, pp. 515–527.

McLaren, D. G., Ries, M. L., Xu, G., and Johnson, S. C. (2012). "A generalized form of context-dependent psychophysiological interactions (gPPI): a comparison to standard approaches". In: *Neuroimage* 61.4, pp. 1277–1286.

Montague, P. R., Dayan, P., and Sejnowski, T. J. (1996). "A framework for mesencephalic dopamine systems based on predictive Hebbian learning". In: *Journal of neuroscience* 16.5, pp. 1936–1947.

Montague, P. R., Dolan, R. J., Friston, K. J., and Dayan, P. (2012). "Computational psychiatry". In: *Trends in cognitive sciences* 16.1, pp. 72–80.

Mourão-Miranda, J., Hardoon, D. R., Hahn, T., Marquand, A. F., Williams, S. C., Shawe-Taylor, J., and Brammer, M. (2011). "Patient classification as an outlier

detection problem: an application of the one-class support vector machine". In: *Neuroimage* 58.3, pp. 793–804.

Muehlhan, M., Lueken, U., Wittchen, H.-U., and Kirschbaum, C. (2011). "The scanner as a stressor: evidence from subjective and neuroendocrine stress parameters in the time course of a functional magnetic resonance imaging session". In: *International Journal of Psychophysiology* 79.2, pp. 118–126.

Müller, V. I., Cieslik, E. C., Serbanescu, I., Laird, A. R., Fox, P. T., and Eickhoff, S. B. (2017). "Altered brain activity in unipolar depression revisited: meta-analyses of neuroimaging studies". In: *JAMA psychiatry* 74.1, pp. 47–55.

Must, A., Horvath, S., Nemeth, V. L., and Janka, Z. (2013). "The Iowa Gambling Task in depression–what have we learned about sub-optimal decision-making strategies?" In: *Frontiers in psychology* 4, p. 732.

Mwangi, B., Ebmeier, K. P., Matthews, K., and Steele, J. D. (2012). "Multi-centre diagnostic classification of individual structural neuroimaging scans from patients with major depressive disorder". In: *Brain* 135.5, pp. 1508–1521.

Mwangi, B., Matthews, K., and Steele, J. D. (2011). "Prediction of illness severity in patients with major depression using structural MR brain scans". In: *Journal of Magnetic Resonance Imaging* 35.1, pp. 64–71.

Nakanishi, S., Hikida, T., and Yawata, S. (2014). "Distinct dopaminergic control of the direct and indirect pathways in reward-based and avoidance learning behaviors". In: *Neuroscience* 282, pp. 49–59.

National Institute for Health and Care Excellence (NICE) (2010). *Depression: The NICE Guideline on the Treatment and Management of Depression in Adults (Updated Edition) (Nice Guidelines)*. Royal College of Psychiatrists. ISBN: 9781904671855.

Navrady, L., Wolters, M., MacIntyre, D., Clarke, T., Campbell, A., Murray, A., Evans, K., Seckl, J., Haley, C., Milburn, K., et al. (2017). "Cohort profile: stratifying resilience and depression longitudinally (STRADL): a questionnaire follow-up of Generation Scotland: Scottish Family Health Study (GS: SFHS)". In: *International journal of epidemiology* 47.1, 13–14g.

Nelson, H. and Willison, J. (1991). "The revised national adult reading test–test manual". In: *Windsor, UK: NFER-Nelson* 991, pp. 1–6.

Nichols, T. E. (2012). "Multiple testing corrections, nonparametric methods, and random field theory". In: *Neuroimage* 62.2, pp. 811–815.

O'Doherty, J., Dayan, P., Schultz, J., Deichmann, R., Friston, K., and Dolan, R. J. (2004). "Dissociable roles of ventral and dorsal striatum in instrumental conditioning". In: *Science* 304.5669, pp. 452–454.

O'Doherty, J. P., Hampton, A., and Kim, H. (2007). "Model-based fMRI and its application to reward learning and decision making". In: *Annals of the New York Academy of sciences* 1104.1, pp. 35–53.

Olfson, M., Blanco, C., and Marcus, S. C. (2016). "Treatment of adult depression in the United States". In: *JAMA internal medicine* 176.10, pp. 1482–1491.

Ormel, J., Bastiaansen, A., Riese, H., Bos, E. H., Servaas, M., Ellenbogen, M., Rosmalen, J. G., and Aleman, A. (2013). "The biological and psychological basis of neuroticism: current status and future directions". In: *Neuroscience & Biobehavioral Reviews* 37.1, pp. 59–72.

Otte, C., Gold, S. M., Penninx, B. W., Pariante, C. M., Etkin, A., Fava, M., Mohr, D. C., and Schatzberg, A. F. (2016). "Major depressive disorder". In: *Nature reviews Disease primers* 2.1, pp. 1–20.

Paulus, M. P., Huys, Q. J., and Maia, T. V. (2016). "A roadmap for the development of applied computational psychiatry". In: *Biological psychiatry: cognitive neuroscience and neuroimaging* 1.5, pp. 386–392.

Pe, M. L., Vandekerckhove, J., and Kuppens, P. (2013). "A diffusion model account of the relationship between the emotional flanker task and rumination and depression." In: *Emotion* 13.4, p. 739.

Pechtel, P., Dutra, S. J., Goetz, E. L., and Pizzagalli, D. A. (2013). "Blunted reward responsiveness in remitted depression". In: *Journal of psychiatric research* 47.12, pp. 1864–1869.

Pedregosa, F., Varoquaux, G., Gramfort, A., Michel, V., Thirion, B., Grisel, O., Blondel, M., Prettenhofer, P., Weiss, R., Dubourg, V., et al. (2011). "Scikit-learn: Machine Learning in Python". In: *Journal of Machine Learning Research* 12, pp. 2825–2830.

Pelli, D. G. (1997). "The VideoToolbox software for visual psychophysics: Transforming numbers into movies". In: *Spatial vision* 10.4, pp. 437–442.

Penny, W., Mattout, J., and Trujillo-Barreto, N. (2006). "Bayesian model selection and averaging". In: *Statistical Parametric Mapping: The analysis of functional brain images. London: Elsevier*.

Perrin, J. S., Merz, S., Bennett, D. M., Currie, J., Steele, J. D., Reid, I. C., and Schwarzbauer, C. (2012). "Electroconvulsive therapy reduces frontal cortical connectivity in severe depressive disorder". In: *Proceedings of the National Academy of Sciences* 109.14, pp. 5464–5468.

Pizzagalli, D. A. (2014). "Depression, stress, and anhedonia: toward a synthesis and integrated model". In: *Annual review of clinical psychology* 10, p. 393.

Pizzagalli, D. A., Evins, A. E., Schetter, E. C., Frank, M. J., Pajtas, P. E., Santesso, D. L., and Culhane, M. (2008). "Single dose of a dopamine agonist impairs reinforcement learning in humans: behavioral evidence from a laboratory-based measure of reward responsiveness". In: *Psychopharmacology* 196.2, pp. 221–232.

Pizzagalli, D. A., Goetz, E., Ostacher, M., Iosifescu, D. V., and Perlis, R. H. (2008). "Euthymic patients with bipolar disorder show decreased reward learning in a probabilistic reward task". In: *Biological psychiatry* 64.2, pp. 162–168.

Pizzagalli, D. A., Holmes, A. J., Dillon, D. G., Goetz, E. L., Birk, J. L., Bogdan, R., Dougherty, D. D., Iosifescu, D. V., Rauch, S. L., and Fava, M. (2009). "Reduced caudate and nucleus accumbens response to rewards in unmedicated individuals with major depressive disorder". In: *American Journal of Psychiatry* 166.6, pp. 702–710.

Pizzagalli, D. A., Iosifescu, D., Hallett, L. A., Ratner, K. G., and Fava, M. (2008). "Reduced hedonic capacity in major depressive disorder: evidence from a probabilistic reward task". In: *Journal of psychiatric research* 43.1, pp. 76–87.

Pizzagalli, D. A., Jahn, A. L., and O'Shea, J. P. (2005). "Toward an objective characterization of an anhedonic phenotype: a signal-detection approach". In: *Biological psychiatry* 57.4, pp. 319–327.

Poldrack, R. A., Mumford, J. A., and Nichols, T. E. (2011). *Handbook of functional MRI data analysis*. Cambridge University Press.

Pornpattananangkul, N., Leibenluft, E., Pine, D. S., and Stringaris, A. (2019). "Association Between Childhood Anhedonia and Alterations in Large-scale Resting-State Networks and Task-Evoked Activation". In: *JAMA psychiatry* 76.6, pp. 624–633.

Pulcu, E., Trotter, P., Thomas, E., McFarquhar, M., Juhász, G., Sahakian, B., Deakin, J., Zahn, R., Anderson, I., and Elliott, R. (2014). "Temporal discounting in major depressive disorder". In: *Psychological medicine* 44.09, pp. 1825–1834.

Pulcu, E. and Browning, M. (2017). "Using Computational Psychiatry to Rule Out the Hidden Causes of Depression". In: *JAMA psychiatry*.

– (2019). "The misestimation of uncertainty in affective disorders". In: *Trends in Cognitive Sciences* 23.10, pp. 865–875.

Queirazza, F., Fouragnan, E., Steele, J. D., Cavanagh, J., and Philiastides, M. G. (2019). "Neural correlates of weighted reward prediction error during reinforcement learning classify response to cognitive behavioral therapy in depression". In: *Science advances* 5.7, eaav4962.

Ramirez-Mahaluf, J. P., Roxin, A., Mayberg, H. S., and Compte, A. (2017). "A computational model of major depression: the role of glutamate dysfunction on cingulo-frontal network dynamics". In: *Cerebral cortex* 27.1, pp. 660–679.

Redish, A. D. (2004). "Addiction as a computational process gone awry". In: *Science* 306.5703, pp. 1944–1947.

Redish, A. D., Jensen, S., and Johnson, A. (2008). "Addiction as vulnerabilities in the decision process". In: *Behavioral and Brain Sciences* 31.4, pp. 461–487.

Reuter, M., Schmansky, N. J., Rosas, H. D., and Fischl, B. (2012). "Within-subject template estimation for unbiased longitudinal image analysis". In: *Neuroimage* 61.4, pp. 1402–1418.

Rizvi, S. J., Pizzagalli, D. A., Sproule, B. A., and Kennedy, S. H. (2016). "Assessing anhedonia in depression: potentials and pitfalls". In: *Neuroscience & Biobehavioral Reviews* 65, pp. 21–35.

Robinson, O. J., Cools, R., Carlisi, C. O., Sahakian, B. J., and Drevets, W. C. (2012). "Ventral striatum response during reward and punishment reversal learning in unmedicated major depressive disorder". In: *American Journal of Psychiatry* 169.2, pp. 152–159.

Rock, P., Roiser, J., Riedel, W., and Blackwell, A. (2014). "Cognitive impairment in depression: a systematic review and meta-analysis". In: *Psychological Medicine* 44.10, p. 2029.

Roiser, J. P., Elliott, R., and Sahakian, B. J. (2012). "Cognitive mechanisms of treatment in depression". In: *Neuropsychopharmacology* 37.1, p. 117.

Romaniuk, L., Sandu, A.-L., Waiter, G. D., McNeil, C. J., Xueyi, S., Harris, M. A., Macfarlane, J. A., Lawrie, S. M., Deary, I. J., Murray, A. D., et al. (2019). "The Neurobiology of Personal Control During Reward Learning and Its Relationship to Mood". In: *Biological Psychiatry: Cognitive Neuroscience and Neuroimaging* 4.2, pp. 190–199.

Rothkirch, M., Tonn, J., Köhler, S., and Sterzer, P. (2017). "Neural mechanisms of reinforcement learning in unmedicated patients with major depressive disorder". In: *Brain* 140.4, pp. 1147–1157.

Rupprechter, S., Romaniuk, L., Seriès, P., Hirose, Y., Hawkins, E., Sandu, A.-L., Waiter, G. D., McNeil, C. J., Shen, X., Harris, M. A., et al. (2020). "Blunted Medial Prefrontal Cortico-Limbic Reward-Related Effective Connectivity and Depression". In: *Brain (accepted)*.

Rupprechter, S., Stankevicius, A., Huys, Q. J. M., Series, P., and Steele, J. D. (2020). "Abnormal reward valuation and event-related connectivity in unmedicated major depressive disorder". In: *Psychological Medicine*, pp. 1–9.

Rupprechter, S., Stankevicius, A., Huys, Q. J. M., Steele, J. D., and Seriès, P. (2018). "Major Depression Impairs the Use of Reward Values for Decision-Making". In: *Scientific Reports* 8.13798.

Rupprechter, S., Valton, V., and Seriès, P. (2020). "Depressive Disorders from a Computational Perspective". In: *Computational Psychiatry: A Primer*. Ed. by P. Seriès. Cambridge, MA, USA: MIT Press. Chap. 7.

Ruscio, A. M. (2019). "Normal versus pathological mood: Implications for diagnosis". In: *Annual review of clinical psychology*.

Rush, A. J., Trivedi, M. H., Ibrahim, H. M., Carmody, T. J., Arnow, B., Klein, D. N., Markowitz, J. C., Ninan, P. T., Kornstein, S., Manber, R., et al. (2003). "The 16-Item Quick Inventory of Depressive Symptomatology (QIDS), clinician rating (QIDS-C), and self-report (QIDS-SR): a psychometric evaluation in patients with chronic major depression". In: *Biological psychiatry* 54.5, pp. 573–583.

Russo, S. J. and Nestler, E. J. (2013). "The brain reward circuitry in mood disorders". In: *Nature Reviews Neuroscience* 14.9, pp. 609–625.

Rutledge, R. B., De Berker, A. O., Espenhahn, S., Dayan, P., and Dolan, R. J. (2016). "The social contingency of momentary subjective well-being". In: *Nature communications* 7.1, pp. 1–8.

Rutledge, R. B., Moutoussis, M., Smittenaar, P., Zeidman, P., Taylor, T., Hrynkiewicz, L., Lam, J., Skandali, N., Siegel, J. Z., Ousdal, O. T., et al. (2017). "Association of Neural and Emotional Impacts of Reward Prediction Errors With Major Depression". In: *JAMA psychiatry* 74.8, pp. 790–797.

Rutledge, R. B., Skandali, N., Dayan, P., and Dolan, R. J. (2014). "A computational and neural model of momentary subjective well-being". In: *Proceedings of the National Academy of Sciences* 111.33, pp. 12252–12257.

Rutledge, R. B., Skandali, N., Dayan, P., and Dolan, R. J. (2015). "Dopaminergic modulation of decision making and subjective well-being". In: *Journal of Neuroscience* 35.27, pp. 9811–9822.

Sanacora, G., Treccani, G., and Popoli, M. (2012). "Towards a glutamate hypothesis of depression: an emerging frontier of neuropsychopharmacology for mood disorders". In: *Neuropharmacology* 62.1, pp. 63–77.

Schmaal, L., Hibar, D., Sämann, P., Hall, G., Baune, B., Jahanshad, N., Cheung, J., Erp, T. van, Bos, D., Ikram, M., et al. (2017). "Cortical abnormalities in adults and adolescents with major depression based on brain scans from 20 cohorts worldwide in the ENIGMA Major Depressive Disorder Working Group". In: *Molecular psychiatry* 22.6, p. 900.

Schmaal, L., Veltman, D. J., Erp, T. G. van, Sämann, P., Frodl, T., Jahanshad, N., Loehrer, E., Tiemeier, H., Hofman, A., Niessen, W., et al. (2016). "Subcortical brain alterations in major depressive disorder: findings from the ENIGMA Major Depressive Disorder working group". In: *Molecular psychiatry* 21.6, p. 806.

Schnack, H. G. and Kahn, R. S. (2016). "Detecting neuroimaging biomarkers for psychiatric disorders: sample size matters". In: *Frontiers in psychiatry* 7, p. 50.

Schultz, W. (1998). "Predictive reward signal of dopamine neurons". In: *Journal of neurophysiology* 80.1, pp. 1–27.

– (2002). "Getting formal with dopamine and reward". In: *Neuron* 36.2, pp. 241–263.

Schultz, W., Dayan, P., and Montague, P. R. (1997). "A neural substrate of prediction and reward". In: *Science* 275.5306, pp. 1593–1599.

Seligman, M. E. (1972). "Learned helplessness". In: *Annual review of medicine* 23.1, pp. 407–412.

Shackman, A. J., Salomons, T. V., Slagter, H. A., Fox, A. S., Winter, J. J., and Davidson, R. J. (2011). "The integration of negative affect, pain and cognitive control in the cingulate cortex". In: *Nature Reviews Neuroscience* 12.3, p. 154.

Sharot, T. (2011). "The optimism bias". In: *Current Biology* 21.23, R941–R945.

Sheehan, D., Lecrubier, Y., Sheehan, K., Amorim, P., Janavs, J., Weiller, E., Hergueta, T., R, B., and GC, D. (1998). "The Mini International Neuropsychiatric Interview (M.I.N.I.): The development and validation of a structured diagnostic psychiatric interview for DSM-IV and ICD-10". In: *Journal of Clinical Psychiatry* 59.20, pp. 22–33.

Shen, X., Reus, L. M., Cox, S. R., Adams, M. J., Liewald, D. C., Bastin, M. E., Smith, D. J., Deary, I. J., Whalley, H. C., and McIntosh, A. M. (2017). "Subcortical volume and white matter integrity abnormalities in major depressive disorder: findings from UK Biobank imaging data". In: *Scientific reports* 7.1, p. 5547.

Shenhav, A., Botvinick, M. M., and Cohen, J. D. (2013). "The expected value of control: an integrative theory of anterior cingulate cortex function". In: *Neuron* 79.2, pp. 217–240.

Shultz, E. and Malone Jr, D. A. (2013). "A practical approach to prescribing antidepressants". In: *Cleve Clin J Med* 80.10, pp. 625–31.

Siegle, G. J. and Hasselmo, M. E. (2002). "Using connectionist models to guide assessment of psycological disorder." In: *Psychological Assessment* 14.3, p. 263.

Siegle, G. J., Steinhauer, S. R., and Thase, M. E. (2004). "Pupillary assessment and computational modeling of the Stroop task in depression". In: *International Journal of Psychophysiology* 52.1, pp. 63–76.

Slotnick, S. D., Moo, L. R., Segal, J. B., and Hart Jr, J. (2003). "Distinct prefrontal cortex activity associated with item memory and source memory for visual shapes". In: *Cognitive Brain Research* 17.1, pp. 75–82.

Smith, B. H., Campbell, A., Linksted, P., Fitzpatrick, B., Jackson, C., Kerr, S. M., Deary, I. J., MacIntyre, D. J., Campbell, H., McGilchrist, M., et al. (2012). "Cohort Profile: Generation Scotland: Scottish Family Health Study (GS: SFHS). The study, its participants and their potential for genetic research on health and illness". In: *International journal of epidemiology* 42.3, pp. 689–700.

Snyder, H. R. (2013). *Major depressive disorder is associated with broad impairments on neuropsychological measures of executive function: A meta-analysis and review.*

Stankevicius, A., Huys, Q. J., Kalra, A., and Seriès, P. (2014). "Optimism as a prior belief about the probability of future reward". In: *PLoS Computational Biololgy* 10.5, e1003605.

Steele, J. D., Christmas, D., Eljamel, M. S., and Matthews, K. (2008). "Anterior cingulotomy for major depression: clinical outcome and relationship to lesion characteristics". In: *Biological psychiatry* 63.7, pp. 670–677.

Steele, J. D. and Paulus, M. P. (2019). "Pragmatic neuroscience for clinical psychiatry". In: *The British Journal of Psychiatry* 215.1, pp. 404–408.

Steele, J., Kumar, P., and Ebmeier, K. P. (2007). "Blunted response to feedback information in depressive illness". In: *Brain* 130.9, pp. 2367–2374.

Stephan, K. E., Bach, D. R., Fletcher, P. C., Flint, J., Frank, M. J., Friston, K. J., Heinz, A., Huys, Q. J., Owen, M. J., Binder, E. B., et al. (2016). "Charting the landscape of priority problems in psychiatry, part 1: classification and diagnosis". In: *The Lancet Psychiatry* 3.1, pp. 77–83.

Stephan, K. E., Binder, E. B., Breakspear, M., Dayan, P., Johnstone, E. C., Meyer-Lindenberg, A., Schnyder, U., Wang, X.-J., Bach, D. R., Fletcher, P. C., et al. (2016). "Charting the landscape of priority problems in psychiatry, part 2: pathogenesis and aetiology". In: *The Lancet Psychiatry* 3.1, pp. 84–90.

Stephan, K. E., Iglesias, S., Heinzle, J., and Diaconescu, A. O. (2015). "Translational perspectives for computational neuroimaging". In: *Neuron* 87.4, pp. 716–732.

Stephan, K. E. and Mathys, C. (2014). "Computational approaches to psychiatry". In: *Current opinion in neurobiology* 25, pp. 85–92.

Stephan, K. E., Penny, W. D., Daunizeau, J., Moran, R. J., and Friston, K. J. (2009). "Bayesian model selection for group studies". In: *Neuroimage* 46.4, pp. 1004–1017.

Strauss, G. P., Robinson, B. M., Waltz, J. A., Frank, M. J., Kasanova, Z., Herbener, E. S., and Gold, J. M. (2010). "Patients with schizophrenia demonstrate inconsistent

preference judgments for affective and nonaffective stimuli". In: *Schizophrenia bulletin* 37.6, pp. 1295–1304.

Stringaris, A., Vidal-Ribas Belil, P., Artiges, E., Lemaitre, H., Gollier-Briant, F., Wolke, S., Vulser, H., Miranda, R., Penttilä, J., Struve, M., et al. (2015). "The brain's response to reward anticipation and depression in adolescence: dimensionality, specificity, and longitudinal predictions in a community-based sample". In: *American Journal of Psychiatry* 172.12, pp. 1215–1223.

Sullivan, P. F., Neale, M. C., and Kendler, K. S. (2000). "Genetic epidemiology of major depression: review and meta-analysis". In: *American Journal of Psychiatry* 157.10, pp. 1552–1562.

Sutton, R. S. and Barto, A. G. (1998). *Reinforcement learning: An introduction*. Vol. 1. MIT press Cambridge.

Taghva, A. S., Malone, D. A., and Rezai, A. R. (2013). "Deep brain stimulation for treatment-resistant depression". In: *World neurosurgery* 80.3-4, S27–e17.

Tavares, J. V. T., Clark, L., Furey, M. L., Williams, G. B., Sahakian, B. J., and Drevets, W. C. (2008). "Neural basis of abnormal response to negative feedback in unmedicated mood disorders". In: *Neuroimage* 42.3, pp. 1118–1126.

Tolomeo, S., Christmas, D., Jentzsch, I., Johnston, B., Sprengelmeyer, R., Matthews, K., and Douglas Steele, J. (2016). "A causal role for the anterior mid-cingulate cortex in negative affect and cognitive control". In: *Brain* 139.6, pp. 1844–1854.

Treadway, M. T., Bossaller, N. A., Shelton, R. C., and Zald, D. H. (2012). "Effort-based decision-making in major depressive disorder: a translational model of motivational anhedonia." In: *Journal of abnormal psychology* 121.3, p. 553.

Treadway, M. T. and Zald, D. H. (2013). "Parsing anhedonia: translational models of reward-processing deficits in psychopathology". In: *Current directions in psychological science* 22.3, pp. 244–249.

Trimmer, P. C., Higginson, A. D., Fawcett, T. W., McNamara, J. M., and Houston, A. I. (2015). "Adaptive learning can result in a failure to profit from good conditions: implications for understanding depression". In: *Evolution, medicine, and public health* 2015.1, pp. 123–135.

Üstün, T., Ayuso-Mateos, J. L., Chatterji, S., Mathers, C., and Murray, C. J. (2004). "Global burden of depressive disorders in the year 2000". In: *The British journal of psychiatry* 184.5, pp. 386–392.

Vallesi, A., Canalaz, F., Balestrieri, M., and Brambilla, P. (2015). "Modulating speed-accuracy strategies in major depression". In: *Journal of psychiatric research* 60, pp. 103–108.

Vinckier, F., Rigoux, L., Oudiette, D., and Pessiglione, M. (2018). "Neuro-computational account of how mood fluctuations arise and affect decision making". In: *Nature communications* 9.1, pp. 1–12.

Vinogradov, S. (2017). "The golden age of computational psychiatry is within sight". In: *Nature Human Behaviour* 1, p. 0047.

Vos, T., Abajobir, A. A., Abate, K. H., Abbafati, C., Abbas, K. M., Abd-Allah, F., Abdulkader, R. S., Abdulle, A. M., Abebo, T. A., Abera, S. F., et al. (2017). "Global, regional, and national incidence, prevalence, and years lived with disability for 328 diseases and injuries for 195 countries, 1990–2016: a systematic analysis for the Global Burden of Disease Study 2016". In: *The Lancet* 390.10100, pp. 1211–1259.

Vos, T., Flaxman, A. D., Naghavi, M., Lozano, R., Michaud, C., Ezzati, M., Shibuya, K., Salomon, J. A., Abdalla, S., Aboyans, V., et al. (2012). "Years lived with disability (YLDs) for 1160 sequelae of 289 diseases and injuries 1990–2010: a systematic analysis for the Global Burden of Disease Study 2010". In: *The Lancet* 380.9859, pp. 2163–2196.

Wang, X.-J. and Krystal, J. H. (2014). "Computational psychiatry". In: *Neuron* 84.3, pp. 638–654.

Watson, D. (2009). "Differentiating the mood and anxiety disorders: A quadripartite model". In: *Annual Review of Clinical Psychology* 5, pp. 221–247.

Wesley, M. J. and Bickel, W. K. (2014). "Remember the future II: meta-analyses and functional overlap of working memory and delay discounting". In: *Biological psychiatry* 75.6, pp. 435–448.

Wetzels, R. and Wagenmakers, E.-J. (2012). "A default Bayesian hypothesis test for correlations and partial correlations". In: *Psychonomic bulletin & review* 19.6, pp. 1057–1064.

Whiteford, H. A., Degenhardt, L., Rehm, J., Baxter, A. J., Ferrari, A. J., Erskine, H. E., Charlson, F. J., Norman, R. E., Flaxman, A. D., Johns, N., et al. (2013). "Global burden of disease attributable to mental and substance use disorders: findings from the Global Burden of Disease Study 2010". In: *The Lancet* 382.9904, pp. 1575–1586.

WHO (2018). *Depression: Fact Sheet (updated Feb 2017)*. Retrieved from http://www.who.int/mediacentre/factsheets/fs369/en/.

Widiger, T. A. and Oltmanns, J. R. (2017). "Neuroticism is a fundamental domain of personality with enormous public health implications". In: *World Psychiatry* 16.2, pp. 144–145.

Wilson, R. C. and Collins, A. G. (2019). "Ten simple rules for the computational modeling of behavioral data". In: *eLife* 8, e49547.

World Health Organization (1992). *The ICD-10 classification of mental and behavioural disorders: clinical descriptions and diagnostic guidelines*. Geneva: World Health Organization.

Wray, N. R., Ripke, S., Mattheisen, M., Trzaskowski, M., Byrne, E. M., Abdellaoui, A., Adams, M. J., Agerbo, E., Air, T. M., Andlauer, T. M., et al. (2018). "Genome-wide association analyses identify 44 risk variants and refine the genetic architecture of major depression". In: *Nature genetics* 50.5, p. 668.

Yang, X., Liu, J., Meng, Y., Xia, M., Cui, Z., Wu, X., Hu, X., Zhang, W., Gong, G., Gong, Q., et al. (2019). "Network analysis reveals disrupted functional brain circuitry in drug-naive social anxiety disorder". In: *Neuroimage* 190, pp. 213–223.

Yarkoni, T., Poldrack, R. A., Nichols, T. E., Van Essen, D. C., and Wager, T. D. (2011). "Large-scale automated synthesis of human functional neuroimaging data". In: *Nature methods* 8.8, p. 665.

Zeidman, P. (2019). *DCM Question [cited 21/06/2019]*. Available from: https://www.jiscmail.ac.uk/cgi-bin/webadmin?A2=SPM;a060cf87.1905.

Zhang, W.-N., Chang, S.-H., Guo, L.-Y., Zhang, K.-L., and Wang, J. (2013). "The neural correlates of reward-related processing in major depressive disorder: a meta-analysis of functional magnetic resonance imaging studies". In: *Journal of affective disorders* 151.2, pp. 531–539.

Zigmond, A. S. and Snaith, R. P. (1983). "The hospital anxiety and depression scale". In: *Acta psychiatrica scandinavica* 67.6, pp. 361–370.